UNIONE EUROPEA
Fondo Sociale Europeo
Fondo Europeo di Sviluppo Regionale

MINISTERO DELL'ISTRUZIONE, DELL'UNIVERSITÀ E DELLA RICERCA

UNIVERSITÀ DEGLI STUDI DI SASSARI

Università degli Studi di Sassari
SCUOLA DI DOTTORATO DI RICERCA

SCIENZE VETERINARIE

Indirizzo: Riproduzione Patologia, Allevamento e Benessere Animale

Ciclo XXXVII

Bacterial Granulomatous Diseases in Teleost Fish from Sardinian Aquaculture and Innovative Strategies for Mycobacteriosis Prevention and Vaccination

Docente Guida:
Prof.ssa Elisabetta Antuofermo

Correlatore:
Prof. Esteban Soto

Coordinatore
Prof. Alberto Alberti

Tesi di dottorato del
Dott. Claudio Murgia

Anno accademico 2023/2024

Abstract

Bacterial granulomatous diseases pose a significant challenge to fish health, particularly in aquaculture systems, where environmental conditions and pathogen exposure contribute to disease outbreaks. Through a multidisciplinary approach that combined histopathological, microbiological, and molecular tools, the study investigated the prevalence and etiology of granulomatous diseases affecting most farmed fish species in Sardinia, including *Argyrosomus regius* (meagre), *Sparus aurata* (gilthead seabream), *Dicentrarchus labrax* (European seabass), and Mugilidae (mullets). Particular attention was given to non-tuberculous mycobacteria (NTM), also referred to as atypical or environmental mycobacteria, which cause a granulomatous chronic disease in fish (Mycobacteriosis) that is also an important zoonosis.

Histopathological analysis revealed a high prevalence of granulomas, with meagre being the most affected fish species (94%), followed by mullets (93%), seabream (42%), and seabass (30%). Granulomas were associated mostly with parasitic infection, especially in mullets (91%), and with *Mycobacterium chelonae* only in a few cases in meagre (13%) and in mullets (5%). No bacteria were associated to granulomas in seabream and seabass. In meagre, the presence of granulomas was almost due to Systemic Granulomatosis (SG), a chronic disorder of unknown origin that shares histological features with fish mycobacteriosis, although nutritional/metabolic etiology is favored. An additional study was conducted to validate commercial antibodies including anti-pancytokeratin, anti-GFAP, anti-vimentin, anti-desmin, and anti-S-100. Immunohistochemical and Western blot analyses confirmed the cross-reactivity of anti-panCK (clone AE1/AE3) and anti-GFAP antibodies in *Sparus aurata, Dicentrarchus labrax, Argyrosomus regius,* and other fish species offering valuable tools for detecting epithelial and glial cells in skin and brain tissues. Furthermore, a key aspect of this research was the development of preventive strategies and vaccination against mycobacterial infections in fish. A first study assessed the susceptibility of mycobacterial biofilms to commonly used aquaculture disinfectants. Using the Minimal Biofilm

Eradication Concentration (MBEC) assay® system, biofilms of *Mycobacterium chelonae, M. salmoniphilum, M. arcueilense,* and *M. marinum* were evaluated and subsequently challenged with disinfectants, highlighting significant species-specific variations in biofilm resistance.

The second study assessed the potential of a mutant *M. chelonae* as a live-attenuated vaccine for fish mycobacteriosis in *Carassius auratus* (goldfish). Two *in vivo* trials, including intraperitoneal injection and oral delivery, were conducted to assess the vaccine's immunogenicity and safety, with gene expression analysis targeting interleukin-12 (*IL-12*) and interferon-gamma (*IFN-γ*). The vaccine demonstrated promising results against *M. marinum*, stimulating a robust immune response, and causing no adverse effects in vaccinated fish.

Overall, this research contributes to a more comprehensive understanding of bacterial granulomatous diseases in farmed fish and provides practical insights into improved diagnostic approaches, vaccination strategies, and biofilm management. These findings support sustainable aquaculture practices in Sardinia and beyond, offering valuable tools for fish mycobacteriosis prevention and control in the aquaculture industry.

Declaration

I declare that this thesis represents my original work, carried out during the designated research project period (2021-2024). This work has not been derived from the work of others, except where such work has been cited and acknowledged within the text. I have had an important role in the study's design, the execution of experiments, sampling, data acquisition, as well as the analysis and interpretation of most of the data.

The thesis project was a collaborative effort involving several research teams from different institutions, including: the Department of Veterinary Medicine and the Department of Agriculture of the University of Sassari; the Department of Veterinary Medicine and Animal Sciences of the University of Milan; the Istituto Zooprofilattico Sperimentale del Piemonte; and the Department of Medicine and Epidemiology at the School of Veterinary Medicine, University of California, Davis (UCD), Aquatic Animal Health Laboratory.

This work was also made possible thanks to the valuable collaboration with several Sardinian farms, including: Maricoltura RiservAzzurra, Marina Torre Grande, Cabras (OR); Compagnie Ittiche Riunite Società Agricola S.r.l., Golfo Aranci (SS); Stagno di San Teodoro S.p.A., San Teodoro (SS); Arrubia, Stagno di S'Ena Arrubia (OR).

Contents

List of abbreviations

AUC: Area Under the Curve

BCG: Bacillus Calmette and Guerin

BGC: Biofilm Growth Check

BHI: Brain Heart Infusion

BSA: Bovine Serum Albumin

CBA: Columbia Blood Agar

CFU: Colony-Forming Units

DAB: Diaminobenzidine

DAPB: Dihydrodipicolinate Reductase

DHA: Docosahexaenoic Acid

d.p.c: Days Post-Challenge

d.p.v: Days Post-Vaccination

ECPs: Extracellular Products

EF1A$_A$: Elongation Factor 1 Alpha A

erp: Exported Repeated Protein

ESX: Early Secretory Antigenic Target (ESAT6) Secretion

FFPE: Formalin-Fixed Paraffin-Embedded

FrFr: Fresh-Frozen

FSW: Filtered Sterilized Water

gDNA: Genomic DNA

GE: Genome Equivalents

GFAP: Glial Fibrillary Acidic Protein

H&E: Hematoxylin & Eosin

H_2O_2: Hydrogen Peroxide

hsp65: Heat Shock Protein 65kD Gene

IHC: Immunohistochemistry

IFN-γ: Interferon-Gamma

IL-12: Interleukin-12

ISH: In Situ Hybridization

KGHfin: Koi-Goldfish Hybrid Fin

LAV: Live-Attenuated Vaccine

LAVs: Live-Attenuated Vaccines

MBEC: Minimal Biofilm Eradication Concentration

MET: Mesenchymal-to-Epithelial Transition

MMCs: Melanomacrophage Centers

MW: Molecular Weight

NCBI: National Center for Biotechnology Information

NTM: Non-Tuberculous Mycobacteria

OTUs: Operational Taxonomic Units

PAS: Periodic Acid-Schiff

PBS: Phosphate-Buffered Saline

PBS-T: Phosphate-Buffered Saline, 0.05% Tween 20

PCR: Polymerase Chain Reaction

qPCR: Real-Time Quantitative PCR

RAS: Recirculation Aquaculture System

rpoB: RNA Polymerase B Subunit

RT-qPCR: Reverse Transcription Quantitative PCR

SBA: Sheep Blood Agar

SG: Systemic Granulomatosis

SDS–PAGE: Sodium Dodecyl Sulfate–Polyacrylamide Gel Electrophoresis

TBARS: Thiobarbituric Acid-Reactive Substances

TSA: Tryptic Soy Agar

WB: Western Immunoblot

WT: Wild-Type Strain

ZN: Ziehl-Neelsen

Δ: Mutant Attenuated Strain

Legend to figures

Legend to tables

Chapter I - Part 1

Global aquaculture production

1.1 General introduction

Global fish production has been growing steadily for the past six decades. In 2022 alone, fisheries and aquaculture activities supplied the world with about 185 million tons of products. In this, aquaculture (excluding algae) contributed 94 million tonnes (live weight equivalent), surpassing for the first time capture fisheries (F.A.O., 2024)(*Fig. 1*). FAO defines aquaculture as the "*farming of aquatic organisms, including fish, molluscs, crustaceans and aquatic plants"* (F.A.O., 2010).

In recent decades, the role of aquaculture in the food supply chain has significantly expanded, providing rich sources of proteins, essential fatty acids, vitamins, and minerals to a wide range of population. Over the last 30 years, fish consumption has surged from 14.3 kg to 20.6 kg per capita, driven by factors such as population growth, urbanization, and advancements in fish production technology (F.A.O., 2024). While traditional fisheries have not significantly increased since the early 1990´s (primarily due to overexploitation of fishing areas and changes in international fishing policies), aquaculture has been responsible for the impressive growth in the supply of fish for human consumption from 7% in 1974, to 57% in 2022 (F.A.O., 2024). This exponential development has been achieved through efforts to optimize efficiency and productivity in both small and large-scale aquaculture systems. Undoubtedly, one of the greatest challenges ahead is securing sustenance for a projected population of 9 billion by 2050, among climate change and increasing competition for natural resources. In addressing this, as highlighted in the *Blue Transformation* initiative (F.A.O., 2022), the development of aquaculture will be pivotal, offering a sustainable solution to meet the rising demand for food and alleviate pressure on conventional food production systems.

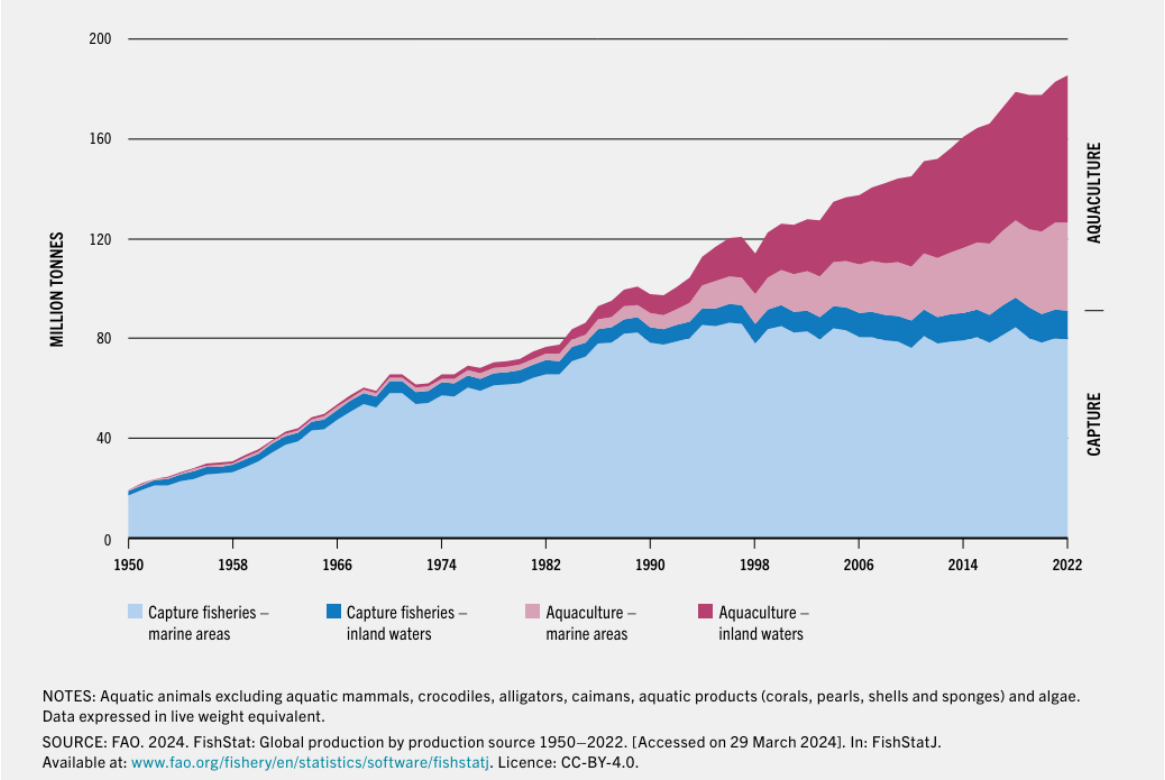

Figure 1*. Trend in world capture fisheries and aquaculture production from 1950 to 2022 (FAO, 2024).*

1.2 Global aquaculture production

Although growth patterns varied across regions and countries, global aquaculture production continued to rise in the last decade, unaffected by the COVID-19 pandemic. In 2022, world aquaculture production valued at USD 312.8 billion, marking an increase USD 34.2 billion from 2020. In 2022, global aquaculture production reached 94.33 million tonnes, with finfish leading at 65.2% (61.5 million tonnes), followed by molluscs at 20% (18.9 million tonnes), crustaceans at 13.5% (12.75 million tonnes), and other aquatic animals at 1.3% (1.18 million tonnes) (F.A.O., 2024). World fisheries and aquaculture trends are summarized in *Fig. 2*.

TABLE 1 WORLD FISHERIES AND AQUACULTURE TRENDS AT A GLANCE

	1990s	2000s	2010s	2020	2021	2022
	Average per year					
	(million tonnes, live weight equivalent)					
Production						
Capture fisheries:						
Inland	7.1	9.3	11.3	11.5	11.4	11.3
Marine	81.9	81.6	79.8	78.3	80.3	79.7
Total capture fisheries	**88.9**	**90.9**	**91.1**	**89.8**	**91.6**	**91.0**
Aquaculture:						
Inland	12.6	25.6	44.8	54.5	56.4	59.1
Marine	9.2	17.9	26.7	33.2	34.7	35.3
Total aquaculture	**21.8**	**43.4**	**71.5**	**87.7**	**91.1**	**94.4**
Total world fisheries and aquaculture	**110.7**	**134.3**	**162.6**	**177.5**	**182.8**	**185.4**
Utilization*						
Human consumption	81.6	109.3	143.1	157.4	162.5	164.6
Non-food uses	29.1	25.0	19.5	20.1	20.3	20.8
Apparent consumption per capita (kg)	14.4	16.9	19.5	20.2	20.6	20.7
Trade**						
Exports – in quantity	39.3	51.2	60.8	63.8	67.8	70.0
Share of exports in total production (%)	*35.4*	*38.3*	*37.5*	*35.8*	*36.9*	*37.6*
Exports – in value (USD billion)	46.6	76.4	141.8	151.0	176.6	192.2
Employment (millions of people)***						
Aquaculture	12.1	15.9	21.9	22.2	22.3	22.1
Fisheries	24.4	29.1	31.9	34.3	33.4	33.6
Unspecified	7.2	6.8	7.0	6.3	6.1	6.1
Fishing fleet (millions of vessels)****						
Motorized and non-motorized vessels	4.5	4.7	5.0	5.3	5.1	4.9

NOTES: Data on production, utilization and trade refer to aquatic animals, excluding aquatic mammals, crocodiles, alligators, caimans, aquatic products (corals, pearls, shells and sponges) and algae. Data may not match totals due to rounding.
* Utilization data for 2020–2022 are provisional estimates. These data might differ from the apparent consumption data as they do not take into account trade.
** Exports including re-exports. Share of trade in total production calculated excluding re-exports. Trade data do not include frogs and turtles.
*** Employment refers to the number of people engaged in the primary sector only. Figures for the 1990s are based on 1995–1999 data.
**** Fishing fleet figures for the 1990s are based on 1995–1999 data.

SOURCES: For production: FAO. 2024. FishStat: Global production by production source 1950–2022. [Accessed on 29 March 2024]. In: FishStatJ. Available at: www.fao.org/fishery/en/statistics/software/fishstatj. Licence: CC-BY-4.0.
For trade: Preliminary data. Final data available here: FAO. 2024. Global aquatic trade statistics. https://www.fao.org/fishery/en/collection/global_commodity_prod. Licence: CC-BY-4.0.
For employment: Preliminary data. Final data available here: FAO. (forthcoming). *Fishery and Aquaculture Statistics – Yearbook 2022*. FAO Yearbook of Fishery and Aquaculture Statistics. Rome. https://www.fao.org/fishery/en/statistics/yearbook
Population data used to calculate apparent consumption per capita are based on United Nations Population Division. 2022. World Population Prospects 2022. [Accessed 13 January 2023]. https://population.un.org/wpp

Figure 2. World fisheries and aquaculture production, utilization, and trade. (FAO 2024)

1.2.1 Regional overview

Asia is the dominant producer in marine, coastal, and freshwater seafood production, accounting for 83.4 million tonnes of farmed aquatic animals representing 91.43% of the total aquaculture production of aquatic animals (F.A.O., 2024). Finfish stand out as the dominant force, accounting for 53.7 million tonnes of production, along with molluscs (17.4 million tonnes), crustaceans (11 million tonnes) and other aquatic animals (1.17 million tonnes) (F.A.O., 2024).

In the Americas, Chile emerges as a major contributor, producing 30.4% of all aquaculture products with 1.5 million tonnes, ranking as the fourth-largest exporter of aquatic products. Chile has the world's second-largest salmonid (F.A.O., 2024). The United States accounts for 9.6% of the production, with 478 thousand tonnes of aquatic animals in 2022. Freshwater aquaculture leads the sector in the U.S., with catfish, crawfish, and trout being the primary species, while marine aquaculture is dominated by Atlantic salmon for finfish and oysters for marine shellfish production (National Marine Fisheries Service, 2024).

In Africa finfish production leads the sector with 2 million tonnes, followed by crustaceans (7 thousand tonnes) and molluscs (5 thousand tonnes). Inland aquaculture is predominant, with tilapia and African catfish as the main farmed species. Egypt, Nigeria, Ghana and Uganda led the production, accounting for about 88,3% of the continent's total aquaculture (F.A.O., 2024).

Oceania's contribution to global aquaculture remains relatively low, with 235 thousand tonnes of aquatic animal products. Australia stands out as the major producer (53.2 thousand tonnes), of Southern Bluefin tuna in offshore cages, salmonids, prawns, and mussel in marine waters (abalone and oysters mainly). New Zealand's aquaculture accounts for 45.1 thousand tonnes focusing on farming green shell mussels, Pacific oysters, and Chinook salmon (Rocha et al., 2022; F.A.O., 2024)

In Europe aquaculture production reached 3.5 million tonnes, with finfish (82%), molluscs (17%), and crustaceans/other species (1%) (FAO, 2024) (Fig. 3). Non-EU countries, including Norway, Turkey, and Russia, have seen growth, while some EU nations, such as France, Italy, and the Netherlands, reported declines. Nordic aquaculture is dominated by salmon and trout (98.4%), with Norway leading in Atlantic salmon (95.6%) (Fig. 4) (Fernández Sánchez et al., 2023). The Mediterranean-EU region farms a diverse range of species, with shellfish (51%) as the largest sector, followed by freshwater and marine finfish (28% and 21%, respectively) (EU Aquaculture Infographic, 2023). France, Greece, Spain, and Italy account for 67% of EU aquaculture (EUROSTAT, 2024).

Despite efforts like the *Blue Growth Strategy* and the *European Green Deal*, EU aquaculture covered only 10% of seafood consumption in 2018 (European Commission, 2021a). Expansion and diversification initiatives aim to improve farming practices and seafood quality.

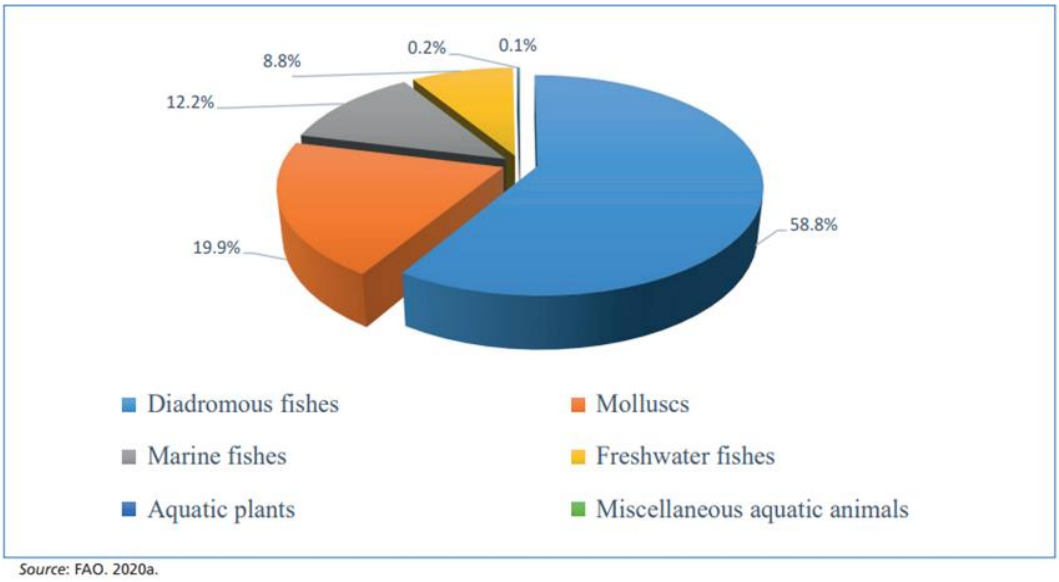

Figure 3. *Division and share of 2018 aquaculture production in the European Region (percent). (FAO 2020a)*

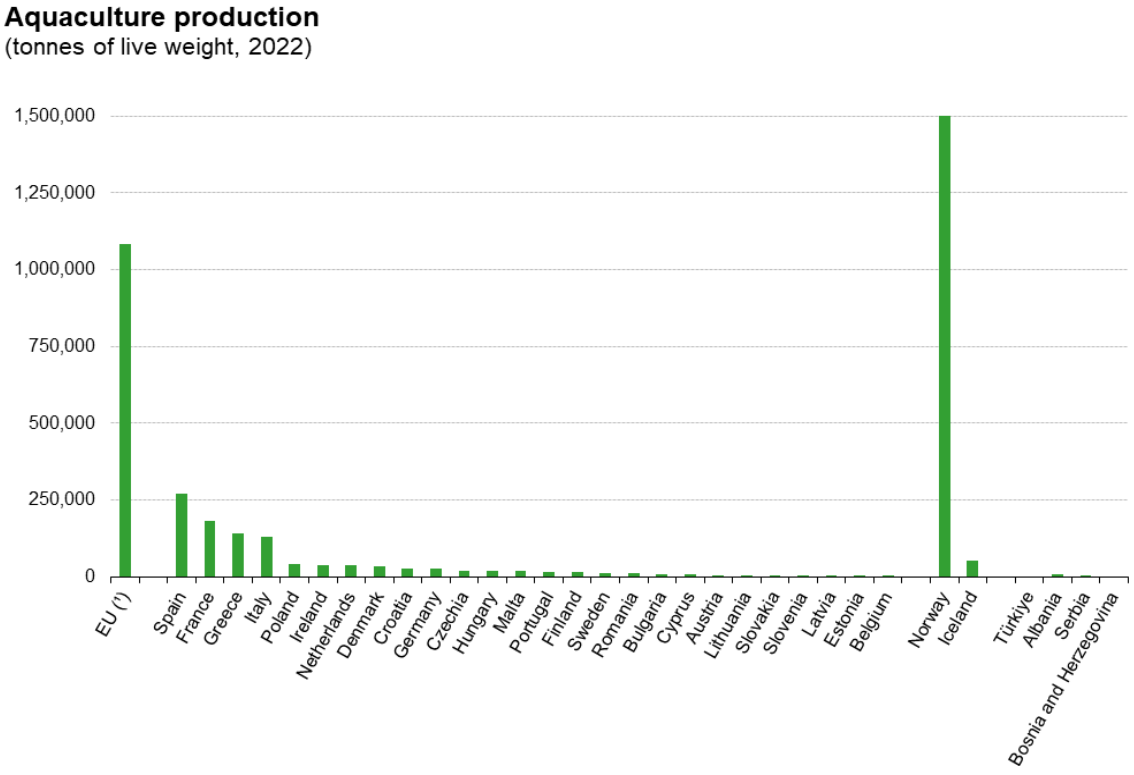

Figure 4. *Aquaculture production, (tonnes of live weight, 2022). (Eurostat (fish_aq2a), 2022)*

	2000	2005	2010	2015	2020	2021	2022	Share in regional total, 2022 (%)	2020/2022 variation
	(thousand tonnes, live weight equivalent)								
Africa	**400**	**646**	**1 289**	**1 788**	**2 266**	**2 328**	**2 317**	100	↗
Egypt	340	540	920	1 175	1 592	1 576	1 552	67.0	↘
Nigeria	26	56	201	317	262	276	259	11.2	↘
Ghana	5	1	10	45	64	89	133	5.7	↗
Uganda	1	11	95	118	124	139	101	4.4	↘
Others	28	38	64	134	225	249	271	11.7	↗
Americas	**1 423**	**2 177**	**2 515**	**3 280**	**4 443**	**4 494**	**4 958**	100	↗
Chile	392	724	701	1 046	1 486	1 427	1 509	30.4	↗
Ecuador	61	139	273	427	775	904	1 123	22.6	↗
Brazil	172	258	411	578	630	649	738	14.9	↗
United States of America	457	514	497	426	448	461	478	9.6	↗
Others	341	543	633	804	1 105	1 053	1 111	22.4	↗
Asia	**28 422**	**39 190**	**51 233**	**64 682**	**77 513**	**80 485**	**83 399**	100	↗
China	21 522	28 121	35 513	43 748	49 620	51 221	52 884	63.4	↗
India	1 943	2 967	3 786	5 341	8 636	9 403	10 230	12.3	↗
Indonesia	789	1 197	2 305	4 342	5 227	5 536	5 414	6.5	↗
Viet Nam	499	1 437	2 683	3 462	4 668	4 736	5 160	6.2	↗
Bangladesh	657	882	1 309	2 060	2 584	2 639	2 731	3.3	↗
Myanmar	99	485	851	997	1 145	1 167	1 197	1.4	↗
Thailand	738	1 304	1 286	921	1 012	991	1 001	1.2	↘
Others	2 177	2 796	3 500	3 810	4 623	4 792	4 783	5.7	↗
Europe	**2 053**	**2 144**	**2 533**	**2 956**	**3 271**	**3 570**	**3 503**	100	↗
Norway	491	662	1 020	1 381	1 490	1 665	1 648	47.0	↗
Russian Federation	74	115	120	152	270	295	320	9.1	↗
Spain	311	225	257	297	277	280	276	7.9	↘
United Kingdom of Great Britain and Northern Ireland	152	173	201	212	220	239	203	5.8	↘
France	267	245	203	163	191	193	200	5.7	↗
Greece	95	106	121	107	132	144	142	4.1	↗
Italy	214	182	153	149	126	146	133	3.8	↗
Others	448	436	457	496	566	608	582	16.6	↗
Oceania	**122**	**154**	**190**	**178**	**225**	**250**	**235**	100	↗
Australia	32	45	76	83	103	129	125	53.2	↗
New Zealand	86	105	111	91	119	117	106	45.1	↘
Papua New Guinea	0	0	2	2	2	2	2	0.8	↗
New Caledonia	2	3	1	1	1	1	1	0.6	↗
Others	2	0	1	0	1	1	1	0.2	↗

NOTE: Data on aquatic animals exclude crocodiles, alligators, caimans, aquatic products (corals, pearls, shells and sponges) and algae.

SOURCE: FAO. 2024. FishStat: Global aquaculture production 1950–2022. [Accessed on 29 March 2024]. In: FishStatJ. Available at: www.fao.org/fishery/en/statistics/software/fishstatj. Licence: CC-BY-4.0.

Figure 5. *World aquaculture production of aquatic animals by region and selected major producers (FAO, 2024)*

1.3 Aquaculture in the Mediterranean Sea

Over the past decade aquaculture production in Mediterranean countries has grown by 160%, mainly driven by non-EU Mediterranean countries (Carvalho & Guillen, 2021).

Aquaculture in Mediterranean countries yielded over 2.3 million tonnes of fish, where Egypt represents 31% of production, followed by Turkey (29%), Greece (14%), Italy (12%), and Spain (5%) (F.A.O., 2023) (*Fig. 6*). Marine cages are the most employed system, accounting for 67.4% of the total volume in Mediterranean and Black Sea countries over 2020–2021 (FAO, 2023). Pond and suspended culture are other methods largely adopted in the region, accounting for 17.9% and 7.8% of total production, respectively (F.A.O., 2023). Other relevant production methods, ranked from highest to lowest use, include bottom culture, dams, reservoirs, barrages, lagoons, raceways, and tanks (F.A.O., 2023).

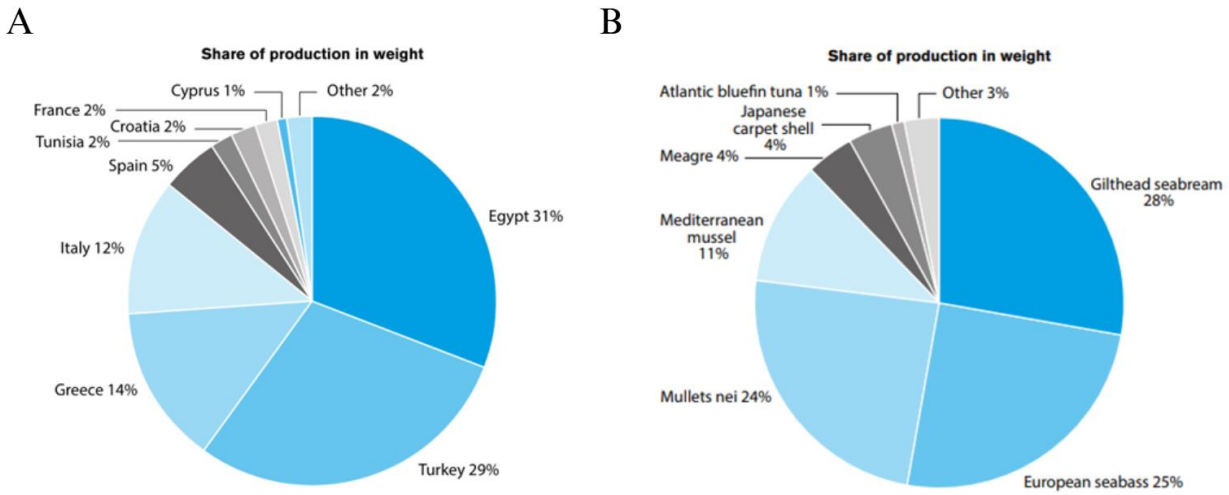

Figure 6. *Aquaculture production in the Mediterranean Sea by country (A) and by species (B) (IEMed. Mediterranean Yearbook 2021)*

Finfish dominate Mediterranean marine aquaculture, comprising 83% of total production, with molluscs covering 16%, and the remaining 1% represented by algal and crustacean species groups (F.A.O., 2023). Among the most farmed finfish species we find Gilthead seabream (*Sparus aurata*) and European seabass (*Dicentrarchus labrax*), accounting for 464.000 tonnes (53%). Other finfish farmed species are meagre (*Argyrosomus regius*) with 48.229 tonnes (5.8%),

followed by Atlantic bluefin tuna (*Thunnus thynnus*) 33.276 tonnes (4 %) and mullets nei (Mugilidae) with 29.322 tonnes (3.5%)(*Fig. 7*).

Other important farmed species are mussels, including Mediterranean mussel (*Mytilus galloprovincialis*) with 86.117 tonnes (10%), and Japanese carpet shell with 23 744 tonnes (3%). The main producers are Italy (62% of the region's production) and Greece (24%)(F.A.O., 2023).

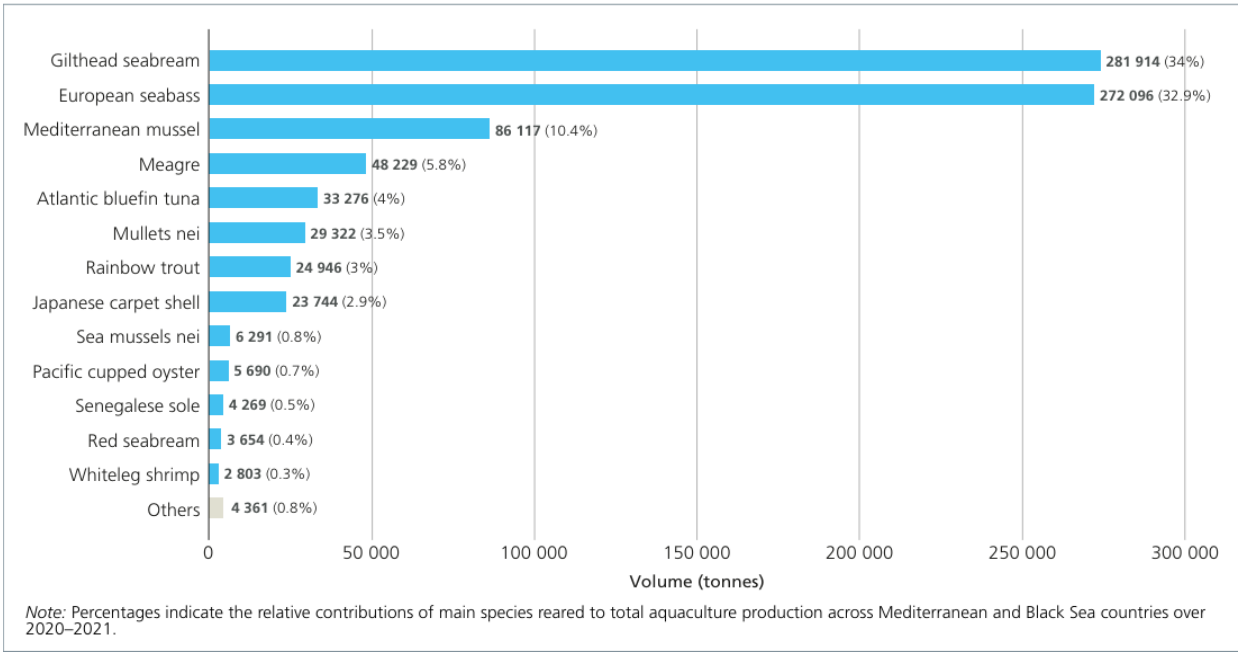

Figure 7. *Annual aquaculture production across Mediterranean and Black Sea countries by main species reared, over 2020–2021. (The State of Mediterranean and Black Sea Fisheries 2023. FAO)*

1.3.1 Aquaculture in Italy

Italy's aquaculture production amounts to 122.760 tonnes, comprising 74.990 tonnes of mollusks (61%), 47.770 tonnes of fish (39%), and 0.5 tonnes of crustaceans, with a total value of 392 million euros. Marine aquaculture accounts for 70% of production, primarily focusing on Mediterranean mussel (*Mytilus galloprovincialis*, 50.338 tonnes), Japanese carpet shell (*Venerupis philippinarum*, 24.337 tonnes), gilthead seabream (*Sparus aurata*, 6.201 tonnes), and European seabass (*Dicentrarchus labrax*, 4.693 tonnes). Other species include mullets (264 tonnes) and meagre (*Argyrosomus regius*, 70.5 tonnes), mainly farmed in offshore cages (CREA, 2020). On

the other hand, freshwater aquaculture contributes 30% of production, farming rainbow trout (*Oncorhynchus mykiss*, 40.441 tonnes) and sturgeon (1.200 tonnes), primarily reared in raceways (*Fig. 8*).

Italy's aquaculture has evolved from traditional extensive practices in coastal lagoons and wetlands to modern intensive systems in inland and marine environments, with both approaches now coexisting (Eurofish, 2023).

The extensive and semi-intensive aquaculture systems are primarily found in coastal lagoons and inland valleys, particularly in Sardinia, Veneto, and Emilia-Romagna. A notable example is *valliculture*, an extensive practice in the Northern Adriatic, which accounts for 66% of confined wetlands (Cautadella et al., 2005). Major species include European seabass, gilthead seabream, mullets, and European eel. However, eel production has declined in favor of seabass and seabream (Cataudella & Spagnolo, 2011).

Intensive farms are highly specialized and typically operate in monoculture, with stocking densities ranging from 0.1% to 5%. Seabream and seabass dominate marine aquaculture, accounting for 97% of total production, while freshwater facilities primarily focus on rainbow trout, sturgeons, and catfish. Intensive aquaculture has expanded from the late 1970s, first in coastal land-based facilities and later in floating sea cages (CREA., 2020).

	Produzione (t)						
	2014	2015	2016	2017	2018	2019	2020
Mitilo	63.700	53.110	62.837	62.502	61.415	52.547	50.338
Vongola verace	36.527	38.964	30.162	37.157	30.991	25.907	24.453
Ostriche	147	157	254	79.5	80	99	181,5
Trote	38.715	36.345	35.655	35.371	33.825	38.103	33.774
Spigola	5.724	6.450	6.800	7.039	5.738	4.947	4.693
Orata	6.830	7.350	7.600	7.173	7.316	6.783	6.201
Storioni	824	950	920	1.097	1.179	1.301	1.124
Cefali	779	832	746	2.604	231	419	264
Anguilla	572	750	710	529	510	464	221,5
Salmerini	533	781	841	557	483	846	799
Pesce gatto	231	392	468	144	138	176	70
Persico spigola	249	307	315	394	358	215	192,5
Carpe	134	241	298	185	179	221	217,1
Ombrina	73	145	145	55	156	70	70,5
Persico trota	60	117	115	50	64	84	87
Tilapia	1	60	115	25	18	ND	ND
Tinca	13	12	15	18	18	17	13,5
Saraghi	19	13	14	16	9	15	23
Sogliola	7	4	4	4	8	11	9
Crostacei	15	15	15	9	13	5	0,5

Figure 8. *Production (t) of the main species produced in Italy from 2014 to 2020 (MIPAAF, Reg. (CE) 762/2008)*

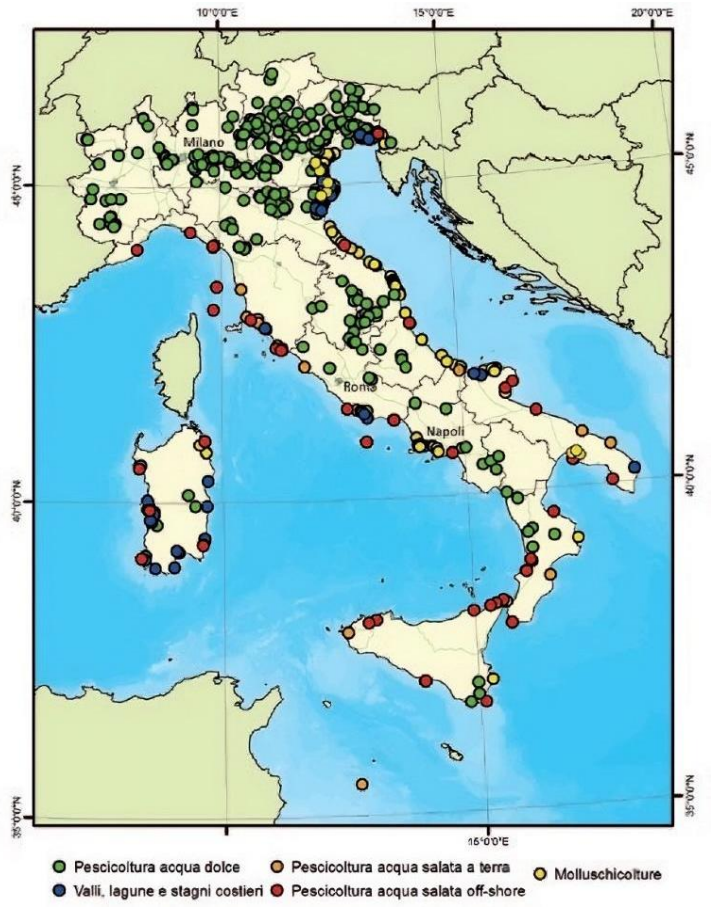

Figure 9*. Illustration of aquaculture systems in Italy. ("Lo stato della pesca e dell'acquacoltura dei mari italiani" S. Cautadella and M. Spagnolo, 2012.)*

1.3.2 Aquaculture in Sardinia

Sardinia is the second-largest island in the Mediterranean and features approximately 1850 kilometers of coastline and 77 bodies of water, forming one of Europe's most extensive lagoon networks, covering around 15.000 hectares (Viale et al., 2016). Currently, 23 of these lagoons are involved for extensive aquaculture practices, occupying roughly 5.700 hectares, primarly concentrated along the central-western coast, with the largest lagoon in Cabras (OR) spanning 2.228 hectares (Cataudella & Spagnolo, 2011). Other major lagoons are distributed in the North-western area ("Nurra"), North-east ("Gallura - Baronia"), South-east ("Ogliastra - Sarrabus - Gergei"), South ("Cagliaritano"), and South-west ("Sulcis - Iglesiente").

The annual aquaculture production in Sardinia amounts to 13.000 tonnes, comprising 17% of fish and 83% of bivalve molluscs, including mussels and oysters (University of Sassari, 2023). Extensive aquaculture serves as a significant productive asset in Sardinia, with production ranging from 50 to 150 kg/ha/year, primarily relying on the management of coastal and inland lagoons (Fenza et al., 2014). In addition to a long tradition in extensive aquaculture, Sardinia has expanded into intensive practices since 1979, particularly for seabass, gilthead seabream, and eels.

Fish species with notable commercial interest include gilthead seabream, European seabass, mullet and eel. Mollusk harvesting is a significant aspect of aquaculture in Sardinia, with a primary focus on mussels (*Mytilus galloprovincialis*), clams (*Ruditapes spp.*), and oysters (*Crassostrea gigas*). According to MIPAAF there are currently 7 floating cage systems (*Fig. 10*) at sea and 2 land-based sites (*Fig. 11*)(CREA., 2020).

While shellfish farming leads production in Sardinia, finfish aquaculture is a growing sector attracting investments from both industry and regional enterprises, as highlighted in the Piano Nazionale Strategico per l'acquacoltura italiana 2021-2027 (CREA., 2020).

Figure 10. *Off-shore mariculture in Sardinia. (Compagnie Ittiche Riunite©)*

Figure 11*. Land-based aquaculture in Sardinia. (Viale et al., 2016)*

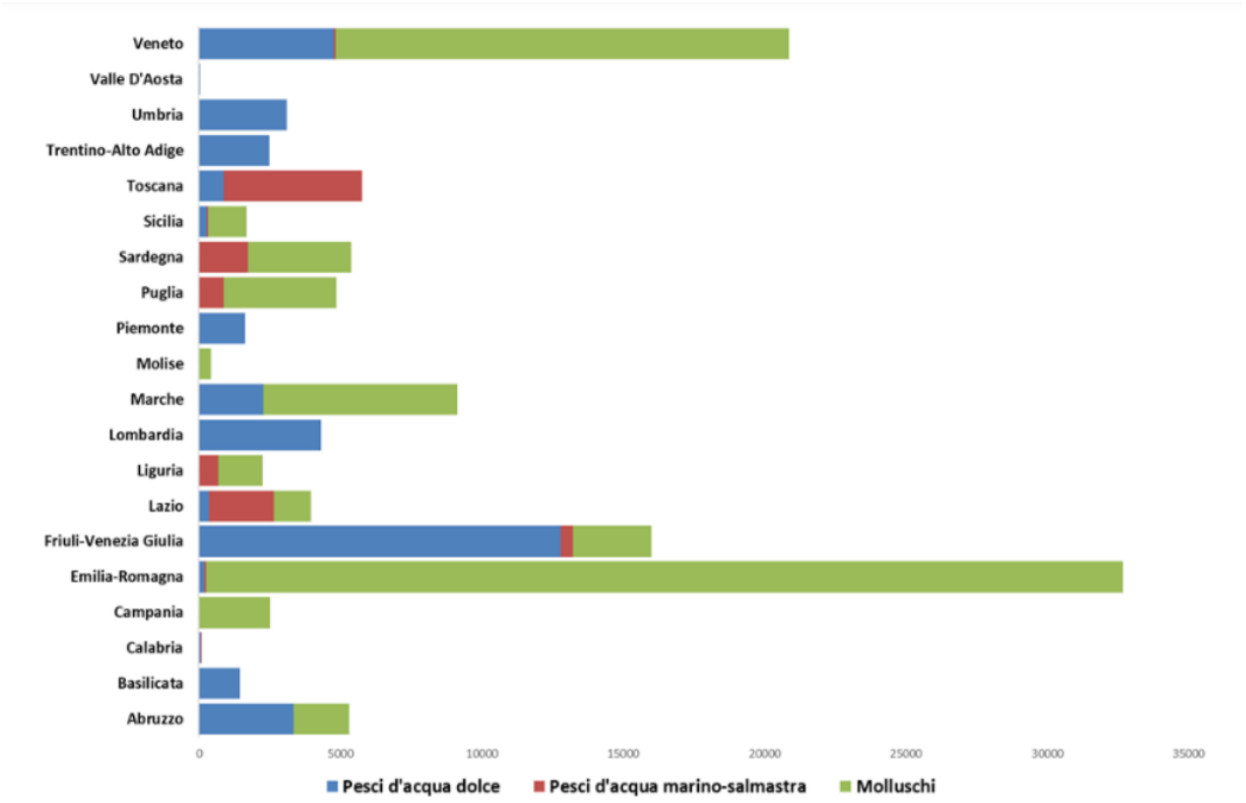

Figure 12. *Production (t) by sector in each region (2020). Piano Nazionale Strategico Acquacoltura Italia 2021-2027)*

1.4 Aquaculture production systems

Aquaculture practices, shaped by cultural traditions and technological advancements, have evolved significantly over time and are generally categorized into three main systems: extensive, semi-intensive, and intensive (*Fig. 13*).

Parameter	Extensive	Semi-Intensive	Intensive
Species Used	Monoculture or Polyculture	Monoculture	Monoculture
Stocking Rate	Moderate	Higher than extensive culture	Maximum
Engineering Design and Layout	May or may not be well laid-out	With provisions for effective water management	Very well engineered system with pumps and aerators to control water quality and quantity
	Very big ponds	Manageable-sized units (up to 2 ha each)	Small ponds, usually 0.5-1 ha each
	Ponds may or may not be fully cleaned	Fully cleaned ponds	Fully cleaned ponds
Fertilizer	Used to enhance natural productivity	Used regularly with lime	Not used
Pesticides	Not used	Used regularly for prohylaxis	Used regularly for prophylaxis
Food and Feeding Regimen	None	Regular feeding of high quality feeds	Full feeding of high-quality feeds
		Depending on stocking density used, formulated feeds may be used partially or totally	
Cropping Frequency (crops/y)	2	2.5	2.5
Quality of Product	Good quality	Good quality	Good quality
	Culture species dominant but extraneous species may occur	Confined to culture species	Confined to culture species
	Variable sizes	Uniform sizes	Uniform sizes

Figure 13. *Comparative features among the three main culture systems. (FAO., 1989)*

1.4.1 Extensive aquaculture

Extensive aquaculture systems have evolved to maximize natural resources, transitioning from basic practices like harvesting fish and aquatic organisms to more advanced techniques for managing fish stocks and juveniles (Anras et al., 2010). These systems rely on natural resources for feeding, depend on tidal flows for water exchange, and lack treatment measures. Fertilization may be used to promote the growth of natural food in the water (Balayut, 1989).

Extensive aquaculture is characterized by low stocking densities (~12.000 fingerlings/ha), and are typically conducted in large ponds, with practices varying regionally based on specific protocols and water management strategies (Oddsson, 2020). Common methods include artisanal

techniques such as fixed capturing systems, nets, or hand tools, along hydraulic barriers like weirs and locks (Anras et al., 2010)(*Fig. 14)*.

In southern Europe, the abundance of coastal lagoons, delta rivers, bays, and inland ponds has supported the development of extensive aquaculture, which continues to play a significant role in fish production despite its modest yields (Anras et al., 2010; Rocha et al., 2022).

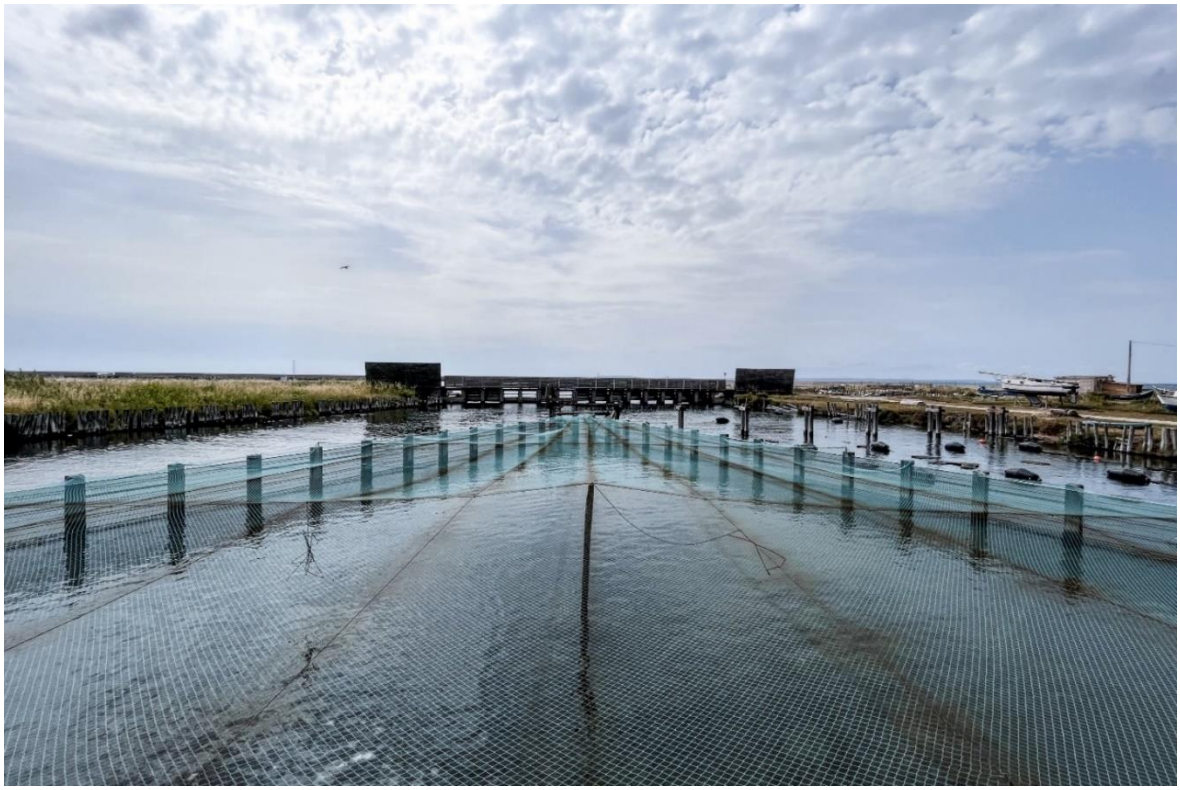

Figure 14. *Extensive aquaculture system in Sardinia (S'Ena Arrubia lagoon).*

1.4.2 Semi-intensive aquaculture

Semi-intensive aquaculture typically follows similar practices of extensive aquaculture, but it's characterized by an intermediate level of stocking (~23.000 fingerling/ha) and includes supplementary feeding and the manipulation of the environment primarily by water management using pumps and aerators (Balayut, 1989; Oddsson, 2020)(*Fig. 15*). Feeding is done at regular intervals during the day and water change is also carried out on a daily basis, with approximately 10-15% of the water in the pond replaced by the entry of new water (Balayut, 1989).

These systems are known for their low input requirements, integration with the natural environment, minimal ecological impact, and positive effects on the ecosystem (Aquaculture Advisory Council, 2021).

Figure 15. *Semi-intensive aquaculture systems. (Cecily Layzell, WorldFish©)*

1.4.3 Intensive aquaculture

Intensive aquaculture systems are characterized by high stocking densities (~36.000 fingerlings per hectare) and the continuous provision of water, feed, and treatments. To support optimal fish growth, these systems ensure appropriate water quality parameters such as dissolved oxygen (DO), carbon dioxide (CO_2), organic matter, nitrogen compounds, and solids (Oddsson, 2020).

In terms of practices, various systems have been developed for intensive aquaculture:

1) *Flow-through systems*: this system involves multiple tanks known as raceways, varying in size and depth based on the growth stages of reared fish (Bronzi et al., 2001; European Commission, 2021b). Water is supplied through a channel from an upstream river and circulates through all the tanks, to return downstream after it has passed through all

of them (*Fig. 16*). Recent advancements in aquaculture practices have enhanced productivity in this system, allowing large-scale production of various species like trout, tilapia, and Siberian sturgeon (European Commission, 2021b; Cappell & Huntington, 2023)

Figure 16. *A flow through raceway for trout production at Sacramento State Aquatic Center. (personal picture)*

2) *Recirculation Aquaculture System* (RAS): these systems are engineered to control rearing conditions, manage waste streams, and minimize water consumption. The main feature of RAS systems is water treatment technology, which continuously eliminates waste products and restores optimal water quality for the fish. Water from the fish tank undergoes filtration through a mechanical and then a biological filter before undergoing aeration, carbon dioxide stripping, and eventually return to the fish tank. It may also undergo processes such as oxygenation, UV or ozone disinfection, automatic pH regulation, and more, depending on specific needs. Commonly reared freshwater species using this method include rainbow trout, catfish, and eel, while turbot is among the most prevalent saltwater fish (European Commission, 2021b). RAS systems represent the most advanced system employed in intensive

freshwater aquaculture, achieving about 100 times greater water efficiency per kilogram of fish produced when compared to traditional flow-through systems (European Commission, 2021b; Bregnballe, 2022; Cappell & Huntington, 2023).

Figure 17. *Recirculating aquaculture systems (RAS) at the Virginia Tech Department of Food Science and Technology. (source: Wikipedia)*

3) *Cages system*: this system includes fixed or floating enclosures that confine fish or within a net for feeding, observation, and harvesting. While the use of cages for holding and transporting fish dates back almost two centuries in Asia, commercial cage culture began in Norway in the 1970s with the rise of salmon farming (Masser & Woods, 2008). Today, cage culture systems vary widely, depending on dimensions, fish stock volumes, distances from shorelines, and their feasibility under different conditions (Cardia & Lovatelli, 2015). Sea cages are classified based on their location as "in-shore," placed in naturally protected areas such as bays and coastal lakes, or "offshore," situated in more exposed sites, typically within a few nautical miles from the coast (*Fig. 18*).

High-density polyethylene (HDPE) cages are extensively used for intensive aquaculture (Chu et al., 2020) and have been adopted primarily for higher-value finfish species such as salmon (Atlantic, coho, and Chinook), as well as various marine and freshwater carnivorous species (e.g., Japanese amberjack, Ghilthead seabream, European seabass) (Cardia & Lovatelli, 2015). While intensive aquaculture has enabled higher production levels, it also carries significant environmental risks, particularly when practiced in unsuitable locations. The high-density stocking of fish in cages can lead to the spread of diseases and parasites, which can impact both farmed and wild species. Additionally, the introduction and migration of non-native species pose further ecological threats, potentially turning these intensive systems into reservoirs and amplifiers of pathogens, which present risks to both production and the surrounding environment (Chu et al., 2020).

Figure 18. *Cage Aquaculture System. Marina Torre Grande, Cabras (OR). (Photo: Gaspare Barbera, 2020)*

1.5 Main farmed fish species

In Italian and Sardinian aquaculture, the most commercially important species include gilthead seabream (*Sparus aurata*), European seabass (*Dicentrarchus labrax*), and meagre (*Argyrosomus regius*), primarily farmed in marine cages, and mullets (Mugilidae) traditionally reared in coastal lagoons and estuarine environments.

1.5.1 Fish farmed in intensive system

Gilthead seabream (Sparus aurata)

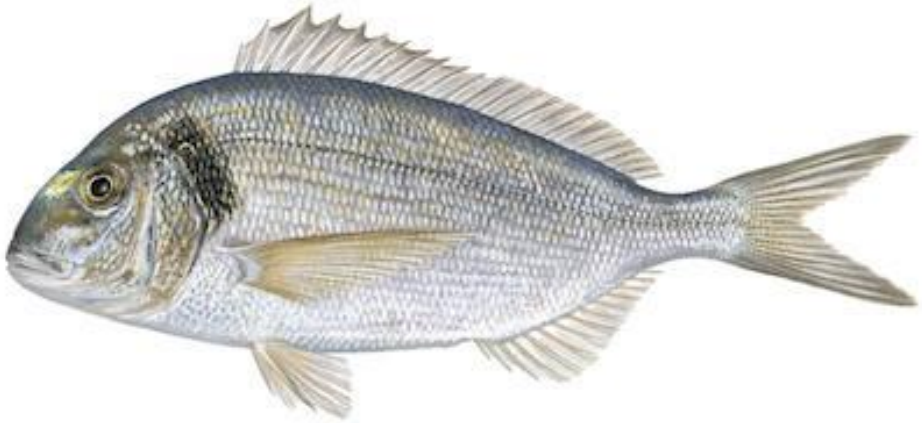

Figure 19. *Sparus aurata (Ghilthead seabream) illustration. From Scandinavian Fishing Yearbook©*

The gilthead seabream (*Sparus aurata*) is a teleost fish belonging to the genus *Sparus* and the family Sparidae. It is a key species in Mediterranean aquaculture, with an annual production of 258.754 tonnes (Mhalhel et al., 2023). Known for being eurythermal and euryhaline, this specie is distributed across the Mediterranean seas and the Eastern Atlantic Ocean, in both marine and brackish water environments, typically inhabiting rocky and seagrass (*Poseidonia oceanica*) meadows in estuaries and coastal waters (Mhalhel et al., 2023). Their diet in the wild is opportunistic, consisting mainly of bivalves and gastropods, but also echinoderms, small fish, and occasionally algae and other marine invertebrates.

This species is a protandrous hermaphrodite – initially maturing as males and later transitioning to females – with sexual maturity developing in males at 2 years of age (20-30 cm) and in females at 2-3 years (33-40 cm). Females are batch spawners and can lay 20.000-80.000 eggs every day for a period up to 4 months, with 90% to 95% fertilization rates (Mhalhel et al., 2023).

Aquaculture practices for gilthead seabream involve various stages tailored to the species' life cycle and production systems. In extensive systems seed is sourced from the wild, while intensive systems rely on hatcheries. To facilitate out-of-season spawning, broodstock conditioning is achieved through controlled temperature and photoperiod, or alternatively females can receive hormonal inoculation with GnRHa to promote spawning. After fertilization, the eggs hatch into larvae within two days. In this phase larvae rely on their yolk sacs for 3-4 days, after which they begin feeding on live organisms. In the initial feeding stage, gilthead seabream larvae are given rotifers (e.g., *Brachionus plicatilis*), and after 10-11 days they are transitioned to *Artemia salina* nauplii for 32-35 days post-hatching. Both rotifers and Artemia are routinely enriched with commercial lipid preparations to boost essential fatty acids (EPA and DHA) and vitamins vital for growth and survival. In Mediterranean hatcheries, microalgae (such as *Chlorella sp., Isochrysis galbana ecc.*) are used to enhance water quality in larval tanks, creating the “green water” environment during initial rearing phases. At around 45 days, as the larvae transition to juveniles (weighing around 5-10 mg), they are gradually weaned onto a high-protein (50-60%) formulated dry diet, and moved to larger tanks. Once the juveniles reach 5g, they are transferred to grow-out systems. Sea cages are the most common grow-out system used in the Mediterranean, providing natural water flow, controlled stocking density, and cost-effective rearing. Under optimal conditions, seabream in sea cages typically take around 16 months to reach a commercial size of 350-400 grams (Mhalhel et al., 2023; F.A.O., 2025b).

Disease management in seabream aquaculture is essential due to the impacts of bacterial, viral, and parasitic infections. Main bacterial diseases include photobacteriosis (*Photobacterium damselae* subsp. *piscicida*), vibriosis (*P. damselae* subsp. *damselae, Vibrio alginolyticus, V.*

anguillarum), and mycobacteriosis (*Mycobacterium marinum*). Viral risks, such as Nervous Necrosis Virus causing viral encephalopathy and retinopathy, particularly affect larvae and juveniles, while Iridoviridae viruses cause lymphocystis, marked by tumor-like growths. Parasitic infections include *Sparicotyle chrysophrii, Sphaerosphora* spp., and *Amyloodinium ocellatum*, each requiring proactive management to ensure fish health and marketability (Mhalhel et al., 2023; F.A.O., 2025b).

European seabass (Dicentrarchus labrax)

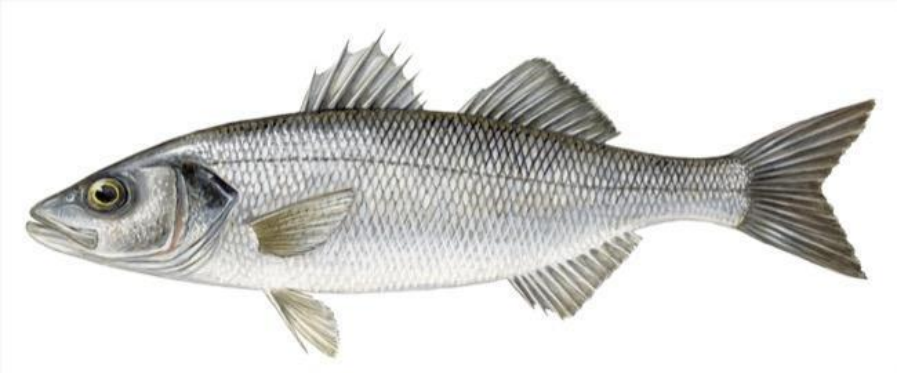

***Figure 20**. Dicentrarchus labrax (European seabass) illustration. From Scandinavian Fishing Yearbook©*

The European seabass (*Dicentrarchus labrax*), classified within the genus *Dicentrarchus* and the family Moronidae, is one of the most commercially important farmed species in the Mediterranean. In 2021, its global production reached 305.000 tonnes, with aquaculture accounting for 98% of the total output (European Commission, 2024). This euryhaline teleost primarily occupies coastal lagoons and estuaries, although it can also be found in rivers. Its ability to thrive in a wide range of salinities (0–40 ppt) and temperatures (2–32°C) enables it to inhabit diverse environments, across the Eastern Atlantic (from Norway to Senegal), as well as the Mediterranean and Black Seas. The European seabass is gonochoristic (distinct sexes) and has polygenic sex determination influenced by both genetic and environmental factors, particularly

temperature (Vázquez & Muñoz-Cueto J.A, 2014). Maturation occurs around two to three years for males and three to four years for females, with breeding seasons varying from December to March in the Mediterranean and March to June in the Atlantic. Female European seabass spawn approximately 200.000 to 500.000 eggs, typically in lower salinity waters, which undergo external fertilization and hatch within three to five days. Post-haching, larvae (4 mm) transition into the post-larval stage (>22 mm) within two to three months, migrating to inshore areas and lagoons for shelter and development/feeding. As they mature, juveniles move to the open sea, shifting their diet to include fish, crustaceans, and other invertebrates until they reach adulthood and sexual maturity (F.A.O., 2009b)

In the Mediterranean, aquaculture practices for European seabass have evolved from traditional extensive methods to modern intensive systems. The production process typically includes a pre-growing phase lasting three to eight months, where fish are raised from 1 to 20 g, followed by an on-growing phase to reach weights of 250-450 g over 12 to 20 months. Hatcheries, usually located inland with temperature-controlled systems, achieve 80-90% hatching success rates by incubating eggs in larval rearing tanks at 14-15°C. This phase is critical since water temperature influences the sex determination of the specimens (F.A.O., 2009b; Kousoulaki et al., 2015).

After hatching, larvae rely on their yolk sac for nutrition and grow to about 5 mm within 3-6 days. Initial feeding involves rotifers (*Brachionus plicatilis*) and brine shrimp *(Artemia salina and nauplii*), that may be enriched with the green water technique (*Nannochloropsis* sp.). As they enter the pre-growing phase (40–50 days), larvae continue feeding on live prey, gradually increasing Artemia while transitioning to microdiets. Once juveniles reach 2-5 g, they are transferred to on-growing facilities, typically off-shore marine cages, where they achieve commercial sizes (300-500 g) within 12-20 months (F.A.O., 2009b; Kousoulaki et al., 2015)

Despite the rapid expansion of intensive European seabass farming, susceptibility to infectious diseases presents a significant challenge. Bacterial infections are particularly concerning, with vibriosis (*V. alginolyticus, V. anguillarum,* and *V. harveyi*), photobacteriosis (*Photobacterium*

damselae subsp. *piscicida*), aeromoniasis (*Aeromonas hydrophila* and *Aeromonas veronii*) and mycobacteriosis (*M. marinum* and *M. chelonae*) being the most threatening. Viral diseases also pose significant challenges, with Viral Encephalopathy and Retinopathy being particularly concerning, leading to high mortality rates in juveniles. Parasitic infections, although less concerning, include ciliates (*Cryptocaryon* and *Philasterides dicentrarchi*) myxozoans (*Kudoa dicentrarchi*) and copepods (*Caligus spp.*). These parasites can cause a range of health issues, including secondary infections and overall deterioration in the health of seabass populations (F.A.O., 2009b; Vázquez & Muñoz-Cueto J.A, 2014; Fernández Sánchez et al., 2022).

Meagre (Argyrosomus regius)

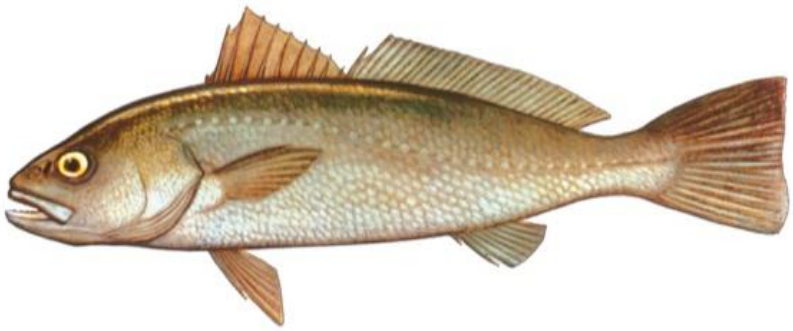

Figure 21. *Argyrosomus regius (Meagre) illustration. From Scandinavian Fishing Yearbook©*

The meagre (*Argyrosomus regius*) is a teleost fish from the genus *Argyrosomus* and the family Sciaenidae. While the term primarily refers to *Argyrosomus regius*, it also includes species like the Southern meagre (*Argyrosomus hololepidotus*) and the Japanese meagre (*Argyrosomus japonicus*). In 2019, its production reached 37.536 tonnes, primarily driven by Egypt (26.355 tonnes) and the EU-27 countries (10.262 tonnes). Spain, Greece, and France are the top EU producers, while Italy remains the largest consumer, relying on imports to meet demand (F.A.O., 2009a; Gil et al., 2013).

Meagre is a eurythermal (2-38°C) and euryhaline (5-39 ppt) fish, adaptable to estuaries, lagoons, and coastal waters. It typically inhabits rocky bottoms and Posidonia fields, with a distribution spanning the eastern Atlantic coast (northward to southern Norway and southward to the Congo), including the entire Mediterranean Sea (F.A.O., 2009a; González-Quirós et al., 2011a; Gil et al., 2013). Meagre are carnivorous, feeding mainly on polychaetes, crustaceans, echinoderms, mollusks, and small fish. They are gonochoristic with seasonal reproduction and multiple spawning events (Zupa et al., 2023). Sexual maturity is reached between 3 and 6 years, with males around 61 cm and females 70-110 cm From March to August adults migrate to estuaries to reproduce, and juveniles move to coastal waters (20-40 m deep) by winter for feeding, returning to estuaries in May (F.A.O., 2009a). Environmental conditions such as temperatures (17-23°C), salinity (10-37 ppt), and photoperiods influence their reproduction (González-Quirós et al., 2011b; Abou Shabana et al., 2012; Gil et al., 2013).

Most production occurs in intensive systems, primarily in off-shore marine cages. Meagre aquaculture began in France and Italy in the late 1990s and has since expanded across the Mediterranean (Monfort, 2010). Rearing protocols for meagre have been successfully adapted from seabream and seabass practices, dividing production into pre-growing and on-growing phases (Gil et al., 2014). In the pre-growing phase, larvae are typically cultured at 22-24°C, starting exogenous feeding three days post-hatching. The initial two weeks usually involve enriched rotifers (*Brachionus plicatilis*) along live or dry/frozen phytoplankton (*Nannochloropsis* sp., *Isochrysis galbana*). In post-hatching, *Artemia* sp. are also included; then, live prey is gradually replaced with dry microparticulate diets (0.3–0.75 μm) . In on-growing conditions, diets are similar to those for other Mediterranean marine species, with extruded feeds containing 45-48% protein and 20-24% lipid (F.A.O., 2009a; Monfort, 2010; Gil et al., 2014). Meagre grows rapidly, with fry reaching over 700 g after 12 months and 2-2.5 kg after 24 months (Monfort, 2010). Meagre's resilience, fast growth and low feed conversion ratio, make it one of the most promising species for Mediterranean aquaculture. However, several health challenges hinder its

expansion. Bacterial diseases, particularly from *Vibrio* spp. (*V. anguillarum*), *Photobacterium damselae* subsp. *piscicida*, *Mycobacterium* spp., and *Nocardia* spp., are significant threats. Parasites, including *Sciaenocotyle*, *Microcotyle pancerii*, *Benedenia sciaenae*, and *Calceostoma* spp., also affect cage-reared meagre. While viral diseases are not a common concern, meagre can be asymptomatic carriers of nodavirus, posing risks to other species like European seabass, which are more vulnerable to the virus (Lopez-Jimena et al., 2010; Soares et al., 2018).

Another notable disease is Systemic Granulomatosis (SG), a condition of unknown etiology that leads to granuloma formation in internal organs. Although SG has been hypothesized to be linked to vitamin deficiencies, its diagnosis remains challenging, particularly in distinguishing it from mycobacterial infections. Further details on SG are provided in Chapter 4.

1.5.2 Fish farmed in extensive system

Mullet (Mugilidae)

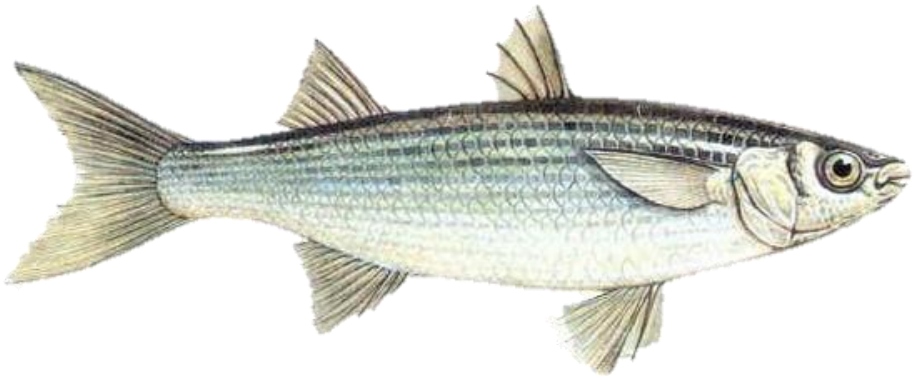

Figure 22. *Grey mullet (Mugilidae) illustration. From Daily Scandinavian Fishing Yearbook©*

The Mugilidae family, commonly known as grey mullets, comprises 26 genera and 77 species that play crucial roles in marine and coastal ecosystems. In 2022, global mullet production reached 697 thousand tonnes, with aquaculture accounting for 54% of the total (375 thousand tonnes) (F.A.O., 2024).

These fish are widely distributed across tropical and temperate regions, including Africa, Asia, Australia, Europe, New Zealand, and the Americas, thriving in offshore and coastal waters,

lagoons, and estuaries (Berra, 1981). Mullets are euryhaline, tolerating salinities from 0 to 90 ppt, and eurythermal, adapting to a wide range of temperatures (Boglione et al., 2006; Fenza et al., 2014). Classified as detritus feeders, mullets consume organic matter from sediment, benthic invertebrates, macroalgae, plankton, and other suspended organic materials (Albertini-Berhaut, 1974; Whitfield & Durand, 2023). They are gonochoristic, showing no sexual dimorphism, and are oviparous, with external fertilization. Their life cycle involves an annual pattern of growth, maturation, and migration, driven by environmental changes, particularly temperature fluctuations: during cooler periods, they migrate to the open sea to spawn, then return to estuaries and lagoons for feeding and shelter. Four genera (Chelon, Liza, Mugil and Oedalechilus) and six species of mullets (*C. labrosus*, *C. auratus*, *C. ramada*, *C. saliens*, *M. cephalus*, *O. labeo*) are endemic in the Mediterranean Sea (De Silva, 1980; Whitfield & Durand, 2023)

Among grey mullet species, *Mugil cephalus* and *Chelon labrosus* are highly valued for their flesh and roe, with the roe, known as "bottarga di muggine," being a prized Mediterranean delicacy (Crosetti, 2015). Mullet aquaculture is practiced in both inland (freshwater and brackish) and marine environments, with Africa leading global production, contributing 60% of the world's output (F.A.O., 2024). In the Mediterranean, mullet farming predominantly follows extensive methods, relying on natural resources and seasonal migrations (F.A.O., 2024).

Despite extensive research, a key challenge to expand mullet aquaculture remains the unreliable large-scale production of fry, forcing many producers to rely on wild-caught individuals (F.A.O., 2023). Fish health also presents a critical challenge in mullet farming, as mullets are susceptible to a range of pathogens and stress-related conditions. Common bacterial diseases include bacterial threats such as *Photobacterium damselae* subsp. *piscicida*, *Streptococcus aquamarinus*, *Aeromonas hydrophila*, and *Vibrio anguillarum* (inserire cit). Viral infections, such as lymphocystis and viral nervous necrosis, along with parasitic infections from protozoa (e.g., *Myxobolus episquamalis*), trematodes (e.g., *Microcotyle mugilis*), and copepods (e.g., *Caligus*

bonito), are also prevalent, especially in polluted or stressed environments (Paperna & Overstreet, 1981; Polinas et al., 2021; Elbahnaswy et al., 2023).

References

Abou Shabana, Nevine M, Soliman H Abd El Rahman, Mohamed A al Absawy, and Samira S Assem. 2012. "Reproductive Biology of *Argyrosomus regius* (Asso, 1801) Inhabiting the South Eastern Mediterranean Sea, Egypt." Egyptian Journal of Aquatic Research 38 (2): 147–56. https://doi.org/https://doi.org/10.1016/j.ejar.2012.12.002.

Albertini-Berhaut, Jocelyne. 1974. "Biologie Des Stades Juveniles de Teleosteens Mugilidae Mugil Auratus Risso 1810, Mugil Capito Cuvier 1829 et Mugil Saliens Risso 1810." Aquaculture 4 (January): 13–27. https://doi.org/10.1016/0044-8486(74)90015-5.

Anras, L, C C Boglione, S Cataudella, M T Dinis, S Livi, P Makridis, G Marino, and M. Ramalho, A., Yúfera. 2010. "The Current Status of Extensive and Semi-Intensive Aquaculture Practices in Southern Europe." Aquaculture Europe 35: 12–16. https://api.core.ac.uk/oai/oai:digital.csic.es:10261/50633.

Anras, L, C Boglione, S Cataudella, M T Dinis, P Makridis, G Marino, A Ramalho Ribeiro, and M Yúfera. 2010. "The Current Status of Extensive and Semi-Intensive Aquaculture Practices in Southern Europe."

Aquaculture Advisory Council, (A.A.C). 2021. "The Provision of Ecosystem Services by European Aquaculture." https://aac-europe.org/wp-content/uploads/2021/06/AAC_Recommendation_-_Ecosystem_Services_2021_08_revised2.pdf.

Balayut, E. 1989. "Aquaculture Systems and Practices: A Selected Review. United Nations Development Programme & Food and Agriculture Organization." https://openknowledge.fao.org/server/api/core/bitstreams/946969fd-d4fb-45c5-a1b8-1dae16148719/content/t8598e.htm.

Berra, T M. 1981. An Atlas of Distribution of the Freshwater Fish Families of the World. London: University of Nebraska Press.

Boglione, C, C Costa, M Giganti, M Cecchetti, P di Dato, M Scardi, and S Cataudella. 2006. "Biological Monitoring of Wild Thicklip Grey Mullet (Chelon Labrosus), Golden Grey Mullet (Liza Aurata), Thinlip Mullet (Liza Ramada) and Flathead Mullet (Mugil Cephalus) (Pisces: Mugilidae) from Different Adriatic Sites: Meristic Counts and Skeletal Anoma." Ecological Indicators 6 (4): 712–32. https://doi.org/10.1016/j.ecolind.2005.08.032.

Borriello, A., M. Calvo SantGhiani, J. Guillén, A. Peralta Baptista, G. Petrucco, M. Pleguezuelo Alonso, G. Pattumelli, and S Quatrini. 2023. The EU Blue Economy Report 2023. Edited by Publications Office of the European Union. European Commission: Directorate-General for Maritime Affairs and Fisheries, Joint Research Centre. https://doi.org/https://data.europa.eu/doi/10.2771/7151.

Bregnballe, J. 2022. "A Guide to Recirculation Aquaculture – An Introduction to the New Environmentally."

Bronzi, P, M Rampacci, and R Ugolini. 2001. "L' Acquacoltura Intensiva." In Acquacoltura.

Cappell, R, and T Huntington. 2023. Research for PECH Committee – Workshop on the European Green Deal – Challenges and Opportunities for EU Fisheries and Aquaculture – Part III: Food Security Aspects. Brussels: European Parliament, Policy Department for Structural and Cohesion Policies.

Cardia, F, and A Lovatelli. 2007. “A Review of Cage Aquaculture: Mediterranean Sea.” Edited by M Halwart, D Soto, and J R Arthur. Cage Aquaculture – Regional Reviews and Global Overview, no. 498: 156–87.

Cardia, F, and A Lovatelli. 2015. “Aquaculture Operations in Floating HDPE Cages: A Field Handbook.” FAO Fisheries and Aquaculture Technical Paper, no. 593: 152.

Carvalho, N, and J Guillen. 2021. Aquaculture in the Mediterranean. Barcelona, Spain: IEMed. https://www.iemed.org/publication/aquaculture-in-the-mediterranean/.

Cataudella, S.; Massa, F.; Crosetti, D. 2005. “Interactions between Aquaculture and Capture Fisheries: A Methodological Perspective.” Edited by S Cataudella, F Massa, and D Crosetti. Studies and Reviews. General Fisheries Commission for the Mediterranean, no. 78: 229. https://www.fao.org/4/a0141e/A0141E00.htm#TOC.

Cataudella, S, and M Spagnolo. 2011. “Lo Stato Della Pesca e Dell’acquacoltura Nei Mari Italiani.” In Ministero Delle Politiche Agricole Alimentari e Forestali. Rome, Italy.

Chu, Y I, C M Wang, J C Park, and P F Lader. 2020. “Review of Cage and Containment Tank Designs for Offshore Fish Farming.” Aquaculture 519: 734928. https://doi.org/https://doi.org/10.1016/j.aquaculture.2020.734928.

Commission, European. n.d. “Benchmarking Project Final Report.” Community Research and Development Information Service (CORDIS. https://cordis.europa.eu/project/id/44483/reporting.

Commission, European, Joint Research Centre, Technical Scientific, Economic Committee Fisheries, J Guillen, J Virtanen, and R Prellezo. n.d. “The 2021 Annual Economic Report on the EU Fishing Fleet.” https://doi.org/https://data.europa.eu/doi/10.2760/60996.

Cozzolino, M, C Iandoli, C Raffaelli, and C M Travisi. 2008a. “Sviluppo Del Bilancio Ambientale Nel Settore Dell’acquacoltura Per Tecnologie Intensive.” In ICRAM (Istituto Centrale Per La Ricerca Scientifica E Tecnologica Applicata Al Mare), IREPA (Istituto Ricerche Economiche Per La Pesca E L’acquacoltura), Fondazione Eni Enrico Mattei.

CREA., 2020 Centro di Zootecnia e Acquacoltura. 2020. “Il Piano Strategico per l’Acquacoltura italiana 2021-2027.”

Crosetti, D. 2015. “Ecological Role of Mugilidae in the Coastal Zone.” In Biology, Ecology and Culture of Grey Mullets (Mugilidae), 334–58. CRC Press. https://doi.org/10.1201/b19927-17.

Elbahnaswy, Samia, Gehad E. Elshopakey, Medhat S. Shakweer, Elsayed A. A. Eldessouki, Abdelwahab A. Abdelwarith, Elsayed M. Younis, Simon J. Davies, and Mai A. M. El-Son. 2023. “Bacterial Co-Infection as a Potential Threat to Farmed Flathead Grey Mullet (Mugil Cephalus): Phenotypic and Molecular Diagnosis, Histopathology, Immunity Response, and In Vitro Antibacterial Evaluation.” Fishes 8 (7): 357. https://doi.org/10.3390/fishes8070357.

EU Commission. n.d. “EU Aquaculture Infographic - Socioeconomic Development.” European Commission. https://aquaculture.ec.europa.eu/system/files/2023-08/EU Aquaculture Sector_Socioeconomic development_Infographic.pdf.

EUMOFA. 2021. “European Market Observatory for Fisheries and Aquaculture Products.” European Commission.

https://eumofa.eu/documents/20124/35725/Species+analysis+EN+2020.pdf/740e165b-0590-233d-8a47-bff08612c769?t=1638437538869.

Eurofish. 2023. “Italy. Eurofish International Organisation.” https://eurofish.dk/member-countries/italy/.

European Commission. 2021. Freshwater Aquaculture in the EU. Edited by Directorate-General for Maritime Affairs and Fisheries. Publications Office. https://data.europa.eu/doi/10.2771/594002.

European Commission. 2022. Meagre in the EU. Edited by Directorate-General for Maritime Affairs and Fisheries. Publications Office of the European Union. https://doi.org/doi/10.2771/28936.

European Commission. 2024. Fresh European Seabass in the EU – Price Structure in the Supply Chain – Focus on Greece, Spain and Italy – Case Study. Edited by Directorate-General for Maritime Affairs and Fisheries. Publications Office of the European Union. https://doi.org/doi/10.2771/88095.

European Commission, Joint Research Centre, Technical Scientific, Economic Committee for Fisheries, J Guillen, J Virtanen, R Prellezo, and N Carvalho. 2021. The 2021 Annual Economic Report on the EU Fishing Fleet (STECF 21-08). Edited by J Guillen, J Virtanen, R Prellezo, and N Carvalho. Publications Office. https://doi.org/doi/10.2760/60996.

European Commission, and Directorate-General for Maritime Affairs and Fisheries. 2021. A New Strategic Vision for Sustainable Aquaculture Production and Consumption in the European Union – Blue Farming in the European Green Deal. Publications Office of the European Union. https://doi.org/doi/10.2771/961425.

F.A.O. 2024. The EU Fish Market – 2024 Edition. Publications Office of the European Union. https://doi.org/doi/10.2771/9420236.

EUROSTAT. 2024. “Aquaculture Statistics.” Eurostat. https://ec.europa.eu/eurostat/statistics-explained/index.php?title=Aquaculture_statistics

F.A.O. 2009a. “*Argyrosomus regius*. In Cultured aquatic species fact sheets.” Edited by P Stipa, M Angelini, Valerio Crespi, and Michael New.

F.A.O. 2009b. “*Dicentrarchus labrax*. In Cultured aquatic species fact sheets.” Edited by M Bagni, Valerio Crespi, and Michael New.

F.A.O. 2010. “Food and Agriculture Organization of the United Nations (2010) FAO Term Portal, Entry: 1222, Collection: Aquaculture FAO.”

F.A.O. 2022. “Blue Transformation - Roadmap 2022–2030: A Vision for FAO’s Work on Aquatic Food Systems. Rome.” https://doi.org/10.4060/cc0459en.

F.A.O. 2022. The State of World Fisheries and Aquaculture 2022. FAO. https://doi.org/10.4060/cc0461en.

F.A.O. 2023. “The State of Mediterranean and Black Sea Fisheries 2023.” In General Fisheries Commission for the Mediterranean, Special. Rome. https://doi.org/10.4060/cc8888en.

F.A.O. 2024. The State of World Fisheries and Aquaculture 2024. Rome: FAO. https://doi.org/10.4060/cd0683en.

F.A.O. 2025a. “Greece. Text by Theodorou, J.A.” In: Fisheries and Aquaculture.

F.A.O. 2025b. “*Sparus aurata*. Cultured Aquatic Species Information Programme.” https://www.fao.org/fishery/en/culturedspecies/sparus_aurata?lang=en.

F.A.O. 2025. “Fishery and Aquaculture Country Profiles.” Fisheries and Aquaculture. Accessed May 3, 2025. https://www.fao.org/fishery/en/facp/ita?lang=en.

Fenza, A, G Olla, F Salati, and I Viale. 2014. “I Principali Ambienti Umidi Della Sardegna.” In Stagni e Lagune Produttive Della Sardegna. Tradizioni, Sapori e Ambiente, edited by A.R.L. Sardegna.

Fernández Sánchez, José L., Alain le Breton, Edgar Brun, Niccolò Vendramin, Georgios Spiliopoulos, Dolors Furones, and Bernardo Basurco. 2022. “Assessing the economic impact of diseases in Mediterranean grow-out farms culturing European sea bass.” Aquaculture 547 (January): 737530. https://doi.org/10.1016/j.aquaculture.2021.737530.

Fernández Sánchez, José L, Ignacio Llorente, and José M Fernández-Polanco. 2023. “Profitability Differences in Aquaculture Firms of the Nordic and Mediterranean-EU Regions.” Aquaculture Economics & Management 27 (3): 335–51. https://doi.org/10.1080/13657305.2022.2163721.

G., Marino, Petochi T., and Cardia F. 2020. Assegnazione Di Zone Marine per l’Acquacoltura (AZA). Guida Tecnica. Guida Tecnica". https://www.isprambiente.gov.it/it/pubblicazioni/documenti-tecnici/assegnazione-di-zone-marine-perlacquacoltura-aza-guida-tecnica.

Gil, Maria del Mar, Amalia Grau, Gualtiero Basilone, Rosalia Ferreri, and Miquel Palmer. 2013. “Reproductive Strategy and Fecundity of Meagre *Argyrosomus regius* Asso, 1801 (Pisces: Sciaenidae): Implications for Restocking Programs.” Scientia Marina 77 (February): 105–18. https://doi.org/10.3989/scimar.03688.28A.

Gil, María del Mar, Miquel Palmer, Amalia Grau, and Sílvia Pérez-Mayol. 2014. “First Evidence on the Growth of Hatchery-Reared Juvenile Meagre *Argyrosomus regius* Released in the Balearic Islands Coastal Region.” Aquaculture 434 (October): 78–87. https://doi.org/10.1016/j.aquaculture.2014.07.032.

González-Quirós, Rafael, Juan del Árbol, María del Mar García-Pacheco, Alfonso J Silva-García, José María Naranjo, and Beatriz Morales-Nin. 2011a. “Life-History of the Meagre *Argyrosomus regius* in the Gulf of Cádiz (SW Iberian Peninsula).” Fisheries Research 109 (1): 140–49. https://doi.org/https://doi.org/10.1016/j.fishres.2011.01.031.

Guillen, J, J Virtanen, and R Nielsen. 2023. “Economic Report on the EU Aquaculture (STECF-22-17).” European Commission: Joint Research Centre, Scientific, Technical and Economic Committee for Fisheries. https://doi.org/10.2760/51391.

Hough, C. 2022. Regional Review on Status and Trends in Aquaculture Development in Europe – 2020. FAO. https://doi.org/10.4060/cb7809en.

Iandoli, C, and A Trincanato. 2007. “Quadro Generale Dell’Acquacoltura Italiana.” ICRAM and API: Ahmedabad, India 56. https://www.isprambiente.gov.it/files/quadro-generale-acquacoltura.pdf.

Kousoulaki, K., B.-S. Saether, S. Albrektsen, and C. Noble. 2015. “Review on European Sea Bass (*Dicentrarchus labrax*, Linnaeus, 1758) Nutrition and Feed Management: A Practical Guide for Optimizing Feed Formulation and Farming Protocols.” Aquaculture Nutrition 21 (2): 129–51. https://doi.org/10.1111/anu.12233.

Lopez-Jimena, B., N. Cherif, E. Garcia-Rosado, C. Infante, I. Cano, D. Castro, S. Hammami, J.J. Borrego, and M.C. Alonso. 2010. “A Combined RT-PCR and Dot-Blot Hybridization Method Reveals the Coexistence of SJNNV and RGNNV Betanodavirus Genotypes in Wild Meagre (*Argyrosomus regius*).” Journal of Applied Microbiology 109 (4): 1361–69. https://doi.org/10.1111/j.1365-2672.2010.04759.x.

Marino, G, E Ingle, and S Cataudella. 2005. “A Short Overview of the Status of Aquaculture in Italy.” In Interactions between Aquaculture and Capture Fisheries: A Methodological Perspective, edited by S Cataudella, F Massa, and D Crosetti, 229–52. https://www.fao.org/3/a0141e/A0141E03.htm.

Masser, M P, and P Woods. 2008. Cage Culture Problems. Southern Regional Aquaculture Center.

Mhalhel, K, M Levanti, F Abbate, R Laurà, M C Guerrera, M Aragona, C Porcino, M Briglia, A Germanà, and G Montalbano. 2023. “Review on Gilthead Seabream (*Sparus aurata*).” Aquaculture: Life Cycle, Growth, Aquaculture Practices and Challenges. Journal of Marine Science and Engineering 11 (10). https://doi.org/10.3390/jmse11102008.

Monfort, M C. 2010. “Present Market Situation and Prospects of Meagre (*Argyrosomus regius*), as an Emerging Species in Mediterranean Aquaculture.” Studies and Reviews. General Fisheries Commission for the Mediterranean, no. 89: 28.

Muniesa, Ana, Bernardo Basurco, Cristóbal Aguilera, Dolors Furones, Carmen Reverté, Anna Sanjuan-Vilaplana, Mona Dverdal Jansen, Edgar Brun, and Saraya Tavornpanich. 2020. “Mapping the Knowledge of the Main Diseases Affecting Sea Bass and Sea Bream in Mediterranean.” Transboundary and Emerging Diseases 67 (3): 1089–1100. https://doi.org/10.1111/tbed.13482.

National Marine Fisheries Service. 2024. “Fisheries of the United States.” Department of Commerce, NOAA Current Fishery Statistics No. https://www.fisheries.noaa.gov/national/sustainable-fisheries/fisheries-united-states.

N.F.I.S.S. 2024. “FishStatJ-Software for Fishery and Aquaculture Statistical Time Series.” https://www.fao.org/fishery/en/topic/166235?lang=en.

Oddsson, Guðmundur Valur. 2020. “A Definition of Aquaculture Intensity Based on Production Functions—The Aquaculture Production Intensity Scale (APIS).” Water 12 (3): 765. https://doi.org/10.3390/w12030765.

Paperna, I, and Robin M Overstreet. 1981. “Parasites and Diseases of Mullets (Mugilidae.” Manter Laboratory of Parasitology 579. https://doi.org/https://digitalcommons.unl.edu/parasitologyfacpubs/579.

Polinas, Marta, Francesc Padrós, Paolo Merella, Marino Prearo, Marina Antonella Sanna, Fabio Marino, Giovanni Pietro Burrai, and Elisabetta Antuofermo. 2021. “Stages of Granulomatous Response Against Histozoic Metazoan Parasites in Mullets (Osteichthyes: Mugilidae).” Animals 11 (6): 1501. https://doi.org/10.3390/ani11061501.

Rajme-Manzur, David, Teresa Gollas-Galván, Francisco Vargas-Albores, Marcel Martínez-Porchas, Miguel Ángel Hernández-Oñate, and Jorge Hernández-López. 2021. "Granulomatous Bacterial Diseases in Fish: An Overview of the Host's Immune Response." Comparative Biochemistry and Physiology Part A: Molecular & Integrative Physiology 261 (August): 111058. https://doi.org/10.1016/j.cbpa.2021.111058.

Raux, P, and D Bailly. n.d. "Sustainable Extensive and Semi-Intensive Coastal Aquaculture in Southern Europe." In Proceedings of the Fourteenth Biennial Conference of the International Institute of Fisheries Economics & Trade, edited by A L Shriver, 1–4. Nha Trang, Vietnam: International Institute of Fisheries Economics & Trade. https://cordis.europa.eu/project/id/44483/reporting.

Rocha, Carolina P, Henrique N Cabral, João C Marques, and Ana M M Gonçalves. 2022. "A Global Overview of Aquaculture Food Production with a Focus on the Activity's Development in Transitional Systems—The Case Study of a South European Country (Portugal)." Journal of Marine Science and Engineering 10 (3): 417. https://doi.org/10.3390/jmse10030417.

Saidi, Houda, Rocío Morales-Medina, Azeddine Abrehouch, Soumia Fahd, Emilia M Guadix Escobar, and Raúl Pérez-Gálvez. 2018. "Effect of the supplementation of live preys enriched in cod liver oil on the survival rate, growth and fatty acid profile of meagre (*Argyrosomus regius*) larvae." Aquaculture Research 49 (3): 1133–41. https://doi.org/10.1111/are.13563.

Silva, S.S. de. 1980. "Biology of Juvenile Grey Mullet: A Short Review." Aquaculture 19 (1): 21–36. https://doi.org/10.1016/0044-8486(80)90004-6.

Soares, Florbela, Ana Roque, and Paulo J Gavaia. 2018. "Review of the Principal Diseases Affecting Cultured Meagre (*Argyrosomus regius*)." Aquaculture Research 49 (4): 1373–82. https://doi.org/10.1111/are.13613.

University of Sassari. 2023. "Overview of Sardinian Farm World and Productions (Appendix 12)." https://veterinaria.uniss.it/sites/st04/files/appendix_12._overview_productions.pdf.

Vázquez, F J S, and Muñoz-Cueto J.A. 2014. Biology of European Sea Bass. Edited by Boca Raton. 1st ed. CRC Press. https://doi.org/10.1201/b16043.

Viale, I, G Olla, and F Salati. 2016. Acquacultura in Sardegna, Tradizioni, Innovazione, Sapori e Ambiente. Agenzia Laore Sardegna: Cagliari, Italy.

Whitfield, A K, and S J M Blaber. 1978. "Resource Segregation among Iliophagous Fish in Lake St Lucia, Zululand." Environmental Biology of Fishes 3: 293–96.

Whitfield, Alan K, and Jean-Dominique Durand. 2023. "An Overview of Grey Mullet (Mugilidae) Global Occurrence and Species-rich Ecoregions, with Indications of Possible Past Dispersal Routes within the Family." Journal of Fish Biology 103 (2): 202–19. https://doi.org/10.1111/jfb.15450.

Zupa, Rosa, Edmond Hala, Gianluca Ventriglia, Chrysovalentinos Pousis, Letizia Passantino, Angelo Quaranta, Aldo Corriero, and Caterina de Virgilio. 2023. "Reproductive Maturation of Meagre *Argyrosomus regius* (Asso, 1801) Reared in Floating Cages." Animals 13 (2). https://doi.org/10.3390/ani13020223.

Chapter I - Part 2

1.6 The disease triangle model

The intensification of aquaculture has led to a significant increase in the global production of fish and seafood, providing a crucial source of protein and economic stability (F.A.O., 2024). However, this rapid expansion is threatened by the emergence and re-emergence of infectious diseases (Murray & Peeler, 2005). As theorized in the disease triangle model, the onset and progression of disease occur through an imbalance between the host defenses, pathogen virulence, and environmental conditions (Scholthof, 2007)(*Fig. 23*). In aquatic animal health, this interplay is particularly relevant, as fish are highly susceptible to environmental stressors such as poor water quality, temperature fluctuations, and high stocking densities, predisposing them to disease outbreak.

Among the infectious diseases affecting fish, bacterial infections represent a major concern due to their persistence in aquatic environments, especially in warm water regions, where pathogens can thrive regardless of host presence (Scholthof, 2007). These diseases can cause high mortality rates, reduced growth performance, and increased costs for treatment and management.

To face these issues, industry commonly relies on the use of antimicrobials, raising production costs and, more critically, contributing to the emergence of antibiotic-resistant bacterial strains in aquatic ecosystems, posing a threat to both aquaculture sustainability, human safety and environmental health (Cabello et al., 2013; Preena et al., 2020; Ziarati et al., 2022). In some cases, infections pose a significant challenge as the pathogens become inaccessible or difficult to target, reducing the effectiveness of chemotherapeutic agents, particularly in chronic conditions such as granulomatous diseases (Martínez-Lara et al., 2021; Rajme-Manzur et al., 2021a).

Beyond antibiotic resistance, these infections have broader implications, as several bacterial pathogens responsible for granulomatous disease in fish have been recognized for their zoonotic potential. Although zoonotic infections from aquatic environments are often perceived as rare,

there is growing concern that they may be underdiagnosed due to a lack of awareness, insufficient surveillance, and the challenges associated with identifying aquatic bacterial pathogens. In cases where infections do occur, they can lead to severe health outcomes, particularly in immunocompromised individuals (Ziarati et al., 2022).

Given the increasing global reliance on aquaculture, the rise of bacterial granulomatous diseases in fish underscores the need for enhanced disease surveillance, improved biosecurity measures, and the implementation of effective management strategies. Furthermore, the potential zoonotic risk associated with some of these bacterial infections highlights the importance of a One Health perspective, recognizing the interconnection between animal, human, and environmental health (Shaheen, 2022).

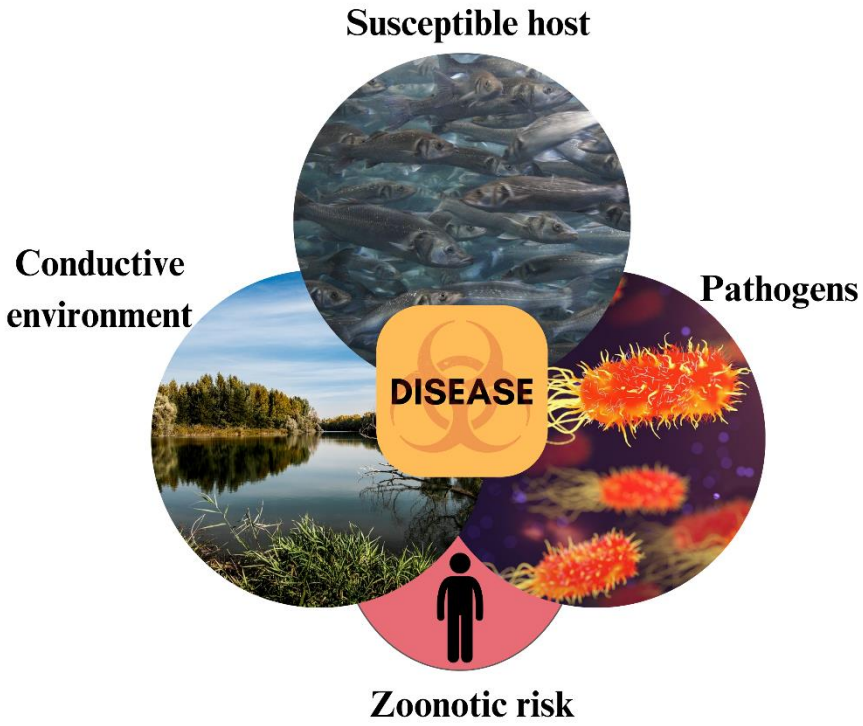

Figure 23. *Disease triangle. Adaptation from Tania Pérez-Sánchez et al., 2018*

1.7 Granulomatous diseases in Teleost fish

Granulomatous diseases in fish encompass a wide range of chronic pathologies, commonly related to infectious agents or autoimmune origin. These are characterized by granulomas or macrophages inflammation (Martínez-Lara et al., 2021; Rajme-Manzur et al., 2021a). Granulomas consist of compact, organized, and dynamic accumulations of immune cells in response to a persistent foreign entity that cannot be easily eliminated (Rajme-Manzur et al., 2021a).

Macroscopically, these diseases manifest as white or yellow nodular lesions in internal organs, often with a rigid or calcified consistency (Noga, 2010). The formation of granulomas begins with the activation of antigen-presenting cells and the recruitment of monocytes to the site of infection, where they differentiate into macrophages to eliminate foreign bodies through phagocytosis. These cells present foreign antigens to lymphocytes, triggering an adaptive immune response characterized by the production of proinflammatory cytokines and chemokines, including tumor necrosis factor (*TNF-α*), interleukins (e.g., *IL-12, IL-2*), CCL2, and interferon-gamma (*IFN-γ*). A Th1-type immune response, orchestrated by CD4+ T cells, plays a pivotal role in organizing effector cells at the site, resulting in macrophage activation and the recruitment of additional immune cells to the site of infection (Rajme-Manzur et al., 2021a). In response, macrophages can fuse to form epithelioid cells and, in some cases, and rarely multinucleated giant cells to contain the infection (Martínez-Lara et al., 2021). This process intensifies the inflammation and promotes the accumulation of more immune cells and spindle cells around the site of infection(Myllymäki et al., 2018), leading to the development of granulomas.

Structures commonly associated with chronic bacterial infections or/and granulomas in teleost are melanomacrophage centers (MMCs), aggregates of pigmented macrophages found in organs such as the kidney, liver, and spleen. MMCs contribute to the immune response and increase in size or frequency in conditions of environmental stress in fish (Agius & Roberts, 2003).

Histologically, granulomas are characterized by a well-organized structure that varies depending on the stage of formation and the immune status of the host. In the *early stages*, granulomas are

generally non-necrotic and are primarily composed of a central cluster of foamy macrophages and epithelioid histiocytes arranged in concentric layers, with few peripheral lymphocytes, plasma cells, and mast cells (Gustinelli et al., 2021). They may lack spindle cells at the periphery, but as the granuloma matures, they are recruited to form a fibrous capsule that encloses the lesion, providing structural integrity and isolating the granuloma from surrounding tissue.

In more advanced granulomas, the central core typically exhibits necrosis with amorphous eosinophilic material, macrophages and degenerating cells with pyknotic nuclei, surrounded by layers of epithelioid macrophages and plasma cells. Epithelioid cells are polygonal, eosinophilic cells with open-faced nuclei, prominent nucleoli, and faintly granular cytoplasm, and unlike their mammalian counterparts, those in fish granulomas exhibit desmosomes, suggesting a distinct lineage (Rajme-Manzur et al., 2021b). Granulomas with central necrosis are typically associated with infectious causes, and as they mature into late-stage lesions, the necrotic areas may coalesce, forming larger inflammatory foci. These granulomas are usually encased by a fibrous capsule formed by spindle cells, isolating persistent pathogens.

In aquaculture, granulomatous diseases threaten productivity causing high mortality and reduced growth, and are often detected in later stages when financial investments in feed and maintenance have already been invested (Rajme-Manzur et al., 2021b).

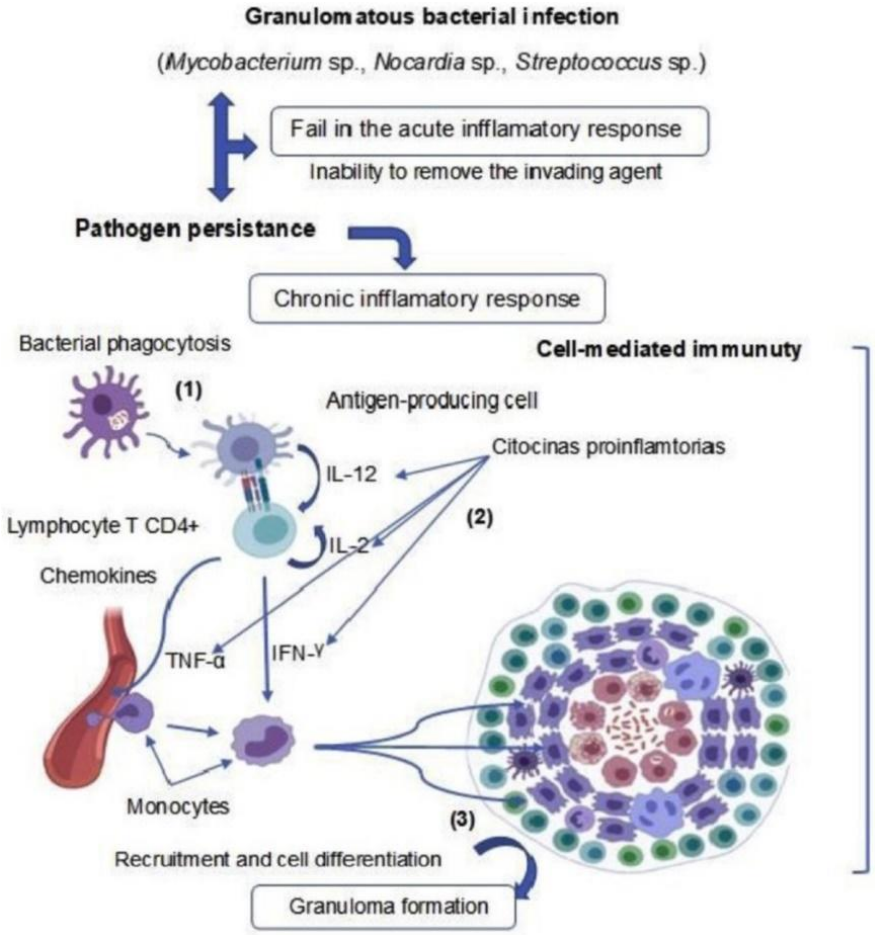

Figure 24. *Graphic illustration of granuloma formation process. (from David Rajme-Manzur et al., 2021)*

1.8 Bacterial agents causing granulomas in teleost

Granulomatous diseases in fish are caused by various bacterial pathogens, primarily from the genera *Mycobacterium, Nocardia, Photobacterium, Francisella, Edwardsiella, Lactococcus,* and *Streptococcus* (Austin & Austin, 2016; Rajme-Manzur et al., 2021b). Transmission generally occurs horizontally through infected fish, exposure to contaminated water, or ingestion of infected materials with pathogens typically entering through skin injuries or the gastrointestinal tract (Austin & Austin, 2016; Maekawa et al., 2018a). Once inside the host, pathogens can survive intracellularly, often within macrophages, evading immune defenses and establishing chronic infections. Clinical signs are generally nonspecific such as lethargy, loss of appetite, skin ulcerations, petechial hemorrhages and exophthalmia. Lesions include nodules on the surface of the organs, mainly in spleen, kidney, and liver, indicative of granulomas.

Clinical signs tend to appear in the late-stage phase, prompting the management and control of outbreaks primarily toward prophylaxis strategies such as vaccination, strict biosecurity measures, and minimizing stress. Antibiotic treatment, while effective to some extent, remains challenging due to the pathogens' intracellular nature and to the emergent problem of antibiotic resistance strains (Martínez-Lara et al., 2021; Rajme-Manzur et al., 2021b).

In the Mediterranean Sea aquaculture, the most reported granulomatous diseases caused by bacterial agents include photobacteriosis, nocardiosis and mycobacteriosis (Cascarano et al., 2021).

Bacteria	Aquatic animal	Evaluated response	Reference
Edwarsiella tarda	West African lungfish (*Protopterus annectens*)	External ulcerative lesions and mortality after developing anorexia. Multifocal areas of necrosis and heterophilic and histiocytic inflammation in multiple tissues. Small numbers of intra- and extracellular monomorphic Gram-negative rod-shaped bacilli. Lung granuloma, kidney and testes showed heterophilic inflammation with phagocytosis of small monomorphic bacilli and some heterophils exhibiting cytoplasmic projections suggesting heterophil extracellular traps	Rousselet *et al.* (2018)
Francisella marina sp. nov.	Spotted Rose Snapper (*Lutjanus guttatus*)	Multifocal granulomatous lesions with small, pleomorphic coccobacilli predominantly in the peritoneum, spleen, kidneys, liver, pancreas, intestine and heart	Soto *et al.* (2018)
Francisella noatunensis subsp. *orientalis*	Nile tilapia (*Oreochromis niloticus* x *O. aureus*)	Numerous white granulomas in kidney, liver, heart and spleen. Head kidney and spleen were markedly swollen	Lin *et al.* (2016)
	Zebrafish (*Danio rerio*)	Granuloma-like structures containing small coccoid bacteria detected in the spleen. Some encapsulated granulomas were also observed even in previously immunized fish	Lagos *et al.* (2017)
	Tilapia (*Oreochromis* sp.)	Reduced appetite, lethargy, dark pigmentation and abnormal distension before death. Necropsy showed widespread of white multifocal nodules in the head kidney, spleen, liver and gill. Histopathology revealed granulomatous inflammation surrounded by numerous macrophages	Pulpipat *et al.* (2019)
Lactococcus garvieae	Rainbow trout (*Oncorhynchus mykiss*)	Haemorrhagic septicaemia was associated with this pathogen. Extensive degenerative and inflammatory changes in eye, kidney, gill and liver were observed.	Shahi *et al.* (2018)
Mycobacterium marinum	Zebrafish (*Danio rerio*)	This approach demonstrated that the zebrafish granuloma contains foam cells and the transdifferentiation of macrophages into foam cells is driven by the mycobacterial ESX1 pathogenicity locus	Johansen *et al.* (2018)
Mycobacterium leprae	Zebrafish (*Danio rerio*)	Rapid development of noncaseating granulomas, but infection was eventually eradicated. The rag1 mutant zebrafish lacking lymphocytes also formed noncaseating granulomas, but these controlled the infection more slowly. These results revealed the interplay between innate and adaptive immune determinants mediating leprosy granuloma formation and function	Madigan *et al.* (2017)
Mycobacterium gordonae	Ginbuna crucian carp (*Carassius auratus langsdorfii*)	Granulomatous responses consisted of central macrophage accumulation and surrounding lymphocytes. Ziehl-Neelsen-positive bacteria were detected in the trunk kidney of fish. The marginal lymphocytes were positive for CD4-1, and the IFNγ-producing cells surrounded the mycobacterial cell-laden phagocytes. CD4-1+ cells and IFNγ2 played important roles in the granulomatous inflammation	Kato *et al.* (2019)
Nocardia seriolae	Spotted butterfish (*Scatophagus argus*, Linn)	Enlargement of spleen, kidney and liver with white nodules varying in size. The pathogen caused systemic granulomas	Wang *et al.* (2014)
	Snubnose pompano (*Trachinotus blochii*)	Fish displayed paleness and lethargy, and exhibited skin haemorrhages and ulcers. Prominent white nodules varying in size were observed in the spleen, kidney and liver. Typical granulomatous lesions in these organs were observed	Vu-Khac *et al.* (2016)
	Tiger barb (*Puntius tetrazona*)	Green fluorescent protein-labelled *Nocardia seriolae* strain was injected in fish. Bacteria were phagocytized by leucocytes and proliferated within these cells, which in turn led to leucocyte aggregation, leucocyte death and granuloma formation. Bacteria could permanently colonize various tissues via leucocyte circulation, causing multi-organ infection	Wang *et al.* (2017)
	Japanese eel (*Anguilla japonica*)	Infected fish exhibited lethargy and skin ulcers. Pathiogen genoma was sequenced and assembled, revealing dozens of antibiotic resistance genes in the genome of *N. seriolae* strains; most of the antibiotics were involved in the inhibition of the biosynthesis of proteins or cell walls	Han et al. (2018)
Streptococcus iniae	Tilapia (*Oreochromis aureus*)	External signs included exophthalmia and cachexia, while internal signs were granulomatous septicaemia and interstitial nephritis, among others	Ortega *et al.* (2018)

***Figure 25**. Granulomatous infections caused by bacteria belonging to different taxonomic groups in diverse marine and freshwater fish species. (from Martinez-Lara et al., 2021)*

1.8.1 Photobacteriosis

Photobacteriosis is caused by *Photobacterium damselae* subsp. *piscicida*, a Gram-negative, non-motile, bipolar rod bacteria that induces chronic granulomatous disease in a wide range of teleost fish, particularly in Mediterranean and Japanese aquaculture (López-Dóriga et al., 2000; Romalde, 2002). The genus *Photobacterium* (family Vibrionaceae) comprises over 35 species found in aquatic ecosystems worldwide, with *Photobacterium damselae* being of particular concern as an emerging pathogen that affects fish, mollusks, crustaceans, and occasionally humans (Rivas et al., 2014; Labella et al., 2017). This species is divided into two subspecies: *P. damselae* subsp. *damselae*, associated with hemorrhagic septicemia in fish and necrotizing fasciitis in humans, and *P. damselae* subsp. *piscicida*, the etiological agent of photobacteriosis. Photobacteriosis outbreaks typically occur in warm water (above 18°C) from late spring to early autumn, being particularly threatening in juveniles and larvae, with mortality rates of 90-100% (Rivas et al., 2014; Essam et al., 2016).

Effective control of photobacteriosis relies on integrated strategies, including vaccination, biosecurity, early diagnosis, and timely treatment. Vaccination options include inactivated bacterins, attenuated strains, and extracellular products, providing variable protection, particularly in sea bream larvae and juveniles (Magariños et al., 1997; Romalde, 2014).

Accurate and timely diagnosis is critical, mainly relying on histopathology, microbiology, and PCR targeting *16S rRNA* and *ureC* genes to effectively identify *P. damselae* subspecies (Essam et al., 2016). Antibiotic treatment, typically involving sulfa-trimethoprim or flumequine, is often complicated by the bacterium's intracellular location and the emergence of multidrug-resistant strains, with documented resistance to tetracyclines, sulfonamides, ampicillin, chloramphenicol, florfenicol, and erythromycin complicating effective disease management (Andreoni & Magnani, 2014). Moreover, transferable genetic elements, such as R plasmids, further exacerbate antibiotic

resistance, highlighting the need for improved prevention and alternative therapeutic strategies (Andreoni & Magnani, 2014).

1.8.2 Nocardiosis

Nocardiosis is caused by filamentous Gram-positive bacteria of the genus Nocardia, primarily *Nocardia seriolae*, which induces chronic granulomatous disease in both freshwater and marine fish species. Other species like *N. salmonicida, N. asteroides*, and *N. crassostreae* have also been implicated in outbreaks across different fish species (Maekawa et al., 2018a).

The pathogen is capable of intracellular survival within macrophages, leading to granuloma formation in the spleen, kidney, liver, and sometimes in the brain. Clinical signs often include external nodules, skin ulcers, and occasional exophthalmia with the disease often being subclinical for extended periods and mortalities occurring in advanced stage. The bacterium thrives in warmer waters, with disease outbreaks occurring predominantly in intensive aquaculture systems, where high stocking densities exacerbate stress and suppress the immune system in fish. Nocardiosis has caused significant economic losses in East Asia aquaculture, affecting species like yellowtail (*Seriola quinqueradiata*) and seabream (Maekawa et al., 2018b), while in the Mediterranean, *Nocardia* spp. has been reported in isolated cases (Carella et al., 2013; Elkesh et al., 2013; Tsertou et al., 2018; Díaz-Santana et al., 2022), yet recently *Nocardia brasiliensis* has been found to cause granulomtaus disease in *Argyrosomus regius* (Acosta et al., 2024).

Diagnosis is typically achieved through histopathological examination, PCR, and culture techniques, though isolation can be difficult due to the slow-growing nature. While treatment with antibiotics like sulfamethoxazole-trimethoprim has been used, antimicrobial resistance is a growing concern, and long-term control strategies remain limited. Preventive measures currently focus on improving farm management practices, including biosecurity and reducing stress-inducing factors, though research into vaccination remains ongoing (Maekawa et al., 2018a).

1.9 Fish mycobacteriosis

Fish mycobacteriosis is a chronic disease that affects a wide range of fish species in both wild and aquaculture environments, caused by ubiquitous, Gram-positive, nonmotile and acid-fast bacteria from the genus *Mycobacterium* (family Mycobacteriaceae, order Actinomycetales)(Decostere et al., 2004; Gauthier & Rhodes, 2009a; Delghandi et al., 2020a; Rovid & Glenda, 2020). A distinctive feature of these bacteria is their lipid-rich cell wall, containing long-chain mycolic acids (with 60 to 90 carbon atoms), which makes them highly resistant to acid-alcohol decolorization and identifiable through staining techniques like the Ziehl-Neelsen (ZN)(Gauthier & Rhodes, 2009a)(*Fig. 26*).

Currently, there are 188 recognized species of mycobacteria, classified into five distinct genera: *Mycobacterium*, *Mycobacteroides* gen. nov., *Mycolicibacillus* gen. nov., *Mycolicibacter* gen. nov., and *Mycolicibacterium* gen. nov. (Gupta et al., 2018). Besides genera, mycobacteria can be also categorized in tuberculous mycobacteria (such as the *M. tuberculosis* complex, *M. leprae*, and *M. lepromatosis*) and non-tuberculous mycobacteria (NTM), also known as atypical or environmental mycobacteria, which do not cause tuberculosis or leprosy. Based on their growth rates, NTM are further classified as rapidly growing (within 2–3 days) or slow-growing (requiring more than 7 days)(Gupta et al., 2018; Delghandi et al., 2020a).

The spectrum of NTM affecting fish ranges from true pathogens, such as *M. marinum* and *M. ulcerans*, which actively cause disease, to opportunistic species like the *M. chelonae-abscessus* complex, *M. fortuitum*, *M. avium* complex, *M. haemophilum*, *M. xenopi*, *M. kansasii*, and *M. simiae*, which primarily infect stressed fish with compromised immunity, while saprophytic species such as *M. smegmatis*, *M. vaccae*, *M. terrae* complex, and *M. gordonae* are typically non-pathogenic and rarely associated with disease

The bacteria primarily infect the host horizontally, through contaminated food, cannibalism of infected fish, or through abrasions on the skin that come into contact with contaminated water or

debris. Although rare, vertical transmission has also been described and can occur in fish through egg or sperm products (Decostere et al., 2004; Gauthier & Rhodes, 2009a; Francis-Floyd, 2011; Delghandi et al., 2020a).

Given the wide variety of bacterial species involved and the broad host range, clinical signs of these infections are often nonspecific and can vary widely. These include skin ulcerations, abnormal swimming behaviors, spinal deformities, exophthalmia, abnormal behavior, poor growth rates, emaciation, and ascites, while gross internal signs include enlargement of the spleen, kidney and liver, and grey or white nodules in internal organs, indicative of multifocal granulomas (Decostere et al., 2004; Gauthier & Rhodes, 2009a; Francis-Floyd, 2011; Delghandi et al., 2020a). Experimentally injection of the organism, mycobacteriosis typically develops over two weeks as a chronic infection with a progressive course often leading to gradual mortality, although acute disease may occur with high bacterial loads (Gauthier & Rhodes, 2009a; Jacobs et al., 2009; Delghandi et al., 2020a).

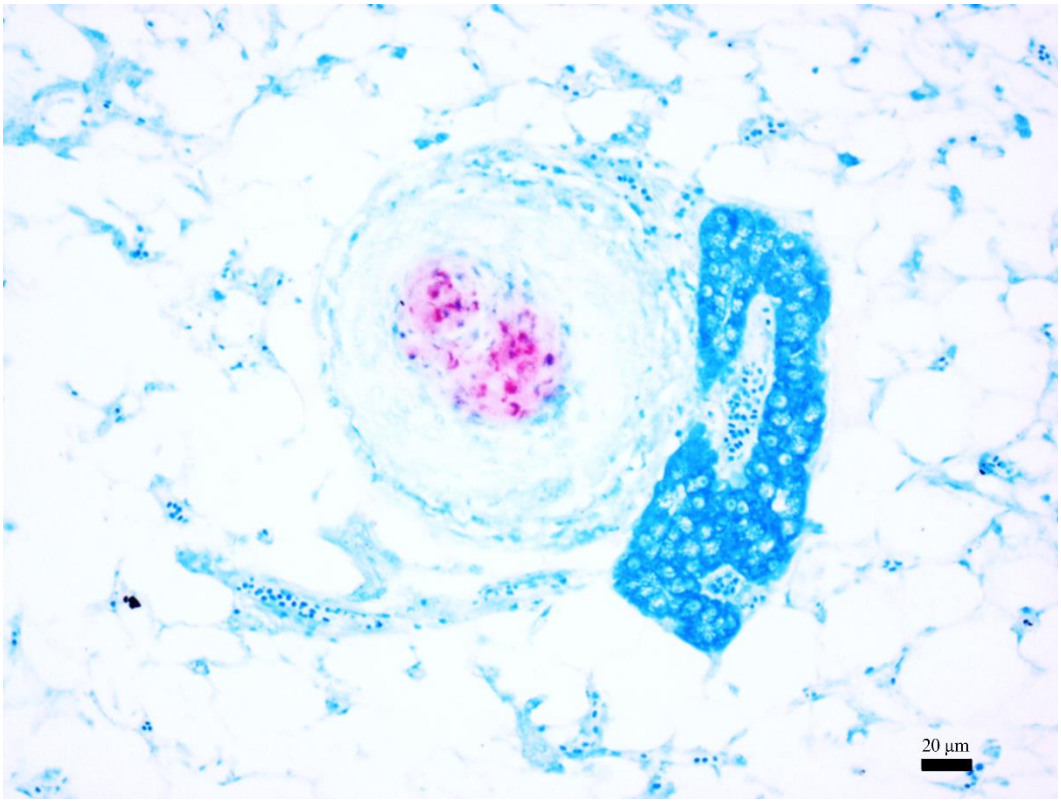

Figure 26. *Focal granuloma in the fish liver with acid fast bacilli (Mycobacterium spp.) in the core of granuloma. Ziehl-Neelsen, Scale bar: 20 µm (Photo by Antuofermo E.)*

1.9.1 Pathogenic mechanisms and virulence factors

Several pathogenic *Mycobacterium* species have evolved to invade, survive, and proliferate within host cells, primarily as intracellular parasites of phagocytes (Volkman et al., 2010; Oksanen et al., 2013). These bacteria evade immune defenses by inhibiting phagolysosomal fusion, delaying phagosome maturation, and resisting reactive nitrogen metabolites, surviving within macrophages (Gauthier & Rhodes, 2009a; Cronan et al., 2016; Ramakrishnan, 2020). Additionally, they can induce apoptosis in T lymphocytes and suppress MHC II expression to evade antigen presentation (Rajme-Manzur et al., 2021b).

A key event in their pathogenesis is the necrosis of infected macrophages, which releases bacteria into the extracellular environment. This process recruits uninfected macrophages, allowing *Mycobacterium* spp. to exploit the immune response, further promoting bacterial dissemination.

In fish, while pathogenic mechanisms are not as thoroughly understood as they are in mammals, pathogenic *Mycobacterium* spp. possess similar adaptations for persistence within host cells. In this regard, *M. marinum* has been extensively studied as a model organism, due to its genetic similarities to *M. tuberculosis* and its capacity to induce granulomatous disease in poikilothermic hosts like zebrafish (*Danio rerio*). Key virulence determinants in this strain include cell wall-associated lipids, such as phthiocerol dimycocerosates and phenolic glycolipids, as well as the type VII secretion system (T7SS), also called the ESX (early secretory antigenic target 6)(Delghandi et al., 2020a). The T7SS functions as a macromolecular nanomachine composed of several proteins, with its core structure being a complex needle-like supramolecular apparatus that translocates virulent proteins into host cells, enabling the manipulation of host cellular processes and contributing to pathogenicity(Mekasha & Linke, 2021; Famelis et al., 2023). Among the ESX pathways, ESX-1, ESX-3, and ESX-5 are particularly significant: ESX-1 plays a critical role in virulence by mediating phagosome rupture within macrophages and enabling the bacteria to escape the phagolysosome. On the other hand, ESX-3 and ESX-5 are essential for iron and fatty

acid uptake and contribute to immune modulation of the host, helping the bacteria to establish the infection and persist within the organism (Y. Wang et al., 2022).

Furthermore, critical pathogenic strategy for *Mycobacterium* spp. survival is their ability to enter a dormant state within the host, minimizing metabolic activity and evading immune detection (Jia et al., 2024). Under certain environmental conditions or in cases of host immune suppression, this dormant state can be reversed, shifting to an active growth state, leading to a rapid bacterial proliferation, granuloma rupture, extensive tissue damage that can ultimately lead to the host's death (Parikka et al., 2012).

1.9.2 Treatment and diagnosis

The management of mycobacteriosis in fish remains a significant challenge due to the chronic nature of the infection and the bacteria's resistance to many common antibiotics. Currently, no approved treatments are available for the disease, although several antibiotics, including rifampicin, kanamycin sulfate, tigecycline, clarithromycin, streptomycin, tetracycline and others, have shown varying degrees of success (Gauthier & Rhodes, 2009a; Delghandi et al., 2020a; Guz & Puk, 2022a). Limitations in their efficacy include species-specific drug susceptibility, prolonged treatments, and differences between slow- and fast-growing strains, often necessitating tailored treatments. Moreover, antibiotic resistance represents one of the most alarming concerns in mycobacterial infections, with several species exhibiting multiple antimicrobial resistance (Francis-Floyd, 2011; Delghandi et al., 2020a).

Given the limitations of antibiotic treatment, prevention remains the most effective approach, relying on stringent biosecurity measures, such as regular disinfection of equipment and tanks, enhancing husbandry practices, quarantining newly introduced fish, and depopulating infected stocks (Francis-Floyd, 2011; Delghandi et al., 2020a).

Early and accurate diagnosis is crucial and often relies on a combination of microbiological, histological, and molecular techniques. Isolation may be challenging due to *Mycobacterium*'s

slow growth and tendency to be overgrown by faster-growing organisms, often necessitating selective media like Löwenstein-Jensen and Middlebrook 7H10, with weeks to months required for colony formation. Histologically, most mycobacteria are detected through specific staining like ZN or Fite-Faraco, although sensitivity can vary with bacterial load. For enhanced precision, immunohistochemistry (IHC) can also be employed to detect specific bacterial antigens within the tissues. Molecular diagnostics, including PCR and RT-qPCR methods targeting genes such as *16S rRNA*, *hsp65*, *rpoB*, and *erp*, are pivotal for early detection and species identification. Complementary techniques, such as high-resolution melting analysis (HRMA), fluorescence resonance energy transfer (FRET), and MALDI-TOF MS, further enhance diagnostic precision and reliability (Gauthier & Rhodes, 2009a; Francis-Floyd, 2011; Van Ingen, 2013; Delghandi et al., 2020a; Maboni et al., 2024;).

1.9.3 Vaccine for fish mycobacteriosis

Immunoprophylaxis has arisen as a promising alternative for effective and sustainable control of the disease. In the last decade, several vaccine strategies have been explored to address mycobacteriosis in fish (Delghandi et al., 2020a). One of the primary approaches involves live attenuated vaccines, consisting in viable strains that mimic natural infections to stimulate both innate and adaptive immunity without causing disease. Examples include the BCG (Bacillus Calmette and Guerin) vaccine, which has enhanced immune responses and survival rates in Japanese flounder (Kato et al., 2010), and live-attenuated *M. marinum* strains in zebrafish, which have elicited strong immune responses and significantly improved survival following infection (Cui et al., 2010). Another extensively studied approach involves inactivated or killed vaccines, such as heat-killed whole cells and extracellular products (ECPs). For instance, heat-killed *M. marinum* has demonstrated effectiveness in reducing mortality in European seabass (Ziklo et al., 2018), while heat-killed *M. bovis* has provided cross-protection in zebrafish (López et al., 2018). In rainbow trout, ECPs from various aquatic *Mycobacterium* spp. have been shown to enhance

phagocyte activity, lysozyme production, and antibody levels, indicating their potential to stimulate a robust immune response (Chen et al., 1996).

More recent technology includes DNA vaccines, using genetic material that encodes for specific mycobacterial antigens that stimulate immune responses (Pasnik & Smith, 2005; Niskanen et al., 2020). A promising example is the DNA vaccine encoding the Ag85A protein, which has shown protective effects in hybrid striped bass against *M. marinum* (Pasnik & Smith, 2005).

1.9.4 Zoonotic implications

Fish mycobacteriosis is an emerging public health concern due to its zoonotic potential (Ziarati et al., 2022). Among NTMs affecting fish, species like *Mycobacterium marinum*, *M. ulcerans*, *M. haemophilum*, *M. fortuitum*, and *M. chelonae* represent significant risks, especially for those handling fish or with open wounds exposed to contaminated water (Wu et al., 2012; Franco-Paredes et al., 2018). In humans, *M. marinum* is particularly notable as the cause of "fish tank granuloma" or "swimming pool granuloma," manifesting as granulomatous skin lesions (Wu et al., 2012) that may develop into painful or necrotic areas (*Fig. 27*). In immunocompromised individuals, these infections can disseminate, leading to severe conditions such as lung abscesses, meningitis, or osteomyelitis (McCracken et al., 2000). A growing concern with NTM infections is the increasing prevalence of multi-antibiotic-resistant strains, which complicates treatment and contributes to higher rates of failure (Brown-Elliott et al., 2012). Resistance to multiple antibiotics poses a significant public health challenge, particularly in industrialized countries where NTM infections are being reported with rising frequency (Muteeb et al., 2023).

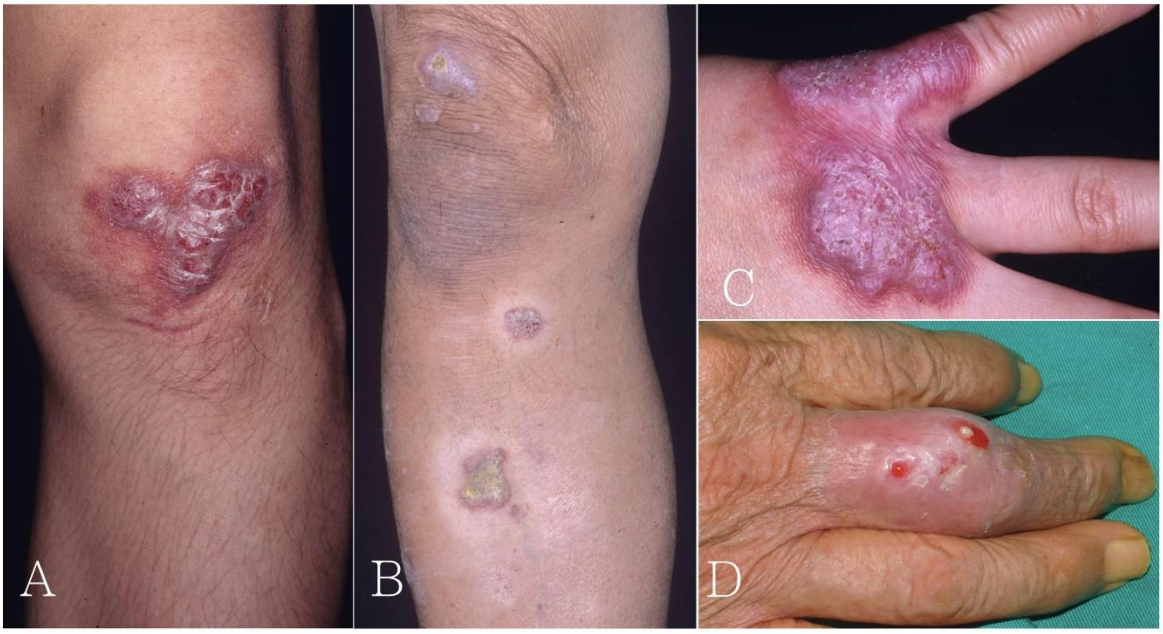

Figure 27. *Fish Tank Granuloma (cutaneous lesions) caused by Mycobacterium marinum. (from Wu et al., 2012)*

References

Acosta, Félix, Belinda Vega, Luis Monzón-Atienza, Joshua Superio, Silvia Torrecillas, Antonio Gómez-Mercader, Pedro Castro, Daniel Montero, and Jorge Galindo-Villegas. 2024. "Phylogenetic Reconstruction, Histopathological Characterization, and Virulence Determination of a Novel Fish Pathogen, Nocardia Brasiliensis." Aquaculture 581 (February). https://doi.org/10.1016/j.aquaculture.2023.740458.

Agius, C, and R J Roberts. 2003. "Melano-macrophage Centres and Their Role in Fish Pathology." Journal of Fish Diseases 26 (9): 499–509. https://doi.org/10.1046/j.1365-2761.2003.00485.x.

Andreoni, Francesca, and Mauro Magnani. 2014. "Photobacteriosis: Prevention and Diagnosis." Journal of Immunology Research 2014 (9): 1–7. https://doi.org/10.1155/2014/793817.

Armstrong, Derek T, Emma Eisemann, and Nicole Parrish. 2023. "A Brief Update on Mycobacterial Taxonomy, 2020 to 2022." Edited by Romney M Humphries. Journal of Clinical Microbiology 61 (4). https://doi.org/10.1128/jcm.00331-22.

Austin, Brian, and Dawn A. Austin. 2016. Bacterial Fish Pathogens. NA. Vol. NA. Cham: Springer International Publishing. https://doi.org/10.1007/978-3-319-32674-0.

Brown-Elliott, Barbara A., Kevin A. Nash, and Richard J. Wallace. 2012. "Antimicrobial Susceptibility Testing, Drug Resistance Mechanisms, and Therapy of Infections with Nontuberculous Mycobacteria." Clinical Microbiology Reviews 25 (3): 545–82. https://doi.org/10.1128/CMR.05030-11.

Cabello, Felipe C., Henry P. Godfrey, Alexandra Tomova, Larisa Ivanova, Humberto Dölz, Ana Millanao, and Alejandro H. Buschmann. 2013. "Antimicrobial Use in Aquaculture Re-examined: Its Relevance to Antimicrobial Resistance and to Animal and Human Health." Environmental Microbiology 15 (7): 1917–42. https://doi.org/10.1111/1462-2920.12134.

Carella, Francesca, Noelia Carrasco, Karl B. Andree, Beatriz Lacuesta, Dolors Furones, and Gionata de Vico. 2013. "Nocardiosis in Mediterranean Bivalves: First Detection of Nocardia Crassostreae in a New Host Mytilus Galloprovincialis and in Ostrea Edulis from the Gulf of Naples (Italy)." Journal of Invertebrate Pathology 114 (3): 324–28. https://doi.org/10.1016/j.jip.2013.10.001.

Cascarano, Maria Chiara, Orestis Stavrakidis-Zachou, Ivona Mladineo, Kim D. Thompson, Nikos Papandroulakis, and Pantelis Katharios. 2021. "Mediterranean Aquaculture in a Changing Climate: Temperature Effects on Pathogens and Diseases of Three Farmed Fish Species." Pathogens. MDPI. https://doi.org/10.3390/pathogens10091205.

Chen, S C, T Yoshida, A Adams, K D Thompson, and R H Richards. 1996. "Immune Response of Rainbow Trout to Extracellular Products of *Mycobacterium* Spp." Journal of Aquatic Animal Health 8 (3): 216–22.

Cronan, Mark R., Rebecca W. Beerman, Allison F. Rosenberg, Joseph W. Saelens, Matthew G. Johnson, Stefan H. Oehlers, Dana M. Sisk, et al. 2016. "Macrophage Epithelial Reprogramming Underlies Mycobacterial Granuloma Formation and Promotes Infection." Immunity 45 (4): 861–76. https://doi.org/10.1016/j.immuni.2016.09.014.

Cui, Z, D Samuel-Shaker, V Watral, and M L Kent. 2010. “Attenuated *Mycobacterium marinum* Protects Zebrafish against Mycobacteriosis.” Journal of Fish Diseases 33 (4): 371–75. https://doi.org/10.1111/j.1365-2761.2009.01115.x.

Decostere, A., K. Hermans, and F. Haesebrouck. 2004. “Piscine Mycobacteriosis: A Literature Review Covering the Agent and the Disease It Causes in Fish and Humans.” Veterinary Microbiology 99 (3–4): 159–66. https://doi.org/10.1016/j.vetmic.2003.07.011.

Delghandi, Mohammad Reza, Mansour El-Matbouli, and Simon Menanteau-Ledouble. 2020. “Mycobacteriosis and Infections with Non-Tuberculous Mycobacteria in Aquatic Organisms: A Review.” Microorganisms. MDPI AG. https://doi.org/10.3390/microorganisms8091368.

Díaz-Santana, Pablo, Antonio Fernández, Josue Díaz-Delgado, Ana Isabel Vela, Lucas Domínguez, Cristian Suárez-Santana, Raquel Puig-Lozano, Carolina Fernández-Maldonado, Eva Sierra, and Manuel Arbelo. 2022. “Nocardiosis in Free-Ranging Cetaceans from the Central-Eastern Atlantic Ocean and Contiguous Mediterranean Sea.” Animals 12 (4): 434. https://doi.org/10.3390/ani12040434.

Elkesh, A., K. P.L. Kantham, A. P. Shinn, M. Crumlish, and R. H. Richards. 2013. “Systemic Nocardiosis in a Mediterranean Population of Cultured Meagre, *Argyrosomus regius* Asso (Perciformes: Sciaenidae).” Journal of Fish Diseases 36 (2): 141–49. https://doi.org/10.1111/jfd.12015.

Essam, H.M., G.S. Abdellrazeq, S.I. Tayel, H.A. Torky, and A.H. Fadel. 2016. “Pathogenesis of *Photobacterium damselae* Subspecies Infections in Sea Bass and Sea Bream.” Microbial Pathogenesis 99 (9): 41–50. https://doi.org/10.1016/j.micpath.2016.08.003.

Falkinham, Joseph O. 2022. “Nontuberculous Mycobacteria in the Environment.” Tuberculosis. Churchill Livingstone. https://doi.org/10.1016/j.tube.2022.102267.

Famelis, Nikolaos, Sebastian Geibel, and Daan van Tol. 2023. “Mycobacterial Type VII Secretion Systems.” Biological Chemistry 404 (7): 691–702. https://doi.org/10.1515/hsz-2022-0350.

F.A.O. 2024. The State of World Fisheries and Aquaculture 2024. Rome: FAO. https://doi.org/10.4060/cd0683en.

Francis-Floyd, R. 2011. “Mycobacterial Infections of Fish.” United States Department of Agriculture, National Institute of Food and Agriculture. https://srac.msstate.edu/pdfs/Fact Sheets/4706 Myobacterial Infections of Fish.pdf.

Franco-Paredes, Carlos, Daniel B. Chastain, Lorna Allen, and Andrés F. Henao-Martínez. 2018. “Overview of Cutaneous Mycobacterial Infections.” Current Tropical Medicine Reports 5 (4): 228–32. https://doi.org/10.1007/s40475-018-0161-7.

Gauthier, David T., and Martha W. Rhodes. 2009. “Mycobacteriosis in Fishes: A Review.” Veterinary Journal. https://doi.org/10.1016/j.tvjl.2008.05.012.

Gupta, Radhey S, Brian Lo, and Jeen Son. 2018. “Phylogenomics and Comparative Genomic Studies Robustly Support Division of the Genus *Mycobacterium* into an Emended Genus Mycobacterium and Four Novel Genera.” Frontiers in Microbiology 9 (February). https://doi.org/10.3389/fmicb.2018.00067.

Gustinelli, Andrea, Slavica Čolak, Francesco Quaglio, Rubina Sirri, Matko Kolega, Danijel Mejdandžić, Monica Caffara, Renata Baric, and Maria Letizia Fioravanti. 2021. "Histological Assessment of Systemic Granulomatosis Progression in Meagre *Argyrosomus regius* during Cage Ongrowing Phase." Diseases of Aquatic Organisms 145: 165–72. https://doi.org/10.3354/dao03606.

Guz, Leszek, and Krzysztof Puk. 2022. "Antibiotic Susceptibility of Mycobacteria Isolated from Ornamental Fish." Journal of Veterinary Research 66 (1): 69–76. https://doi.org/10.2478/jvetres-2022-0011.

Ingen, Jakko van. 2013. "Diagnosis of Nontuberculous Mycobacterial Infections." Seminars in Respiratory and Critical Care Medicine 34 (ue 01): 103–9. https://doi.org/10.1055/s-0033-1333569.

Jacobs, J M, C B Stine, A M Baya, and M L Kent. 2009. "A Review of Mycobacteriosis in Marine Fish." Journal of Fish Diseases 32 (2): 119–30. https://doi.org/10.1111/j.1365-2761.2008.01016.x.

Jia, Pingping, Shize Peng, Yi Zhang, Jianyuan Zhao, Qianqian Zhao, Xiaoxiao Wu, Fangqi Shen, Kai Sun, Liyan Yu, and Shan Cen. 2024. "Identification of Immune-Associated Genes Involved in Latent *Mycobacterium marinum* Infection." Microbes and Infection 75 (9): 105407. https://doi.org/10.1016/j.micinf.2024.105407.

Kato, Goshi, Hidehiro Kondo, Takashi Aoki, and Ikuo Hirono. 2010. "BCG Vaccine Confers Adaptive Immunity against Mycobacterium Sp. Infection in Fish." Developmental & Comparative Immunology 34 (2): 133–40. https://doi.org/10.1016/j.dci.2009.08.013.

Labella, Alejandro M., David R. Arahal, Teresa Lucena, Manuel Manchado, Dolores Castro, and Juan J. Borrego. 2017. "Photobacterium Toruni Sp. Nov., a Bacterium Isolated from Diseased Farmed Fish." International Journal of Systematic and Evolutionary Microbiology 67 (11): 4518–25. https://doi.org/10.1099/ijsem.0.002325.

López, Vladimir, María Angeles Risalde, Marinela Contreras, Lourdes Mateos-Hernández, Joaquin Vicente, Christian Gortázar, and José de la Fuente. 2018. "Heat-inactivated Mycobacterium Bovis Protects Zebrafish against Mycobacteriosis." Journal of Fish Diseases 41 (10): 1515–28. https://doi.org/10.1111/jfd.12847.

López-Dóriga, M. Victoria, Andrew C. Barnes, Nuno M. S. dos Santos, and Anthony E. Ellis. 2000. "Invasion of Fish Epithelial Cells by *Photobacterium damselae* Subsp. Piscicida: Evidence for Receptor Specificity, and Effect of Capsule and Serum." Microbiology 146 (1): 21–30. https://doi.org/10.1099/00221287-146-1-21.

Maboni, G, N Prakash, and M A S Moreira. 2024. "Review of Methods for Detection and Characterization of Non-Tuberculous Mycobacteria in Aquatic Organisms." Journal of Veterinary Diagnostic Investigation 36 (ue 3): 299–311. https://doi.org/10.1177/10406387231194619.

Maekawa, S, T Yoshida, P-C Wang, and S-C Chen. 2018. "Current Knowledge of Nocardiosis in Teleost Fish." Journal of Fish Diseases 41 (3): 413–19. https://doi.org/10.1111/jfd.12782.

Magariños, Beatriz, Carlos R. Osorio, Alicia E. Toranzo, and Jesús L. Romalde. 1997. "Applicability of Ribotyping for Intraspecific Classification and Epidemiological Studies of *Photobacterium Damselae* subsp. *Piscicida*." Systematic and Applied Microbiology 20 (4): 634–39. https://doi.org/10.1016/S0723-2020(97)80035-5.

Martínez-Lara, Pablo, Marcel Martínez-Porchas, Teresa Gollas-Galván, Jorge Hernández-López, and Glen R. Robles-Porchas. 2021. "Granulomatosis in Fish Aquaculture: A Mini Review." Reviews in Aquaculture. Wiley-Blackwell. https://doi.org/10.1111/raq.12472.

McCracken, D., P. Flanagan, D. Hill, and I. Hosein. 2000. "Cluster of Cases of *Mycobacterium Chelonae* Bacteraemia." European Journal of Clinical Microbiology & Infectious Diseases 19 (1): 43–46. https://doi.org/10.1007/s100960050008.

Mekasha, Sophanit, and Dirk Linke. 2021. "Secretion Systems in Gram-Negative Bacterial Fish Pathogens." Frontiers in Microbiology 12 (9): 1497–1517. https://doi.org/10.3389/fmicb.2021.782673.

Muñoz-Egea, Maria-Carmen, Arij Akir, and Jaime Esteban. 2023. "Mycobacterium Biofilms." Biofilm 5 (December): 100107. https://doi.org/10.1016/j.bioflm.2023.100107.

Murray, Alexander G., and Edmund J. Peeler. 2005. "A Framework for Understanding the Potential for Emerging Diseases in Aquaculture." Preventive Veterinary Medicine 67 (2–3): 223–35. https://doi.org/10.1016/j.prevetmed.2004.10.012.

Muteeb, Ghazala, Md Tabish Rehman, Moayad Shahwan, and Mohammad Aatif. 2023. "Origin of Antibiotics and Antibiotic Resistance, and Their Impacts on Drug Development: A Narrative Review." Pharmaceuticals 16 (11): 1615. https://doi.org/10.3390/ph16111615.

Niskanen, Mirja, Henna Myllymäki, and Mika Rämet. 2020. "DNA Vaccination with the *Mycobacterium marinum* MMAR_4110 Antigen Inhibits Reactivation of a Latent Mycobacterial Infection in the Adult Zebrafish." Vaccine 38 (35): 5685–94. https://doi.org/10.1016/j.vaccine.2020.06.053.

Noga, Edward J. 2010. Fish Diseases: Diagnosis and Treatment. Edited by John Wiley & Sons. 2nd ed.

Oksanen, Kaisa E., Nicholas J.A. Halfpenny, Eleanor Sherwood, Sanna-Kaisa E. Harjula, Milka M. Hammarén, Maarit J. Ahava, Elina T. Pajula, Marika J. Lahtinen, Mataleena Parikka, and Mika Rämet. 2013. "An Adult Zebrafish Model for Preclinical Tuberculosis Vaccine Development." Vaccine 31 (45): 5202–9. https://doi.org/10.1016/j.vaccine.2013.08.093.

Parikka, Mataleena, Milka M. Hammarén, Sanna-Kaisa E. Harjula, Nicholas J. A. Halfpenny, Kaisa E. Oksanen, Marika J. Lahtinen, Elina T. Pajula, Antti Iivanainen, Marko Pesu, and Mika Rämet. 2012. "*Mycobacterium marinum* Causes a Latent Infection That Can Be Reactivated by Gamma Irradiation in Adult Zebrafish." Edited by Marcel A. Behr. PLoS Pathogens 8 (9): e1002944. https://doi.org/10.1371/journal.ppat.1002944.

Pasnik, David J., and Stephen A. Smith. 2005. "Immunogenic and Protective Effects of a DNA Vaccine for *Mycobacterium marinum* in Fish." Veterinary Immunology and Immunopathology 103 (3–4): 195–206. https://doi.org/10.1016/j.vetimm.2004.08.017.

Preena, Prasannan Geetha, Thangaraj Raja Swaminathan, Vattiringal Jayadradhan Rejish Kumar, and Isaac Sarojini Bright Singh. 2020. "Antimicrobial Resistance in Aquaculture: A Crisis for Concern." Biologia 75 (9): 1497–1517. https://doi.org/10.2478/s11756-020-00456-4.

Rajme-Manzur, David, Teresa Gollas-Galván, Francisco Vargas-Albores, Marcel Martínez-Porchas, Miguel Ángel Hernández-Oñate, and Jorge Hernández-López. 2021. "Granulomatous Bacterial Diseases in Fish: An Overview of the Host's Immune Response."

Comparative Biochemistry and Physiology -Part A : Molecular and Integrative Physiology 261 (November). https://doi.org/10.1016/j.cbpa.2021.111058.

Ramakrishnan, Lalita. 2020. "Mycobacterium Tuberculosis Pathogenicity Viewed through the Lens of Molecular Koch's Postulates." Current Opinion in Microbiology 54 (9): 103–10. https://doi.org/10.1016/j.mib.2020.01.011.

Ravid-Peretz, Shay, Angelo Colorni, Galit Sharon, and Michal Ucko. 2019. "Vaccination of European Sea Bass *Dicentrarchus labrax* with Avirulent *Mycobacterium marinum* (IipA::Kan Mutant)." Fish & Shellfish Immunology 90 (July): 317–27. https://doi.org/10.1016/j.fsi.2019.04.057.

Rivas, Amable J., Alejandro M. Labella, Juan J. Borrego, Manuel L. Lemos, and Carlos R. Osorio. 2014. "Evidence for Horizontal Gene Transfer, Gene Duplication and Genetic Variation as Driving Forces of the Diversity of Haemolytic Phenotypes in *Photobacterium damselae* Subsp. Damselae." FEMS Microbiology Letters 355 (2): 152–62. https://doi.org/10.1111/1574-6968.12464.

Romalde, Jesús L. 2002. "*Photobacterium damselae* Subsp. Piscicida: An Integrated View of a Bacterial Fish Pathogen." International Microbiology 5 (1): 3–9. https://doi.org/10.1007/s10123-002-0051-6.

Romalde, Jesús L. 2014. "Vaccination against Photobacteriosis." In Fish Vaccination, 19:200–210. Wiley. https://doi.org/10.1002/9781118806913.ch17.

Rovid, Spickler Anna, and Dvorak Glenda. 2020. "Mycobacteriosis." http://www.cfsph.iastate.edu/DiseaseInfo/factsheets.php.

Scholthof, Karen-Beth G. 2007. "The Disease Triangle: Pathogens, the Environment and Society." Nature Reviews Microbiology 5 (2): 152–56. https://doi.org/10.1038/nrmicro1596.

Shaheen, Mohamed N. F. 2022. "The Concept of One Health Applied to the Problem of Zoonotic Diseases." Reviews in Medical Virology 32 (4): 1497–1517. https://doi.org/10.1002/rmv.2326.

Tsertou, M. I., M. Smyrli, C. Kokkari, E. Antonopoulou, and P. Katharios. 2018. "The Aetiology of Systemic Granulomatosis in Meagre (*Argyrosomus regius*): The 'Nocardia' Hypothesis." Aquaculture Reports 12 (November): 5–11. https://doi.org/10.1016/j.aqrep.2018.08.002.

Volkman, Hannah E., Tamara C. Pozos, John Zheng, J. Muse Davis, John F. Rawls, and Lalita Ramakrishnan. 2010. "Tuberculous Granuloma Induction via Interaction of a Bacterial Secreted Protein with Host Epithelium." Science 327 (5964): 466–69. https://doi.org/10.1126/science.1179663.

Wang, Yuchen, Yuting Tang, Chen Lin, Junli Zhang, Juntao Mai, Jun Jiang, Xiaoxiao Gao, et al. 2022. "Crosstalk between the Ancestral Type VII Secretion System ESX-4 and Other T7SS in *Mycobacterium marinum*." IScience 25 (1): 103585. https://doi.org/10.1016/j.isci.2021.103585.

Wu, Ting-Shu, Cheng-Hsun Chiu, Chih-Hsun Yang, Hsieh-Shong Leu, Ching-Tai Huang, Yi-Chieh Chen, Tsu-Lan Wu, et al. 2012. "Fish Tank Granuloma Caused by *Mycobacterium marinum*." Edited by David M. Ojcius. PLoS ONE 7 (7): e41296. https://doi.org/10.1371/journal.pone.0041296.

Ziarati, Mina, Mohammad Jalil Zorriehzahra, Fatemeh Hassantabar, Zibandeh Mehrabi, Manish Dhawan, Khan Sharun, Talha bin Emran, Kuldeep Dhama, Wanpen Chaicumpa, and Shokoofeh Shamsi. 2022. "Zoonotic Diseases of Fish and Their Prevention and Control." Veterinary Quarterly 42 (1): 95–118. https://doi.org/10.1080/01652176.2022.2080298.

Ziklo, N., A. Colorni, L.-Y. Gao, S. J. Du, and M. Ucko. 2018. "Humoral and Cellular Immune Response of European Seabass *Dicentrarchus labrax* Vaccinated with Heat-Killed *Mycobacterium marinum* (IipA::Kan Mutant)." Journal of Aquatic Animal Health 30 (4): 312–24. https://doi.org/10.1002/aah.10042.

Chapter II

2. Investigation of the prevalence of granulomatous diseases caused by bacteria in fish species in Sardinia (*Sparus aurata, Dicentrarchus labrax*, Mugilidae)

2.1 Introduction

Aquaculture in the Mediterranean area has become an essential industry, playing a key role in ensuring food security and driving economic growth (Carvalho & Guillen, 2021). However, bacterial diseases pose a growing threat due to their persistence, treatment challenges, and zoonotic potential. These infections are of particular concern in warm-water environments, where pathogens can persist independently of a host (Rajme-Manzur et al., 2021b). Given that the Mediterranean is highly responsive to climate change (Lionello & Scarascia, 2018), rising water temperatures could further exacerbate bacterial disease outbreaks in aquaculture (Nichols et al., 2018).

Among bacterial diseases affecting fish, granulomatous infections are primarily caused by pathogens from the genera *Mycobacterium, Nocardia,* and *Photobacterium* (Rajme-Manzur et al., 2021b; Austin & Austin, 2016). To the best of our knowledge, no previous studies have investigated the presence of these pathogens in association with granulomatous lesions in fish organs in Sardinia.

The aim of this study was to investigate, through an integrated approach combining histopathological, microbiological, and molecular techniques, the prevalence and distribution of bacterial granulomatous diseases in *Sparus aurata* and *Dicentrarchus labrax* from intensive aquaculture, as well as in extensively farmed Mugilidae in Sardinia.

2.2 Materials and methods

2.2.1 Samplings

Between June and July 2022, sixty adult specimens of European seabass (*Dicentrarchus labrax*), gilthead seabream (*Sparus aurata*), and mullets (Mugilidae) were sampled from aquaculture sites

across Sardinia. Seabream and seabass were collected from off-shore intensive farms in Golfo Aranci (40°58'59.5"N 9°38'05.4"E) and Torregrande (39°52'00.3"N 8°29'36.6"E), while mullets were obtained from extensive lagoon farms in San Teodoro (40°47'51.7"N 9°40'00.1"E) and S'Ena Arrubia (39°49'19.092"N, 8°33'48.989"E) (Table 2; *Fig. 28*).

Samplings were conducted according to the EU Directive 2010/63/EEC. Institutional ethical approval was not required, as the fish were collected as part of a routine surveillance and health monitoring plan. Fish were euthanized using an overdose of tricaine methanesulfonate (MS-222, Sigma-Aldrich) and transferred on ice to the Department of Veterinary Medicine, University of Sassari (Uniss) for necropsy.

Tissues from the brain, heart, liver, spleen, kidney, intestine, and gonads were collected, and aliquots of each tissue were both fixed in 10% buffered formalin for 48 hours for histopathological analysis and stored at -80°C for microbiological analysis and molecular studies.

2.2.2 Histopathology

For histopathology, a total of 1260 formalin-fixed tissues coming from a total of 240 fish (see *Table 3*) were dehydrated with increasing alcohol concentrations and xylene in an automatic tissue processor, and paraffin-embedded (FFPE). Tissue sections (3 µm) were stained with Hematoxylin and Eosin (H&E) and examined under a light microscope. Specific stains, including Gram, Ziehl-Neelsen (ZN), Giemsa, and Periodic acid–Schiff (PAS), were also employed to detect bacteria associated with granulomatous lesions.

2.2.3 Microbiological analysis

Tissues showing granulomas at histology (brain, heart, liver, spleen, kidney, intestine, and gonads) from seabream, seabass, and mullets were submitted for microbiological analysis at the Fish Diseases Laboratory of the "Istituto Zooprofilattico Sperimentale del Piemonte, Liguria e Valle d'Aosta" (Turin). Organs without granulomas were also included as negative control (see *Table 3*).

For pathogen isolation, fresh frozen (FrFr) tissues were individually suspended in physiological solution (0.8% NaCl) and homogenized using a Sewar Stomacher™ Model 400 circulator lab blender (Thermo Fisher Scientific, Waltham, MA, USA). Approximately 10 µL of the homogenate was inoculated onto Columbia Blood Agar (CBA) and Tryptic Soy Agar (TSA) supplemented with 2% NaCl as the primary isolation media. Plates were incubated at 22 ± 2°C for 72 hours and monitored daily for bacterial growth.

For mycobacteria isolation, organ homogenates were decontaminated with a 1.5% solution of 1-hexadecylpyridinium chloride monohydrate (HPC) for 30 minutes and then centrifuged at 3000 rpm for 20 minutes. A 10 µL pellet from each sample was inoculated onto Löwenstein-Jensen medium (Microbiol, Uta-Cagliari, Italy) and Stonebrink medium (Microbiol) tubes using a sterile loop. Two sets of tubes were prepared for each medium: one set was incubated at 28 ± 1°C and the other at 37 ± 1°C, with daily monitoring for up to 60 days. Colonies were subsequently stained using the ZN technique with cold-modified carbolfuchsin (Kinyoun staining) as described by Sun et al. (2009).

2.2.4 Molecular Biology

2.2.4.1 DNA extraction

DNA was extracted from fresh frozen tissues affected by granulomatous lesions (see *Table 3*). Corresponding organs without granulomas on histology were also included as negative controls. DNA was extracted using QIAGEN DNeasy Blood and Tissue Kit, following the manufacturer's guidelines. The concentration and purity of the extracted DNA were evaluated using a NanoDrop ND-2000 (ThermoScientific) spectrophotometer and the DNA extracts were frozen at −20°C until used.

2.2.4.2 PCR assays and sequencing

PCR assays were performed to identify and molecularly characterize pathogens in granuloma-affected tissues. The primers and targeted genes are detailed in *Table 1*.

Specific methods for each assay are described below:

- ***16S rDNA gene:*** a 1500 bp fragment of the 16S rDNA gene was amplified from tissues using primers described by Weisburg et al. (1991). Each 25 µL reaction mixture included 12.5 µL of 2× Dream Taq Green Master Mix (Thermo Fisher Scientific, USA), 0.2 µM of each primer, 2 µL of bacterial genomic DNA, and RNase-free water to complete the volume. The thermal cycling conditions were as follow: initial denaturation at 95°C for 5 minutes, followed by 35 cycles of 95°C for 30 seconds, 50°C for 35 seconds, and 72°C for 65 seconds, with a final extension at 72°C for 5 minutes. Positive controls (*M. chelonae* DSM 43804) and negative controls (tissues without granulomas and DEPC-treated water) were included to validate results.
- ***hsp65 gene:*** a 441 bp fragment of the *hsp65* gene was amplified from tissues to detect *Mycobacterium spp.* and *Nocardia spp.*, following the protocol of Telenti et al. (1993). Each 50 µL reaction contained 1× reaction buffer (1.5 mM MgCl2), 1× CoralLoad, 200 µM dNTPs, 25 pmol of each primer, 1 U of TopTaq DNA polymerase (Qiagen), and 5 µL of template DNA. The PCR cycling program included an initial denaturation at 93°C for 10 minutes, followed by 45 cycles of 94°C for 1 minute, 60°C for 1 minute, and 72°C for 1 minute, with a final extension at 72°C for 7 minutes. Positive controls (*Mycobacterium marinum* DSM 44344 DNA) and negative controls (tissues without granulomas and DEPC-treated water) were included in each reaction series.
- ***Photobacterium damselae*** **subspecies:** to detect *Photobacterium damselae* and differentiate between the *damselae* and *piscicida* subspecies, two distinct PCR assays were conducted on tissues. A 297 bp fragment of the penicillin-binding protein gene was

amplified for the *piscicida* subspecies, while a 448 bp fragment of the urease C gene was targeted for the *damselae* subspecies. The reaction mixture for both assays was the same as described for the *hsp65* assay adopting primers described by Amagliani et al. (2009) and Osorio et al. (2000). The thermal cycling conditions were as follow: initial denaturation at 95°C for 4 minutes, followed by 50 cycles of 95°C for 30 seconds, 65°C for 30 seconds, and 72°C for 1 minute, with a final extension at 72°C for 10 minutes. Positive controls (*Photobacterium damselae* subsp. *damselae* ATCC 33539 and subsp. *piscicida* ATCC 29688) and negative controls (tissues without granulomas and DEPC-treated water) were included to ensure assay specificity and accuracy.

Amplified DNA fragments were analyzed via electrophoresis on a 2% agarose gel stained with GelRed staining and visualized under UV light. Positive PCR products were purified using the QIAquick Gel Extraction Kit (Qiagen) and sequenced on an ABI PRISM 3500 Genetic Analyzer (Applied Biosystems). Sequence accuracy was verified by manually editing electropherograms with BioEdit v.7.2.5.

To determine sequence similarity, the edited sequences were queried against the GenBank database using the Basic Local Alignment Search Tool (BLAST) available at https://www.ncbi.nlm.nih.gov/.

2.2.4.3 Real-time quantitative PCR (qPCR)

Quantification and detection of *Mycobacterium spp.* DNA in fresh tissues were performed using real-time quantitative PCR (qPCR) targeting the genus-specific *atpE* gene as described by Radomski et al. (2013). Each 12 µL reaction contained 6 µL of TaqMan Environmental Master Mix 2.0 (EMM; Applied Biosystems), 0.25 µM of each primer, 0.05 µM of probe, 5 µL of template DNA, and RNase-free water to complete the volume. *Mycobacterium chelonae* (DSM 43804) was used as a positive control and DEPC-treated H_2O as a negative control. All samples, including positive and negative controls, were run in triplicate. Thermal cycling was conducted

using a QuantStudio3 qPCR System (Thermo Fisher Scientific) under the following conditions: 30 seconds at 60°C, 10 minutes at 95°C, 40 cycles of 15 seconds at 95°C (denaturation) and 60 seconds at 60°C (annealing and extension). The Presence/Absence analysis module was selected for data interpretation. The cycle threshold (Cq) was set at 0.05 ΔRn units, and values above 36 were classified as negative based on a previously established standard curve (detailed in Section 6.3.7) using known quantities of *Mycobacterium* spp. DNA.

Table 1. *List of primers used in this study.*

	Gene name	Primer name	Sequence (5′-3′)	Size	Reference
PCR	16srDNA	20F:	AGAGTTTGATCATGGCTCAG	~1500 bp	Weisburg et al., 1991
		1500R	GGTTACCTTGTTACGACTT		
	Hsp65	Tb11	ACCAACGATGGTGTGTCCAT	~441 bp	Telenti et al., 1993
		Tb12	CTTGTCGAACCGCATACCCT		
	penicillinbinding protein (1A)	PdP_F	CCGACTCAACTACAGATCACCCAGTC	297 bp	Amagliani et al. 2009
		PdP_R	GTGCGGCCTAAATTTCGACGA		
	UreasiC	UreC_F	TCCGGAATAGGTAAAGCGGG	448 bp	Osorio et al. 2000
		UreC_R	CTTGAATATCCATCTCATCTGC		
qPCR	*atpE*	atpE_F	CGGYGCCGGTATCGGYGA	182 bp	Radomski et al., 2013
		atpE_R	CGAAGACGAACARSGCCAT		
		probe PatpE	ACSGTGATGAAGAACGGBGTRAA		

2.3 Results

2.3.1 Prevalence of granulomatous infections in fish

Histopathological evaluation revealed a high prevalence of granulomas among the examined fish species, with mullets being the most affected (93%), followed by gilthead seabream (42%), and European seabass (30%) (see *Table 2*).

Below, in detail the number of visceral granulomas associated to bacteria in fish (see *Table 3*).

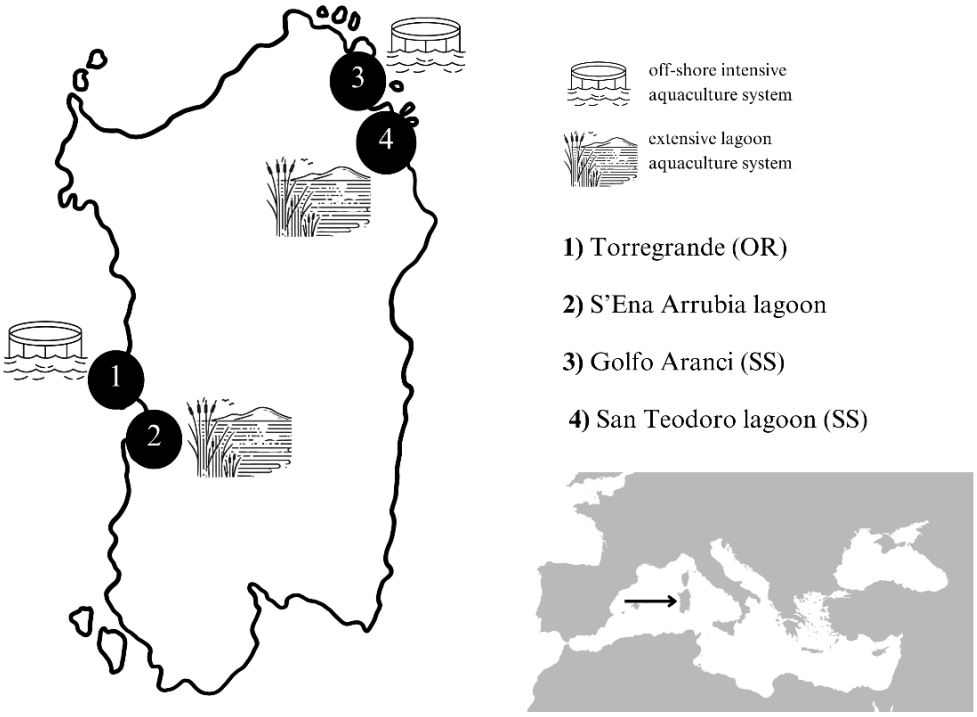

Figure 28. *Study area and sampling sites.*

Table 2*. Prevalence of granulomatous lesions in histology in sampled fish associated with parasites.*

Fish species	**Site of sampling**	**Sampled fish**	**Fish with granulomas**	**Fish with parasites associated granulomas**
Dicentrarchus labrax	Torregrande[1] Golfo Aranci[3]	60	18/60 (30%)	14/18 (78%)
Sparus aurata	Torregrande[1] Golfo Aranci[3]	60	25/60 (42%)	19/25 (76%)
Mugilidae	S'Ena Arrubia[2] San Teodoro[4]	60	56/60 (93%)	50/56 (91%)
Tot.		180	99/180 (75%)	83/99 (84%)

Table 3. *Number of visceral granulomas in total organs associated with bacteria in fish. Microbiology, acid fast, and molecular biology assays were performed based on histopathology results.*

Fish species	**Histology**	**Microbiology positivity**	**Acid fast positivity**	**Molecular biology (PCR + qPCR)**
Dicentrarchus labrax	19/420 (4.5%)	0/19	0/19	0/19
Sparus aurata	63/420 (15%)	0/63	0/63	0/30*
Mugilidae	77/420 (18.3%)	3/77 (4%) 3/3 *M. chelonae*	1/77 positivity (1%)	2/30* (6%) 1 Enterovibrio + 1 *Photobacterium damselae*
Organs	219/1260 (17%)			

*Based on histopathology, 30 representative tissues were selected for molecular biology investigations

2.3.2 Mullets

2.3.2.1 Gross examination

Among the 60 mullet specimens, at postmortem examination, no external clinical signs were observed in the majority of fish, except for a single individual presenting a skin erosion and hemorrhage on the caudal fin (*Fig. 29*).

Figure 29*. Mullet with skin erosion and hemorrhage (arrow) on the caudal fin.*

2.3.2.2 Histopathology results

Granulomas were detected mostly on the kidney (n=29), followed by the liver (n=19), spleen (n=7), intestine (n=6), gonads (n=4), heart (n=2), and brain (n=1).

Microscopically, the affected organs were characterized by a multifocal expansion of the parenchyma due to nodular formations compatible with granulomas. These structures, ranging from 200 to 900 microns in diameter, consisted of a large center containing abundant eosinophilic granular material intermixed with numerous cellular debris and surrounded by multiple layers of spindle cells (*Fig. 30A*). Multifocal aggregates of melanomacrophages were also observed within the affected tissues (*Fig. 30D*). Gram, PAS, and Giemsa stains tested negative in all evaluated sections except for ZN that identified the presence of red, rod-shaped, acid-fast bacilli within granuloma in one spleen.

In addition, parasites were associated with granulomas at different stages of severity in 50/56 (91%) of the specimens affected by granulomas. Trematode metacercariae, within cystic structures, were identified in the kidney, spleen, and liver (*Fig. 30C*). These structures were mixed with mild to moderate inflammation. Furthermore, myxozoa parasites measuring 100 to 450 microns and containing variable numbers of spores were detected within tissues or melanomacrophage centers (*Fig. 30B-D*).

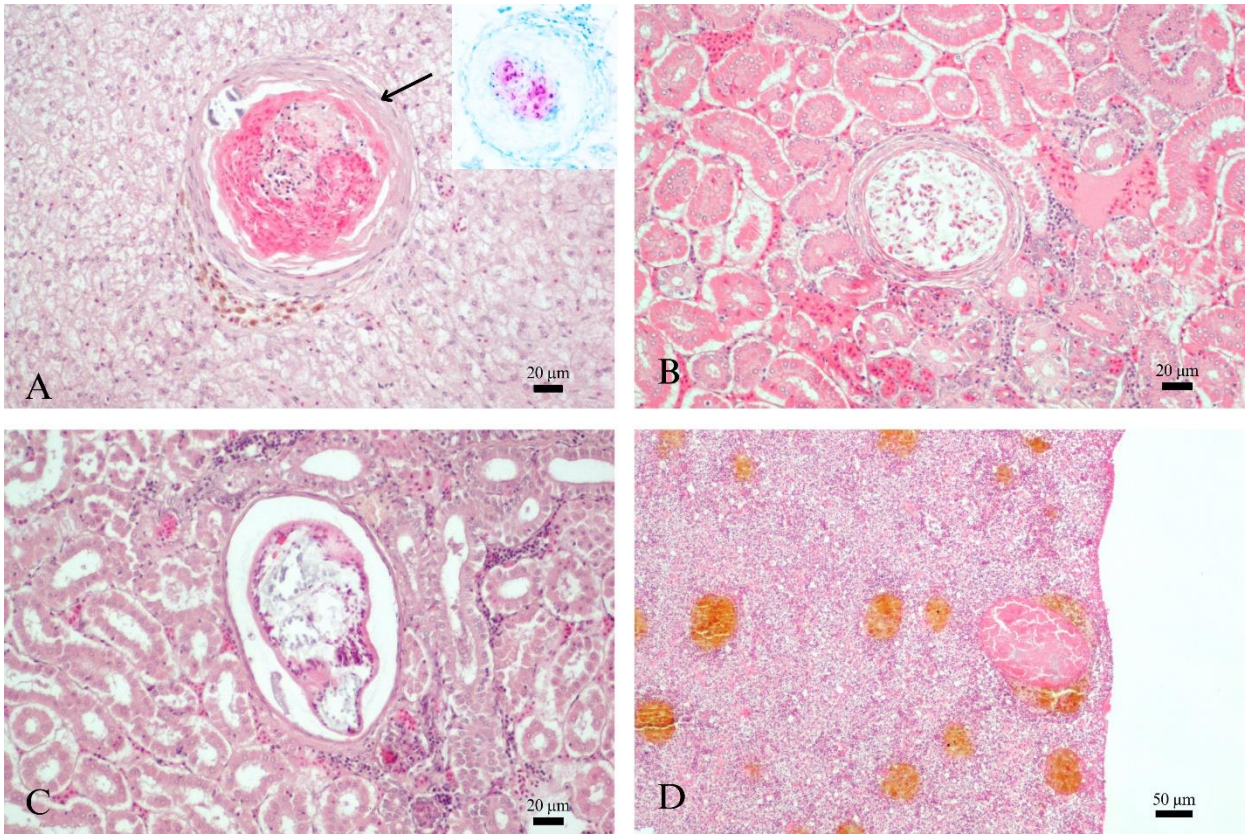

***Figure 30**. Histopathological features of granulomatous lesions in affected mullet tissues. (A) Granuloma with central eosinophilic granular material (necrosis) and peripheral spindle cell layers (arrow); i*nset: ZN staining revealing Acid-Fast bacilli. *(B) Myxozoa parasites within a granuloma in a kidney. (C) Trematode metacercariae encysted in tubular renal tissue. (D) Multifocal melanomacrophage aggregates in affected spleen tissue. Hematoxylin and eosin (H&E) staining.*
Scale bars: 20 µm (A–C), 50 µm (D)

2.3.2.3 Microbiology results

Colonies have grown from cultured spleen in 3 out of 60 (5%) mullets and were clearly visible in Löwenstein-Jensen and Stonebrink media tubes (*Fig. 31A*), showing acid-fast bacilli at Kinyoun staining (*Fig. 31B*). All the other samples were negative for the presence of other bacteria.

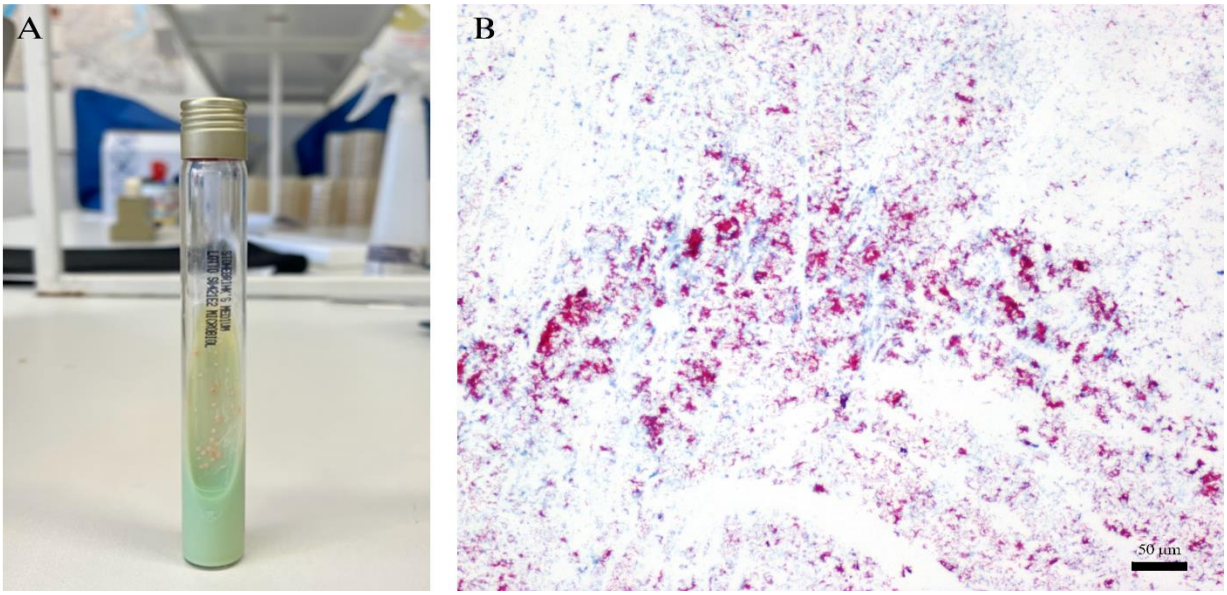

***Figure 31**. (A) Colonies (yellowish in color) of Mycobacterium spp. in Löwenstein-Jensen tube. (B) Colonies with fite Faraco Stain showing acid fast bacilli.*

2.3.2.4 Molecular Analyses results

Sequencing from 16S rDNA PCR identified *Enterovibrio* sp. and *Photobacterium damselae* sp. with 95.4% and 95.5% of identity respectively in two out of sixty livers. Moreover, *hsp65* confirmed the presence of *Mycobacterium* spp in three out sixty spleens.

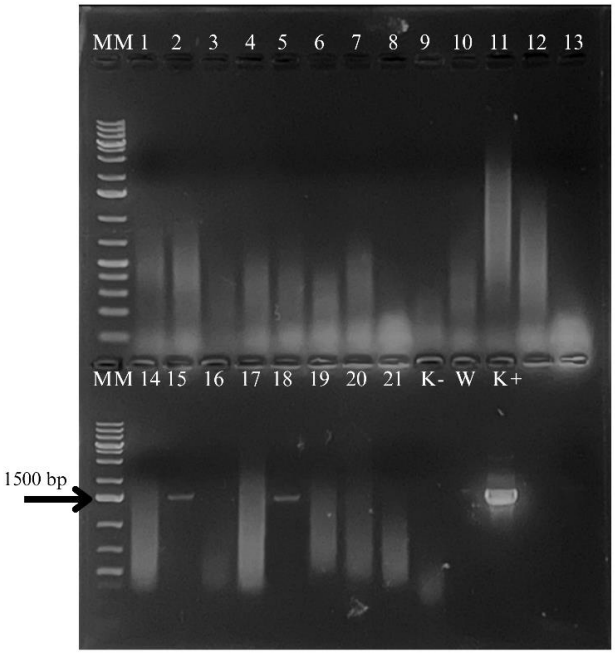

Figure 32. *16S rDNA amplicons (1500 bp) from granuloma-affected organs in mullets. Samples 15 and 18 correspond to liver tissues, where Enterovibrio sp. and Photobacterium damselae sp. were identified. (MM = 1 Kb plus; K-: organs without granuloma; W: DEPC treated water; K+ = M. chelonae DNA)*

Moreover, sequencing from *hsp65* PCR identified *Mycobacterium* spp. in 5% of affected specimens, sharing 99–100% identity with *Mycobacterium chelonae* strains in GenBank. The *atpE* qPCR tested positive from a spleen (the same one that tested positive at ZN staining in histopathology) with a Ct average value of 34.4.

2.3.3 Gilthead Seabream (Sparus aurata)

2.3.3.1 Gross Examination

No visible external abnormalities were observed in the examined seabream specimens (*Fig.* 33A). Upon opening the coelomic cavity, 4 out of 60 specimens (6.6%) displayed marked splenic anomalies. In one particularly severe case, the spleen was firmly adhered to the surrounding adipose tissue, showing extensive fibrosis and calcified nodules.

The spleen appeared significantly enlarged showing numerous, multifocal to coalescing, firm nodules of variable sizes, ranging to 1-2 mm in diameter (*Fig. 33B*).

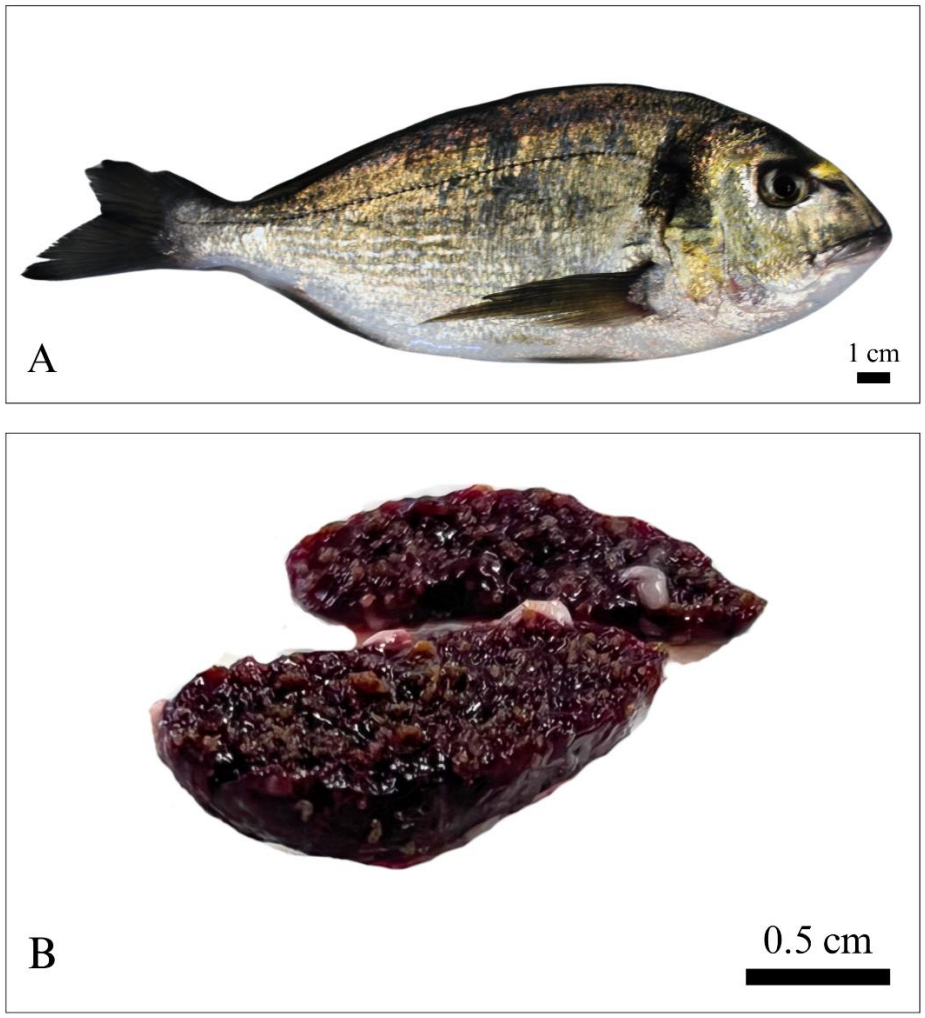

Figure 33. *(A) Ghilthead seabream (Sparus aurata) specimen with no external clinical signs.. (B) Spleen showing numerous multifocal to coalescing, firm nodules of variable sizes.*

2.3.3.2 Histopathology

Granulomas were detected mostly in the kidney (n=11), followed by the spleen (n=9), liver (n=8), heart (n=4), gonads (n=2), and intestine (n=1). Histological examination revealed focal granulomatous myocarditis in the heart, with nodular structures ranging from 200 to 900 µm in diameter. These nodules were characterized by eosinophilic granular material mixed with cellular debris and multiple layers of spindle cells. In the liver, moderate chronic granulomatous hepatitis

were observed. Fibrosis of the bile ducts and eosinophilic hepatitis were noted in association with granulomas caused by myxozoa parasites.

Severe chronic multifocal granulomatous oophoritis was detected in two gonads. The intestine showed diffuse eosinophilic enteritis. The spleen showed multifocal to coalescent eosinophilic inflammation within the parenchyma, surrounded by scattered melanomacrophage centers. The eosinophilic material appears amorphous and variably sized, with some areas showing central necrosis (*Fig. 34A*).

The kidney displayed multifocal eosinophilic glomerulonephritis and granulomas associated with myxozoa parasites (*Fig. 34B*). Parasites were associated with granulomas at different stages of severity in 23/25 (92%) of the specimens affected by granulomas.

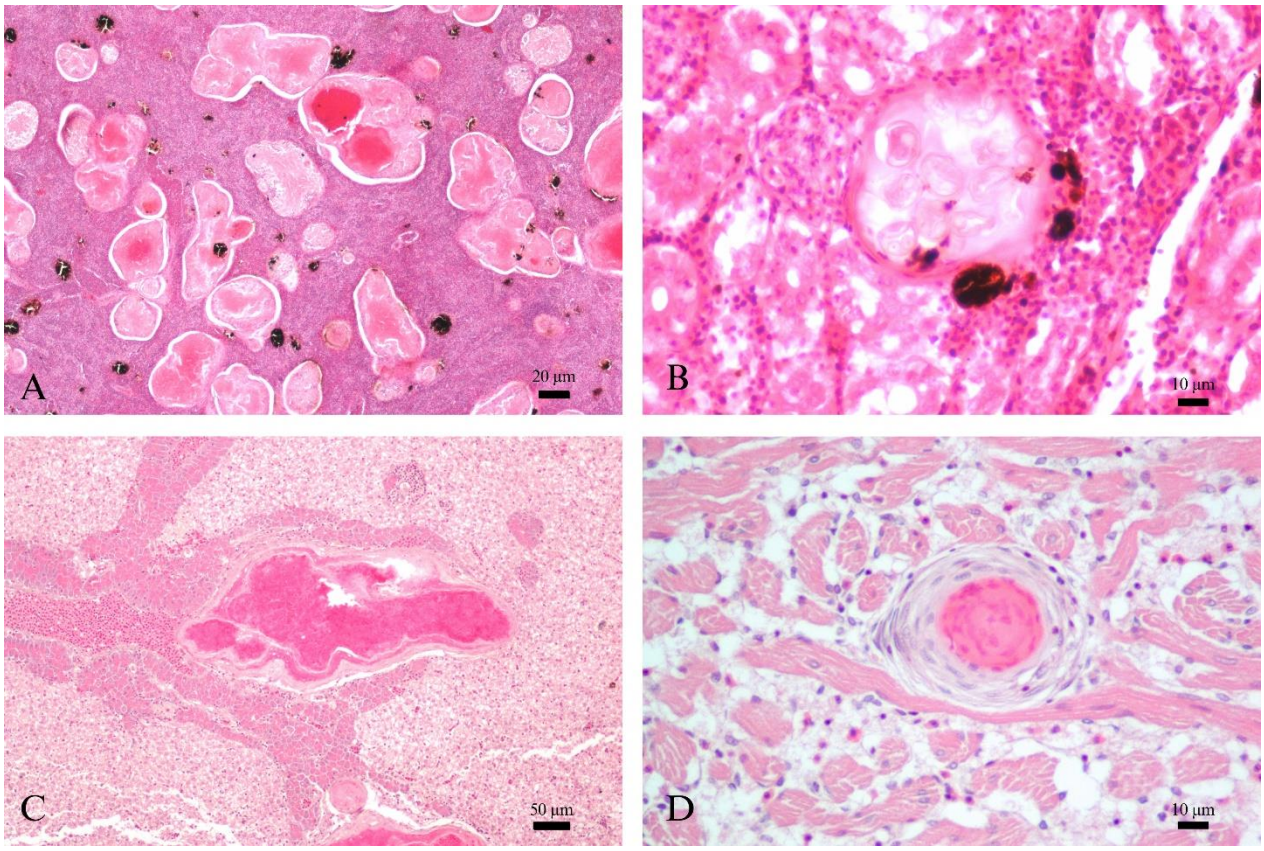

Figure 34. *A) Multifocal irregular in shape granulomas in the spleen (same subject of figure33 B). B) Kidney section showing focal granuloma associated with myxozoa parasite, surrounded by melanomacrophage and multifocal glomerulonephritis. C) Liver. Focal granuloma within hepatopancreatic tissue. D) Heart. Focal granuloma in the heart. Hematoxylin and eosin (H&E) staining. Scale bars: 20 µm (A), 10µm (B-D), 50 µm (C).*

2.3.3.3 Microbiological and Molecular Analyses

No bacteria were recovered in the inoculated Columbia Blood Agar, TSA (2% NaCl) in Löwenstein-Jensen or Stonebrink medium. Furthermore, all samples tested negative in molecular assays.

2.3.4 European Seabass (Dicentrarchus labrax)

2.3.4.1 Gross Examination

No external signs of disease were detected in the examined seabass specimens, except for severe hyperemia observed in the operculum and fins in 1/60 specimens.

Figure 35. *European seabass (Dicentrarchus labrax) from intensive aquaculture system with severe hyperemia in the operculum and fins.*

2.3.4.2 Histopathology

Granulomas were detected mostly on the kidney (n=8) being the most affected organ, followed by the gonads (n=3), liver (n=2), spleen (n=1), heart (n=1), and brain (n=1).

Trematode metacercarie were identified in kidney, spleen, and liver (*Fig. 36A*) within cystic structures often mixed with mild to moderate inflammation. Furthermore, myxozoa parasites measuring 100 to 450 microns and containing variable numbers of spores were detected within tissues or melanomacrophage centers (*Fig. 36B*). In most cases, granulomas showed signs of mineralization and calcification.

Parasites were associated with granulomas in 15/18 (83%) of the specimens affected by granulomas.

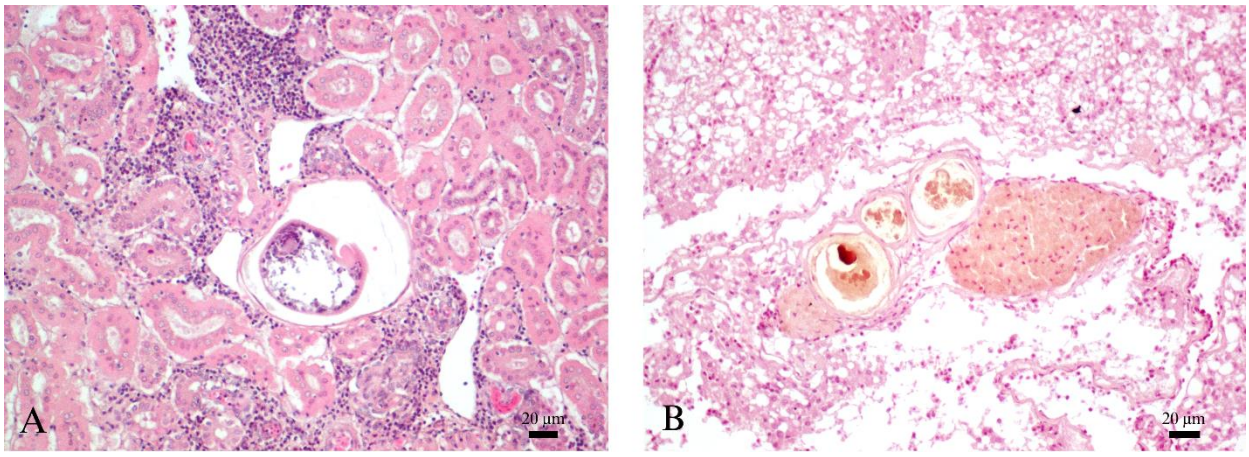

Figure 36. *A) Trematode metacercaria encisted in the kidney of European seabass . B) Multifocal granulomas in European seabass liver associated with myxozoa parasites admixed to calcification close to a melanomacrophagic center. Hematoxylin and eosin (H&E) staining. Scale bars: 20 µm (A-B)*

2.3.4.3 Microbiological and Molecular Analyses

No bacteria were recovered in the inoculated Columbia Blood Agar, TSA (2% NaCl) in Löwenstein-Jensen or Stonebrink medium. All samples also tested negative in molecular assays.

2.4 Discussion

This study explored granulomas in organs of farmed fish species in Sardinia, investigating the etiology and variability in prevalence among these species.

Mullets emerged as the fish with the highest number of granulomas (93%), where the kidney was the most affected organ by granulomas (48%). Pathogenic bacteria were isolated in only 5% of the specimens with granulomas, identified as *Mycobacterium chelonae*. The isolation of this microorganism in mullets confirms their role in granulomatous diseases (Delghandi et al., 2020), supporting previous studies in mullets in Sardinia (Antuofermo et al., 2017).

Molecular analysis identified in liver (3%) other bacteria belonging to *Enterovibrio* and *Photobacterium damselae* species.

Interestingly, the highest percentage of granulomas (91%) were associated with trematode and myxozoan parasites, suggesting that the etiology of granulomatous diseases in mullets is mostly due to parasites infection. This result aligns with previous studies from other authors that reported Mugilidae as a widely parasitized species (Paperna et al., 1981; Polinas et al. 2021). Parasites such as trematodes and myxozoa, are commonly found in Sardinian brackish waters and other Mediterranean regions, where mullets is an intermediate hosts. Moreover, the detritivorous diet of mullets increases exposure to parasite carriers such as gastropods, invertebrates, and small crustaceans, which may harbor spores or larval stages, ultimately leading to infections and granulomatous inflammation.

Nevertheless, coinfection with bacteria should also be considered (Martinez-Lara et al., 2020; Dezfuli et al., 2023).

In contrast, the incidence of granulomas in intensively farmed gilthead seabream and European seabass was lower (42% and 30%, respectively), with no pathogenic bacteria detected through microbiological analyses or molecular methods. However, the results in both species were similar to mullets, with granulomas primarily associated with parasites (92% for seabream and 83% for seabass) where myxozoan and other species such as *Polysporoplasma sparis*, were found.

The fact that bacteria were not detected in seabream and seabass samples could be attributed to the stage of granulomas, where pathogen may not be longer viable, complicating isolation and detection (Ramírez-Castillo et al., 2015). On the other hand, the lack of detectable pathogens in seabream and seabass reared in intensive offshore systems is encouraging and likely reflects effective management practices, including optimal stocking densities, stringent biosecurity protocols, and good water exchange, which appear to limit pathogen proliferation and support fish health (Morro et al., 2022).

2.5 Conclusion

In conclusion, this study evaluated the incidence of granulomatous diseases in economically significant fish species farmed in Sardinia. These results suggest a multifactorial etiology for granulomatous diseases, mostly including parasites.

The scarcity of bacteria associated with granulomas emphasizes the positive impact of good aquaculture practices adopted by Sardinian farms, demonstrating that the sector can serve as a promising strategy for economic development while balancing environmental sustainability, fish health, and productivity.

However, the isolation of atypical mycobacteria in mullets with granulomas poses significant concerns for their zoonotic potential risks for fisheries and aquaculture workers.

References

Amagliani, G, E Omiccioli, F Andreoni, R Boiani, I Bianconi, R Zaccone, M Mancuso, and M Magnani. 2009. "Development of a Multiplex PCR Assay for *Photobacterium damselae* Subsp. Piscicida Identification in Fish Samples." Journal of Fish Diseases 32 (8): 645–53. https://doi.org/10.1111/j.1365-2761.2009.01027.x.

Antuofermo, E, A Pais, M Polinas, T Cubeddu, M Righetti, M A Sanna, and M Prearo. 2017. "Mycobacteriosis Caused by *Mycobacterium marinum* in Reared Mullets: First Evidence from Sardinia (Italy." Journal of Fish Diseases 40 (ue 3): 327–37. https://doi.org/10.1111/jfd.12515.

Austin, Brian, and Dawn A. Austin. 2016. Bacterial Fish Pathogens. NA. Vol. NA. Cham: Springer International Publishing. https://doi.org/10.1007/978-3-319-32674-0.

Carvalho, N, and J Guillen. 2021. Aquaculture in the Mediterranean. Barcelona, Spain: IEMed. https://www.iemed.org/publication/aquaculture-in-the-mediterranean/.

Delghandi, Mohammad Reza, Mansour El-Matbouli, and Simon Menanteau-Ledouble. 2020. "Mycobacteriosis and Infections with Non-Tuberculous Mycobacteria in Aquatic Organisms: A Review." Microorganisms. MDPI AG. https://doi.org/10.3390/microorganisms8091368.

Kumar, Sudhir, Glen Stecher, and Koichiro Tamura. 2016. "MEGA7: Molecular Evolutionary Genetics Analysis Version 7.0 for Bigger Datasets." Molecular Biology and Evolution 33 (7): 1870–74. https://doi.org/10.1093/MOLBEV/MSW054.

Lionello, Piero, and Luca Scarascia. 2018. "The Relation between Climate Change in the Mediterranean Region and Global Warming." Regional Environmental Change 18 (5): 1481–93. https://doi.org/10.1007/s10113-018-1290-1.

Martínez-Lara, Pablo, Marcel Martínez-Porchas, Teresa Gollas-Galván, Jorge Hernández-López, and Glen R. Robles-Porchas. 2021. "Granulomatosis in Fish Aquaculture: A Mini Review." Reviews in Aquaculture. Wiley-Blackwell. https://doi.org/10.1111/raq.12472.

Morro, Bernat, Keith Davidson, Thomas P. Adams, Lynne Falconer, Max Holloway, Andrew Dale, Dmitry Aleynik, et al. 2022. "Offshore Aquaculture of Finfish: Big Expectations at Sea." Reviews in Aquaculture 14 (2): 791–815. https://doi.org/10.1111/raq.12625.

Nichols, Gordon, Iain Lake, and Clare Heaviside. 2018. "Climate Change and Water-Related Infectious Diseases." Atmosphere 9 (10): 385. https://doi.org/10.3390/atmos9100385.

Osorio, CR, AE Toranzo, JL Romalde, and JL Barja. 2000. "Multiplex PCR Assay for UreC and 16S RRNA Genes Clearly Discriminates between Both Subspecies of *Photobacterium damselae*." Diseases of Aquatic Organisms 40 (1): 177–83. https://doi.org/10.3354/dao040177.

Paperna, I, and Robin M Overstreet. 1981. "Parasites and Diseases of Mullets (Mugilidae." Manter Laboratory of Parasitology 579. https://doi.org/https://digitalcommons.unl.edu/parasitologyfacpubs/579.

Polinas, Marta, Francesc Padrós, Paolo Merella, Marino Prearo, Marina Antonella Sanna, Fabio Marino, Giovanni pietro Burrai, and Elisabetta Antuofermo. 2021. "Stages of Granulomatous

Response Against Histozoic Metazoan Parasites in Mullets (Osteichthyes: Mugilidae)." Animals 11 (6): 1501. https://doi.org/10.3390/ani11061501.

Radomski, Nicolas, Adélaïde Roguet, Françoise S. Lucas, Frédéric J. Veyrier, Emmanuelle Cambau, Héberte Accrombessi, Régis Moilleron, Marcel A. Behr, and Laurent Moulin. 2013. "AtpE Gene as a New Useful Specific Molecular Target to Quantify Mycobacterium in Environmental Samples." BMC Microbiology 13 (1). https://doi.org/10.1186/1471-2180-13-277.

Rajme-Manzur, David, Teresa Gollas-Galván, Francisco Vargas-Albores, Marcel Martínez-Porchas, Miguel Ángel Hernández-Oñate, and Jorge Hernández-López. 2021. "Granulomatous Bacterial Diseases in Fish: An Overview of the Host's Immune Response." Comparative Biochemistry and Physiology -Part A : Molecular and Integrative Physiology 261 (November). https://doi.org/10.1016/j.cbpa.2021.111058.

Ramírez-Castillo, Flor, Abraham Loera-Muro, Mario Jacques, Philippe Garneau, Francisco Avelar-González, Josée Harel, and Alma Guerrero-Barrera. 2015. "Waterborne Pathogens: Detection Methods and Challenges." Pathogens 4 (2): 307–34. https://doi.org/10.3390/pathogens4020307.

Sayyaf Dezfuli, Bahram, Massimo Lorenzoni, Antonella Carosi, Luisa Giari, and Giampaolo Bosi. 2023. "Teleost Innate Immunity, an Intricate Game between Immune Cells and Parasites of Fish Organs: Who Wins, Who Loses." Frontiers in Immunology 14 (1): 417–34. https://doi.org/10.3389/fimmu.2023.1250835.

Sun Shan-Shan; Lee Shih-Yi; Lu Jang-Jih, Jun-Ren; Hsieh. 2009. "Evaluation of Cord Formation in Kinyoun-Stained Smears of MGIT Cultures as a Rapid Identification Method for Mycobacterium Tuberculosis Complex." Journal of Rapid Methods & Automation in Microbiology 17 (3): 339–49. https://doi.org/10.1111/j.1745-4581.2009.00157.x.

Telenti, A, F Marchesi, M Balz, F Bally, E C Böttger, and T Bodmer. 1993. "Rapid Identification of Mycobacteria to the Species Level by Polymerase Chain Reaction and Restriction Enzyme Analysis." Journal of Clinical Microbiology 31 (ue 2): 175–78. https://doi.org/10.1128/jcm.31.2.175-178.1993.

Weisburg, W G, S M Barns, D A Pelletier, and D J Lane. 1991. "16S Ribosomal DNA Amplification for Phylogenetic Study." Journal of Bacteriology 173 (ue 2): 697–703. https://doi.org/10.1128/jb.173.2.697-703.1991.

Chapter III

https://doi.org/10.3390/vetsci11120597

3. Systemic granulomatosis in the meagre *Argyrosomus regius*: fishing for a plausible etiology.

3.1 Introduction

Meagre (*Argyrosomus regius*) is one of the fast-growing species considered for sustainable aquaculture development along the Mediterranean and Eastern Atlantic coasts (Monfort, 2010; Duncan et al. 2013). In 2022, the global production of meagre amounted to 49,723.58 tonnes of live weight, primarily concentrated in Europe, contributing 11,430.68 tonnes (FAO, 2024). Greece led European production with 5,697.02 tonnes (49.83%), followed by Spain with 4,524.93 tonnes (39.59%), Croatia with 1,085.74 tonnes (9.50%), and Italy with 123 tonnes (1.08%) (FAO, 2024). Despite meagre production increasing, farms face significant challenges due to systemic granulomatosis (SG), a prevalent disease of unknown etiology that hampers growth and production performance (Ghittino et al. 2004; Katharios et al. 2011; Tsertou et al. 2018).

Systemic granulomatosis is a chronic condition characterized by low mortality, high prevalence and severity, and non-specific clinical signs and gross changes such as emaciation, skin erosion, and exophthalmia. The disease is marked by multifocal white nodules visible throughout the viscera, particularly in the kidney, spleen, and liver (Ghittino et al. 2004). Microscopically, the nodules correspond to granulomas consisting of aggregates of epithelioid cells arranged in concentric layers around a necrotic core, which may become calcified over time and surrounded by spindle cells. As the condition progresses, these nodules can advance to form larger inflammatory foci because of granulomas merging, leading to significant growth impairment and reduced production performance (Ghittino et al. 2004; Katharios et al. 2011; Gustinelli et al. 2021; Rajme-Manzur et al. 2021; Pavloudi et al. 2023).

Although SG is a disease of unknown aetiology, two possible causes are thought to be related to the appearance of the disease: an infectious agent or a nutrient deficiency (Ghittino et al. 2004;

Katharios et al. 2011; Avsever et al. 2014; Timur et al. 2015; Ruiz et al. 2018; Tsertou et al. 2018; Ruiz et al. 2019; Pavloudi et al. 2023; Pfalzgraff et al. 2023).

Recent studies have explored the impact of nutritional factors on SG incidence. Specifically, Ruiz and co-authors (2018, 2019) evaluated how antioxidants, particularly vitamins E and C, and variations in diet composition affect granuloma development in meagre. *Artemia* spp.-fed larvae was found to decrease the incidence of granulomas and reduce thiobarbituric acid-reactive substances (TBARS) levels, which improved growth and survival. Furthermore, an association between SG and larval oxidative status was identified, with diets high in docosahexaenoic acid (DHA) and low in vitamin E correlating with a higher frequency of granulomas and increased lipid peroxidation in meagre larvae (Ruiz et al. 2018, 2019). Recent findings revealed a higher incidence of granulomas in meagre fed with lower concentrations of long-chain polyunsaturated fatty acids (Pfalzgraff et al. 2023). Furthermore, Pavloudi and co-authors (2023) conducted metagenomic analyses on meagre kidney tissues revealing distinct microbial profiles in healthy and granuloma-affected tissues, identifying specific operational taxonomic units (OTUs) enriched in diseased fish, though none were linked to known granuloma-causing species (Pavloudi et al. 2023).

On the other hand, *Photobacterium damselae* subsp. *piscicida* (Costa et al. 2017; Labella et al. 2011) and *Nocardia* spp. have been reported in diseased meagre (Elkesh et al. 2012; Acosta et al. 2024), and their role as etiological agents of SG has been investigated (Tsertou et al. 2018). Several other bacterial species have been associated with granulomas in fish (Rajme-Manzur et al. 2021), and nontuberculous mycobacteria (NTM) have been frequently reported in aquaculture outbreaks in the Mediterranean Sea (Antuofermo et al. 2017; Carella et al. 2019; Mugetti et al. 2020). Increases in water temperature, coupled with high stocking densities typical of intensive marine cages aquaculture, are suspected to increase the frequency and intensity of disease outbreaks, including piscine mycobacteriosis (Cascarano et al. 2021; Falkinham, 2022).

From a histological point of view, the maegre's SG mirrors mycobacteriosis in fish, a systemic infectious disease caused by NTM that leads to the formation of multiple granulomas, particularly in the kidney, liver and spleen (Delghandi et al. 2020; Rajme-Manzur et al. 2021).

Mycobacteriosis caused by *Mycobacterium marinum* infections was first described in farmed meagre, in Turkey in 2014, with subsequent cases documented in the same region in 2015 (Avsever et al. 2014; Timur et al. 2015). More recently, *M. pseudoshottsii* was isolated from a meagre presenting granulomas in a Greek aquaculture farm (Stathopoulou et al. 2020).

Several NTM mycobacterial species have been associated with mycobacteriosis in fish, including *M. marinum*, *M. chelonae*, and *M. fortuitum*, as well as other species such as *M. shottsii*, *M. pseudoshottsii*, *M. ulcerans*, *M. abscessus*, *M. salmoniphilum*, *M. haemophilum*, and *M. gordonae* (Decostere et al. 2004; Francis-Floyd et al. 2011; Delghandi et al. 2020). In particular, *M. chelonae* was identified in a wide range of aquatic environments, affecting both freshwater and marine fish species, including salmonids (Bruno et al. 1998; Nguyen et al. 2021), sturgeons (Antuofermo et al. 2014), mugilidae (Varello et al. 2010), and several ornamental species (Zanoni et al. 2008).

Isolation of Mycobacteria may be challenging due to the fastidious nature and slow growth of *Mycobacterium* spp. and their peculiar cell wall (Delghandi et al. 2020). Isolation typically requires nutrient-rich and sometimes selective media such as Löwenstein-Jensen and Stonebrink. Colonies can take 2 to 28 days to form, sometimes requiring 2 to 3 months of incubation to rule out infection. Histologically, most mycobacteria are regarded as acid-fast positive typically stained with Ziehl-Neelsen (ZN) or Fite-Faraco, however depending on species and bacterial load, acid-fast negative granulomas can be found. Molecular diagnostics methods typically target different Mycobacteria conserved regions of the heat shock protein 65kD gene (*hsp65*), the exported repeated protein (*erp*), the RNA polymerase B subunit (*rpoB*), and others (Delghandi et al. 2020). The detection of pathogenic agents such as acid-fast mycobacteria within granulomas can be sometimes challenging (Cribier et al. 2011; Crothers et al. 2020). Nevertheless, the presence of NTM and other etiologic agents within affected tissues by PCR alone does not

necessarily prove a link between agents and diseases. To solve this problem in *situ* hybridization (ISH) techniques have been largely used in mammals and recently ISH has emerged as a powerful tool to detect and localize specific RNA or DNA sequences within fish tissues (Jensen, 2014; Adams et al. 2011; Fritsvold et al. 2022).

This study aimed at exploring a mycobacteria etiology in systemic granulomatosis by using 34 adult's meagres from an offshore aquaculture facility in Sardinia, Italy. Histological, metagenomic, microbiological, and molecular analyses, including in *situ* hybridization, were conducted to assess any possible link between SG-granulomas and NTM, in particular *M. chelonae*.

3.2 Materials and methods

3.2.1 Sample collection and gross examination

In June 2022, 34 seemingly healthy adult meagres (*Argyrosomus regius*) were collected from an offshore aquaculture facility located in Sardinia, Italy. The facility maintained a stocking density of 10-20 kg/m³, with water salinity levels between 37-40 ‰, and a surface temperature of 25 ± 1.0°C. The adult fish averaged 34.5 ± 3.5 cm in total length and 389 ± 67 g in total weight. Fish were euthanized by an overdose of tricaine methanesulfonate MS222 (MS-222, Sigma-Aldrich). The sampling was performed in accordance with the EU Directive 2010/63/EEC. For this study, ethical approval from an institutional ethical committee was not required because all the fish examined were collected as a part of a plan of surveillance and sanitary controls on fish health.

Necropsies of fish were performed at the Department of Veterinary Medicine, Sassari University, and aliquots of fish tissues (i.e., brain, heart, liver, spleen, kidney, and intestine) were frozen at -80°C (FrFr) for molecular and microbiological analysis or fixed in 10% buffered formalin for 48 h for histopathology.

3.2.2 Histopathology

For histopathology, 34 adults' meagre formalin-fixed tissues were dehydrated with increasing alcohol concentrations and xylene in an automatic tissue processor, and paraffin-embedded (FFPE). Sections of 3 μm thickness were obtained with a microtome (RM2245, Leica Biosystems, Wetzlar, Germany) and stained with hematoxylin and eosin (HE) in an automatic multistainer (ST5020, Leica Biosystems, Wetzlar, Germany). Slides were then evaluated at light microscopy (Nikon Eclipse 80i, Amsterdam, Netherlands). Additionally, ZN, PAS and Giemsa staining was performed to rule out the occurrence of acid-fast organisms, fungi, or parasites.

3.2.3 Metagenomic analysis

Based on histopathological analyses confirming the presence of evident granulomas in multiple organs, brain, heart, spleen, kidney and intestine tissues of a meagre were tested by 16S ribosomal rRNA PCR (Takahashi et al., 2014) and sequencing.

Briefly, DNA extracted with a DNeasy Blood and Tissue Kit (Quiagen), amplified as described, treated with Thermolabile Exonuclease I (NEB) and finally used in Illumina Nextera XT indexing. Afterwards, sample DNA concentrations were normalized to equal concentrations. Paired-end sequencing was performed on the MiSeq platform (Illumina, San Diego, CA, USA) with the v3-600 cycles chemistry.

Sequencing data were analyzed as previously reported using the operational taxonomic unit (OTU) approach, with 97% sequence similarity, using the Qiime2 package v. 2019.10 and Greengenes v. 13.8 database (Bolyen et al., 2019; Banchi et al., 2023). Graphical representations were created using GraphPad Prism (version 8.0.2, GraphPad Software, La Jolla, CA USA).

3.2.4 Microbiological analysis and nontuberculous mycobacterial (NTM) culture screening

Microbiological analysis was performed on kidneys of 33 out of the 34 of meagre. Aseptically collected kidneys were initially homogenized in 0.8% NaCl solution and a sterile loop with ~10

µL was inoculated in Columbia Blood Agar (CBA) and Tryptic Soy Agar (TSA) supplemented with 2% NaCl as the primary isolation media. Plates were incubated at 22 ± 2 °C for a total of 72 hours, with daily checks for bacterial growth.

Additionally, liver, brain, heart, spleen, and intestine tissues from 33 out of the 34 meagres, were individually suspended in a physiological solution and homogenized using a Seward™ Stomacher™ Model 400 circulator lab blender (Thermo Fisher Scientific, Waltham, MA, USA). Following decontamination with a 1.5% solution of 1-hexadecylpyridinium chloride monohydrate (Thermo Scientific) for 30 minutes, the homogenates were centrifugated at 3000 rpm for 20 minutes. A 10 µL pellet was then inoculated onto Löwenstein-Jensen medium (Microbiol, Uta-Cagliari, Italy) and Stonebrink medium (Microbiol) tubes using a sterile loop. Two tubes were prepared for each medium; one set was incubated for 60 days at 28 ± 1°C and the other at 37 ± 1°C, with daily monitoring. The colonies were stained using ZN technique with cold-modified carbolfuchsin (Kinyoun staining) (Sun et al., 2009). The meagre that was submitted to metagenomic analysis did not undergo microbiology.

3.2.5 Molecular identification of Mycobacterium spp.

DNA extraction

DNA extraction was performed from 34/34 FFPE and FrFr livers of meagre with SG and 30/34 FrFr kidneys with SG. Based on histology, 3/34 meagre did not show granulomas and livers from these were used as negative controls. For the FFPE tissues, 15 sections of 3 µm in thickness were obtained with a Leica RM2245 microtome (Leica Biosystems, Nussloch, Germany) and placed into 1.5-mL sterile microtubes. To avoid cross-contamination, the samples were collected using disposable gloves and masks. The blades were changed for each FFPE block, while the microtome, instruments, and all work surfaces were cleaned with 70% ethanol. The sections were then deparaffinized using xylene. Briefly, the sections were submerged in 1 ml of xylene vortexed

and centrifuged at 10,000 x g for 10 min. The xylene was carefully removed, and the tissue was washed twice with 100% ethanol to remove any residual xylene and centrifuged at 14,000 x g for 5 minutes to pellet the tissue. Following the ethanol washes, the tissue pellets were air-dried at 37 °C for 15-20 minutes to evaporate any remaining ethanol and subjected to DNA extraction using QIAGEN DNEasy Blood and Tissue kit according to the manufacturer's instructions. For the 30 FrFr kidneys, DNA extraction was also performed using the QIAGEN DNEasy Blood and Tissue kit following the manufacturer's instructions. DNA concentration and purity were assessed using a NanoDrop ND-2000 (ThermoScientific).

Polymerase chain reaction (PCR)

Molecular identification and characterization of pathogens were conducted using PCR amplification and sequencing of the 65-kDa heat shock protein (*hsp65*) gene on both 34/34 FFPE and FrFr livers. Meagres without granulomas (3/34) were used as negative controls. The amplification of a ~441 bp fragment of the *hsp65* gene was carried out according to Telenti et al. (1993). The PCR mix contained 1 x reaction buffer (with 1.5 mM MgCl2), 1 x CoralLoad, 200 mM dNTP, 25 pmoles of each primer, 1U TopTaq DNA polymerase (Qiagen), and 200 ng of total DNA in 50 µl of reaction. PCR amplification consisted of an initial denaturation at 93°C for 10 minutes, followed by 45 cycles of 94°C for 1 minute, 60°C for 1 minute, and 72°C for 1 minute, with a final extension at 72°C for 7 minutes. PCR products were analyzed by 2% agarose gel electrophoresis, and fragments were detected using GelRed staining and a UV transilluminator. *Mycobacterium marinum* (DSM 44344) was used as a positive control. DNA isolated from meagres without granulomas and DEPC-treated H_2O were used as negative controls.

The positive PCR products were gel purified using the QIAquick Gel Extraction Kit (Qiagen) and confirmed by sequencing on an ABPRISM 3500 Genetic Analyser (Applied Biosystem). The electropherograms were manually edited for sequence accuracy using BioEdit v. 7.2.5 (Hall, 1999). Subsequently, the sequences were queried against GenBank's Basic Local Alignment and

Search Tool (BLAST) at https://www.ncbi.nlm.nih.gov/ to identify closely related sequences. For phylogenetic analysis, MEGA v.7 software was employed (Kumar et al., 2016). The phylogenetic tree was constructed using the maximum-likelihood method, and evolutionary distances were calculated utilizing the Kimura 2-parameter model with 1000 bootstrap replicates

Real-time quantitative PCR (qPCR)

Detection and quantification of *Mycobacterium* spp. DNA was performed on 30/34 FrFr kidneys from SG-affected meagre samples using qPCR, targeting the genus-specific *Mycobacterium atpE* gene according to Radomski et al. (2013). Samples that underwent metagenomic and kidneys from meagre without granulomas were not included. The 12 µl reactions consisted of 6 µl TaqMan Environmental Master Mix 2.0 (EMM; Applied Biosystems), 0.25 µM of each primer and 0,05 µM of probe, 5 µl of template DNA, and RNase free water to volume. *Mycobacterium chelonae* (DSM 43804) was used as a positive control and DEPC-treated H_2O as a negative control. All samples, including positive and negative controls, were run in triplicate. Cycling conditions were as follows: 30 s at 60°C, 10 min at 95°C followed by 40 cycles of 15 s at 95°C (denaturation), 60 s at 60°C for the annealing and 30s at 60°C of final extension. All qPCRs were analyzed using the QuantStudio3 qPCR System (Thermo Fisher Scientific). Cycle threshold line was set at 0.05 ΔRn units; Cq values above 36 were considered negative. All primers used for molecular analysis are listed in Table 4.

Table 4. Primers used in this study for molecular analyses.

	Gene name	Primer name	Sequence (5′-3′)	Reference
Metagenomic	*16S rRNA*	Pro341F	TCGTCGGCAGCGTCAGATGTGTATAAGAGACAGCCTACGGGNBGCASCAG	Takahashi et al. 2014
		Pro805R	GTCTCGTGGGCTCGGAGATGTGTATAAGAGACAGGACTACNVGGGTATCTAATCC	
PCR	*Hsp65*	Tb11	ACCAACGATGGTGTGTCCAT	Telenti et al. 1993
		Tb12	CTTGTCGAACCGCATACCCT	
qPCR	*atpE*	FatpE	CGGYGCCGGTATCGGYGA	Radomski et al. 2013
		RatpE	CGAAGACGAACARSGCCAT	
		probe PatpE	ACSGTGATGAAGAACGGBGTRAA	

3.2.6 In situ Hybridization Assay

Manual RNAscope assay was set up and performed at the Department of Veterinary Medicine-University of Sassari on FFPE of the 30/34 SG-affected meagre using BaseScopeTM v2 Assay (cod. # 322350, Bio-Techne, Milan, Italy) according to the manufacturer's protocol. Briefly, after deparaffinization and rehydration steps, tissues were immerged in a solution of 1% SDS containing 200 mM of boric acid, pH 7.0 at room temperature followed by ½ hour a 37°C in the same solution. Then slides were washed 3 times with 0.2% Tween-20 - PBS. Tissue sections were treated with RNAscope® Hydrogen Peroxide (Bio-techne, Milan, Italy) for 10 min at room temperature. Target retrieval was performed for 15 min at 100–104°C. Probes were then hybridized for 2 h at 40°C followed by RNAscope amplification and red chromogenic detection. Sections were counterstained with hematoxylin and mounted with Bio-Mount (Bio-Techne, Milan, Italy).

In this study, the following RNAscope probes were used: probe encodes for B-*Mycobacterium chelonae*-16SrRNA targeting 169-209 of DQ866772.1. (cod. # 1301541-C1, Bio-Techne, Milan, Italy) and dihydrodipi-colinate reductase (dapB), a bacterial gene (cod. #310043, Bio-Techne, Milan, Italy) as negative control probe.

As a positive control of the probe encodes for B-*M. chelonae*-16SrRNA targeting 169-209 of DQ866772.1, a FFPE goldfish *Carassius auratus* block experimentally infected with *M. chelonae* kindly provided by the Aquatic Animal Health Laboratory at the School of Veterinary Medicine, University of California-Davis was used.

3.3 Results

3.3.1 Gross examination

At gross examination, exophthalmia and skin hyperemia were observed in 5/34 (15%) meagres (*Fig. 37 A*), whereas 1/34 (2%) exhibited macroscopic multifocal white, slide raised, 0.2 x 0.2 cm ovoidal nodules both in the posterior kidney and in the heart (*Fig. 37 B*).

Figure 37*. (**A**) Affected meagre showing bilateral exophthalmia. (**B**) Heart of meagre with visible white nodules (white arrows) on the epicardium. Bar: 0.2 cm.*

3.3.2 Histopathology

Histopathological examination revealed the presence of multifocal granulomas in 31/34 (91%) adult meagres. The kidney was the most affected organ (30/34; 88%), followed by the liver (16/34; 47%), the heart (14/34; 41%), the intestine (6/34; 18%), and the brain (2/34; 6%) (*Fig. 38 A-B*). Notably, 3/34 (9%) meagre specimens were negative for granulomas in all examined organs and were considered non-SG-affected fish.

Microscopically, the parenchyma was characterized by severe granulomatous inflammation with the presence of multiple, 200 to 900 microns of diameter, nodules. Granulomas were characterized by a central region rich in abundant eosinophilic granular material, intermixed with numerous cellular debris (lytic necrosis) and surrounded by multiple layers of epithelioid cells and a rim of elongated spindle cells (*Fig. 38 C*). No lymphoplasmacytic inflammation was noticed. ZN staining (*Fig. 38 D*), as well as PAS and Giemsa tested negative in all evaluated organs and sections.

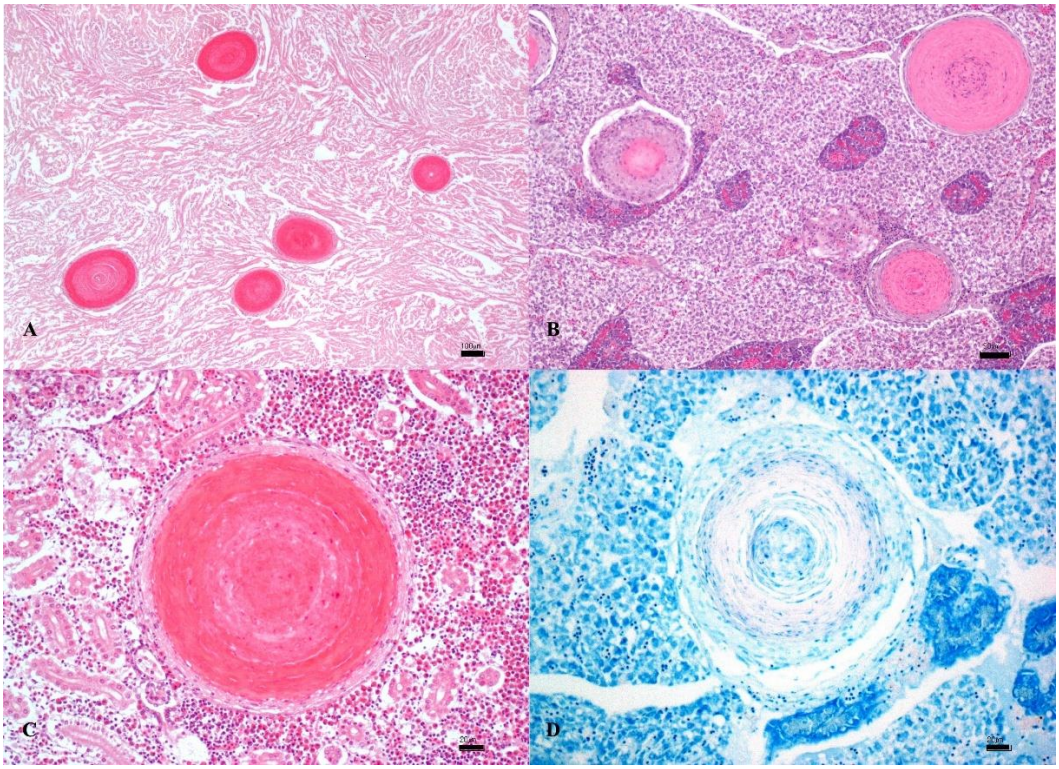

Figure 38. *(**A**) Multifocal granulomas in the heart (H&E). (**B**) Multifocal granulomas in the liver (H&E). (**C**) High power field of a granuloma in the kidney characterized by a necrotic hypereosinophilic centre surrounded by epithelioid and spindle cells arranged in concentric layers (H&E.). (**D**). Negative Ziehl-Neelsen stain of a granuloma in the kidney (ZN). Scale bars: 100 µm (A-B), 20µm (C-D).*

3.3.3 Metagenomic analysis

The metagenomic analysis, along with unclassified species, showed that the most predominant phyla were Proteobacteria (88.6% for the intestine, 24.1% for the brain, 37.2% for the heart, 14.1% for the kidneys) and Bacteroidetes (46.8% for the spleen), followed by Firmicutes (31.6% for the heart, 12.3% for the kidneys, 9.4% for the brain, 7.7% for the intestine, 31.9% for the spleen). In the phylum Proteobacteria, the most predominant class was Gammaproteobacteria (43.9% for the intestine, 33.4% for the heart, 18.9% for the brain, 11.2% for the kidneys, 8.2% for the spleen), with the most abundant species *Sulfitobacter donghicola* (41.7%) for the intestine, *Faecalibacterium prausnitzii* (4.9%) for the kidney, *Acinetobacter johnsonii* (18.2%) for the heart, and *Veillonella dispar* (0.6%) in the spleen.

In the phylum Firmicutes, the most predominant classes were Bacilli (31.5% in the heart), Alphaproteobacteria (41.7% in the spleen and 7.7% in the intestine), and Clostridia (10.1% in the kidney and 7.8% in the brain). The most abundant species were Acin*etobacter lwoffii* (12.9%) in the heart, *Chitinibacter tainanensis* (1.4%) across various organs, and *Bacteroides uniformis* (0.6%) in the kidney. For Bacteroidetes, Bacteroidia was the class with the most reads for the spleen with the most abundant species *Faecalibacterium prausnitzii* (11.6%) (*Fig.39*).

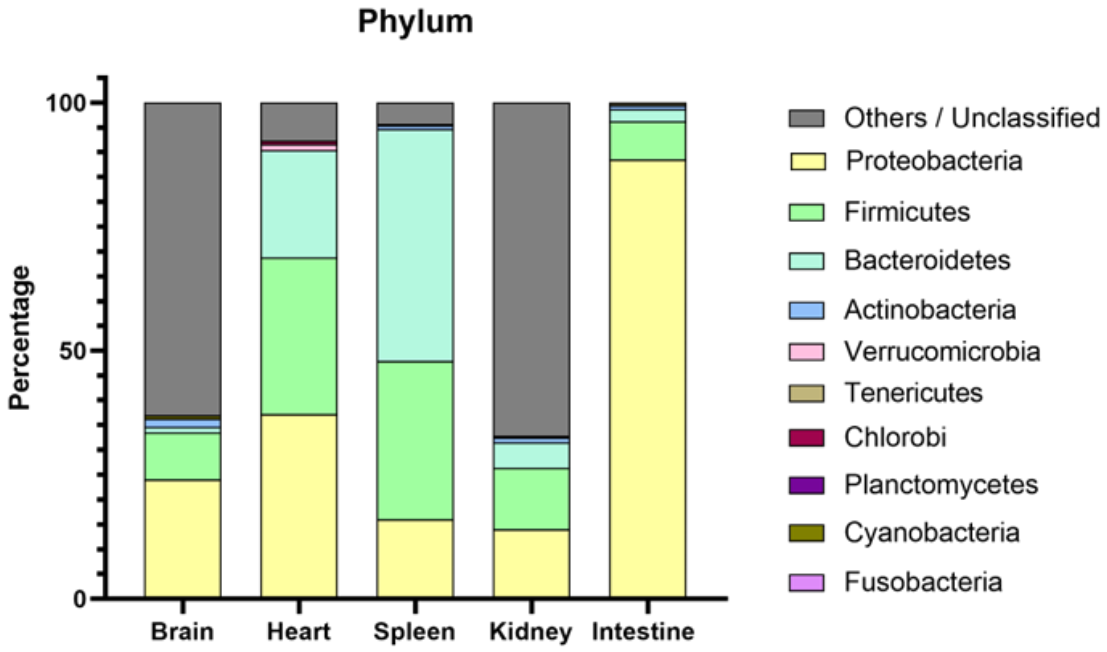

Figure 39. *Bar chart illustrating the relative abundance (in percentage) of the main microbial taxa at the phylum level in the brain, heart, spleen, kidney, and intestine of a meagre affected by SG.*

3.3.4 Microbiological analysis

No bacteria were recovered in the inoculated CBA, TSA (2% NaCl) in Löwenstein-Jensen or Stonebrink medium.

3.3.5 Molecular detection and identification of Mycobacterium spp.

From PCR analysis, 7/34 (20%) FFPE livers as well as 6/34 (18%) FrFr livers showed a ~ 440bp band. The PCR products were purified and sequenced, and electropherograms were edited for sequence accuracy and were aligned. *Mycobacterium chelonae* was detected in 5/31 (16%) SG-affected meagre, and in particular in 4/31(13%) FFPE livers and in 4/31(13%) livers FrFr of SG-affected meagre (*Table 5; Fig.40*). Mycobacteria sequences share 99-100 % nucleotide identity with *hsp65* of *Mycobacterium chelonae* strains available on GenBank database. The derived sequences were submitted to GenBank and their accession numbers are PQ340275-PQ340276-PQ340277-PQ340278-PQ340279. The *atpE* qPCR resulted negative for *Mycobacterium* spp. detection in all the tested kidneys.

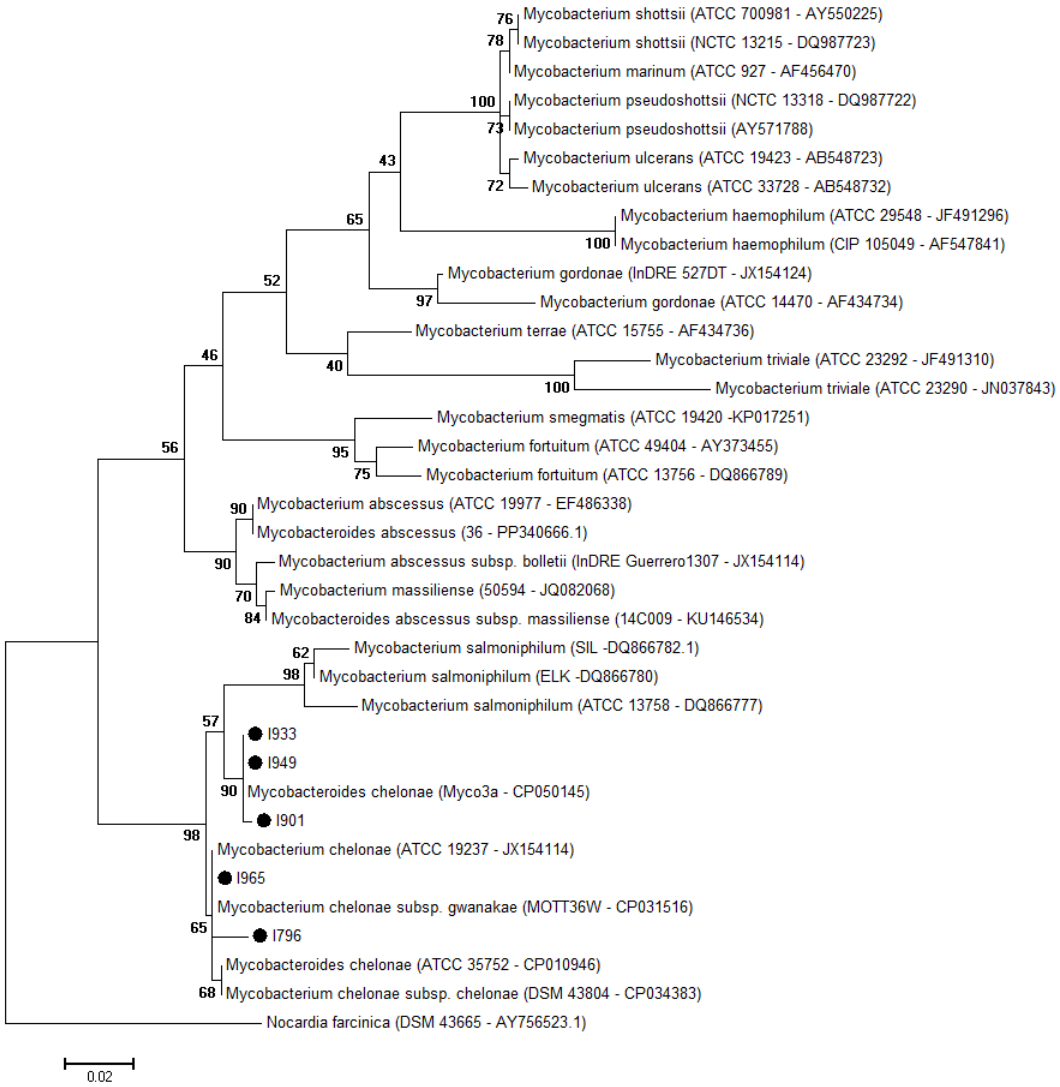

Figure 40. *Maximum Likelihood tree shows how the hsp65 sequences obtained from SG-affected meagre cluster with the Mycobacterium chelonae. Nocardia farcinica was selected as outgroup. The other sequences are the most probable species causing mycobacteriosis in fish. Evolutionary analyses were conducted in MEGA7, performed using Maximum Likelihood method, Tamura-Nei model, bootstrap 1000 replicates.*

3.3.6 Association between Histology and Mycobacteriun chelonae

In 16/31 (52%) livers showing granulomas from meagre with SG, *M. chelonae* was detected in 4/16 (25%) samples, whereas *M. chelonae* was not identified in 15/31 (48%) in non-affected livers, both FFPE and FrFr, except for one case (1/15; 0.6%) (Table 2).

Table 5. *Association between granulomas in meagre's livers, PCR and sequencing.*

Meagres Id	Liver Granulomas	PCR *hsp65* (FFPE)	PCR *hsp65* (FrFr)	Sequencing
1	Yes	-	-	
2	Yes	+	+	***Mycobacterium chelonae***
3	Yes	+	-	*Propionibacterium*
4	Yes	+	+	*Corynebacterium*
5	Yes	-	-	
6	No	-	-	
7	No	-	-	
8	No	-	-	
9	No	-	-	
10	No	-	-	
11	Yes	-	-	
12	Yes	-	-	
13	**No**	+	+	***M. chelonae***
14	Yes	+	+	*Propionibacterium*
15	Yes	-	-	
16	No	-	-	
17	Yes	+	-	***M. chelonae***
18	Yes	-	-	
19	Yes	+	+	***M. chelonae***
20	Yes	-	+	***M. chelonae***
21	No	-	-	
22	No	-	-	
23	Yes	-	-	
24	No	-	-	
25	Yes	-	-	
26	No	-	-	
27	Yes	-	-	
28	No	-	-	
29	No	-	-	
30	No	-	-	
31	Yes	-	-	
32	No	-	-	
33	No	-	-	
34	No	-	-	

FFPE: Formalin-Fixed and paraffin-embedded tissue; FrFr: fresh-frozen

3.3.7 In situ Hybridization Assay

No positive ISH signals were observed in any of the meagre evaluated organs, whereas in the control tissues of the *Carassius auratus* experimentally infected with *M. chelonae* numerous, 1-2 micron in length, bacillary rods inside a granuloma were observed (*Fig. 41 A-B*).

A summary of the results obtained by histopathological examination, microbiology, PCR and ISH is presented in *Table 6.*

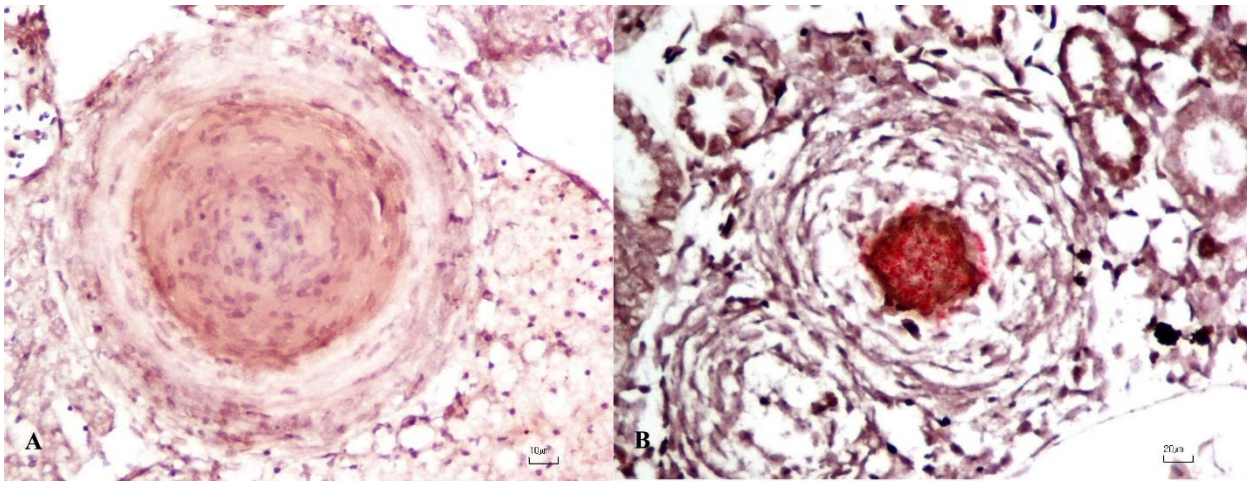

Figure 41. *ISH (Red chromogen. Hematoxylin counterstain)* ***(A)*** *Granuloma in meagre's liver without ISH signals (Hematoxylin counterstain).* ***(B)*** *Numerous red rods (inside a granuloma of a Carassius auratus experimentally infected with M. chelonae. Scale bars: 20 µm (A-B).*

Table 6. Summary of the results obtained by histopathological examination, microbiology, PCR and ISH.

Analysis	**Results**	**Meagre**
Histopathology	Presence of granuloma	31/34
Histochemistry	Ziehl-Neelsen, positivity in granulomas	0/34
Microbiology	Bacteria and mycobacteria isolation	0/33
qPCR in kidney	*atpE* qPCR +	0/30
PCR FrFr livers	*Hsp65* PCR +	8/34
	M. chelonae	4/8
PCR FFPE livers	*Hsp65* PCR +	7/34
	M. chelonae	4/7
ISH	*M. chelonae* +	0/30

3.4 Discussion

Granulomatous diseases in fish are commonly associated with chronic infections and inflammatory responses to persistent antigens, often caused by bacteria, fungi, or non-infectious agents.

The meagre, a valuable aquaculture species, has been observed to develop systemic granulomatosis (SG), characterized by the widespread formation of granulomas in multiple organs, prompting this investigation into its underlying causes and manifestations. However, SG, characterized by forming granulomas in multiple organs, poses a challenge in diagnosing and managing affected fish populations. The study focused on describing gross findings, histopathology, metagenomic analysis, microbiology, and molecular identification of SG disease in maegre.

However, it is important to highlight the limitation of using only meagre from a single farm sampled at one single time point. Nevertheless, this approach served to reduce confounding variables such as environmental factors (water quality, surface temperature, salinity), involving different farms and different sampling periods, allowing for a more focused analysis of SG disease aetiology and manifestation in meagre.

Gross examination revealed exophthalmia and skin hyperemia in 5 out of 34 meagres. Similar aspecific signs have been reported in various fish species suffering from systemic infections, including those caused by *Mycobacterium* spp. and other pathogens (Delghandi et al. 2020).

Histopathological analysis further confirmed the presence of granulomas characterized by a central region of eosinophilic granular material and cellular debris, surrounded by multiple layers of epithelioid cells and spindle cells in different organs, with the kidney being the most affected (30/34), followed by the liver (16/34) and heart (14/34). Granulomas in the kidney, liver, and heart align with findings in other studies on fish granulomatous diseases, where these organs are commonly affected (Gustinelli et al. 2021). Furthermore, while the kidney is often reported as a

primary site of granulomatous inflammation, the prevalence of granulomas in the heart and liver observed in this study is relatively high compared to some reports, which may suggest species-specific responses or environmental factors influencing disease manifestation (Decostere et al. 2004; Roberts, 2012; Noga, 2010; Austin and Austin, 2016). Likewise, as previously described by other authors, no acid-fast bacteria, fungi, or parasites were observed within the granulomas in our study using histological staining including ZN (Ghittino et al. 2004; Avsever et al. 2014; Timur et al. 2015; Katharios et al. 2011; Ruiz et al. 2018; Tsertou et al. 2018; Ruiz et al. 2019;).

Granuloma's pathogenesis is variable and of a complex nature, and granuloma can be defined as a localized inflammation or a hypersensitive reaction to substances leading to different layers of macrophages (Decostere et al. 2004). Etiologies of granulomatous disorders can be divided into infectious and noninfectious causes (autoimmune conditions, toxins, body reactions, etc.) (Aubry, 2012). In some cases, it is hard to distinguish infectious from noninfectious granulomas. However, pathologists agree that when granulomas exhibit a necrotic "core" extracellular bacteria can persist surrounded by cellular necrotic debris. Accordingly, in our study, the histopathological pattern of the disease with the necrosis centrally located in meagre's granulomas directs the investigations towards identifying target pathogen-causing granulomas in fish (Aubry et al. 2012).

Metagenomic analyses revealed the prevalence of various bacterial phyla in different organs reflecting the complex microbiota associated with granulomatous inflammation. Bacteroidetes were predominant in the spleen, while Proteobacteria were more common in other organs. Firmicutes were also significantly present, whereas Actinobacteria had a low prevalence in the kidney, the most affected organ. Of note, the low prevalence of Actinobacteria, particularly *Mycobacterium* spp., despite their known pathogenicity, would decrease their likelihood as a cause of SG (Gauthier & Rhodes, 2009; Maboni et al. 2024). These data do not differ from what has been recently proposed by Pavloudi et al. (2023), suggesting that a "new" pathogenic bacteria species or a single predominant pathogen is not present in SG. Although their specific roles remain to be elucidated, this diverse bacterial community might contribute to the observed granulomatous

inflammation, and their presence in significant proportions implies potential interactions with the host immune system that may exacerbate inflammation. Although the metagenomic experiment was conducted in a representative case of meagre affected by SG involving multiple organs including the brain, we had to be aware of the inherent limitations of these studies regarding the single case used for metagenomics analysis.

Furthermore, culture, which remains the gold standard in cases of bacteria-causing diseases, tested negative for bacteria and mycobacteria in our work. The absence of cultivable bacteria might indicate that the granulomas had a non-bacterial etiology. However, many pathogens, including certain species of *Mycobacterium*, exhibit stringent growth requirements or are slow-growing, which may not be met by conventional culture media (Forbes et al. 2018; Delghandi et al. 2020). Overall, culture supports the hypothesis that mycobacteria were not the causative agents of the granulomas, although granulomas without visible acid-fast bacilli have been reported in several experimentally infected species (Colorni et al. 1998; Watral and Kent, 2007; Gauthier et al. 2009). Nevertheless, molecular diagnostic methods are now considered the most practical and efficient approach to detect and identify mycobacteria at the species level, mainly overcoming the limitations of culture and biochemical tests (van Ingen et al. 2013). These PCR methods may involve the amplification of DNA from fresh, frozen, or ethanol-preserved tissues and often target highly discriminatory regions, such as *hsp65*, *rpoB*, and the 16S–23S internal transcriber spacer (McNabb et al. 2004; Meritet DM et al. 2017; Delghandi et al. 2020). In our study, PCR targeting the *hsp65* gene of mycobacteria yielded positive results in a subset of FFPE and FrFr liver samples, with sequencing identifying *M. chelonae* in 4/34 FFPE and FrFr liver samples.

Mycobacterial infections in fish are frequently reported in both wild and farmed species, across marine and freshwater environments (Colorni et al. 1998; Decostere et al. 2004; Beran et al. 2006; Volpe et al., 2019; Mandrioli et al., 2022). Less frequent cases of systemic mycobacteriosis caused by *M. marinum* were reported in the meagre (Avsever et al. 2014; Timur et al. 2015). However,

to our knowledge, *M. chelonae* has not been previously identified in farmed meagres showing systemic granulomas.

On the other hand, in our study, the qPCR analysis targeting the *atpE* gene for *Mycobacterium* spp. quantification in kidney samples tested negative, not supporting the SG infection caused by NTM (atypical mycobacteria, as reported by Avsever et al. (2014) and Timur et al. (2015).

Previous studies have compared methods of detecting mycobacteria in fish tissues, including histological and bacteriological examination and nucleic acid-based techniques (Knibb et al. 1993, Kaattari et al. 2005). However, Gauthier and co-authors (2009) pointed out several drawbacks in the different detection methods due to their focus on varying biological phenomena. Histological methods can identify disease and infection but are not powerful in cryptic infections in which the pathogen is undetectable in the histological sections and not cultivable.

Bacteriological examinations detect culturable organisms, indicating the presence of live bacteria capable of multiplying and infecting new hosts. However, as suggested by Pourahmad and co-authors (2014), a robust immune response in fish might resolve an active mycobacterial infection, rendering the bacteria nonviable and unculturable.

Conversely, molecular methods detect mycobacterial DNA without confirming bacterial viability or disease presence. In such cases, significant amounts of mycobacterial DNA might still be detected by PCR, indicating mycobacteriosis even if the bacteria are no longer viable (Pourahmad et al. 2014).

Overall, different scenarios are therefore possible, including infection due to some cryptic bacteria, a state of non-infection but with mycobacterial DNA present within affected tissue, as well granulomas caused by noninfectious agents (Gauthier et al. 2009).

In addition to SG, a well known condition in fish pathology named visceral granulomatosis exists, as aspecific tissue response to numerous aetiologic agents, of which Mycobacteria are most recognized and described in the literature; in the study about doctor fish (*Garra rufa*, Heckel., 1843), granulomas were detected in all of the batches analysed and *Mycobacterium* antigens have

been immunohistochemically (IHC) labelled, confirming their presence within pathologic tissue (Volpe et al., 2019), stressing the relevance to flank an in *situ* technique as IHC to histochemistry and/or molecular analyses, especially in research or from the field studies.

Moreover, the diagnostic challenge of mycobacteria in the case of granulomas containing few bacilli has driven pathologists to the increased use of RNA scope. This technique is highly sensitive and specific, using a unique probe design to amplify target RNA signals, allowing for the detection and visualization of a colorimetric signal within formalin-fixed paraffin-embedded tissue samples.

In this study, the decisive value of RNAscope was demonstrated on various granuloma-affected meagre organs, including the kidneys, liver, heart, and intestine showing that mycobacterial RNA was not detected, although *M. chelonae* DNA was detectable in a few liver samples.

The goal of this study was achieved in particular due to the set-up of ISH. The absence of specific ISH signal reinforce the lack of association between mycobacteria and granulomas and confirms that there was no active infection or significant bacterial load in tissues examined of meagre affected by SG.

3.5 Conclusions

Meagres may be affected by various classical bacterial diseases (e.g., vibriosis, photobacteriosis, mycobacteriosis, nocardiosis, etc.), viral infections (e.g., betanodaviruses, etc.), and parasitic diseases (e.g., monogenean trematodes, etc.) (Lopez-Jimena, 2010; Soares et al., 2018; Tedesco et al., 2022)

However, SG in meagres is still regarded as a non-infectious condition forming granulomas ZN negative, potentially stemming from unproven nutritional or autoimmune causes.

We can conclude that, while *Mycobacterium chelonae* DNA can be detected within granulomas-affected tissue, it is unlikely that this mycobacterium is the causative agent of SG in meagres.

Searching for infectious agents causing granulomas can be increased by straight sampling directly on granuloma by microscopic examination, molecular detection or NGS. Notably, at histopathology, the SG resembles the systemic mycobacteriosis in meagre, caused by *M. marinum* (Delghandi et al. 2020; Rajme-Manzur et al. 2021), this requiring expertise for interpreting the type of granulomas.

Based on these considerations, future studies should be aimed at identifying the diagnostic features in distinguishing between types of granulomas in meagre, considering not only the economic impact but also the potential zoonotic implications of pathogens causing granulomas in meagre.

References

Acosta, Félix, Belinda Vega, Luis Monzón-Atienza, Joshua Superio, Silvia Torrecillas, Antonio Gómez-Mercader, Pedro Castro, Daniel Montero, and Jorge Galindo-Villegas. 2024. "Phylogenetic Reconstruction, Histopathological Characterization, and Virulence Determination of a Novel Fish Pathogen, Nocardia Brasiliensis." *Aquaculture* 581 (December 2023). https://doi.org/10.1016/j.aquaculture.2023.740458.

Adams, A, and K D Thompson. 2011. "Development of Diagnostics for Aquaculture: Challenges and Opportunities." In *Aquaculture Research*, 42:93–102. Hindawi Limited. https://doi.org/10.1111/j.1365-2109.2010.02663.x.

Antuofermo, E, A Pais, and S Nuvoli. 2014. "Mycobacterium Chelonae Associated with Tumor-like Skin and Oral Masses in Farmed Russian Sturgeons (Acipenser Gueldenstaedtii." *BMC Vet Res* 10: 18. https://doi.org/10.1186/1746-6148-10-18.

Antuofermo, E, A Pais, M Polinas, T Cubeddu, M Righetti, M A Sanna, and M Prearo. 2017. "Mycobacteriosis Caused by *Mycobacterium marinum* in Reared Mullets: First Evidence from Sardinia (Italy." *Journal of Fish Diseases* 40 (ue 3): 327–37. https://doi.org/10.1111/jfd.12515.

Aubry, M.-C. 2012. "Necrotizing Granulomatous Inflammation: What Does It Mean If Your Special Stains Are Negative?" In *Modern Pathology*, 25:31–38. Elsevier BV. https://doi.org/10.1038/modpathol.2011.155.

Austin Brian, Austin, and Dawn A. 2016. *Bacterial Fish Pathogens*. *Springer Nature*. 2016th ed. Vol. 27. https://doi.org/10.1145/276305.276383.

Avsever, M. L., M. Z. Günen, S. Eskiizmirliler, B. I. Didinen, G. Erdal, and M. Özden. 2014. "The First Report of *Mycobacterium marinum* Isolated from Cultured Meagre, *Argyrosomus regius*." *Bulletin of the European Association of Fish Pathologists* 34 (4): 343–54. https://avesis.ege.edu.tr/yayin/c1f0d3d5-9fa8-4b98-8622-0e14754686fb/the-first-report-of-mycobacterium-marinum-isolated-from-cultured-meagre-argyrosomus-regius.

Banchi, Penelope, Barbara Colitti, Andrea del Carro, Michela Corrò, Alessia Bertero, Ugo Ala, Angela del Carro, Ann van Soom, Luigi Bertolotti, and Ada Rota. 2023. "Challenging the Hypothesis of in Utero Microbiota Acquisition in Healthy Canine and Feline Pregnancies at Term: Preliminary Data." *Veterinary Sciences* 10 (5): 331. https://doi.org/10.3390/vetsci10050331.

Beran, V, L Matlova, L Dvorska, P Svastova, and I Pavlik. 2006. "Distribution of Mycobacteria in Clinically Healthy Ornamental Fish and Their Aquarium Environment," 383–93.

Bolyen, Evan, Jai Ram Rideout, Matthew R. Dillon, Nicholas A. Bokulich, Christian C. Abnet, Gabriel A. Al-Ghalith, Harriet Alexander, et al. 2019. "Reproducible, Interactive, Scalable and Extensible Microbiome Data Science Using QIIME 2." *Nature Biotechnology* 37 (8): 852–57. https://doi.org/10.1038/s41587-019-0209-9.

Bruno, D. W., J. Griffiths, C. G. Mitchell, B. P. Wood, Z. J. Fletcher, F. A. Drobniewski, and T. S. Hastings. 1998. "Pathology Attributed to Mycobacterium Chelonae Infection among Farmed and Laboratory-Infected Atlantic Salmon Salmo Salar." *Diseases of Aquatic Organisms* 33 (2): 101–9. https://doi.org/10.3354/dao033101.

Carella, F, S Aceto, and F Pollaro. 2019. “A Mycobacterial Disease Is Associated with the Silent Mass Mortality of the Pen Shell Pinna Nobilis along the Tyrrhenian Coastline of Italy.” *Sci Rep* 9: 2725. https://doi.org/10.1038/s41598-018-37217-y.

Cascarano, M. C., Stavrakidis-Zachou, O., Mladineo, I., Thompson, K. D., Papandroulakis, N., & Katharios, P. 2021. “Mediterranean Aquaculture in a Changing Climate: Temperature Effects on Pathogens and Diseases of Three Farmed Fish Species.” *Pathogens* 10 (ue 9): 1205. https://doi.org/10.3390/pathogens10091205.

Colorni, Angelo, Rami Avtalion, Wayne Knibb, Evelyn Berger, Barbara Colorni, and Bracha Timan. 1998. “Histopathology of Sea Bass (*Dicentrarchus labrax*) Experimentally Infected with *Mycobacterium marinum* and Treated with Streptomycin and Garlic (Allium Sativum) Extract.” *Aquaculture* 160 (1–2): 1–17. https://doi.org/10.1016/S0044-8486(97)00234-2.

Costa, J Z, Ú McCarthy, and O Perez. 2017. “Occurrence of *Photobacterium damselae* Subsp. Piscicida in Sea-Cage Farmed Meagre (*Argyrosomus regius*) in Tenerife, Canary Islands, Spain.” *Thalassas* 33: 65–71. https://doi.org/10.1007/s41208-017-0022-5.

Cribier, B., A. Aubry, E. Caumes, E. Cambau, V. Jarlier, and O. Chosidow. 2011. “Aspects Histopathologiques de l’infection *Mycobacterium marinum*.” *Annales de Dermatologie et de Venereologie* 138 (1): 17–22. https://doi.org/10.1016/j.annder.2010.10.025.

Crothers, Jessica W, Alvaro C Laga, and Isaac H Solomon. 2021. “Clinical Performance of Mycobacterial Immunohistochemistry in Anatomic Pathology Specimens: The Beginning of the End for Ziehl-Neelsen?” *American Journal of Clinical Pathology* 155 (1): 97–105. https://doi.org/10.1093/ajcp/aqaa119.

Decostere, A, K Hermans, and F Haesebrouck. 2004. “Piscine Mycobacteriosis: A Literature Review Covering the Agent and the Disease It Causes in Fish and Humans.” *Veterinary Microbiology* 99 (ues 3-4): 159–66. https://doi.org/10.1016/j.vetmic.2003.07.011.

Delghandi, M R, M El-Matbouli, and S Menanteau-Ledouble. 2020. “Mycobacteriosis and Infections with Non-Tuberculous Mycobacteria in Aquatic Organisms: A Review.” *Microorganisms* 8 (ue 9): 1368. https://doi.org/10.3390/microorganisms8091368.

Duncan, N J, A Estévez, H Fernández-Palacios, I Gairin, C M Hernández-Cruz, J Roo, D Schuchardt, and R Vallés. 2013. “Aquaculture Production of Meagre (*Argyrosomus regius*): Hatchery Techniques, Ongrowing and Market.” In *Advances in Aquaculture Hatchery Technology*, 519–41. Elsevier. https://doi.org/10.1533/9780857097460.3.519.

Elkesh, A, K P L Kantham, A P Shinn, M Crumlish, and R H Richards. 2013. “Systemic Nocardiosis in a Mediterranean Population of Cultured Meagre, *Argyrosomus regius* Asso (Perciformes: Sciaenidae.” *Journal of Fish Diseases* 36 (ue 2): 141–49. https://doi.org/10.1111/jfd.12015.

Falkinham, Joseph O. 2022. “Nontuberculous Mycobacteria in the Environment.” *Tuberculosis* 137 (September): 28–31. https://doi.org/10.1016/j.tube.2022.102267.

F.A.O. n.d. “FishStatJ, a Tool for Fishery Statistics Analysis Release: 4.04.00.” https://www.fao.org/fishery/statistics/software/fishstatj/en.

Forbes, Betty A., Geraldine S. Hall, Melissa B. Miller, Susan M. Novak, Marie Claire Rowlinson, Max Salfinger, Akos Somoskövi, David M. Warshauer, and Michael L. Wilson. 2018.

"Practice Guidelines for Clinical Microbiology Laboratories: Mycobacteria." *Clinical Microbiology Reviews* 31 (2). https://doi.org/10.1128/CMR.00038-17.

Francis-Floyd, R. 2011. "Mycobacterial Infections of Fish." United States Department of Agriculture, National Institute of Food and Agriculture. https://srac.msstate.edu/pdfs/Fact Sheets/4706 Myobacterial Infections of Fish.pdf.

Fritsvold, C, A B Mikalsen, Ø Haugland, H Tartor, and H Sindre. 2022. "Characterization of Early Phases of Cardiomyopathy Syndrome Pathogenesis in Atlantic Salmon (Salmo Salar L.) through Various Diagnostic Methods." *Journal of Fish Diseases* 45 (ue 9): 1267–79. https://doi.org/10.1111/jfd.13659.

Gauthier, D T, and M W Rhodes. 2009. "Mycobacteriosis in Fishes: A Review." *The Veterinary Journal* 180 (ue 1): 33–47. https://doi.org/10.1016/j.tvjl.2008.05.012.

Ghittino, Claudio, Elisabetta Manuali, Mario Latini, Francesco Agnetti, Fabio Rogato, Roberto Agonigi, Silvia Colussi, and Marino Prearo. 2004. "Caso Di Granulomatosi Sistemica in Ombrina Boccadoro (*Argyrosomus regius*) e Raffronto Con Le Lesioni Istologiche Presenti Nell ' Orata Case of Systemic Granulomatosis in Meagre (*Argyrosomus regius*) and Comparison with the Histological Features Present," no. August 2014: 59–67.

Gupta, E., P. Bhalla, N. Khurana, and T. Singh. 2009. "Histopathology for the Diagnosis of Infectious Diseases." *Indian Journal of Medical Microbiology* 27 (2): 100–106. https://doi.org/10.4103/0255-0857.49423.

Gustinelli, A, S Čolak, F Quaglio, R Sirri, M Kolega, D Mejdandžić, M Caffara, R Baric, and M Fioravanti. 2021. "Histological Assessment of Systemic Granulomatosis Progression in Meagre *Argyrosomus regius* during Cage Ongrowing Phase." In *Diseases of Aquatic Organisms*, 145:165–72. Inter-Research Science Center. https://doi.org/10.3354/dao03606.

Ingen, Jakko van. 2013. "Diagnosis of Nontuberculous Mycobacterial Infections." *Seminars in Respiratory and Critical Care Medicine* 34 (ue 01): 103–9. https://doi.org/10.1055/s-0033-1333569.

Jensen, Ellen. 2014. "Technical Review: In Situ Hybridization." *Anatomical Record* 297 (8): 1349–53. https://doi.org/10.1002/ar.22944.

Kaattari, I, M Rhodes, H Kator, and S Kaattari. 2005. "Comparative Analysis of Mycobacterial Infections in Wild Striped Bass Morone Saxatilis from Chesapeake Bay." In *Diseases of Aquatic Organisms*, 67:125–32. Inter-Research Science Center. https://doi.org/10.3354/dao067125.

Katharios, P, K Kokkari, M Papadaki, and N Papandroulakis. 2011. "Systemic Granulomas in Cultured Meagre, *Argyrosomus regius*." *Aquaculture Europe* 11: 537–38.

Knibb, Wayne, Angelo Colorni, Amir Zlotkin, and Arik Diamant. 1992. "Detection and Identification of *Mycobacterium marinum* in Fish Using Polymerase Chain Reaction Technique." https://www.researchgate.net/publication/273319130.

Kumar, Sudhir, Glen Stecher, and Koichiro Tamura. 2016. "MEGA7: Molecular Evolutionary Genetics Analysis Version 7.0 for Bigger Datasets." *Molecular Biology and Evolution* 33 (7): 1870–74. https://doi.org/10.1093/MOLBEV/MSW054.

Labella, A., C. Berbel, M. Manchado, D. Castro, and J.J. Borrego. 2011. "*Photobacterium damselae* Subsp. Damselae, an Emerging Pathogen Affecting New Cultured Marine Fish Species in Southern Spain." *Recent Advances in Fish Farms*. https://doi.org/10.5772/26795.

Lopez-Jimena, B., N. Cherif, E. Garcia-Rosado, C. Infante, I. Cano, D. Castro, S. Hammami, J. J. Borrego, and M. C. Alonso. 2010. "A Combined RT-PCR and Dot-Blot Hybridization Method Reveals the Coexistence of SJNNV and RGNNV Betanodavirus Genotypes in Wild Meagre (*Argyrosomus regius*)." *Journal of Applied Microbiology* 109 (4): 1361–69. https://doi.org/10.1111/j.1365-2672.2010.04759.x.

Maboni, G, N Prakash, and M A S Moreira. 2024. "Review of Methods for Detection and Characterization of Non-Tuberculous Mycobacteria in Aquatic Organisms." *Journal of Veterinary Diagnostic Investigation* 36 (ue 3): 299–311. https://doi.org/10.1177/10406387231194619.

Mandrioli, L, V Codotto, G D'Annunzio, E Volpe, F Errani, Y Eishi, K Uchida, M Morini, G Sarli, and S Ciulli. 2022. "Pathological and Tissue-Based Molecular Investigation of Granulomas in Cichlids Reared as Ornamental Fish." In *Animals (Basel*. Vol. 26;12(11): https://doi.

McNabb, A, D Eisler, K Adie, M Amos, M Rodrigues, G Stephens, W A Black, and J Isaac-Renton. 2004. "Assessment of Partial Sequencing of the 65-Kilodalton Heat Shock Protein Gene (*Hsp65*) for Routine Identification of Mycobacterium Species Isolated from Clinical Sources." *Journal of Clinical Microbiology* 42 (ue 7): 3000–3011. https://doi.org/10.1128/jcm.42.7.3000-3011.2004.

Meritet, D M, D M Mulrooney, M L Kent, and C v Löhr. 2017. "Development of Quantitative Real-Time PCR Assays for Postmortem Detection of Mycobacterium Spp. Common in Zebrafish (*Danio rerio*." *Research Colonies. J Am Assoc Lab Anim Sci*.

Monfort, Marie Christine. 2002. *Present Market Situation and Prospects of Meagre (Argyrosomus regius), as an Emerging Species in Mediterranean Aquaculture. Studies and Reviews. General Fisheries Commission for the Mediterranean*.

Mugetti, D, K Varello, A Gustinelli, P Pastorino, V Menconi, D Florio, M L Fioravanti, et al. 2020. "Mycobacterium Pseudoshottsii in Mediterranean Fish Farms: New Trouble for European Aquaculture?" *Pathogens* 9 (ue 8): 610. https://doi.org/10.3390/pathogens9080610.

Nargan, Kievershen, Joel N. Glasgow, Sajid Nadeem, Threnesan Naidoo, Gordon Wells, Robert L. Hunter, Anneka Hutton, et al. 2024. "Spatial Distribution of Mycobacterium Tuberculosis MRNA and Secreted Antigens in Acid-Fast Negative Human Antemortem and Resected Tissue." *EBioMedicine* 105: 105196. https://doi.org/10.1016/j.ebiom.2024.105196.

Nguyen, Diem Thu, David Marancik, Cynthia Ware, Matt J. Griffin, and Esteban Soto. 2021. "Mycobacterium Salmoniphilum and M. Chelonae in Captive Populations of Chinook Salmon." *Journal of Aquatic Animal Health* 33 (2): 107–15. https://doi.org/10.1002/aah.10124.

Noga, Edward J. 2010. *Fish Diseases: Diagnosis and Treatment*. Edited by John Wiley & Sons. 2nd ed.

Pavloudi, C, M I Tsertou, E Antonopoulou, and P Katharios. 2023. "Investigation of Systemic Granulomatosis in Cultured Meagre, *Argyrosomus regius*, Using Clinical Metagenomics."

In *Aquaculture*, 567:739249. Elsevier BV. https://doi.org/10.1016/j.aquaculture.2023.739249.

Pfalzgraff, T, P Borges, L Robaina, S Kaushik, and M Izquierdo. 2023. "Essential Fatty Acid Requirement of Juvenile Meagre (*Argyrosomus regius*." In *Aquaculture*, 572:739532. Elsevier BV. https://doi.org/10.1016/j.aquaculture.2023.739532.

Pourahmad, Fazel, Mostafa Nemati, and Randolph H. Richards. 2014. "Comparison of Three Methods for Detection of *Mycobacterium marinum* in Goldfish (Carassius Auratus)." *Aquaculture* 422–423: 42–46. https://doi.org/10.1016/j.aquaculture.2013.11.026.

Radomski, Nicolas, Adélaïde Roguet, Françoise S. Lucas, Frédéric J. Veyrier, Emmanuelle Cambau, Héberte Accrombessi, Régis Moilleron, Marcel A. Behr, and Laurent Moulin. 2013. "AtpE Gene as a New Useful Specific Molecular Target to Quantify Mycobacterium in Environmental Samples." *BMC Microbiology* 13 (1). https://doi.org/10.1186/1471-2180-13-277.

Rajme-Manzur, D, T Gollas-Galván, F Vargas-Albores, M Martínez-Porchas, M Á Hernández-Oñate, and J Hernández-López. 2021. "Granulomatous Bacterial Diseases in Fish: An Overview of the Host's Immune Response." In *Comparative Biochemistry and Physiology Part A: Molecular & Integrative Physiology*, 261:111058. Elsevier BV. https://doi.org/10.1016/j.cbpa.2021.111058.

Roberts, Ronald J. 2012. *Fish Pathology*. John Wiley & Sons.

Ruiz García, Miguel Ángel, Carmen M. Hernández-Cruz, Maria Jose Caballero, Hipólito Fernández-Palacios, Reda Saleh, Marisol Izquierdo, and Mónica Beatriz Betancor Quintana. 2019. "Incidence of Systemic Granulomatosis Is Modulated by the Feeding Sequence and Type of Enrichment in Meagre (*Argyrosomus regius*) Larvae." *Aquaculture Research* 50 (1): 284–95. https://doi.org/10.1111/are.13896.

Ruiz, M. A., M. B. Betancor, L. Robaina, D. Montero, C. M. Hernández-Cruz, M. S. Izquierdo, G. Rosenlund, R. Fontanillas, and M. J. Caballero. 2019. "Dietary Combination of Vitamin E, C and K Affects Growth, Antioxidant Activity, and the Incidence of Systemic Granulomatosis in Meagre (*Argyrosomus regius*)." *Aquaculture* 498 (February 2018): 606–20. https://doi.org/10.1016/j.aquaculture.2018.08.078.

Ruiz, Miguel Ángel, Mónica Beatriz Betancor, Daniel Montero, Maria Jose Caballero, Carmen Maria Hernández-Cruz, Grethe Rosenlund, Ramon Fontanillas, and Marisol S. Izquierdo. 2021. "The Effect of Fish Stocking Density and Dietary Supplementation of Vitamin C and Micronutrients (Mn, Zn and Se) on the Development of Systemic Granulomatosis in Juvenile Meagre (*Argyrosomus regius*)." *Aquaculture Research* 52 (11): 5703–18. https://doi.org/10.1111/are.15446.

Soares, F, A Roque, and P J Gavaia. 2018. "Review of the Principal Diseases Affecting Cultured Meagre (*Argyrosomus regius*." *Aquaculture Research* 49 (ue 4): 1373–82. https://doi.org/10.1111/are.13613.

Stathopoulou, P, E Asimakis, Y Petropoulos, G Apostolopoulou, and G Tsiamis. 2020. "Genomic Insights into the Fish-Pathogenic Mycobacterium Pseudoshottsii Strain AR Recovered from Meagre (*Argyrosomus regius*." Edited by V Bruno. *Microbiology Resource Announcements* 9 (ue 47)). https://doi.org/10.1128/mra.01099-20.

Sun, Jun Ren, Shan Shan Hsieh, Shih Yi Lee, and Jang Jih Lu. 2009. "Evaluation of Cord Formation in Kinyoun-Stained Smears of Mgit Cultures as a Rapid Identification Method for Mycobacterium Tuberculosis Complex." *Journal of Rapid Methods and Automation in Microbiology* 17 (3): 339–49. https://doi.org/10.1111/j.1745-4581.2009.00157.x.

Takahashi, S, J Tomita, K Nishioka, T Hisada, and M Nishijima. 2014. "Development of a Prokaryotic Universal Primer for Simultaneous Analysis of Bacteria and Archaea Using Next-Generation Sequencing." *PLOS ONE* 9 (8): 105592. https://doi.org/10.1371/journal.pone.0105592.

Tedesco, P, A Gustinelli, M Caffara, M Kolega, S Čolak, D Mejdandžić, V Baranović, and M L Fioravanti. 2022. "First Report of Ktariella Polyorchis (Monogenea: Calceostomatidae) Infection in Farmed Meagre *Argyrosomus regius* (Actinopterygii: Sciaenidae), with a Review of Calceostomatid Parasites of Wild and Cultured Fish." In *Aquaculture Reports*, 24:101105. Elsevier BV. https://doi.org/10.1016/j.aqrep.2022.101105.

Telenti, A, F Marchesi, M Balz, F Bally, E C Böttger, and T Bodmer. 1993. "Rapid Identification of Mycobacteria to the Species Level by Polymerase Chain Reaction and Restriction Enzyme Analysis." *Journal of Clinical Microbiology* 31 (ue 2): 175–78. https://doi.org/10.1128/jcm.31.2.175-178.1993.

Timur, G., Ürkü, Çanak, G. Erköse Genç, and Z. Erturan. 2015. "Systemic Mycobacteriosis Caused by *Mycobacterium marinum* in Farmed Meagre (*Argyrosomus regius*), in Turkey." *Israeli Journal of Aquaculture - Bamidgeh* 67 (January 2017): 1–8. https://doi.org/10.46989/001c.20714.

Tomasoni, Mattia, Giuseppe Esposito, Davide Mugetti, Paolo Pastorino, Nadia Stoppani, Vasco Menconi, Flavio Gagliardi, et al. 2022. "The Isolation of Vibrio Crassostreae and V. Cyclitrophicus in Lesser-Spotted Dogfish (Scyliorhinus Canicula) Juveniles Reared in a Public Aquarium." *Journal of Marine Science and Engineering* 10 (1). https://doi.org/10.3390/jmse10010114.

Tsertou, M I, M Smyrli, C Kokkari, E Antonopoulou, and P Katharios. 2018. "The Aetiology of Systemic Granulomatosis in Meagre (*Argyrosomus regius*): The 'Nocardia' Hypothesis." In *Aquaculture Reports*, 12:5–11. Elsevier BV. https://doi.org/10.1016/j.aqrep.2018.08.002.

Volpe, E, L Mandrioli, F Errani, P Serratore, E Zavatta, A Rigillo, and S Ciulli. 2019. "Evidence of Fish and Human Pathogens Associated with Doctor Fish (Garra Rufa, Heckel, 1843) Used for Cosmetic Treatment." *Journal of Fish Diseases*. https://doi.

Watral, V, and M L Kent. 2006. "Pathogenesis of Mycobacterium Spp. in Zebrafish (*Danio rerio*) from Research Facilities." *Comparative Biochemistry and Physiology Part C: Toxicology & Pharmacology* 145 (ue 1): 55–60. https://doi.org/10.1016/j.cbpc.2006.06.004.

Zanoni, R G, D Florio, M L Fioravanti, M Rossi, and M Prearo. 2008. "Occurrence of Mycobacterium Spp. in Ornamental Fish in Italy." *Journal of Fish Diseases* 31 (ue 6): 433–41. https://doi.org/10.1111/j.1365-2761.2008.00924.x.

Chapter IV

https://doi.org/10.3390/ani13182934

4. Exploring Immunohistochemistry in Fish: Assessment of Antibody Reactivity by Western Immunoblotting

4.1 Introduction

In recent years, research on fish has made unprecedented steps forward, propelled by the increase in aquaculture species production, the ornamental fish industry, and biomedical studies involving aquatic organisms. Despite notable advancements, several challenges persist. One prominent issue revolves around the vast array of fish species and their phylogenetic diversity, each characterized by distinct biology and physiology. Furthermore, diagnosing fish diseases presents a complex undertaking, requiring precise tools and methodologies specifically designed and validated for aquatic animals.

Among the different assays, immunohistochemistry (IHC) is an effective technique that has rapidly gained popularity in veterinary research, finding applications in physiological and pathological studies (Ramos-Vara & Miller, 2014). IHC has emerged as a valuable microscopy-based method in anatomic, physiological, and pathological fish studies (Markl Werner W., 1988; Bunton, 1993; Germanà F. et al., 2007; Iaria A. et al., 2019; Ronza A. et al., 2019; Šálková H. et al., 2022), specifically in identifying infectious disease agents and characterizing neoplastic lesions (Romano & Pedrosa, 2020). Except for zebrafish (*Danio rerio*), researchers often rely on antibodies developed against human or mouse proteins, commonly lacking species-specificity. Despite their extensive use (Paquette et al., 2015; Quaglio et al., 2016; Rahmati-Holasoo et al., 2018; Denk et al., 2020; Galeotti et al., 2021; Polinas et al., 2021; Sirri et al., 2021; Stilwell et al., 2021), mammalian antibodies must be optimized for aquatic animals (Grunow et al., 2013; Stilwell et al., 2021). Thus, false positives, negatives, and aberrant labelling are commonly described, despite manufacturers' data sheets providing some information regarding expected cross-species reactivity.

Antibody cross-reactivity in IHC refers to the ability of an antibody to bind to the same antigen in

different species or when the antibody is designed to recognize a conserved epitope on the antigen (Ramos-Vara & Miller, 2014). In aquatic animals, an antibody that reacts effectively in one species may not exhibit similar performance in others (Grunow et al., 2013; Stilwell et al., 2021). The clonality of antibodies represents another confounding element related to IHC, as polyclonal antibodies may show cross-reactivity with common epitopes expressed by different proteins, leading to a non-specific background. Finally, interspecies variations in antibody reactions stem from changes in the amino acid sequence of antigens, leading to different reactivity among species, even for identical antibody clones targeting the same antigen. It is, therefore, essential to validate the IHC cross-reactivity of antibodies with the corresponding antigen in the fish tissue species of interest using specific methods. Among the many approaches to validate the IHC assay's specificity, the Western blotting (WB) technique is the preferred choice for evaluating cross-reactivity, allowing the detection of the protein's molecular weight and determining the specificity of detection (Hewitt et al., 2014; Webster et al., 2021).

Antibodies frequently used for IHC with variable results in fish research are cytokeratins, vimentin, glial fibrillary acidic protein (GFAP), S-100, and desmin. Cytokeratin antibodies are used to detect a group of cytoplasmic proteins playing a role in maintaining cellular integrity, serving as markers for epithelial tissues. The expression of the 20 existent different cytokeratins is complex as their pattern has been restricted during evolution (Markl & Franke, 1988) and can change during a lifetime (Bunton, 1993). Pan-cytokeratin AE1/AE3 antibodies are commonly employed to identify and characterize epithelial cells in various fish species (Markl & Franke, 1988; Bunton, 1993; Grunow et al., 2013; Faílde et al., 2014), and positive reactions were found in teleost skin, intestine, renal tubules, certain glia, and thymic epithelial cells (Bunton, 1993; Faílde et al., 2014; Šálková et al., 2022). In pathological studies, neoplastic tissues such as carcinomas, adenocarcinomas, and papillomas were characterized by using cytokeratin antibodies (Paquette et al., 2015; Yasumoto et al., 2015; Lanteri et al., 2016).

As an intermediate filament protein, vimentin exhibits widespread cytoplasmic expression in

mesenchymal cell types, including fibroblasts, endothelial cells, melanocytes, and smooth muscle cells (Herrmann et al., 1996). However, vimentin staining in normal teleost tissues and neoplastic disease has been reported with variable positivity (Faílde et al., 2014; Yasumoto et al., 2015; Iaria et al., 2019; Sirri et al., 2021).

The S-100 protein, belonging to the EF-hand superfamily, plays an essential role in cell proliferation, differentiation, apoptosis, gene transcription, and intracellular calcium homeostasis (Moore, 1965). In teleosts, S-100 used to detect calcium-binding proteins is a moderately non-specific marker capable of staining cells of neurocrest origin, nerve fibers, melanocytes, sensory organs, brain, spinal cord (Abbate et al., 2002; Germanà et al., 2008; Fonseca et al., 2011), and neoplasia such as schwannoma (Sirri et al., 2015; Iaria et al., 2019).

GFAP, a protein belonging to the family of intermediate filaments, plays a crucial role in providing structural support to astrocytes and maintaining the integrity of the central nervous system (CNS). GFAP is associated with various neurological disorders such as brain injury, inflammation, and neurodegenerative diseases, or as a marker of neoplasms originating from glial cells in the CNS. GFAP expression is used in combination with other markers and histological features to classify gliomas into various subtypes, such as astrocytomas, oligodendrogliomas, and glioblastomas in mammals (Ramos-Vara & Borst, 2016). In fish, GFAP has been used to map glial structures both in the brain and other areas such as the gut (Kálmán, 1998; Hagström & Olsson, 2010), as well as a tumor marker (Marino et al., 2012).

Desmin is a type of intermediate filament protein that is an essential component of skeletal and cardiac muscle, maintaining the integrity of muscle fibers. In IHC, antibodies against desmin are used as specific markers for muscle tissue and are often utilized to differentiate muscle-related neoplasms, such as rhabdomyosarcoma, from other types of tumors (Ramos-Vara & Borst, 2016). Desmin antibodies have been employed to identify muscle cells in teleost species, making them helpful in investigating muscle-related diseases and disorders (Rowlerson et al., 1997; Clemen et al., 2013).

This study aims to assess the cross-reactivity of commercially available antibodies (CK AE1/AE3, vimentin, S-100, GFAP, and desmin) in IHC assays conducted on *Sparus aurata*, *Dicentrarchus labrax*, *Oncorhynchus mykiss*, *Carassius auratus* and *Argyrosomus regius*. By systematically testing and validating these antibodies by WB, we ascertain their specificity, sensitivity, and reproducibility across various commonly encountered teleost fish tissues.

4.2 Materials and methods

4.2.1. Sample Preparation and Histology

Paraffin-embedded and frozen (at 80°C) tissues of the skin, brain, heart, and intestine from a total of 12 fish were included in this study. In particular, fish were selected as follows: three farmed gilthead sea bream (*Sparus aurata*—Mediterranean seabream, adult fish, ranging from 30 to 38 cm in length and between 350 and 450 g in weight), three European sea bass (*Dicentrarchus labrax*—Western Mediterranean seabass, adult fish, ranging from 35 to 42 cm in length and between 300 and 450 g in weight); three goldfish (*Carassius auratus*—Ryukin strain, adult fish, ranging from 10 to 15 cm in length and weight between 20 and 25 g) and three rainbow trout (*Oncorhynchus mykiss*—Danish strain, adult fish, ranging from 52 to 55 cm in length and weight between 250 and 350 g from the diagnostic archives of Sassari and Udine Universities, respectively.

In addition, healthy tissues (skin, brain, heart, and intestine) and tissues affected by granulomas of *Argyrosomus regius* (kidney, liver, and heart) previously sampled and used in experiments of chapter III were selected.

Before inclusion in paraffin, all the tissues were previously fixed in 10% buffered formalin for 48 h, dehydrated with increasing alcohol concentrations and xylene in an automatic tissue processor. Sections of 3 µm thickness were obtained with a microtome (RM2245, Leica Biosystems, Wetzlar, Germany) and stained with hematoxylin and eosin in an automatic multi-stainer (ST5020, Leica Biosystems, Wetzlar, Germany). The inclusion criteria for this study were: the

absence of gross and microscopically significant lesions and the presence of known antigen expression in tissue. Canine tissues from archive diagnostic material (brain, heart, intestine, skin) were included as a positive control. Experiment permission was not required from the University's Animal Care Ethics Committee since all the samples were used for diagnostic purposes.

4.2.2. Antibodies and Sequence Alignments

The following antibodies were used for the study: Dako, monoclonal mouse anti-cytokeratin CKAE1/AE3; Dako, monoclonal mouse anti-vimentin, clone V9; Dako, polyclonal rabbit anti-S100, code Z0311; Dako, polyclonal rabbit anti-glial fibrillary acidic protein, code Z0334; Dako, mouse monoclonal anti-human desmin, clone D33. For all the antibodies providing sufficient information, the UniProt entry sequence of the antigen was retrieved and aligned with the respective protein sequences of *S. aurata*, *D. labrax*, *C. auratus*, and *O. mykiss*. When more than one sequence was available, the one with the highest annotation level was selected for the alignment; when available, the UniProtKB reviewed sequence was used. Protein sequence alignments were carried out with the Align tool of the Universal Protein KnowledgeBase (https://www.uniprot.org/, accessed on 24 August 2023).

4.2.3. SDS–PAGE and Western Immunoblotting

SDS-PAGE and WB were performed on tissues collected from three fish per species (n=12), including *Sparus aurata, Dicentrarchus labrax, Carassius auratus*, and *Oncorhynchus mykiss*. Additionally, fresh-frozen healthy tissues (skin, brain, heart, and intestine) from *Argyrosomus regius* were included. Fresh-frozen aliquots of all tissues were minced with a sterile scalpel. Then, 100 mg of each tissue was separately resuspended in 500 µL of Laemmli Buffer (Sigma-Aldrich, St. Louis, MO, USA) and incubated at 100°C for 10 min at 1500 rpm in a Thermomixer Comfort (Eppendorf, Hamburg, Germany). All extracts were clarified for 5 min at 10,000 g at 4°C and separated by sodium dodecyl sulfate–polyacrylamide gel electrophoresis (SDS–PAGE) in

AnykDTM polyacrylamide gels on a Protean Tetra Cell (Bio-Rad, Hercules, CA, USA) following manufacturer's instructions. After the run, gels were stained with SimplyBlue™ Protein SafeStain (Thermo Fisher Scientific, Waltham, MA, USA).

For WB, separated proteins were transferred to nitrocellulose membranes with the Trans-Blot® TurboTM Transfer System (Bio-Rad). Nitrocellulose membranes were checked for quality by reversible Ponceau S staining (Sigma-Aldrich), destained with water, blocked with EveryBlot Blocking Buffer (Bio-Rad) for 5 min and then incubated for 1 h with the following primary antibodies diluted in EveryBlot Blocking Buffer: anti-cytokeratin, dilution 1:1000, anti-vimentin, dilution 1:1000, anti-S-100, dilution 1:5000, glial fibrillary acidic protein (GFAP), dilution 1:5000, and desmin, dilution 1:1000. The membranes were then washed five times with PBS-T (phosphate buffered saline, 0.05% Tween 20) and incubated with appropriate HRP-conjugated anti-mouse antibodies or with HRP- conjugated anti-rabbit antibodies (Sigma-Aldrich) diluted in blocking buffer (1:2000) for 30 min. After five washes with PBS-T, the reactivity was visualized with a chemiluminescent peroxidase substrate (Clarity Western ECL substrate, Bio-Rad). Chemiluminescent images were digitalized with an iBright 1500 (Thermo Fisher Scientific). Molecular weight (MW) was estimated using the MagicMark markers (Thermo Fisher Scientific). Same samples from a dog were used as positive control.

4.2.4. Immunohistochemistry

IHC was performed on formalin-fixed paraffin-embedded (FFPE) tissues collected from three fish per species (n=12), including *Sparus aurata, Dicentrarchus labrax, Carassius auratus*, and *Oncorhynchus mykiss*. Additionally, FFPE healthy tissues (skin, brain, heart, and intestine) and granuloma-affected tissues (kidney, liver, and heart) from *Argyrosomus regius* were included. Serial 3 µm-thick FFPE sections of all tissues were mounted on positively charged slides (Superfrost, Fisher Scientific) for immunostaining. Slides were immersed for 20 min in a 98 ◦C, preheated solution (WCAP, citrate pH 6, BiOptica, Milan, Italy) for antigen unmasking. Tissues

were blocked for endogenous peroxidase (Dako REAL Peroxidase- Blocking Solution S2023, Dako, Glostrup, Denmark) and non-specific binding with 2.5% normal horse serum (ImmPRESS reagent kit, Vector Labs, Burlingame, CA, USA) and 2% bovine serum albumin (BSA) Sections were incubated overnight at 4 ◦C with the same primary antibodies as reported above at the following dilutions: anti-cytokeratin AE1/AE3, 1:200, anti-vimentin, 1:200, S-100, 1: 2000, GFAP, 1:2000, anti-desmin, 1:200. Then, the sections were incubated with an anti-mouse/rabbit secondary antibody (ImmPRESS reagent kit—peroxidase—MP-7500; Vector Laboratories, Burlingame, CA, USA) for 30 min at room temperature and treated with 3,30 -Diaminobenzidine (DAB) chromogen (ImmPACT DAB; Vector Laboratories). Tissues were then counterstained with hematoxylin, dehydrated, and mounted. Slides were evaluated under light microscopy (Nikon Eclipse 80i) and digital computer images were recorded with a Nikon Ds-fi1 camera. Normal canine tissue, including skin, brain, heart, and intestine were used as positive controls. Negative controls were established by replacing the primary antibodies with only antibody diluent.

Same samples from a dog were used as positive control.

4.3. Results

4.3.1. Antibodies and Sequence Alignments

The pan-cytokeratin antibody could not be assessed as the antigen is an uncharacterized protein mixture from a human callus extract; therefore, protein sequence information is not available. Concerning the other proteins, the vimentin antigen displayed a sequence homology ranging from 76.4% for *C. auratus* to 74.34% for *O. mykiss*. The sequence homology for the S100 antigen ranged from 33.33% for *C. auratus* to 62.77% for *D. labrax*. The sequence homology for the GFAP antigen ranged from 33.10% for *S. aurata* to 72.05% for *C. auratus*. Finally, the sequence homology of desmin ranged from 37.18% for *C. auratus* to 74.16% for *D. labrax*.

4.3.2. Pan-Cytokeratin

The reactivity of mouse monoclonal anti-human cytokeratin AE1/AE3 antibodies was assessed by WB against skin tissue extracts. Several clear bands within the predicted molecular mass range of 45–65 kDa were observed in all the species tested (*Fig. 42A*). In goldfish and rainbow trout, lower molecular weight bands in the range of 30 kDa were also observed, indicating possible additional non-specific reactivity of the tested antibody in these two species. By IHC, a strong and diffuse cytoplasmic immunostaining highlighting the cellular membrane in the squamous epithelium of the skin was observed both in the dog (*Fig. 42 B*) and all fish species (*Fig. 42 C–F*), using the same monoclonal antibody (*Table 7*).

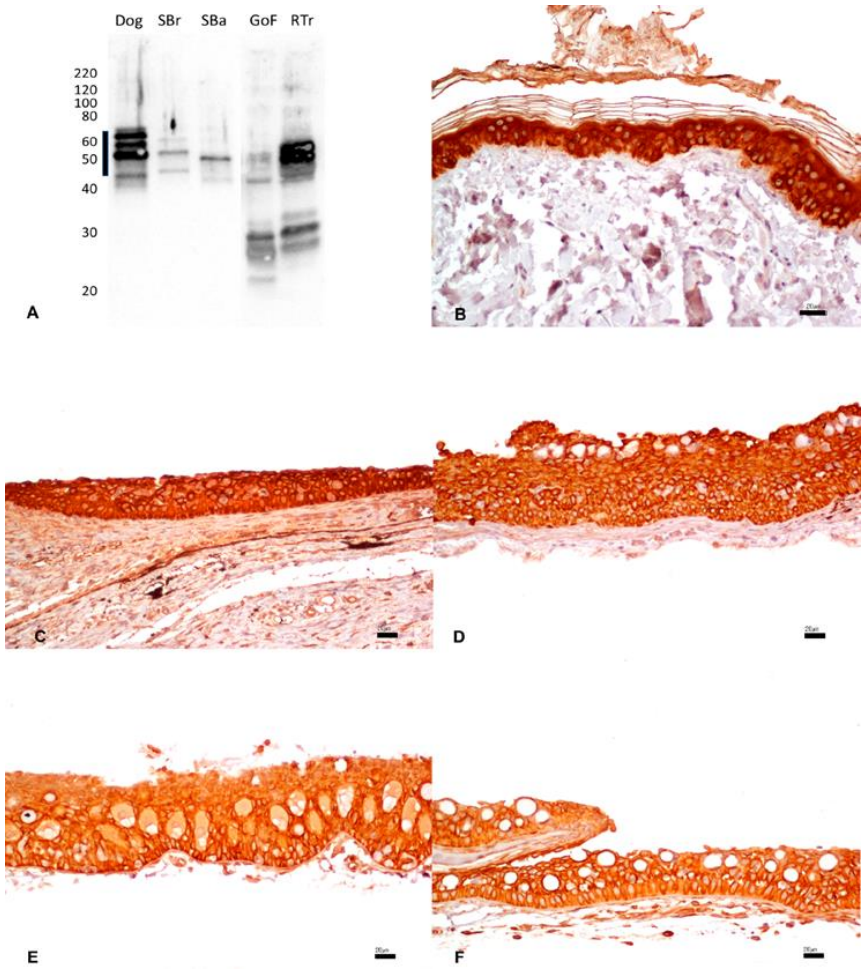

Figure 42. *(A) Western immunoblotting of skin tissues incubated with the monoclonal anti-pan-cytokeratin antibody. Molecular weight markers are indicated on the left. The predicted molecular weight range of 45–65 kDa is indicated with a thick line. Dog tissue extract loaded as a positive*

control; SBr, sea bream; SBa, sea bass; GoF, goldfish; RTr, rainbow trout. (A–F). IHC shows strong and diffuse cytoplasmic immunostaining with accentuation of the cellular membrane in the squamous epithelium of the skin in the dog (B), sea bream (C), sea bass (D), goldfish (E), and rainbow trout (F). Scale Bar: 20 µm.

4.3.3. Vimentin

The reactivity of mouse monoclonal anti-vimentin antibody was tested against intestinal tissue extracts. The dog tissue proteins tested as a positive control produced a band at the expected MW of ~60 kDa (*Fig. 43A*). No reactivity was observed for sea bream, sea bass, or goldfish. The rainbow trout extract displayed a band at ~35, indicating possible non-specific reactivity. By IHC, strong and diffuse cytoplasmic staining was observed with the same anti-vimentin antibody in the mesenchymal cells of the intestine in dog tissues (*Fig. 43B*). No immunostaining was present in fish tissues (*Fig. 43C–F*) (*Table 7*).

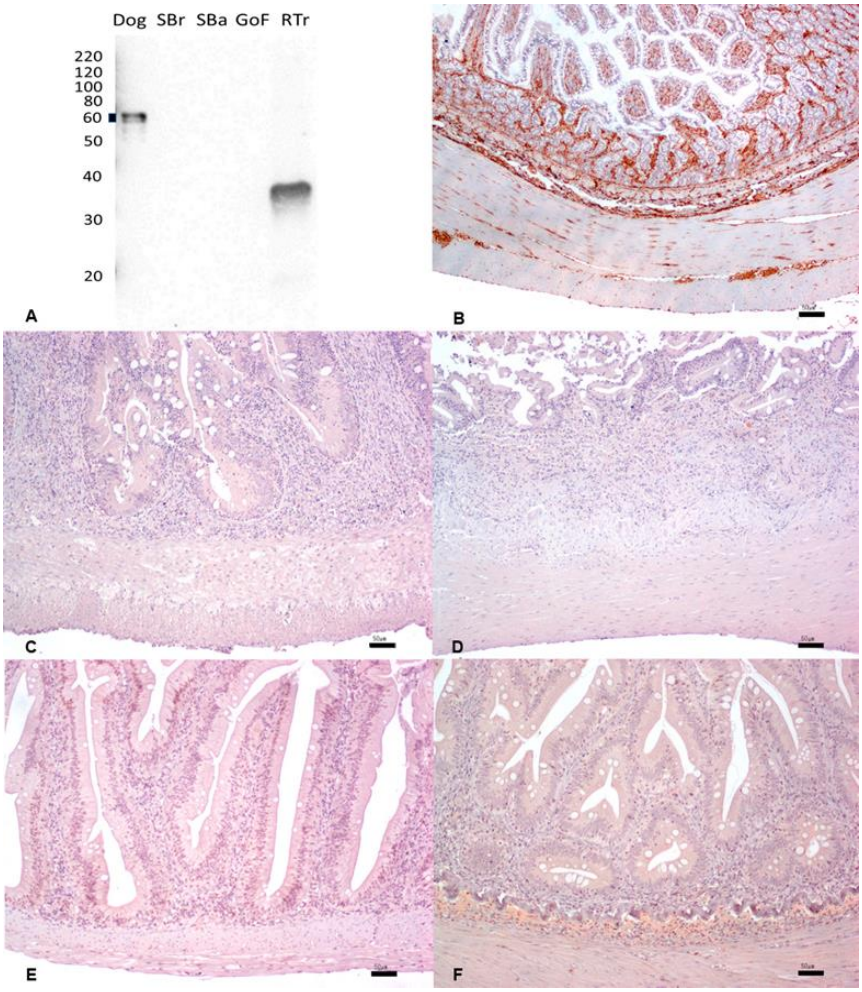

Figure 43. *(A) Western immunoblotting of intestinal tissues incubated with the mouse monoclonal anti-vimentin antibody. Molecular weight markers are indicated on the left. The predicted molecular weight of 60 kDa is indicated with a thick line. Dog tissue extract loaded as a positive control; SBr, sea bream; SBa, sea bass; GoF, goldfish; RTr, rainbow trout. (B–F). IHC shows strong and diffuse cytoplasmic immunostaining of the intestinal mesenchymal cells of the dog (B), while no immunosignals were observed in sea bream (C), sea bass (D), goldfish (E), and rainbow trout (F). Scale Bar: 5.0 µm.*

4.3.4. S100 Protein

The reactivity of rabbit polyclonal anti-S100 antibodies was assessed against brain tissue extracts. The dog tissue proteins tested as a positive control did not produce any band, indicating a lack of reactivity of the antibody in this species. The same was observed for sea bass proteins. On the other hand, the antibody produced a faint band in sea bream tissues and a very intense band in goldfish and rainbow trout at ~10 kDa. In these species, the findings shown in *Figure 44A* indicate the likelihood of specific S100 protein isoforms being recognized by the antibody (*Fig. 44A*). In

contrast, IHC demonstrated a strong and diffuse nuclear and cytoplasmic expression of S100 protein in all species' cytoplasm, and in nuclei in the brain tissues. (*Fig. 44B–F*) (*Table 7*).

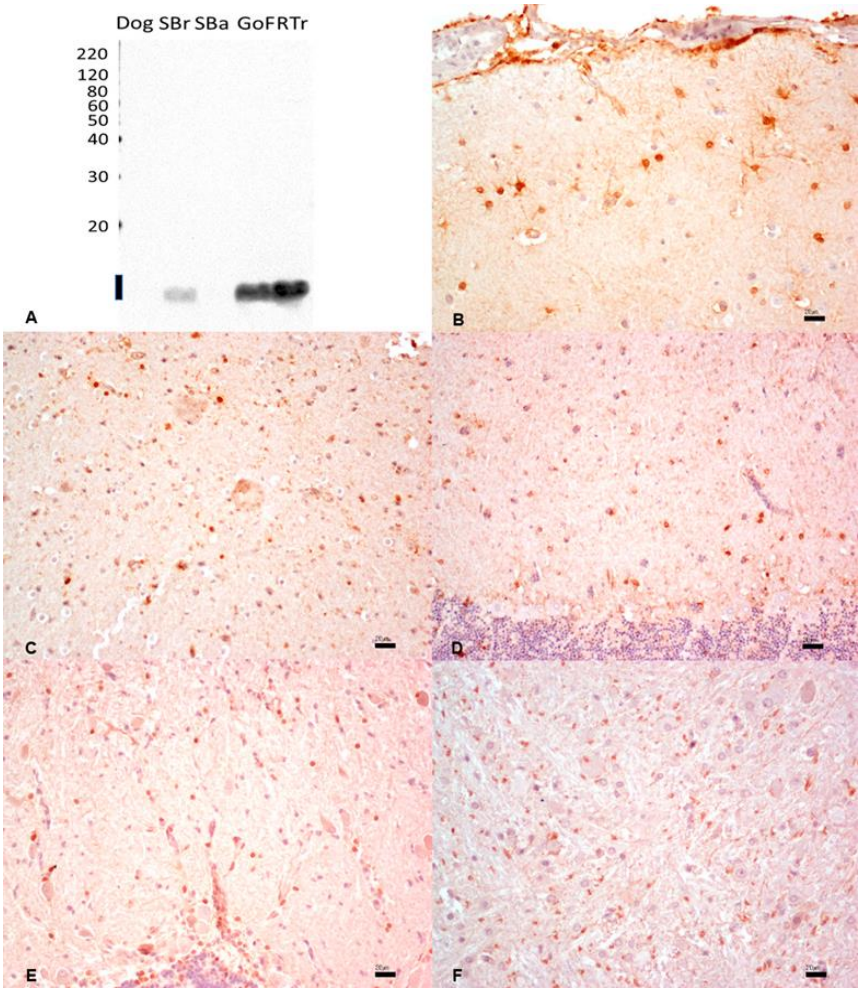

Figure 44. *(A) Western immunoblotting of brain tissues incubated with the rabbit polyclonal anti-S100 protein. Molecular weight markers are indicated on the left. The predicted molecular weight of 10–12 kDa is indicated with a thick line. Dog tissue extract loaded as a positive control; SBr, sea bream; SBa, sea bass; GoF, goldfish; RTr, rainbow trout. (B–F). IHC shows a strong and diffuse cytoplasmic and nuclear expression in the dog (B), in sea bream (C), sea bass (D), goldfish (E), and rainbow trout (F). Scale Bar: 20 µm.*

4.3.5. Glial Fibrillary Acidic Protein

The reactivity of rabbit polyclonal anti-GFAP was tested against brain tissue extracts. The dog tissue proteins tested as a positive control produced a band at the expected MW of ~50 kDa plus other minor bands, possibly due to multiple protein isoforms. Bands of similar MW were observed

in all the fish species tested, although with minor differences, which might be related to species-specific isoforms. Higher molecular weight bands observed in sea bream and sea bass (~100 kDa) may represent protein dimers (*Fig. 45A*). The immunostaining performed by IHC with the same anti-GFAP antibodies produced a strong and diffuse cytoplasmic staining of glial cells (i.e., astrocytes) in all tested species (*Fig. 45B–F*) (*Table 7*).

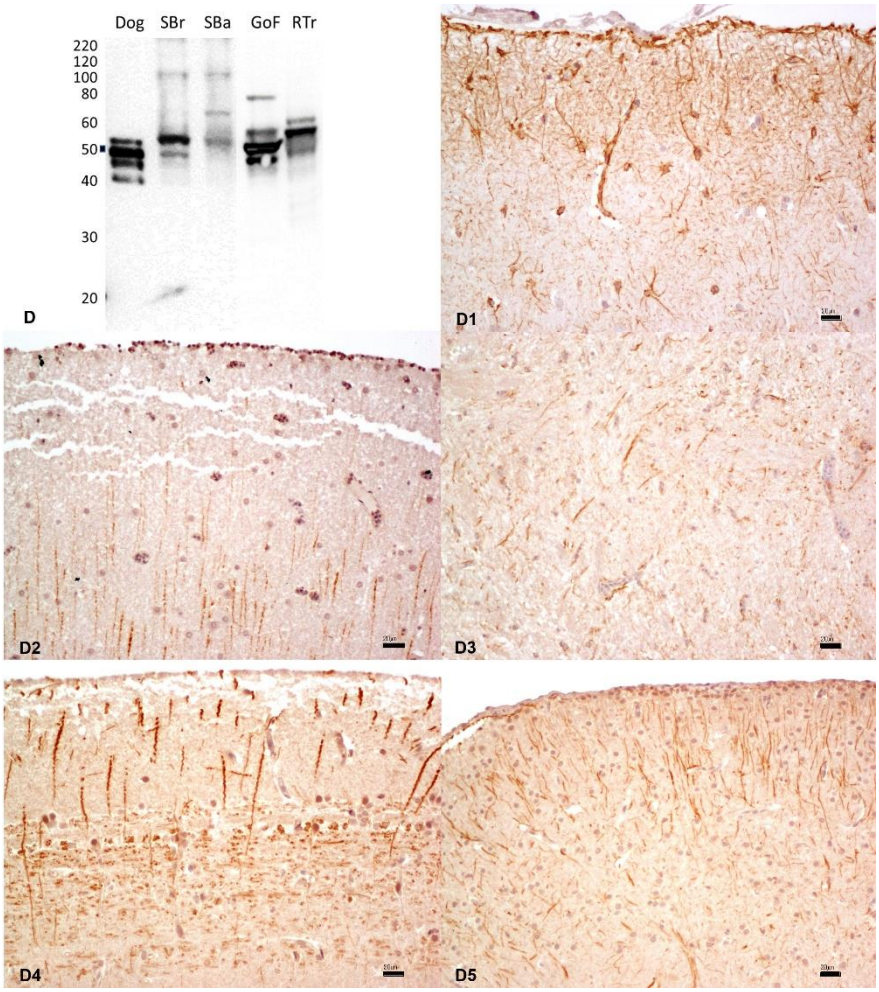

Figure 45. *Western immunoblotting of brain tissues incubated with the rabbit polyclonal anti-glial fibrillary acidic protein (GFAP). Molecular weight markers are indicated on the left. The predicted molecular weight of 50 kDa is indicated with a thick line. Dog tissue extract loaded as*

a positive control; SBr, sea bream; SBa, sea bass; GoF, goldfish; RTr, rainbow trout. (B–F). IHC shows strong and diffuse cytoplasmic staining in the dog (B), sea bream (C), sea bass (D), goldfish (E), and rainbow trout (F). Scale Bar: 20 µm.

4.3.6. Desmin

The reactivity of the mouse monoclonal anti-human desmin antibody was assessed against heart tissue extracts. The dog tissue proteins tested as a positive control produced a band at the expected MW of ~50 kDa. Fish tissues displayed a band in the 30 kDa molecular weight, indicating possible non-specific reactivity (*Fig. 46A*). By IHC, the same anti-desmin antibody did not show any reactivity in the cardiac tissues of all examined fishes (*Fig. 46C–F*). Conversely, a strong signal was observed in dog myocardium (*Fig. 46B*) (*Table 7*).

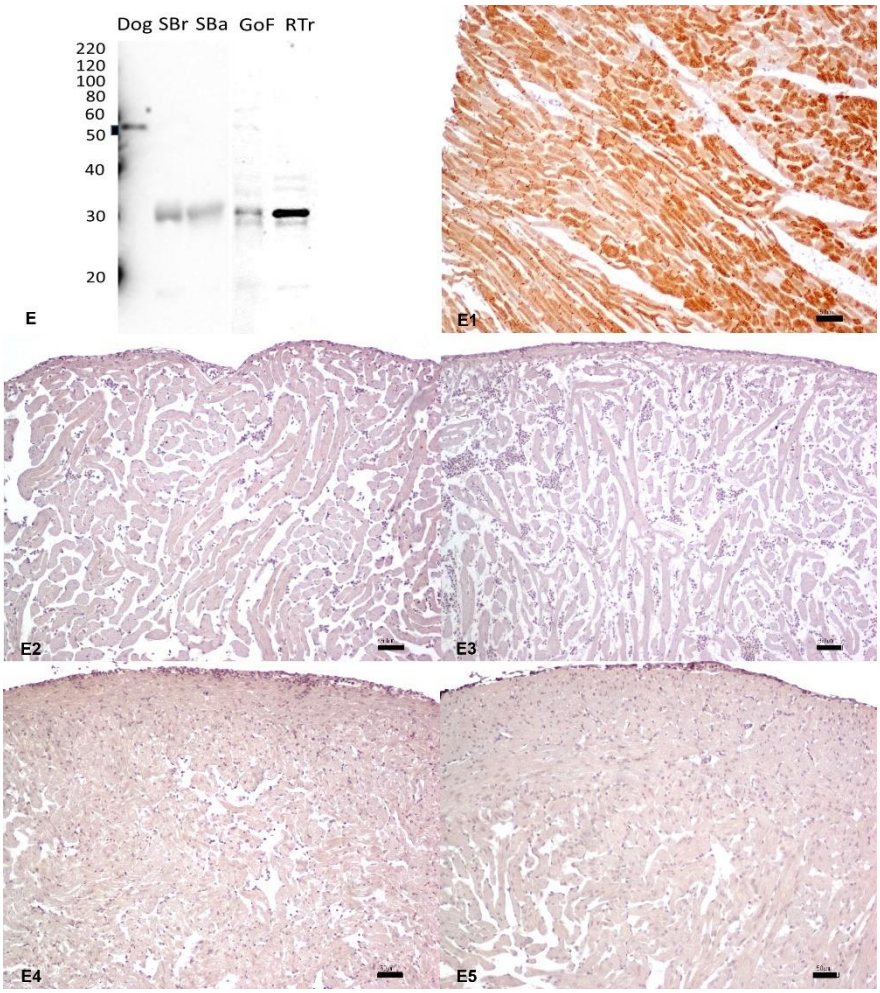

***Figure 46**. (A) Western immunoblotting of cardiac tissues incubated with the monoclonal anti-human desmin antibody. Molecular weight markers are indicated on the left. The predicted molecular weight of ~50 kDa is indicated with a thick line. Dog tissue extract loaded as a positive control; SBr, sea bream; SBa, sea bass; GoF, goldfish; RTr, rainbow trout. (B–F). By IHC, a strong and diffuse cytoplasmic expression was observed in the dog (B), while no immunostaining was observed in sea bream (C), sea bass (D), goldfish (E), and rainbow trout (F). Scale Bar: 50 µm.*

4.3.7 Argyrosomus regius antibody validation in healthy and granulomatous affected tissues

Regarding meagre, WB analysis confirmed the reactivity of the anti-cytokeratin (clone AE1/AE3) antibody, producing a distinct band at ~50 kDa in both meagre and dog skin tissue. This finding was supported by immunohistochemistry (IHC), which revealed strong cytoplasmic staining in the squamous epithelium of both species. For the anti-vimentin (clone V9) antibody, WB demonstrated reactivity with dog intestinal tissue (positive control) at ~60 kDa, while no bands

were detected in meagre. Consistently, IHC showed strong cytoplasmic staining in mesenchymal cells of the dog intestine, but no immunostaining was observed in meagre tissues.

Testing with polyclonal anti-GFAP antibodies identified bands around ~50 kDa in both dog and meagre brain extracts, with additional minor bands in meagre that may correspond to protein dimers. IHC using the same antibody revealed strong and diffuse cytoplasmic staining of glial cells, likely astrocytes, in both species. No reactivity was observed for the anti-desmin antibody in meagre heart tissues by either WB or IHC. For anti-S100 antibodies, WB failed to detect bands in both meagre and dog brain extracts, despite the expected reactivity in the positive control. In contrast, IHC demonstrated robust nuclear and cytoplasmic staining of S100 protein in glial cells within brain tissues of both species.

Regarding granulomas in meagre, as outlined in Chapter 3, Systemic Granulomatosis is characterized by multifocal granulomas within the parenchyma of internal organs, composed of layers of epithelioid cells, often accompanied by central necrosis and/or calcifications. By applying our research outcomes, anti-cytokeratin (clone AE1/AE3) IHC assay revealed a strong cytoplasmic staining within epithelioid cells and the ductal epithelium of the liver(*Fig. 47A-B*); conversely, vimentin (clone V9) staining was entirely negative (*Fig. 47 B-C*).

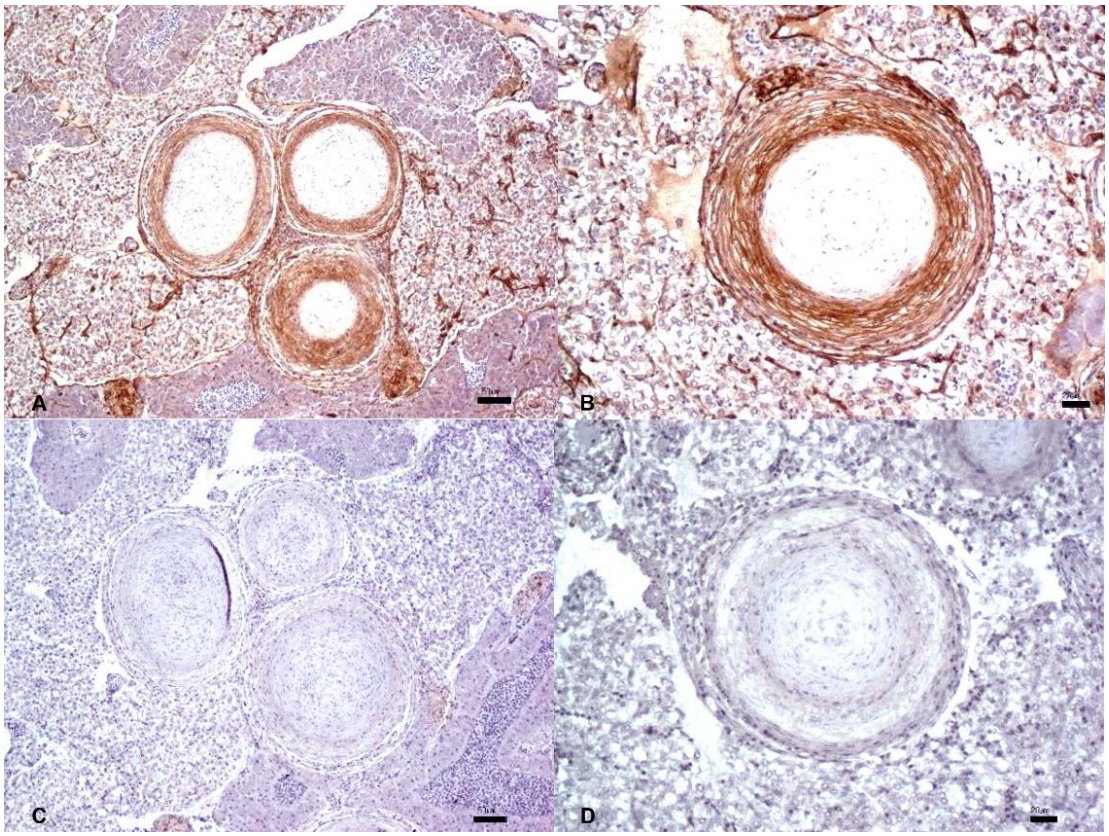

Figure 47*. Immunohistochemical analysis of granulomatous lesions in meagre. A) and B) show strong and diffuse cytoplasmic immunoreactivity with the monoclonal anti-pan-cytokeratin antibody in the layers of epithelioid cells and in the biliary ducts. C) and (D) display the negative staining for vimentin. Scale bars: 50 µm (a, c) and 20 µm (b, d).*

Table 7. Summary of the results obtained by Western immunoblotting (WB) and immunohistochemistry (IHC) with all the assessed antibodies and tissues. The (+) symbol indicates antibody reactivity, whereas the (-) symbol the absence of antibody reactivity, and (×) possible non-specific reactivity.

Antibody and tissue	**Species**	**WB**	**IHC**
Pan-cytokeratin (skin) Monoclonal mouse anti-human cytokeratin CKAE1/AE3	Canine	+	+
	Sparus aurata	+	+
	Dicentrarchus labrax	+	+
	Carassius auratus	+	+
	Oncorhynchus mykiss	+	+
	Argyrosomus regius	+	+
Vimentin (intestine) Monoclonal mouse anti-vimentin, clone V9	Canine	+	+
	Sparus aurata	-	-
	Dicentrarchus labrax	-	-
	Carassius auratus	-	-
	Oncorhynchus mykiss	x	-
	Argyrosomus regius	-	-
S-100 (brain) Polyclonal rabbit, code Z0311	Canine	-	+
	Sparus aurata	+	+
	Dicentrarchus labrax	-	+
	Carassius auratus	+	+
	Oncorhynchus mykiss	+	+
	Argyrosomus regius	+	+
GFAP (brain) Polyclonal rabbit anti-glial fibrillary acidic protein, code Z0334	Canine	+	+
	Sparus aurata	+	+
	Dicentrarchus labrax	+	+
	Carassius auratus	+	+
	Oncorhynchus mykiss	+	+
	Argyrosomus regius	+	+
Desmin (skin) Mouse monoclonal anti-human desmin, clone D33	Canine	+	+
	Sparus aurata	x	-
	Dicentrarchus labrax	x	-
	Carassius auratus	x	-
	Oncorhynchus mykiss	x	-
	Argyrosomus regius	x	-

4.4. Discussion

Immunohistochemistry is a fundamental technique widely employed in biomedical research and diagnostic pathology, constituting a potent tool that provides crucial insights into protein expression, antigens cellular localization, and disease-related alterations within tissues. Its applications extend across various fields, including veterinary science, where it significantly advances our understanding of the biology and pathogenesis of animal diseases.

In aquatic organisms, IHC has found prominent utility in exploring anatomical and pathological aspects, particularly concerning neoplastic disorders in farmed and ornamental fish species (Paquette et al., 2015; Rahmati-Holasoo et al., 2018; Iaria et al., 2019; Denk et al., 2020; Galeotti et al., 2021; Stilwell et al., 2021; Šálková et al., 2022). Nevertheless, the specificity of antibodies holds paramount importance in ensuring accurate results, and it is worth noting that many commercially available antibodies might have yet to undergo thorough validation for their application in fish tissues. Antibodies such as cytokeratin (AE1/AE3), vimentin, S-100 protein, GFAP, and desmin, primarily developed for human or mouse proteins, may lack the species-specificity for fish. Consequently, the potential for false positives or negatives arises, leading to misinterpretation of results (Stilwell et al., 2021). To address this concern, WB has emerged as a preferred technique for testing antibody cross-reactivity and enhancing the reliability of IHC in fish research (Hewitt et al., 2014). This study investigates the immunolocalization of the most encountered antibodies in teleosts, assessing their specificity through WB to establish their applicability in fish species.

The clone AE1/AE3 represents a cocktail of antibodies capable of detecting cytokeratins 1–8, 10, 14–16, and 19, with its expression visualized through membrane positivity. Our findings indicate that this clone exhibited cross-reactivity in all tested fish species, producing bands between 52 and 65 kDa, corresponding to the predicted molecular weight range. Notably, it demonstrated a robust cytoplasmic staining reaction, focusing on the epithelial cells of the species under investigation. These results are consistent with those revealed by previous IHC studies in fish, highlighting the role played by the monoclonal mouse anti-CK antibody in recognizing cytokeratins in epithelial cells of diverse fish species, both in healthy tissues and neoplasms (Markl & Franke, 1988; Bunton, 1993; Grunow et al., 2013; Faílde et al., 2014; Paquette et al., 2015; Lanteri et al., 2016; Iaria et al., 2019; Šálková et al., 2022). The results strongly suggest that the clone AEl/AE3 antibody exhibits significant cross-reactivity between mammals and fish

proteins. Hence, it can be considered a viable option for conducting immunohistochemical studies in tested fish species.

In mammals, vimentin is a common immunohistochemical marker for distinguishing between epithelial and mesenchymal tissues and identifying tumors exhibiting a mesenchymal phenotype, such as sarcomas (Roccabianca et al., 2020). In fish pathology, the V9 mouse monoclonal antibody is widely used for immunohistochemical analysis to identify normal and neoplastic mesenchymal cells with variable results (Quaglio et al., 2016; Stilwell et al., 2019; Iaria et al., 2019; Armando et al., 2021;). The results of the present study show that the V9 clone does not effectively bind to its intended target protein in tested fish tissues, except for a non-specific WB-detectable band in rainbow trout. Given the protein homology between the antigen used for antibody generation and the fish proteins (>70% for all species), the observed lack of reactivity may be attributed to other factors, including crucial sequence differences in the epitope region, potential cross-reactivity issues, or variations in protein expression levels in the investigated fish tissues. These findings are in line with recent studies in which the V9 clone failed to cross-react with goldfish peripheral nerve sheath tumors (atypical neurofibroma)(Armando et al., 2021). However, our results differ from prior reports wherein vimentin exhibited a positive reaction in adult ovarian cells and a gonadal tumor in koi carp (SCST) (Faílde et al., 2014), as well as in the outer layers (fibroblasts) of granulomas developed against histozoic metazoan parasites in mullet (Polinas et al., 2021). Moreover, our results do not agree with what was reported by Šálková and coauthors (2022), as they successfully utilized the anti-vimentin antibody (clone V9) in both sterlet and carp without conducting a validation test such as WB. Based on the findings of this study, it is reasonable to conclude that the monoclonal mouse anti-human vimentin clone V9 is unsuitable for immunohistochemical studies in the examined fish species.

S-100 is another commonly used marker in IHC studies for identifying normal cells, tumors, and diseases originating from the neural crest in fish: its effectiveness as an IHC marker shows slight variation across different fish species (Abbate et al., 2002; Germanà et al., 2008; Fonseca et al.,

2011; Šálková et al., 2022). Our study confirms this data in IHC, showing a strong and diffuse cytoplasmic and nuclear expression of S-100 in the brain of all tested species. However, WB results showed the presence of bands at approximately 10 kDa for sea bream, goldfish, rainbow trout and meagre tissues. Our WB results closely aligned with other researchers who reported bands using polyclonal antibodies against the S100 protein, revealing a molecular weight of 10 kDa (Moore, 1965; Germanà et al., 2008). Interestingly, a weaker band was observed in sea bream, and no bands were observed in sea bass, suggesting a lack of antibody reactivity in this latter species. When examining the percentage identity matrix for this antigen, the sea bass showed the highest homology (62.77%). On the other hand, the strongest reactivity was observed for goldfish, for which the percentage homology between antigen and target protein was the lowest (33.33%). Likely, the sequence differences occurring in the epitope play a vital role in the antibody's ability to recognize the fish protein variants. Unfortunately, the epitope sequences are not available. Additionally, no band was detected in the dog brain extracts; further investigation would be advisable, considering the extensive use of this marker in veterinary medicine. Given these considerations, the polyclonal rabbit S-100 antibody may constitute a useful tool when considering the species-specific diversity in fish.

GFAP antibodies facilitate the differential diagnosis of peripheral nervous sheet tumors such as Schwannomas and neurofibromas in fish (Rowlerson et al., 1997; Ramos-Vara & Borst, 2016; Armando et al., 2021). Our results showed that the polyclonal anti-rabbit GFAP antibody displays strong specificity at approximately 50 kDa molecular weight and exhibits cytoplasmic expression in brain glial cells across all tested species, confirming the antibody's specificity. In this case, Western immunoblotting in sea bream and sea bass observed a slightly weaker reactivity in line with their lower protein sequence homology with the antigen used for antibody generation. Our results align with those highlighted by a previous study, where a monoclonal GFAP anti-mouse antibody was employed, validating the expression of GFAP proteins at 90 kDa and 50–52 kDa in the brain and spinal cord of two larval stages and adult rainbow trout (Alunni A et al., 2005).

Therefore, similar to cytokeratin, we can conclude that there is a good cross-reactivity between mammals and fish when using this polyclonal rabbit anti-GFAP antibody, which is now validated for immunohistochemical investigation in fish species.

In contrast to dogs, where a strong signal was detected, no immunostaining reaction of the anti-desmin antibody against the target protein, commonly utilized as a specific marker for muscle tissue and for distinguishing muscle-related neoplasms, was observed in the heart of all the examined fish species. By WB, the anti-desmin mouse monoclonal antibody demonstrated the presence of an expected 53 kDa band in the dog heart. However, no signal was evident at this molecular weight in fish. Additional bands at lower molecular weights were detected in all fish examined, suggesting potential antibody cross-reactivity with different peptides. These results collectively indicate that clone D33 may not be suitable for studying muscle-related tissues in tested fish. This observation is consistent with findings from various other authors (Rowlerson et al., 1997; Armando et al., 2021), suggesting that desmin might be a helpful marker only for newly formed or regenerating fibers in fish (Rowlerson et al., 1997) or should be considered unsuitable for immunohistochemical studies in fish species, as indicated by Armando and coauthors (Armando et al., 2021). This discrepancy exists despite a substantial sequence homology with the protein antigen (>70% for sea bass, rainbow trout, and sea bream).

Regarding granulomas in meagre (*Argyrosomus regius*), anti-cytokeratin (clone AE1/AE3) IHC assay revealed a strong cytoplasmic staining within epithelioid cells and the ductal epithelium while vimentin (clone V9) staining was entirely negative. These findings, together with prior literature, shed light on a potential epithelium-like phenotype of epithelioid cells, raising questions about their origin and function in teleost's granuloma biology.

Traditionally, epithelioid cells are described as transformed macrophages that play a key role in granuloma formation and structure, acting as a barrier to contain and neutralize pathogens (Sayyaf Dezfuli et al., 2023). However, our findings challenge the mesenchymal nature of these cells in fish, suggesting potential phenotypic plasticity and raising the possibility that epithelioid cells

might undergo processes similar to the mesenchymal-to-epithelial transition (MET). This assumption aligns with a previous study in zebrafish, where epithelioid cells in mycobacterial granulomas exhibited elevated levels of E-cadherin, a critical protein in epithelial cell adhesion (Nathan, 2016; Sayyaf Dezfuli et al., 2023). MET is a well-documented biological process in which mesenchymal cells acquire epithelial traits, such as cell polarity and adhesion. This process is primarily studied in contexts like embryogenesis and tumor progression, but our results suggest that a similar mechanism could occur during granulomatous inflammation in teleosts. The granuloma microenvironment, characterized by chronic inflammation, cytokine signaling, and tissue remodeling, may serve as a trigger for molecular pathways linked to this transition. Supporting this hypothesis, recent research by Nathalie Chênais et al. (2023) demonstrated that TGF-β inhibition regulates MET in goldfish somatic cells. TGF-β is a cytokine with a key role in immune modulation and granulomas formation (Letterio and Roberts, 1998), and could plausible influence the epithelioid cells' transition during granulomatous inflammation.

However, these hypotheses remain speculative and require dedicated studies to confirm whether TGF-β and related pathways may be directly involved in this phenotypic shift. Morover, while our findings support the presence of epithelial traits in epithelioid cells, the potential involvement of vimentin in this process, or in the transition from macrophages to epithelioid cells, cannot be excluded as the antibody used was not validated for the fish species tested. To address these limitations, future studies should prioritize the use of monoclonal antibodies tailored to the species of interest or validating other antibodies.

4.5 Conclusions

The results of this study underscore the importance of validating antibodies for IHC assays in the specific species of interest, especially in teleost fish where cross-reactivity with mammalian antibodies can vary significantly. While the tested clones of anti-cytokeratin, GFAP, and S-100

(only for sea bream, goldfish, rainbow trout and meagre) antibodies provided reliable results, other antibodies, such as vimentin and desmin exhibited no cross-reactivity in fish species examined. For future studies involving immunohistochemical analysis in fish, it is recommended to carefully select antibodies that have been specifically validated to assess antibody specificity and cross-reactivity in fish tissues. Additionally, species-specific antibodies or those specifically optimized for aquatic animals should be sought to ensure accurate and reproducible results in fish research. In conclusion, this study provides valuable insights into the performance of commonly used antibodies in fish tissues, highlighting the need for cautious selection and validation of antibodies in aquatic animal studies. By employing appropriate antibodies and optimizing IHC protocols, understanding fish biology, pathology, and disease can advance, contributing to the continued progress in aquaculture, the ornamental fish industry, and biomedical studies involving aquatic organisms.

References

A Vaccari; S Torcia; Me Meomartini; A Nicotra; L Alfei, Alunni; S. 2005. "Characterization of Glial Fibrillary Acidic Protein and Astroglial Architecture in the Brain of a Continuously Growing Fish, the Rainbow Trout." *European Journal of Histochemistry : EJH* 49 (2): 157–66. https://doi.org/NA.

Abbate, F, S Catania, A Germanà, T González, B Diaz-Esnal, G Germanà, and J.A Vega. 2002. "S-100 Protein Is a Selective Marker for Sensory Hair Cells of the Lateral Line System in Teleosts." *Neuroscience Letters* 329 (2): 133–36. https://doi.org/10.1016/S0304-3940(02)00597-9.

Alunni A, S Vaccari, S Torcia, M E Meomartini, A Nicotra, and L Alfei. 2005. "Characterization of Glial Fibrillary Acidic Protein and Astroglial Architecture in the Brain of a Continuously Growing Fish, the Rainbow Trout." *European Journal of Histochemistry : EJH* 49 (2): 157–66. https://doi.org/https://doi.org/10.4081/940.

Armando, Federico, Claudio Pigoli, Matteo Gambini, Andrea Ghidelli, Gabriele Ghisleni, Attilio Corradi, Benedetta Passeri, et al. 2021. "Peripheral Nerve Sheath Tumors Resembling Human Atypical Neurofibroma in Goldfish (Carassius Auratus, Linnaeus, 1758)." *Animals* 11 (9): 2621. https://doi.org/10.3390/ani11092621.

Bunton, T. E. 1993. "The Immunocytochemistry of Cytokeratin in Fish Tissues." *Veterinary Pathology* 30 (5): 418–25. https://doi.org/10.1177/030098589303000503.

Chênais, Nathalie, Aurelie le Cam, Brigitte Guillet, Jean-Jacques Lareyre, and Catherine Labbé. 2023. "TGFβ Inhibition and Mesenchymal to Epithelial Transition Initiation by Xenopus Egg Extract: First Steps towards Early Reprogramming in Fish Somatic Cell." *Scientific Reports* 13 (1): 9967. https://doi.org/10.1038/s41598-023-36354-3.

Clemen, Christoph S., Harald Herrmann, Sergei v. Strelkov, and Rolf Schröder. 2013. "Desminopathies: Pathology and Mechanisms." *Acta Neuropathologica* 125 (1): 47–75. https://doi.org/10.1007/s00401-012-1057-6.

Denk, Daniela, Ranieri Verin, Lorenzo Ressel, Eleanor Lewis, and Mark F Stidworthy. 2020. "Spontaneous Neoplasia in Captive Syngnathid Species: A Retrospective Case Series (2003–2014) and Literature Review." *Journal of Fish Diseases* 43 (8): 929–39. https://doi.org/10.1111/jfd.13203.

Faílde, L.D., R. Bermúdez, F. Vigliano, G.A. Coscelli, and M.I. Quiroga. 2014. "Morphological, Immunohistochemical and Ultrastructural Characterization of the Skin of Turbot (Psetta Maxima L.)." *Tissue and Cell* 46 (5): 334–42. https://doi.org/10.1016/j.tice.2014.06.004.

Fonseca, Vera G., Joana Rosa, Vincent Laizé, Paulo J. Gavaia, and M. Leonor Cancela. 2011. "Identification of a New Cartilage-Specific S100-like Protein up-Regulated during Endo/Perichondral Mineralization in Gilthead Seabream." *Gene Expression Patterns* 11 (7): 448–55. https://doi.org/10.1016/j.gep.2011.07.003.

Galeotti, M., G. Sarli, R. Sirri, L. Mandrioli, P. Beraldo, P. Bronzatti, R. Giavenni, M. Orioles, G.E. Magi, and D. Volpatti. 2021. "Red Mark Syndrome of Trout (*Oncorhynchus Mykiss* ; Walbaum, 1792): Histopathological Scoring and Correlation with Gross Lesions." *Journal of Fish Diseases* 44 (9): 1325–36. https://doi.org/10.1111/jfd.13391.

Germanà, A., F. Marino, M.C. Guerrera, S. Campo, P. de Girolamo, G. Montalbano, G.P. Germanà, F.J. Ochoa-Erena, E. Ciriaco, and J.A. Vega. 2008. "Expression and Distribution of S100 Protein in the Nervous System of the Adult Zebrafish (*Danio rerio*)." *Microscopy Research and Technique* 71 (3): 248–55. https://doi.org/10.1002/jemt.20544.

Grunow, B., B. Böhmert, and K. Fechner. 2013. "Specificity of Antibodies Established from Mammals in Rainbow Trout (*Oncorhynchus Mykiss)*." *Journal of Applied Ichthyology* 29 (5): 1129–33. https://doi.org/10.1111/jai.12146.

Hagström, Christina, and Catharina Olsson. 2010. "Glial Cells Revealed by GFAP Immunoreactivity in Fish Gut." *Cell and Tissue Research* 341 (1): 73–81. https://doi.org/10.1007/s00441-010-0979-3.

Herrmann, Harald, Michaela D. Münick, Monika Brettel, Bernadette Fouquet, and Jürgen Markl. 1996. "Vimentin in a Cold-Water Fish, the Rainbow Trout: Highly Conserved Primary Structure but Unique Assembly Properties." *Journal of Cell Science* 109 (3): 569–78. https://doi.org/10.1242/jcs.109.3.569.

Hewitt, Stephen M., Denis G. Baskin, Charles W. Frevert, William L. Stahl, and Eduardo Rosa-Molinar. 2014. "Controls for Immunohistochemistry." *Journal of Histochemistry & Cytochemistry* 62 (10): 693–97. https://doi.org/10.1369/0022155414545224.

Iaria, C., A. Ieni, I. Corti, R. Puleio, C. Brachelente, G. Mazzullo, and G. Lanteri. 2019. "Immunohistochemical Study of Four Fish Tumors." *Journal of Aquatic Animal Health* 31 (1): 97–106. https://doi.org/10.1002/aah.10058.

Kálmán, Mihály. 1998. "Astroglial Architecture of the Carp (Cyprinus Carpio) Brain as Revealed by Immunohistochemical Staining against Glial Fibrillary Acidic Protein (GFAP)." *Anatomy and Embryology* 198 (5): 409–33. https://doi.org/10.1007/s004290050193.

Lanteri, G, A Ieni, A Toffan, J Abbate, M Saraò, V Barresi, and B Macrì. 2016. "Immunohistochemical patterns of a non-viral papilloma in goldfish (Carassius auratus, L." *Bull. Eur. Assoc. Fish Pathol* 36: 208–13. https://scholar.google.com/scholar_lookup?title=Immunohistochemical+patterns+of+a+non-viral+papilloma+in+goldfish+(Carassius+auratus,+L.)&author=Lanteri,+G.&author=Ieni,+A.&author=Toffan,+A.&author=Abbate,+J.&author=Sara%C3%B2,+M.&author=Barresi,+V.&author=Macr%C3%AC,+B.&publication_year=2016&journal=Bull.+Eur.+Assoc.+Fish+Pathol.&volume=36&pages=208%E2%80%93213.

Letterio, John J., and Anita B. Roberts. 1998. "REGULATION OF IMMUNE RESPONSES BY TGF-β." *Annual Review of Immunology* 16 (1): 137–61. https://doi.org/10.1146/annurev.immunol.16.1.137.

Marino, F, G Lanteri, G Rapisarda, A Perillo, and B Macrì. 2012. "Spontaneous Schwannoma in Zebrafish, *Danio rerio* (Hamilton)." *Journal of Fish Diseases* 35 (3): 239–42. https://doi.org/10.1111/j.1365-2761.2011.01335.x.

Markl, Jürgen, and Werner W. Franke. 1988. "Localization of Cytokeratins in Tissues of the Rainbow Trout: Fundamental Differences in Expression Pattern between Fish and Higher Vertebrates." *Differentiation* 39 (2): 97–122. https://doi.org/10.1111/j.1432-0436.1988.tb00086.x.

Moore, Blake W. 1965. “A Soluble Protein Characteristic of the Nervous System.” *Biochemical and Biophysical Research Communications* 19 (6): 739–44. https://doi.org/10.1016/0006-291x(65)90320-7.

Nathan, Carl. 2016. “Macrophages’ Choice: Take It In or Keep It Out.” *Immunity* 45 (4): 710–11. https://doi.org/10.1016/j.immuni.2016.10.002.

Paquette, CE, ML Kent, TS Peterson, R Wang, RH Dashwood, and CV Löhr. 2015. “Immunohistochemical Characterization of Intestinal Neoplasia in Zebrafish *Danio rerio* Indicates Epithelial Origin.” *Diseases of Aquatic Organisms* 116 (3): 191–97. https://doi.org/10.3354/dao02924.

Polinas, Marta, Francesc Padrós, Paolo Merella, Marino Prearo, Marina Antonella Sanna, Fabio Marino, Giovanni pietro Burrai, and Elisabetta Antuofermo. 2021. “Stages of Granulomatous Response Against Histozoic Metazoan Parasites in Mullets (Osteichthyes: Mugilidae).” *Animals* 11 (6): 1501. https://doi.org/10.3390/ani11061501.

Quaglio, F, V Zappulli, L Poppi, P Capovilla, F Capparucci, and F Marino. 2016. “Squamous Cell Carcinoma in a Wild European Bullhead Cottus Gobio.” *Diseases of Aquatic Organisms* 122 (1): 73–76. https://doi.org/10.3354/dao03065.

Rahmati-Holasoo Sara; Masoudifard Majid; Davudypoor S.; Vaseghi M, Hooman; Shokrpoor. 2018. “Telangiectatic Osteosarcoma and Renal Adenocarcinoma in an Oscar (Astronotus Ocellatus, Agassiz): Diagnostic Imaging and Immunohistochemical Study.” *Journal of Fish Diseases* 41 (7): 1165–72. https://doi.org/10.1111/jfd.12788.

Ramos-Vara, J. A., and M. A. Miller. 2014. “When Tissue Antigens and Antibodies Get Along.” *Veterinary Pathology* 51 (1): 42–87. https://doi.org/10.1177/0300985813505879.

Ramos-Vara, José A., and Luke B. Borst. 2016. “Immunohistochemistry.” In *Tumors in Domestic Animals*, edited by Ed., 5th ed., 44–87. Meuten, D.J: Wiley. https://doi.org/10.1002/9781119181200.ch3.

Roccabianca, P, Y Schulman, G Avallone, R Foster, J Scruggs, K Dittmer, and M Kiupel. 2020. “Surgical Pathology of Tumors of Domestic Animals.” 3: Tumors of Soft Tissue. https://scholar.google.com/scholar_lookup?title=Surgical+Pathology+of+Tumors+of+Domestic+Animals.+3:+Tumors+of+Soft+Tissue&author=Roccabianca,+P.&author=Schulman,+Y.&author=Avallone,+G.&author=Foster,+R.&author=Scruggs,+J.&author=Dittmer,+K.&author=Kiupel,+M.&publication_year=2020.

Romano, L A, and V F Pedrosa. 2020. “Neoplasias in Fish: Review of the Last 20 Years. A Look from the Pathology.” *Annu. Res. Rev. Biol* 35: 134–53.

Ronza Antonio; Méndez Lucía; Pardo Belén G.; Bermúdez Roberto; Quiroga María Isabel, Paolo; Villamarín. 2019. “Immunohistochemical Expression of E–Cadherin in Different Tissues of the Teleost Fish Scophthalmus Maximus.” *Aquaculture* 501 (NA): 465–72. https://doi.org/10.1016/j.aquaculture.2018.12.009.

Rowlerson, A., G. Radaelli, F. Mascarello, and A. Veggetti. 1997. “Regeneration of Skeletal Muscle in Two Teleost Fish: *Sparus aurata* and Brachy*Danio rerio*.” *Cell and Tissue Research* 289 (2): 311–22. https://doi.org/10.1007/s004410050878.

Šálková, Eva, Heike Schmidt-Posthaus, Ilka Lutz, Hana Kocour Kroupová, and Christoph Steinbach. 2022. “Immunohistochemical Investigation of Epithelial, Mesenchymal,

Neuroectodermal, Immune and Endocrine Markers in Sterlet (Acipenser Ruthenus), Shortnose Sturgeon (Acipenser Brevirostrum) and Common Carp (Cyprinus Carpio)." *Fish Physiology and Biochemistry* 48 (6): 1737–49. https://doi.org/10.1007/s10695-022-01145-6.

Sayyaf Dezfuli, Bahram, Massimo Lorenzoni, Antonella Carosi, Luisa Giari, and Giampaolo Bosi. 2023. "Teleost Innate Immunity, an Intricate Game between Immune Cells and Parasites of Fish Organs: Who Wins, Who Loses." *Frontiers in Immunology* 14 (1): 417–34. https://doi.org/10.3389/fimmu.2023.1250835.

Sirri Giorgia; Budai Jane; Beraldo Paola; Fiorentino Michelangelo; Barbé Tim; Galeotti Marco; Sarli Giuseppe; Mandrioli Luciana, Rubina; Tura. 2020. "Histological and Immunohistochemical Characterization of 17 Gonadal Tumours in Koi Carp (Cyprinus Carpio Koi)." *Journal of Fish Diseases* 44 (3): 273–85. https://doi.org/10.1111/jfd.13280.

Sirri, Rubina, Giorgia Tura, Jane Budai, Paola Beraldo, Michelangelo Fiorentino, Tim Barbé, Marco Galeotti, Giuseppe Sarli, and Luciana Mandrioli. 2021. "Histological and Immunohistochemical Characterization of 17 Gonadal Tumours in Koi Carp (*Cyprinus Carpio Koi*)." *Journal of Fish Diseases* 44 (3): 273–85. https://doi.org/10.1111/jfd.13280.

Stilwell, Justin M., Shane M. Boylan, Bryan Vorbach, and Alvin C. Camus. 2021. "Epizootic Neoplasia in a Managed Population of Atlantic Bumper Fish, *Chloroscombrus Chrysurus* (Osteichthyes: Carangidae), at a Public Aquarium." *Journal of Fish Diseases* 44 (4): 415–27. https://doi.org/10.1111/jfd.13326.

Stilwell, Justin M., Rita McManamon, Ginger L. Sturgeon, Melinda S. Camus, and Alvin C. Camus. 2019. "Microscopic, Immunohistochemical and Ultrastructural Characterization of Spontaneous Lepidosarcomas in a Neon Tetra, *Paracheirodon Innesi* , and a Black Crappie, *Pomoxis Nigromaculatus*." *Journal of Fish Diseases* 42 (7): 1077–83. https://doi.org/10.1111/jfd.13011.

Webster, Joshua D., Margaret Solon, and Katherine N. Gibson-Corley. 2021. "Validating Immunohistochemistry Assay Specificity in Investigative Studies: Considerations for a Weight of Evidence Approach." *Veterinary Pathology* 58 (5): 829–40. https://doi.org/10.1177/0300985820960132.

Yasumoto, Shinya, Daiji Koga, Kazuyuki Tanaka, Masakazu Kondo, and Yukinori Takahashi. 2015. "Histopathological and Immunohistochemical Studies of Gonadal Undifferentiated Carcinoma in Common Carp <I>Cyprinus Carpio</I>" *Fish Pathology* 50 (2): 53–59. https://doi.org/10.3147/jsfp.50.53.

Chapter V – Part 1

Prevention and therapy of fish mycobacteriosis

https://doi.org/10.1111/jfd.14091

5. Susceptibility of non-tuberculous mycobacteria biofilm to common disinfectants in aquaculture systems

5.1 Introduction

The family Mycobacteriaceae consists of a diverse group of Gram-positive, rod-shaped, acid-fast positive bacteria within the phylum Actinobacteria. This family includes many important pathogens within the *M. tuberculosis* complex, most notably *Mycobacterium tuberculosis, M. bovis*, *M. avium*, and a wide range of non-tuberculous mycobacteria (NTM) (Hartmans et al., 2006; Gao and Gupta, 2012; Gopalaswamy et al., 2020). The latter, also known as atypical or environmental mycobacteria (Shinnick et al., 1994), are typically free-living organisms ubiquitous in the environment, with over 200 identified species, approximately 140 of which are known to be pathogenic to humans and animals (Porvaznik et al., 2016; Matsumoto et al., 2019; Armstrong et al., 2023). Within the NTM group, species can be categorized based on their growth rates into two types: slow-growing bacteria, which take more than 7 days to form colonies, and rapid-growing bacteria, which form colonies in less than 7 days (Gupta et al., 2018). NTMs can cause a wide range of infections, impacting diverse hosts including mammals, reptiles, and fish (Pereira et al., 2020).

In fish, the impact of NTMs is particularly noteworthy, causing a disease known as piscine mycobacteriosis affecting aquaculture and wildlife, with significant economic and health implications (Decostere et al., 2004; Francis-Floyd., 2011; Delghandi et al., 2020). NTMs affecting fish include species like *M. marinum, M. chelonae*, and *M. fortuitum*, along with other less frequently isolated species such as *M. salmoniphilum, M. abscessus, M. pseudoshottsii, M. ulcerans, M. gordonae, M. haemophilum* (Francis-Floyd., 2011; Delghandi et al., 2020). Furthermore, many of these pathogens have zoonotic potential, posing additional risks to human health, particularly for veterinarians, biologists, and aquarium workers. Mycobacterial infections are typically linked to cleaning aquaria or injuries from contact with fish, leading to skin lesions

known as “fish tank granuloma” or “fish handler’s disease” (Aubry et al., 2002; Decostere et al., 2004; Francis-Floyd., 2011; Delghandi et al., 2020).

In natural environments, NTMs are often found in biofilms, especially polymicrobial ones, where mycobacteria interact with other microorganisms (Johansen et al., 2020; Muñoz-Egea et al., 2023). In this community-like condition, bacteria improve their ability to survive in harsh environments through a self-organized 3D microbial structure, with cells enclosed within a self-produced extracellular matrix that may be attached to a biotic or abiotic substratum (Yin et al., 2019; Guzmán-Soto et al., 2021). Biofilm bacteria also exhibit distinct metabolism and gene expression compared to their planktonic counterparts and present an altered phenotype with increased tolerance to host immune defense mechanisms and exogenously administered antimicrobial substances (Guzmán-Soto et al., 2021). The ability of mycobacteria to form biofilms, coupled with their unique cell wall properties represent a critical pathogenic factor in many NTM infections (Muñoz-Egea et al., 2023). To further complicate the scenario, significant differences have been reported between species and strains, with variations observed between clinical and collection isolates (Zamora et al., 2007).

Although attempts have been made, no vaccines are currently commercially available for the disease (Delghandi et al., 2020) and treatment is challenging due to the slow drug absorption and prolonged treatment required for mycobacteria, with differences between fast and slow-growing species (van Ingen et al.; 2012). Acquired antibiotic resistance further complicates treatments (Uruén et al., 2020; Sharma et al., 2021; Muñoz-Egea et al., 2023). Therefore, prophylaxis remains the best control option, including disinfection, eradication of infected stocks and optimizing husbandry practices (Francis-Floyd., 2011; Delghandi et al., 2020).

Extensive research has explored the susceptibility of various NTM *Mycobacterium* spp. to disinfectants and antimicrobials, primarily focusing on their planktonic forms (Mainous et al., 2005; van Ingen et al.; 2012; Chang et al., 2015; Burgess et al., 2017; Wang et al., 2019), and then addressing biofilm (Bardouniotis et al., 2001, 2003; Steed et al., 2006; Kolpen et al., 2020; Saxena

et al., 2021). Yet, a notable gap in understanding persists regarding the formation of mycobacterial biofilms and their susceptibility to disinfectants within aquaculture environments. The increasing resistance of Mycobacteria biofilms to disinfectants and antibiotics presents a significant challenge (Tarashi et al., 2022; Conyers et al., 2024), particularly in aquaculture systems where the resilience of mycobacterial biofilms remains inadequately studied and can act as a reservoir for bacterial outbreaks.

Thus, our study aimed to compare biofilm formation among different *Mycobacterium* spp. previously recovered from outbreaks of mycobacteriosis in fish, employing the Minimal Biofilm Eradication Concentration (MBEC) Assay® system, and investigating their resistance to common disinfectants used in aquaculture systems.

5.2. Materials and methods

5.2.1 Bacterial strains and phylogenetic analysis

Four *Mycobacterium* spp. previously isolated from diseased fish at the Aquatic Animal Health Laboratory, School of Veterinary Medicine, University of California Davis, were selected for this study (*Fig. 48, Table 9*). Isolates were stored in 1 mL aliquots in brain heart infusion broth (BHI; MP Biomedicals) with 20% glycerol at −80°C. Prior to each experiment, isolates were revived from frozen stock on trypticase soy agar with 5% sheep blood agar (SBA; University of California, Biological Media Services) at 28°C in aerobic conditions. All strains were then expanded in BHI at 100 rpm until they reached the early stationary phase, which was 3-4 days for the rapid-growers (*M. chelonae, M. salmoniphilum, M. arcueilense*) and 7-10 days for *M. marinum*.

5.2.2. rpoB amplification and sequence analysis

Genomic DNA (gDNA) from all isolates was extracted using the DNeasy Blood and Tissue Kit (Qiagen, Hilden, Germany) according to the manufacturer's protocol for Gram-positive bacteria.

The extracted gDNA was quantified using a NanoDrop ND-1000 spectrophotometer (Thermo Fisher Scientific) and stored at −20°C until further analysis.

Molecular characterization was performed by PCR amplification and sequencing of a 723-bp fragment of the RNA polymerase β-subunit (*rpoB*) gene, using primers described by Adamek et al. (2003). The amplification was conducted by using 2X DreamTaq Master Mix (Thermo Fisher Scientific) on a SimpliAmp Thermal Cycler (Applied Biosystems, Foster City, California, USA) using the following thermal profile: 2 min. initial denaturation at 94 °C; followed by 35 cycles of denaturation at 94°C, annealing at 60°C and extension at 72 °C, each for 1 min; and final incubation at 72°C for 5 min. Amplification products, along with the marker (GeneRuler 1 kb plus DNA Ladder; Thermo Fisher Scientific) were electrophoresed through 1.2% agarose gel that was supplemented with SYBR Safe DNA gel stain (Invitrogen, Carlsbad, California, USA) and visualized under ultraviolet light. Amplicons were purified using the QIAquick PCR Purification Kit (Qiagen) and quantified spectrophotometrically. The purified products and corresponding primers were submitted for Sanger sequencing at AZENTA/GENEWIZ (South Plainfield, New Jersey, USA). Partial *rpoB* sequences were analyzed using BioEdit (version 7.2.5) and aligned with MUSCLE (Edgar 2004). Sequences were compared with those of closely related species through non-redundant nucleotide BLASTn searches in the National Center for Biotechnology Information's (NCBI) GenBank database.

A maximum-likelihood phylogenetic tree was generated using MEGA X software, based on the General Time Reversible model with a gamma distribution, and bootstrap analysis with 1,000 replicates. Reference sequences from the *M. chelonae-abscessus, fortuitum-vaccae*, and *tuberculosis-simiae* clades were included to determine the phylogenetic positioning of the isolates.

5.2.3 Biofilm formation assay

Biofilms were formed using an inoculator with a 96-well base and hydroxyapatite coated pegs (Innovotech Inc., Edmonton, Canada) following methods adapted from the manufacturer protocol (MBEC Assay® Procedural Manual Version 2.1, 2019) and Heckman et al. (2021). A 0.5 McFarland solution (optical density at 600 nm between 0.08 and 0.1) was generated for each bacterial isolate from BHI at early stationary time points, and solutions diluted to ~1.5×10^5 CFU (colony-forming units) ml^{-1} in sterile BHI. Aliquots of 150 µl of either diluted bacterial suspension or sterile media (as controls) were dispensed into the wells of the MBEC™ biofilm inoculator. The inoculator plates were then sealed with the pegged lid and incubated at 25°C under constant agitation (110 rpm). Biofilm formation by mycobacterial isolates was assessed at 2, 4, 8, 12, and 14 days after inoculation. At each time point, the corresponding pegs were rinsed in sterile phosphate-buffered saline (PBS) for 10 seconds to eliminate non-adherent cells. Pegs were then detached using flame-sterilized pliers and placed into 200 µl of sterile PBS in a round-bottom 96-well plate. To dislodge the biofilm into suspension, the plates were sonicated at high power for 30 minutes. The resulting suspensions were serially diluted, and 10 µl aliquots were spot-plated in triplicate to determine the number of viable, biofilm-associated cells for each isolate and time point. This procedure was used consistently for all subsequent sonication and quantification steps. Each strain was tested in triplicate, with the entire experiment independently replicated twice.

5.2.4 Susceptibility to Different Disinfectants

The resistance of *Mycobacterium* spp. biofilms to disinfectants was evaluated using a modified version of the MBEC Assay® protocol adapted from Heckman et al. (2021). Sodium hypochlorite (bleach), povidone iodine (Ovadine®), hydrogen peroxide, Virkon® Aquatic, and 70% ethanol were selected for testing based on their common usage in aquaculture systems (Table 1) (Yanong and Erlacher-Reid, 2012) (*Table 8*).

Proper working concentrations were achieved by diluting the following stock solutions: 5.25% sodium hypochlorite (bleach), 1% available iodine (povidone-iodine), 30% hydrogen peroxide (H_2O_2), Virkon® Aquatic, and 100% ethanol. Working concentrations were prepared using filtered sterilized water (FSW) obtained from the Center for Aquatic Biology and Aquaculture (Davis, CA, USA). FSW was sterilized through a 0.2 μm filter (Millipore Sigma, USA) to ensure sterility. All solutions were freshly prepared immediately before each experimental challenge using non-expired stock materials to minimize the risk of degradation of active ingredients.

Table 8. Treatment conditions for testing biofilm susceptibility to common disinfectants selected from recommended protocols in aquaculture (Yanong and Erlacher-Reid, 2012).

DISINFECTANT	ACTIVE INGREDIENT	CONCENTRATION	CONTACT TIME (MINUTES)
BLEACH	Sodium hypochlorite	200 mg L−1 available chlorine	30
OVADINE®	Povidone-iodine	50 mg L−1 free iodine	30
VIRKON® AQUATIC	21.4% potassium peroxymonosulfate, 1.5% sodium chloride	10 g L−1	15
HYDROGEN PEROXIDE	Hydrogen peroxide	3% H_2O_2	15
ETHANOL	Ethyl alcohol	70% Ethanol	30 - 15

Briefly, mature biofilms were cultivated over 12 days, following previously established protocols. A subset of two pegs per strain was removed and quantified to serve as a biofilm growth check (BGC). The remaining pegs (three pegs per strain for each disinfectant) were exposed to the disinfectants in a round-bottom 96-well "challenge" plate containing the disinfectants at proper concentrations. Pegs exposed only to FSW served as positive controls. After the recommended contact times, the biofilms were transferred to a new round-bottom 96-well plate containing 200 μl sterile PBS and incubated for 30 min at room temperature to equilibrate. The plates were then sonicated on high for 30 minutes to dislodge the biofilm-associated bacteria into suspension. The

suspensions were serially diluted, and 10 µL aliquots were spot-plated in triplicate to quantify the remaining viable bacteria. Spot plates were incubated at 28°C and checked for growth for 10 days. The absence of colony growth on the SBA after 10 days indicated full susceptibility to the treatment.

5.2.5 Statistical analysis

Statistical tests were performed using GraphPad Prism (version 8.0.2, GraphPad Software, La Jolla, CA USA). The dynamics of biofilm growth were first assessed through Area Under the Curve (AUC), followed by one-way ANOVA and Tukey's multiple comparison test to compare biofilm formation across the different isolates. Additionally two-way ANOVA was used to determine the significance of different treatments with Dunnet's multiple comparison test to compare biofilm formation and to evaluate the impact of disinfectant on biofilm persistence for all isolates.

5.3. Results

5.3.1 Bacterial identification

According to the phylogenomic framework proposed by Gupta et al. (2018), the isolates clustered into distinct clades: *M. chelonae-abscessus* clade (*M. chelonae* and *M. salmoniphilum)*, the *fortuitum-vaccae* clade (*M. arcueilense*), and the *tuberculosis-simiae* clade (*M. marinum*) (*Fig. 48; Table 9*).

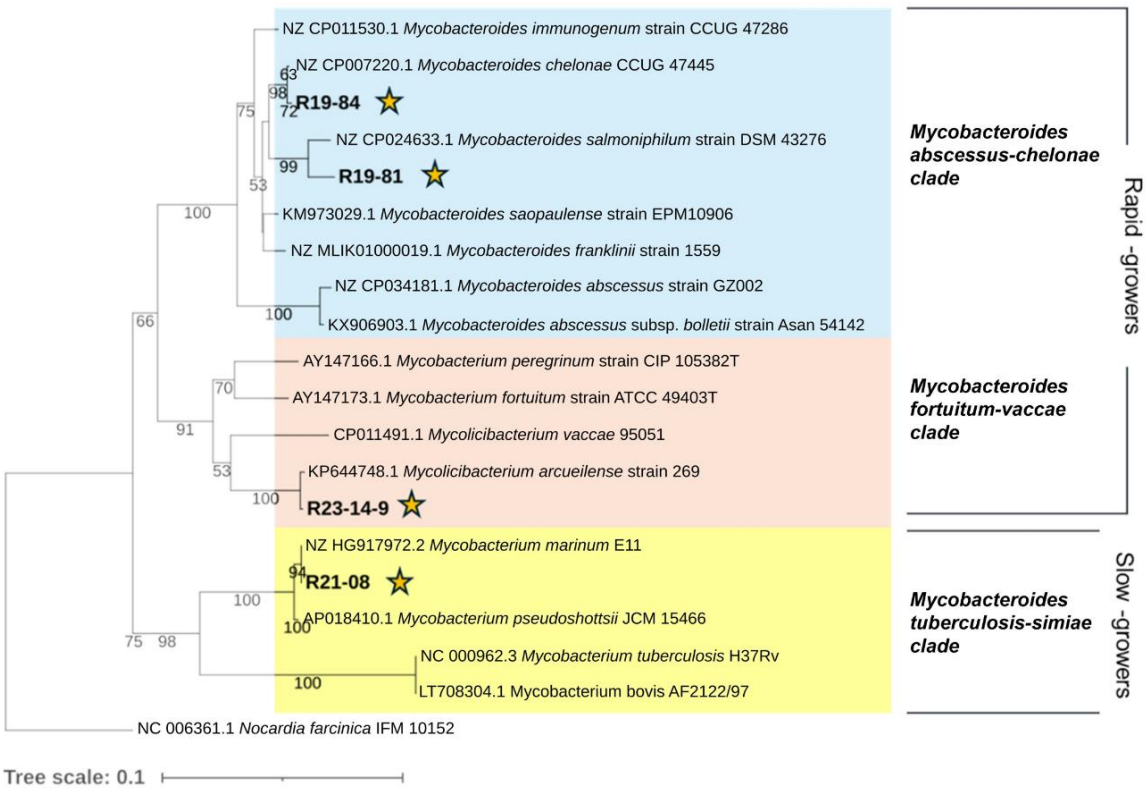

Figure 48. *Maximum-likelihood phylogenetic tree for Mycobacterium isolates based on rpoB. Stars indicate Mycobacterium spp. used in this study and colors indicate different clades. The analysis was done on 1000 bootstrapped data sets and values. The scale bar indicates substitutions per nucleotide position.*

Table 9. *Mycobacterium spp. isolates used in this study. Clade denotation was determined by rpoB analysis following phylogenomic from Gupta et al. (2018).*

ID UC DAVIS	SPECIES	SOURCE	RAPID/SLOW GROWER	*rpoB* PHYLOGENY (CLADE)
R19-84	*M. chelonae*	Chinook salmon (*Oncorhynchus tshawytscha*)	Rapid (3-4 days)	*abscessus-chelonae*
R19-81	*M. salmoniphilum*	Chinook salmon	Rapid (3-4 days)	*abscessus-chelonae*
R21-08	*M. marinum*	Delta smelt (*Hypomesus transpacificus*)	Slow (7-10 days)	*tuberculosis – simiae*
R23-14-9	*M. arcueilense*	Largemouth bass (*Micropterus salmoides*)	Rapid (3-4 days)	*fortuitum – vaccae*

5.3.2 Biofilm formation kinetics

All isolates exhibited the ability to form biofilms, with significant variation in the extent and rate of biofilm development among different species. The kinetics of biofilm formation are illustrated in *Fig. 49*. The growth followed the expected sigmoidal pattern: an initial lag phase, followed by rapid growth, and finally, a stationary phase. The kinetics of biofilm formation varied among species, reflecting inherent biological differences. *Mycobacterium chelonae* and *M. salmoniphilum*, both rapid-grower species, showed robust biofilm formation starting from day 2, with a substantial increase by day 8 for *M. chelonae* and day 12 and 14 for *M. salmoniphilum*. The biofilm density plateaued from day 12 onwards. *Mycobacterium arcueilense* also formed biofilms rapidly, similar to *M. chelonae* and *M. salmoniphilum*, with biofilm presence by day 4 and maximum formation observed by day 12. In contrast, *M. marinum*, being a slow-grower, demonstrated delayed biofilm formation, becoming noticeable around day 8 and reaching its peak by day 12. The AUC analysis revealed statistically significant differences between *M. chelonae* and *M. salmoniphilum* compared to *M. marinum* (***p < 0.0001, **p < 0.001) (*Fig. 50*).

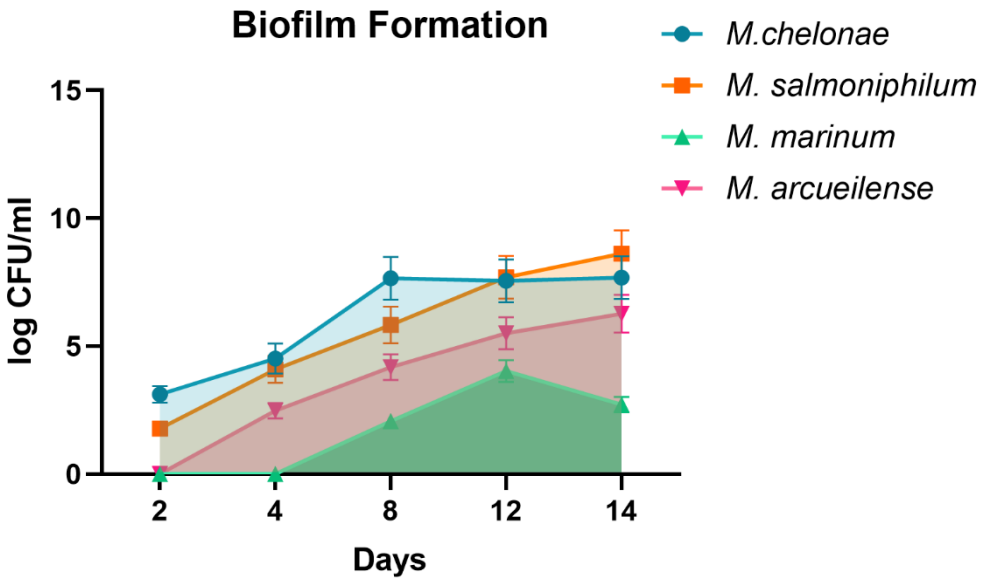

Figure 49. *Quantification of non-tuberculous (NTM) Mycobacterium spp. biofilm (log CFU/mL) using the MBEC Assay in BHI at 25°C. Error bars represent the standard error.*

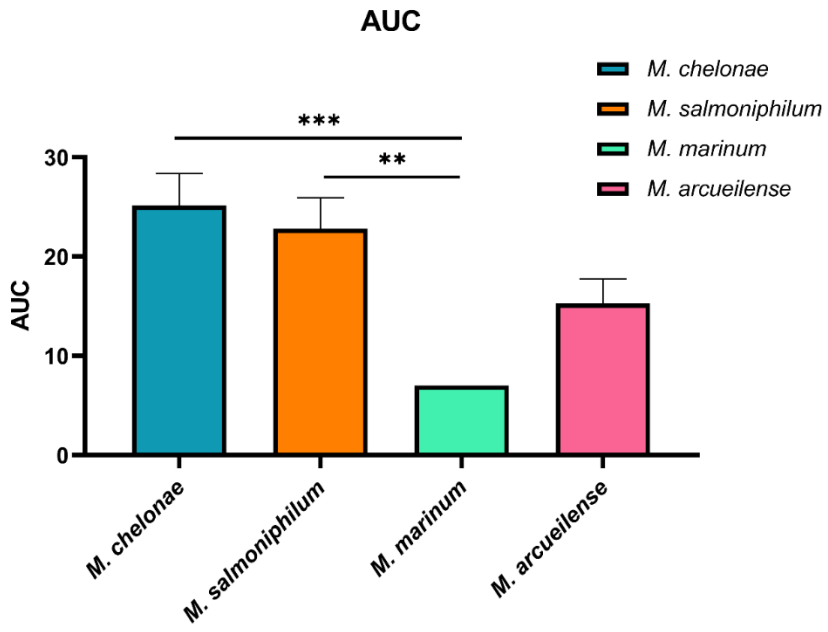

Figure 50*. Area Under the Curve (AUC) Analysis: The AUC analysis was used to quantify biofilm formation dynamics across different Mycobacterium species. Error bars represent standard error. Asterisks (*) indicate significant differences (***: p < 0.001; **: p<0.005).*

5.3.3 *Disinfectant efficacy on biofilm-associated Mycobacterium spp.*

Disinfection efficacy varied by strain and exposure time (*Fig. 51*). *Mycobacterium marinum* was susceptible to all disinfectants at both 15-minute and 30-minute treatments, achieving complete eradication of viable bacteria. *Mycobacterium arcueilense* was susceptible to bleach, povidone-iodine, and 70% ethanol after a 30-minute exposure. However, substantial biofilm-associated bacteria were still detectable after the 15-minute treatment, with only partial effectiveness of 70% ethanol. Conversely, no treatments were effective against *M. chelonae* and *M. salmoniphilum* biofilms at either time point. For *M. chelonae* only the 30-minute treatments with bleach and 70% ethanol showed partial effectiveness, with substantial biofilm-associated bacteria still remaining. The statistical analysis confirmed significant differences in biofilm formation after the 30-minute treatment with bleach (**p < 0.001) and 70% ethanol (*p < 0.01) for *M. chelonae*, while 70%

ethanol was also significantly effective after the 15-minute treatment for *M. chelonae* (***p < 0.0001), *M. salmoniphilum*, and *M. arcueilense* (*p < 0.01).

Bleach	Ovadine®	Ethanol	Virkon® Aquatic	Hydrogen peroxide	FSW
200 mg L^{-1} available chlorine	50 mg L^{-1} free iodine	70% Ethanol	10 g L^{-1}	3% H_2O_2	Filtered Sterilized Water

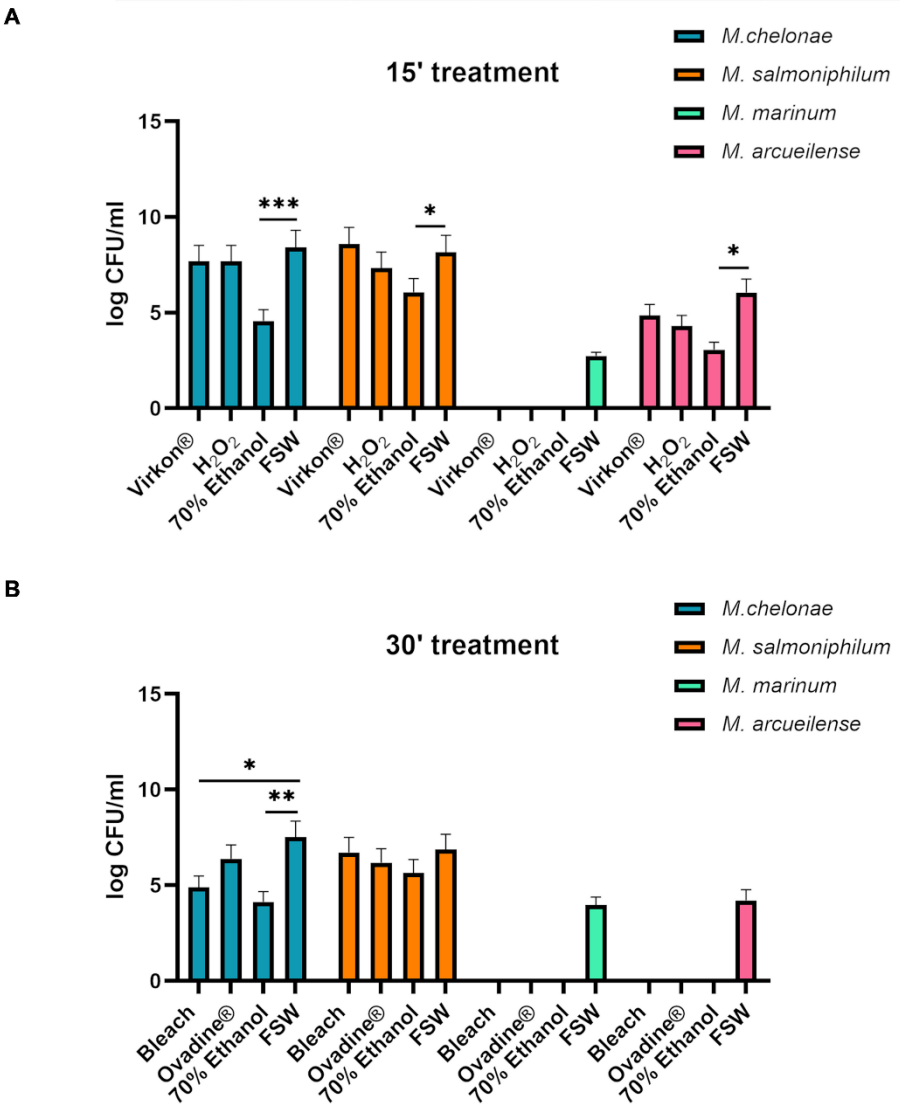

Figure 51. *Quantification of non-tuberculous (NTM) Mycobacterium spp. biofilm (log CFU/ml) after challenge with the recommended treatment (bleach, Ovadine®, 70% ethanol) for 15 (A) or 30 minutes (B). FSW (filtered-sterilized water) served as the positive control. Error bars represent standard error. Asterisks indicate significant differences (*p < 0.05; **p < 0.01; ***p < 0.001).*

5.4. Discussion and conclusion

Biofilm formation by NTMs is a critical survival mechanism that provides protection against environmental stressors, including disinfectants and antibiotics (Esteban & García-Coca, 2018; Muñoz-Egea et al., 2023). The emergence of highly resistant NTM strains to different antibiotics and disinfectants has increasingly drawn attention from the research community due to their implications for human and animal health (Tarashi et al., 2022; Conyers et al., 2024).

All *Mycobacterium* spp. isolates formed significant biofilms under the tested conditions, including *M. salmoniphilum* and *M. arcueilense*, which had not been previously tested for biofilm formation. These findings align with other studies, confirming that both rapid- and slow-growing NTMs can form biofilms (Muñoz-Egea et al., 2023). *Mycobacterium chelonae* and *M. salmoniphilum* exhibited substantial biofilm formation, reaching significant biomass levels by days 8 and 12, respectively. Despite limited knowledge about *M. salmoniphilum*'s biofilm, it is closely related to *M. chelonae*, known for robust biofilm formation and resistance to disinfectants and antimicrobials (Williams et al., 2009; Wang et al., 2019; Tarashi et al., 2022).

None of the tested disinfectants effectively eliminated *M. chelonae* or *M. salmoniphilum* biofilm-associated cells. These findings corroborate those of Chang et al. (2015), who reported resistance of *M. chelonae* to bleach, hydrogen peroxide, and povidone-iodine. However, it is important to note that Chang et al.'s study was performed on planktonic bacteria under different conditions, including temperature, disinfectant concentration and exposure time. Furthermore, Steed and Falkinham (2006) found that biofilms of *M. avium* and *M. intracellulare* exposed to chlorine were significantly more resistant than their planktonic counterparts.

Mycobacterium arcueilense also formed biofilm rapidly, with significant presence by day 4 and maximum formation observed by day 12. Biofilm-associated cells of *M. arcueilense* showed varying responses to disinfectants depending on exposure time. The species was susceptible to bleach, povidone-iodine, and 70% ethanol after 30 minutes of exposure, while shorter exposure

times (15 minutes) with hydrogen peroxide, Virkon® Aquatic, and 70% ethanol were less effective. Similar results were reported by Chang et al. (2015), who found susceptibility in planktonic cells of *M. peregrinum* to bleach and povidone-iodine, but higher resistance to hydrogen peroxide.

Mycobacterium marinum displayed the slowest biofilm formation rate, becoming noticeable around day 8 and peaking by day 12. The lower number of biofilm-associated cells may be due to its slow-growth nature and possibly influenced by lower temperatures, given that the optimal growth for this bacterium is around 30-32°C (Ramakrishnan et al., 1994). Yet, the vulnerability to disinfectants of *M. marinum* biofilms observed in our study is somewhat encouraging, as this species is one of the most reported and threatening NTMs found in fish mycobacteriosis outbreaks (Delghandi et al., 2020). Our results align with previous findings by Bardouniotis et al. (2003), where the experimental MBEC for *M. marinum* biofilms for 30 minutes were lower than those used in this study, particularly for bleach, hydrogen peroxide, and Virkon® Aquatic. Of note, in the mentioned study authors highlighted an increase in biocide resistance of *M. marinum* planktonic cells when compared to biofilms, recommending that each biofilm organism must be considered on its own as to its susceptibility to antibiotics and biocides.

Disinfectant susceptibility was tested using the MBEC method, which was previously employed in other NTM biofilm studies (Bardouniotis et al., 2001; 2003; García-Coca et al., 2020). Consistent with these studies, our findings demonstrate the robust nature of NTM biofilms, particularly those of *M. chelonae, M. salmoniphilum,* and *M. arcueilense*, which showed significant resistance to various disinfectants. The work of Bardouniotis et al. (2003) is particularly relevant as it highlighted that while biofilms are generally more resistant, the susceptibility of *M. marinum* biofilms increased with prolonged exposure to biocides, aligning with our observations. However, a crucial difference between our study and those by Bardouniotis et al. lies in our exclusive focus on biofilm-associated cells. Bardouniotis et al. also evaluated

planktonic cells, discovering that in some cases, planktonic forms exhibited resistance comparable to biofilms.

Although the exact mechanism of disinfectant resistance of these NTM is unknown, a recent review by Tarashi et al. (2022) suggests that their hydrophobic cell wall rich in mycolic acids, their tendency to form clumps, and their accumulation within biofilms play a significant role. Various molecules have been described in biofilm development, particularly glycopeptidolipids, as components of the mycobacterial cell wall, conferring hydrophobic properties to the cell surface and facilitating cell-cell interaction. Further research in the topic is warranted as the growing human population become more dependent on cultured fish, and potentially zoonotic pathogens become more prevalent in human and animal populations.

References

Adamek, Adékambi, T., Colson, P., & Drancourt, M. (2003). rpoB -Based Identification of Nonpigmented and Late-Pigmenting Rapidly Growing Mycobacteria. Journal of Clinical Microbiology, 41(12), 5699–5708. https://doi.org/10.1128/JCM.41.12.5699-5708.2003

Armstrong, D. T., Eisemann, E., & Parrish, N. (2023). A Brief Update on Mycobacterial Taxonomy, 2020 to 2022. Journal of Clinical Microbiology, 61(4). https://doi.org/10.1128/jcm.00331-22

Aubry, A., Chosidow, O., Caumes, E., Robert, J., & Cambau, E. (2002). Sixty-three Cases of *Mycobacterium marinum* Infection. Archives of Internal Medicine, 162(15), 1746. https://doi.org/10.1001/archinte.162.15.1746

Bardouniotis, E., Huddleston, W., Ceri, H., & Olson, M. E. (n.d.). Characterization of biofilm growth and biocide susceptibility testing of Mycobacterium phleiusing the MBEC® assay system. FEMS Microbiology Letters, 203(ue 2), 263–267. https://doi.org/10.1111/j.1574-6968.2001.tb10851.x

Bardouniotis, E., Ceri, H., & Olson, M. E. (2003). Biofilm Formation and Biocide Susceptibility Testing of Mycobacterium fortuitum and *Mycobacterium marinum*. Current Microbiology, 46(1), 28–32. https://doi.org/10.1007/s00284-002-3796-4

Burgess, W., Margolis, A., Gibbs, S., Duarte, R. S., & Jackson, M. (2017). Disinfectant Susceptibility Profiling of Glutaraldehyde-Resistant Nontuberculous Mycobacteria. Infection Control & Hospital Epidemiology, 38(7), 784–791. https://doi.org/10.1017/ice.2017.75

Chang, C. T., Colicino, E. G., DiPaola, E. J., Al-Hasnawi, H. J., & Whipps, C. M. (2015). Evaluating the effectiveness of common disinfectants at preventing the propagation of Mycobacterium spp. isolated from zebrafish. Comparative Biochemistry and Physiology Part C: Toxicology & Pharmacology, 178, 45–50. https://doi.org/10.1016/j.cbpc.2015.09.008

Conyers, L. E., & Saunders, B. M. (2024). Treatment for non-tuberculous mycobacteria: challenges and prospects. Frontiers in Microbiology, 15. https://doi.org/10.3389/fmicb.2024.1394220

Decostere, A., Hermans, K., & Haesebrouck, F. (2004). Piscine mycobacteriosis: a literature review covering the agent and the disease it causes in fish and humans. Veterinary Microbiology, 99(3–4), 159–166. https://doi.org/10.1016/j.vetmic.2003.07.011

Delghandi, M. R., El-Matbouli, M., & Menanteau-Ledouble, S. (2020). Mycobacteriosis and Infections with Non-tuberculous Mycobacteria in Aquatic Organisms: A Review. Microorganisms, 8(ue 9), 1368. https://doi.org/10.3390/microorganisms8091368

Esteban, J., & García-Coca, M. (2018). Mycobacterium Biofilms. Frontiers in Microbiology, 8. https://doi.org/10.3389/fmicb.2017.02651

Falkinham, J. O. (2022). Nontuberculous mycobacteria in the environment. Tuberculosis, 137, 102267. https://doi.org/10.1016/j.tube.2022.102267

Francis-Floyd, R. (2011). Mycobacterial infections of fish. United States Department of Agriculture, National Institute of Food and Agriculture.

Gao, B., & Gupta, R. S. (2012). Phylogenetic Framework and Molecular Signatures for the Main Clades of the Phylum Actinobacteria. Microbiology and Molecular Biology Reviews, 76(1), 66–112. https://doi.org/10.1128/MMBR.05011-11

García-Coca, M., Rodríguez-Sevilla, G., Pérez-Domingo, A., Aguilera-Correa, J.-J., Esteban, J., & Muñoz-Egea, M.-C. (2020). Inhibition of Mycobacterium abscessus, M. chelonae, and M. fortuitum biofilms by Methylobacterium sp. The Journal of Antibiotics, 73(1), 40–47. https://doi.org/10.1038/s41429-019-0232-6

Gopalaswamy, R., Shanmugam, S., Mondal, R., & Subbian, S. (2020). Of tuberculosis and non-tuberculous mycobacterial infections – a comparative analysis of epidemiology, diagnosis and treatment. Journal of Biomedical Science, 27(1), 74. https://doi.org/10.1186/s12929-020-00667-6

Gupta, R. S., Lo, B., & Son, J. (2018). Phylogenomics and Comparative Genomic Studies Robustly Support Division of the Genus Mycobacterium into an Emended Genus Mycobacterium and Four Novel Genera. Frontiers in Microbiology, 9. https://doi.org/10.3389/fmicb.2018.00067

Guzmán-Soto, I., McTiernan, C., Gonzalez-Gomez, M., Ross, A., Gupta, K., Suuronen, E. J., Mah, T.-F., Griffith, M., & Alarcon, E. I. (2021). Mimicking biofilm formation and development: Recent progress in in vitro and in vivo biofilm models. IScience, 24(5), 102443. https://doi.org/10.1016/j.isci.2021.102443

Hartmans, S., de Bont, J. A. M., & Stackebrandt, E. (2006). The Genus Mycobacterium--Nonmedical. In The Prokaryotes (pp. 889–918). Springer New York. https://doi.org/10.1007/0-387-30743-5_33

Heckman, T. I., & Soto, E. (2021). Streptococcus iniae biofilm formation enhances environmental persistence and resistance to antimicrobials and disinfectants. Aquaculture, 540, 736739. https://doi.org/10.1016/j.aquaculture.2021.736739

Johansen, M. D., Herrmann, J.-L., & Kremer, L. (2020). Non-tuberculous mycobacteria and the rise of Mycobacterium abscessus. Nature Reviews Microbiology, 18(7), 392–407. https://doi.org/10.1038/s41579-020-0331-1

Kolpen, M., Jensen, P. Ø., Qvist, T., Kragh, K. N., Ravnholt, C., Fritz, B. G., Johansen, U. R., Bjarnsholt, T., & Høiby, N. (2020). Biofilms of Mycobacterium abscessus Complex Can Be Sensitized to Antibiotics by Disaggregation and Oxygenation. Antimicrobial Agents and Chemotherapy, 64(2). https://doi.org/10.1128/AAC.01212-19

Mainous, M. E., & Smith, S. A. (2005). Efficacy of Common Disinfectants against *Mycobacterium marinum*. Journal of Aquatic Animal Health, 17(3), 284–288. https://doi.org/10.1577/H04-051.1

Matsumoto, Y., Kinjo, T., Motooka, D., Nabeya, D., Jung, N., Uechi, K., Horii, T., Iida, T., Fujita, J., & Nakamura, S. (2019). Comprehensive subspecies identification of 175 nontuberculous mycobacteria species based on 7547 genomic profiles. Emerging Microbes & Infections, 8(1), 1043–1053. https://doi.org/10.1080/22221751.2019.1637702

Muñoz-Egea, M.-C., Akir, A., & Esteban, J. (2023). Mycobacterium biofilms. Biofilm, 5, 100107. https://doi.org/10.1016/j.bioflm.2023.100107

Pereira, A. C., Ramos, B., Reis, A. C., & Cunha, M. V. (2020). Non-Tuberculous Mycobacteria: Molecular and Physiological Bases of Virulence and Adaptation to Ecological Niches. Microorganisms, 8(9), 1380. https://doi.org/10.3390/microorganisms8091380

Porvaznik, I., Solovič, I., & Mokrý, J. (2016). Non-Tuberculous Mycobacteria: Classification, Diagnostics, and Therapy. In Advances in Experimental Medicine and Biology (pp. 19–25). Springer International Publishing. https://doi.org/10.1007/5584_2016_45

Ramakrishnan, L., & Falkow, S. (1994). *Mycobacterium marinum* persists in cultured mammalian cells in a temperature-restricted fashion. Infection and Immunity, 62(8), 3222–3229. https://doi.org/10.1128/iai.62.8.3222-3229.1994

Saxena, S., Spaink, H. P., & Forn-Cuní, G. (2021). Drug Resistance in Nontuberculous Mycobacteria: Mechanisms and Models. Biology, 10(2), 96. https://doi.org/10.3390/biology10020096

Sharma, D., Misba, L., & Khan, A. U. (2019). Antibiotics versus biofilm: an emerging battleground in microbial communities. Antimicrobial Resistance & Infection Control, 8(1), 76. https://doi.org/10.1186/s13756-019-0533-3

Shinnick, T. M., & Good, R. C. (1994). Mycobacterial taxonomy. European Journal of Clinical Microbiology & Infectious Diseases, 13(11), 884–901. https://doi.org/10.1007/BF02111489

Steed, K. A., & Falkinham, J. O. (2006). Effect of Growth in Biofilms on Chlorine Susceptibility of Mycobacterium avium and Mycobacterium intracellulare. Applied and Environmental Microbiology, 72(6), 4007–4011. https://doi.org/10.1128/AEM.02573-05

Tarashi, S., Siadat, S. D., & Fateh, A. (2022). Nontuberculous Mycobacterial Resistance to Antibiotics and Disinfectants: Challenges Still Ahead. BioMed Research International, 2022, 1–12. https://doi.org/10.1155/2022/8168750

Uruén, C., Chopo-Escuin, G., Tommassen, J., Mainar-Jaime, R. C., & Arenas, J. (2020). Biofilms as Promoters of Bacterial Antibiotic Resistance and Tolerance. Antibiotics, 10(1), 3. https://doi.org/10.3390/antibiotics10010003

van Ingen, J., Boeree, M. J., van Soolingen, D., & Mouton, J. W. (2012). Resistance mechanisms and drug susceptibility testing of nontuberculous mycobacteria. Drug Resistance Updates, 15(3), 149–161. https://doi.org/10.1016/j.drup.2012.04.001

Wang, J., Sui, M., Yuan, B., Li, H., & Lu, H. (2019). Inactivation of two Mycobacteria by free chlorine: Effectiveness, influencing factors, and mechanisms. Science of The Total Environment, 648, 271–284. https://doi.org/10.1016/j.scitotenv.2018.07.451

Williams, M. M., Yakrus, M. A., Arduino, M. J., Cooksey, R. C., Crane, C. B., Banerjee, S. N., Hilborn, E. D., & Donlan, R. M. (2009). Structural Analysis of Biofilm Formation by Rapidly and Slowly Growing Nontuberculous Mycobacteria. Applied and Environmental Microbiology, 75(7), 2091–2098. https://doi.org/10.1128/AEM.00166-09

Yanong, R. P. E., & Erlacher-Reid, C. (2012). Biosecurity in Aquaculture, Part 1: An Overview (Issue 4707). Southern Regional Aquaculture Center.

Yin, W., Wang, Y., Liu, L., & He, J. (2019). Biofilms: The Microbial "Protective Clothing" in Extreme Environments. International Journal of Molecular Sciences, 20(14), 3423. https://doi.org/10.3390/ijms20143423

Zamora, N., Esteban, J., Kinnari, T. J., Celdrán, A., Granizo, J. J., & Zafra, C. (2007). In-vitro evaluation of the adhesion to polypropylene sutures of non-pigmented, rapidly growing mycobacteria. Clinical Microbiology and Infection, 13(9), 902–907. https://doi.org/10.1111/j.1469-0691.2007.01769.x

Chapter V - Part 2

Prevention and therapy of fish mycobacteriosis

6. Testing a Live-Attenuated *Mycobacterium chelonae* in *Carassius auratus* as a vaccine for fish mycobacteriosis

6.1 Introduction

The expansion of aquaculture over the past two decades has led to a rise in infectious diseases, with mycobacterial infections emerging as a major concern due to their persistence, high mortality rates, and potential zoonotic risks (Gauthier & Rhodes, 2009b; Delghandi et al., 2020b). The disease, known as fish mycobacteriosis, is caused by various species of non-tuberculous mycobacteria (NTMs), manifesting as chronic infection with nonspecific symptoms, including ulcerative skin lesions, weight loss, and white nodules in internal organs (Gauthier & Rhodes, 2009b; Delghandi et al., 2020b;). Reports of mycobacteriosis span a wide range of freshwater, marine, and brackish-water fish species, with an increasing incidence observed in the ornamental fish sector in recent years (Zanoni et al., 2008; McDermott & Palmeiro, 2020; Puk & Guz, 2020; Phillips Savage et al., 2022). The management of mycobacteriosis in fish remains a significant challenge due to the chronic nature of the infection and the bacteria's resistance to many common antibiotics. Although some antibiotics have shown varying degrees of success (Guz & Puk, 2022b), limitations in their efficacy include species-specific drug susceptibility, prolonged treatments, and differences between slow- and fast-growing strains, often necessitating tailored treatments (Delghandi et al., 2020b). Moreover, antibiotic resistance represents one of the most alarming concerns in mycobacterial infections, with several species exhibiting multiple antimicrobial resistance (Saxena et al., 2021; Tarashi et al., 2022; Conyers & Saunders, 2024;).

Given the limitations of antibiotic treatment, prevention remains the most effective approach, relying on stringent biosecurity measures, such as regular disinfection of equipment and tanks, enhancing husbandry practices, quarantining newly introduced fish, and depopulating infected stocks (Delghandi et al., 2020b).

On the prophylaxis side, several vaccination strategies have been explored for fish mycobacteriosis, including the use of BCG (Bacillus Calmette and Guerin) vaccine in Japanese flounder (Kato et al., 2010), heat-killed *M. marinum* in European seabass (Ziklo et al., 2018), mycobacterial extracellular products in rainbow trout (Chen et al., 1996), and DNA vaccine in hybrid-striped bass and zebrafish (Pasnik & Smith, 2005; Niskanen et al., 2020;). Moreover, vaccination with live-attenuated and mutant strains have been employed in European seabass and zebrafish with promising results (Cui et al., 2010; Ravid-Peretz et al., 2019). Live-attenuated vaccines (LAVs) are developed by reducing the virulence of pathogenic bacteria. Attenuation can be achieved through physical, chemical, or genetic modifications, including prolonged subculturing under selective conditions (Shoemaker et al., 2009; Mohd-Aris et al., 2019;). This approach has been successfully applied to various microorganisms, including *Mycobacterium spp.*, leading to the development of *Mycobacterium bovis* BCG, which is widely used worldwide to protect humans against *M. tuberculosis* (Flores-Valdez et al., 2022).

These vaccines can replicate pathogenic mechanisms without causing clinical disease by triggering both humoral antibody and cell-mediated responses (Shoemaker et al., 2009; Mohd-Aris et al., 2019). In particular, cell-mediated immunity (Th1-mediated immunity) is essential in promoting host defense against intracellular pathogens. This response is mainly triggered by interleukin 12 (*IL-12)* and interferon gamma (*IFN-γ*), two key proinflammatory cytokines. Antigen-presenting cells, upon activation by PAMPs and DAMPs secrete *IL-12*, stimulating NK and T cells to produce *IFN-γ*. This cytokine enhances macrophage activation, increasing their phagocytic activity and promoting the release of other proinflammatory cytokines (e.g., *IL-1β, TNF-α*). *IFN-γ* also establishes a positive feedback loop by amplifying its own production and upregulating IL-12 receptor expression, as well as MHC-I and MHC-II molecules, strengthening the Th1 response (T. Wang & Secombes, 2013). These processes culminate in the recruitment of other immune cells to the site of infection, ultimately leading to granuloma formation to prevent pathogen dissemination (Myllymäki et al., 2018).

This study aimed to evaluate the efficacy and immunogenicity of LAV derived from a WT strain of *Mycobacterium chelonae*, using goldfish (*Carassius auratus*) as a model organism. In vivo trials were conducted to assess the Δ*M. chelonae* (mutant attenuated strain) immunogenicity and protection in goldfish, subsequently challenged with *M. chelonae* WT (wild type strain) in the first trial and with *M. marinum* WT in the second trial.

Gene expression analysis was performed from both vaccinated and non-vaccinated fish, focusing on interleukin-12 (*IL-12*) and interferon-gamma (*IFN-γ*) as key markers of cell-mediated immune responses.

6.2 Background of study

This study is based on previous research outcomes conducted by the Aquatic Animal Health research group at UC Davis, which aimed to develop a LAV against fish mycobacteriosis. Briefly, a *M. chelonae* WT was isolated from a diseased Chinook salmon during a mycobacteriosis outbreak in Northern California (Nguyen et al., 2021). Subsequently, the *M. chelonae* WT underwent an attenuation process through continuous subculturing on Sheep Blood Agar (SBA) plates for 100 passages. Afterwards, the Δ*M. chelonae* was tested for *in vitro* cytotoxicity using koi-goldfish hybrid fin (*KGHfin*) cells (Soto et al., 2024). Cytotoxicity was assessed by measuring lactate dehydrogenase release, revealing a significant reduction in virulence for the Δ*M. chelonae* compared to the *M. chelonae* WT. Moreover, whole-genome sequencing was performed to evaluate genetic modifications associated with the attenuation, finding a key in-frame deletion in the *TetR/AcrR* family transcriptional regulator gene.

These results supported the *M. chelonae* attenuation *in vitro*, prompting its evaluation with *in vivo* experiments.

6.3 Materials and methods

6.3.1 Source of fish and ethic statement

A total of 330 apparently healthy goldfish (*Carassius auratus*) with average weight 23.6 ± 7 g and length 11.3 ± 1.5 cm were kindly gifted from a commercial fish farm (Blackwater Creek Koi Farms Inc., Florida). Fish were acclimatized in recirculated freshwater at 19 ± 2 °C with dissolved oxygen levels kept at ~9 mg/L and fed with a dry pellet food (Skretting, Tooele, UT) at a rate of 1% body weight per day. Prior to the experiments, a representative subset of the fish (n=20) underwent comprehensive clinical, bacteriological, histopathological and molecular analysis to confirm the absence of *Mycobacterium* spp.

All animal experimental procedures were carried out under protocols approved by the University of California, Davis Institutional Animal Care and Use Committee. When required, anesthesia and euthanasia were performed using buffered MS-222 at different concentrations (100 mg/L for anesthesia and 1000 mg/L for euthanasia).

6.3.2 ***In vivo*** **Trial 1***:* Δ*M. chelonae* vs *M. chelonae* WT

A total of 80 goldfish were acclimatized for one week in aerated 40 L tanks filled with static dechlorinated water. The fish were distributed across eight tanks, each containing 10 individuals. Water quality parameters, including unionized ammonia, pH, nitrate, and nitrite levels, were regularly monitored using test kits (API, Freshwater Master Kit). To maintain optimal conditions, 25% water changes were performed weekly. Each tank was equipped with a box-type aquarium filter containing activated carbon for biological filtration (Marineland Penguin Bio-Wheel Power Filter and Aqueon QuietFlow 20 LED Pro Power Filter), which was replaced monthly to prevent water quality deterioration.

To evaluate the protective efficacy of Δ*M. chelonae*, goldfish (n=40) were immunized via intracelomic injection with 0.1 mL of a bacterial suspension containing $4x10^6$ CFU/fish. Control fish (n=40) were injected with 0.1 mL of sterile PBS to serve as sham-vaccinated controls.

Following vaccination, fish were maintained at 22–25°C and monitored for any adverse effects related to the injection or vaccine.

At 26 days post-vaccination (d.p.v), the immunized fish (n = 40) and sham-vaccinated positive control fish (n = 20) were challenged via intracelomic injection with $1.0x10^7$ CFU/fish of virulent *M. chelonae* WT. The negative control group received 0.1 mL of sterile PBS. Both the vaccine and challenge doses were confirmed by spot-plating on Sheep Blood Agar (SBA). Fish were monitored twice daily for mortality and clinical signs over a 52-day period.

At both 1- and 52-days post-challenge (d.p.c.), three fish per tank were sacrificed (n = 6 for the negative control, n = 6 for the positive control, and n = 12 for the vaccinated group). Spleen and posterior kidney tissues were aseptically collected from each fish, suspended in RNAlater (Thermo Fisher Scientific, Waltham, MA, USA), and stored at -80°C for molecular analysis.

At 52 d.p.c., all surviving fish were euthanized using a lethal dose of MS-222 and processed for microbiological analysis. For microbiological evaluation, posterior kidney swabs were aseptically collected from all dead fish after each sampling, plated on SBA, and incubated at 28°C for 7–10 days.

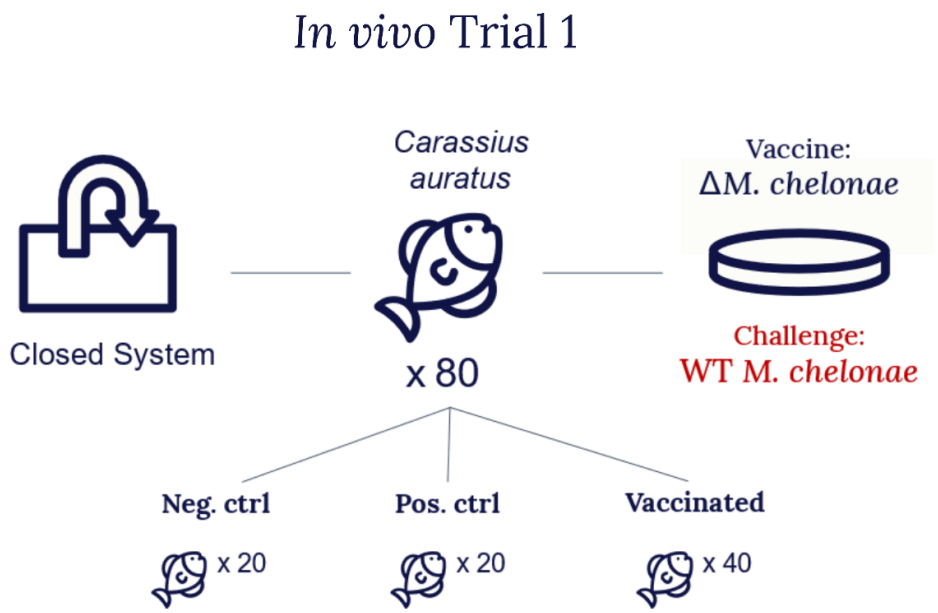

Figure 52. *Schematic representation of in vivo* Trial 1.

6.3.3 ***In vivo trial 2****:* Δ*M. chelonae* vs *M. marinum* WT

In the second trial, a total of 144 fish were housed in 100 L aerated tanks with recirculating freshwater maintained at 18-19°C. Goldfish were divided into three groups: controls (no vaccination), intracelomic vaccine administration, and oral (in-feed) vaccine administration (*Fig. 53*). Each group had 48 fish across duplicate tanks, with 24 fish per tank. After one-week acclimatization, fish received 4×10^6 CFU/fish of Δ*M. chelonae* either by intracoelomic injection or mixed with their feed for oral administration. Sham-vaccinated fish were given sterile PBS or standard feed. Fish were monitored for adverse effects from the injection procedure or the vaccine.

At 1 d.p.v, 4 fish/tank (n=8 for the controls, n=8 for the oral vaccinated group, and n=8 for the injected vaccinated group) were euthanized, and samples of spleen, posterior kidney, and the distal part of the intestine were aseptically collected from each fish, suspended in RNAlater, and stored at -80°C.

Twenty-eight d.p.v, ten immunized fish in each tank were intracelomically challenged with $4x10^6$ CFU/fish of *M. marinum* WT. In this phase one tank from the control group served as a positive control, following the same procedure. The injected fish were identified by a dorsal fin tip excision, acting as "shedders" in a co-habitation challenge, while the remaining 10 fish served as "cohabitants". The negative control group received 0.1 ml of sterile PBS. Morbidity and mortality were monitored for 90 days, with fish checked twice daily for signs of mycobacteria infection. At 90 d.p.c, all the survived fish were euthanized with a lethal dose of MS-222. Spleen and posterior kidney samples were collected suspended in RNAlater, and stored at -80°C. For microbiological evaluation, posterior kidney swabs were aseptically collected from all dead fish after each sampling, plated on SBA, and incubated at 28°C for 7–10 days.

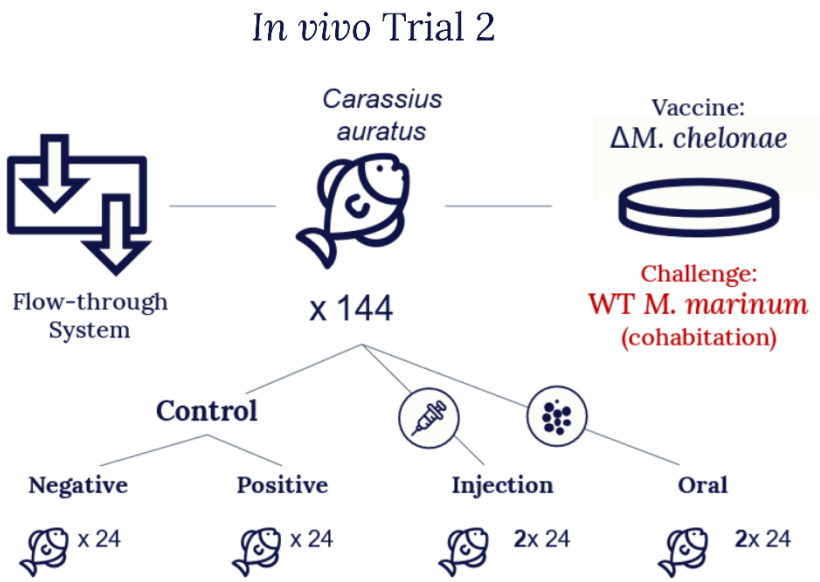

Figure 53. *Schematic representation of in vivo Trial 2.*

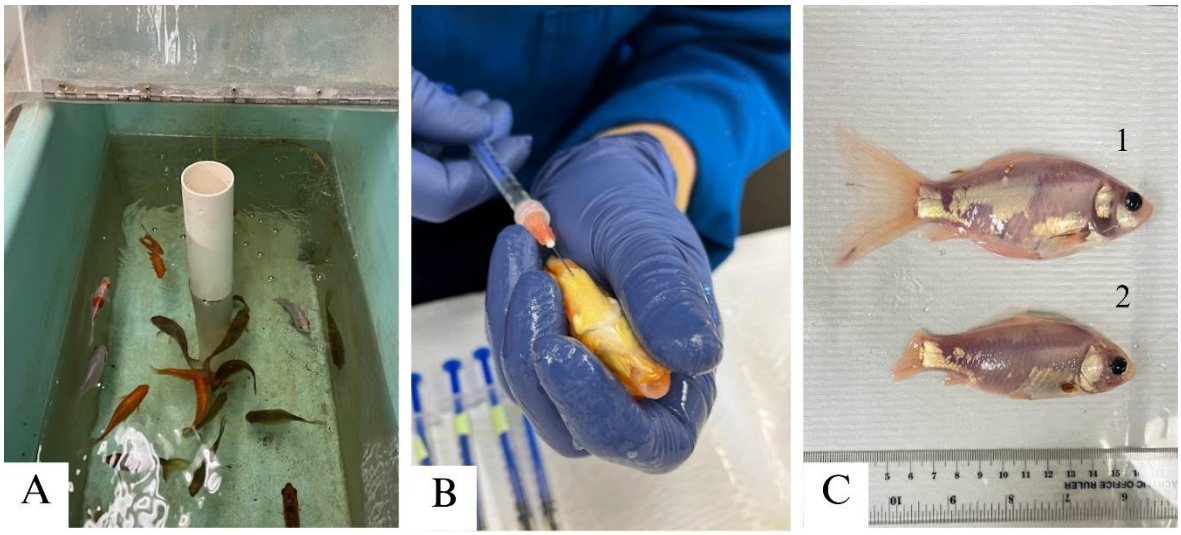

Figure 54. *In vivo trial 2. (A) Flow-through system tank. (B) Intraperitoneal vaccination of goldfish with 4×10⁶ CFU/fish of ΔM. chelonae. (C) Co-habitation challenge: injected fish (shedders) were marked by dorsal fin tip excision (2), while unmarked fish (1) were cohabitants.*

6.3.4 Stress event

For both trials, 22 days post challenge all groups underwent a stress event to enhance mycobacterial infections and evaluate variations in the immune response among the groups

(Ramsay et al., 2009). The stressor event consisted of temporarily removing fish from the water for 30 seconds on two occasions, with an interval of 15 seconds between each stress event.

6.3.5 Nucleic acid extraction

Nucleic acid extraction was performed homogenizing ~5 mg of tissues with a ceramic bead mixture (Omni International), comprising two 2.8 mm beads to disrupt clumped cells and five 1.4 mm beads to ensure thorough lysis of individual cells. Samples were homogenized twice for 20 s each, using an Omni Bead Ruptor 12 (Omni International). Subsequently, DNA and RNA extraction was carried out using the DNeasy Blood & Tissue kit (QIAGEN) and RNeasy Mini Kit (QIAGEN, Redwood City, CA), respectively, following the manufacturer's instructions. Total gDNA was eluted in 100 µl of elution buffer, while total RNA was eluted in 60 µl of RNA-free water. Concentrations and purity were assessed with NanoDrop ND-2000 (ThermoScientific).

For the cDNA generation, reverse transcription of 1 µg of extracted RNA in 20 µL reactions was conducted using the QuantiTect Rev. Transcription Kit (QIAGEN, Hilden, Germany), following the manufacturer's instructions. Post-reverse transcription, DNA concentration was measured, and the samples were used as templates for reverse transcription quantitative PCR (RT-qPCR).

6.3.6 Gene expression analysis

In Trial 1, gene expression analysis was performed at 1 and 52 d.p.c. using spleen and posterior kidney samples from 6 negative control fish, 6 positive control fish, and 12 vaccinated fish at each time point. In Trial 2, analysis was conducted 1 d.p.v on spleen, posterior kidney, and distal intestine samples from 8 fish per group (control, orally vaccinated, and intraperitoneally vaccinated).

The quantitatively real-time PCR (qRT-PCR) investigated the effect of immunization on the expression of immune-related genes, including interleukin 12 (*IL-12*) and interferon γ (*IFN-γ*)(Dharmaratnam et al., 2021). Relative gene expression was calculated using the $2^{-\Delta\Delta Ct}$ method and normalized against the expression of the average of β-actin (*ACTB*) and elongation factor

(*EF1A*$_A$) reference genes (Das et al., 2021). The sequences of all primers used in this study are listed in Table 1.

The PCR mixture contained 5 µL of template cDNA, 1x SYBR Green PCR Master Mix (ThermoFisher Scientific, Waltham, MA, USA), and 0.2 µM of the appropriate forward and reverse primers (Invitrogen, Carlsbad, CA, USA). Conditions for the RT-qPCR were as follows: 1 cycle at 50 °C 2 min, 1 cycle at 95 °C 10 min, and 40 cycles of amplification at 95 °C for 15 s and annealing at 60 °C for 1 min. A melting curve determination was performed at 95 °C for 15 s, 60 °C for 1 min, and 95 °C for 15 s. Negative controls (DEPC-treated H_2O) were included in each run and all samples were run in duplicate.

6.3.7 Mycobacteria load quantification

In Trial 1, total mycobacterial load was estimated from posterior kidney samples (n = 6 for the negative control, n = 6 for the positive control, and n = 12 for the vaccinated group) at 1 and 52 d.p.c using qPCR targeting the *Mycobacterium*-specific *atpE* gene (Radomski et al., 2013).

For *trial 2*, mycobacterial loads were quantified from the spleen and posterior kidney samples (n=10 negative control, n = 20 for the positive control, n = 40 for the oral vaccinated, n = 40 for the injected vaccinated) at 90 d.p.c. with different molecular tools. *M. marinum* load was determined using qPCR targeting the *erp* gene as described by Slany et al. (2013), while Δ*M. chelonae* load was quantified using a specific set of primers designed for the *TetR/AcrR* transcriptional regulator region (see *Table 10*).

To ensure accurate quantification of bacterial loads in tissue samples, distinct standard curves were prepared for each assay. The first standard curve was developed using the *atpE* gene as the target, with known quantities of *M. chelonae* WT, Δ*M. chelonae* and *M.marinum* WT DNA. For the second set of analyses, separate standard curves were generated to target the *erp* gene for *M.*

marinum and the *TetR/AcrR* transcriptional regulator region for Δ*M. chelonae*. Cross-reactivity between the assays was also evaluated using the *M. marinum* and Δ*M. chelonae* DNA.

The conversion from copy number to genome equivalents (GE) was performed by considering the total DNA concentration and the genome size of *M. chelonae* (5092469 bp) and the WT M. marinum (6455215 bp).

The number of GE/ng of DNA was calculated using the following formula:

$$\text{Genome equivalents (GE)} = \frac{DNA\ (ng) \times 6.022 \times 10^{23}}{Genome\ size\ (bp) \times 1.096 \times 10^{-21}}$$

In the qPCR analysis, for the standard curve, results were expressed as $\log_{10}$ GE/reaction.

Serial dilutions ranging from 1 to 1×10^6 GE/reaction were used for both standard curves. Each dilution was run in triplicate to assess the repeatability and reproducibility of the assays. These standard curves were then used to quantify mycobacterial loads in tissue samples, expressed as $\log_{10}$ GE/µg of total DNA. The number of GE per reaction was based on the Ct value from the qPCR and determined using the standard curve equation. The obtained value was then divided by 5, corresponding to the volume of DNA used in each reaction (5 µl), to obtain GE per µl of DNA. This value was then normalized to the initial DNA concentration by dividing by the total DNA concentration (ng/µl), thus obtaining GE per ng of DNA. Finally, the value was divided by 1000 to obtain GE per µg of DNA and expressed as $\log_{10}$ GE/µg of total DNA.

qPCR reactions (12 µL) consisted of 6 µL of TaqMan Environmental Master Mix 2.0 (Applied Biosystems), 0.25 µM of each primer (Table 2), 5 µL of template DNA, and RNase-free water to volume. All reactions, including standards, positive controls, and negative controls, were performed in triplicate. Cycling conditions were as follows: 30 s at 60°C, 10 min at 95°C, followed by 40 cycles of 15 s at 95°C (denaturation), 60 s at 60°C (annealing), and 30 s at 60°C (final extension). All qPCR data were analyzed using the QuantStudio3 qPCR System (Thermo Fisher

Scientific). The cycle threshold (Cq) line was set at 0.05 ΔRn units, and Cq values above 36 were considered negative.

6.3.8 ΔM. chelonae persistence

The safety of the Δ*M. chelonae* was assessed through an in vivo experiment involving 10 healthy goldfish. In separate tanks, five fish were vaccinated intracelomically with 0.1 mL of Δ*M. chelonae* suspension (4×10^6 CFU/fish), while the remaining five served as controls and were injected with 0.1 mL of sterile PBS. Fish were maintained under standard husbandry conditions and monitored daily for 30 days for any clinical signs of illness or behavioral changes. At the end of the trial, all fish were euthanized, and spleen and posterior kidney samples were aseptically collected to estimate the total mycobacterial load. Posterior kidney swabs were taken aseptically from all fish, plated on SBA, and incubated at 28°C for 7–10 days to observe bacterial growth. *atpE* qPCR was used to estimate total mycobacterial load, following the protocol described in section 6.3.8.

6.3.9 Statistical analysis

Gene expression analysis and mycobacterial loads comparisons were performed using GraphPad Prism (version 8.0, GraphPad Software, La Jolla, CA, USA). Statistical differences in gene expression values and bacteria load were determined by two-way ANOVA and Tukey's multiple comparisons test.

Table 10. Primers used in this study for gene expression analysis and mycobacteria quantification.

		Gene name	Primer name	Sequence (5′-3′)	Reference
RT-qPCR (gene expression)	House-keeping genes	*ACTB*	ACTB_F	CAAAGCCAACAGGGAGAAGA	(Dharmaratnam et al., 2021)
			ACTB_R	TGAAGCATACAGGGAGAGCA	
		EF1A$_A$	EF1A$_A$_F	CCTGGCCACAGAGATTTCAT	
			EF1A$_A$_R	TTTGACTCCCAGGGTGAAAG	
	CMI response gene	*IFNγ*	IFN-γ_F	GACTTCAGGATGGGCAACAT	(Das et al., 2021)
			IFN-γ_R	TGCTCAGGTTCCTCGAGATT	
		IL12	IL-12_F	GCTTGTGGTGGATGTTGATG	
			IL-12_R	TCAGGTAGGAGCCCTCATTG	
qPCR (mycobacteria quantification)	*Total mycobacteria load*	*atpE*	atpE_F	CGGYGCCGGTATCGGYGA	(Radomski et al., 2013)
			atpE_R	CGAAGACGAACARSGCCAT	
			probe PatpE	ACSGTGATGAAGAACGGBGTRAA	
	ΔM. chelonae	*TetR/AcrR*	TetR/AcrR_F	CGATGACCAAGCGCATGTT	This study
			TetR/AcrR_R	GGACGAGCTACTACCACTAC	
			Probe TetR	ACCTCATCGAGTCCGTC	
	WT M. marinum strain	*erp*	MAR-erp_F	TTGGCAGGACGACAAGGTCA	(Slany, 2014)
			MAR-erp_R	ATGGTACGAGTGAGGTTGGTGA	
			MAR-probe	FAM-TTCGACAACCCAAGCAGGCCCTAAGCA-BHQ	

6.4 Results

6.4.1 Trial 1*: vaccination and immune response*

In Trial 1, goldfish were intracelomically vaccinated with 10^6 CFU/fish of Δ *M. chelonae*, and at 26 d.p.v, they underwent intracelomic challenge with 10^7 CFU/fish of the *M. chelonae* WT strain. Throughout the 52 d.p.c period, neither the control nor vaccinated groups experienced any mortalities, and no clinical symptoms were observed. However, intracelomic vaccination with the Δ*M. chelonae* resulted in a diverse immune response when challenged with the WT strain (*Fig. 55*). In the vaccinated group, mRNA expression levels of immune-related genes *IL-12* and *IFN-γ*,

evaluated from the spleen and posterior kidney, exhibited an increase at both 1- and 52-days post-challenge, comparing with the levels observed in the negative and positive control groups. The differences in the expression levels were found to be statistically significant for *IFN-γ* in spleen at 1 d.p.c.

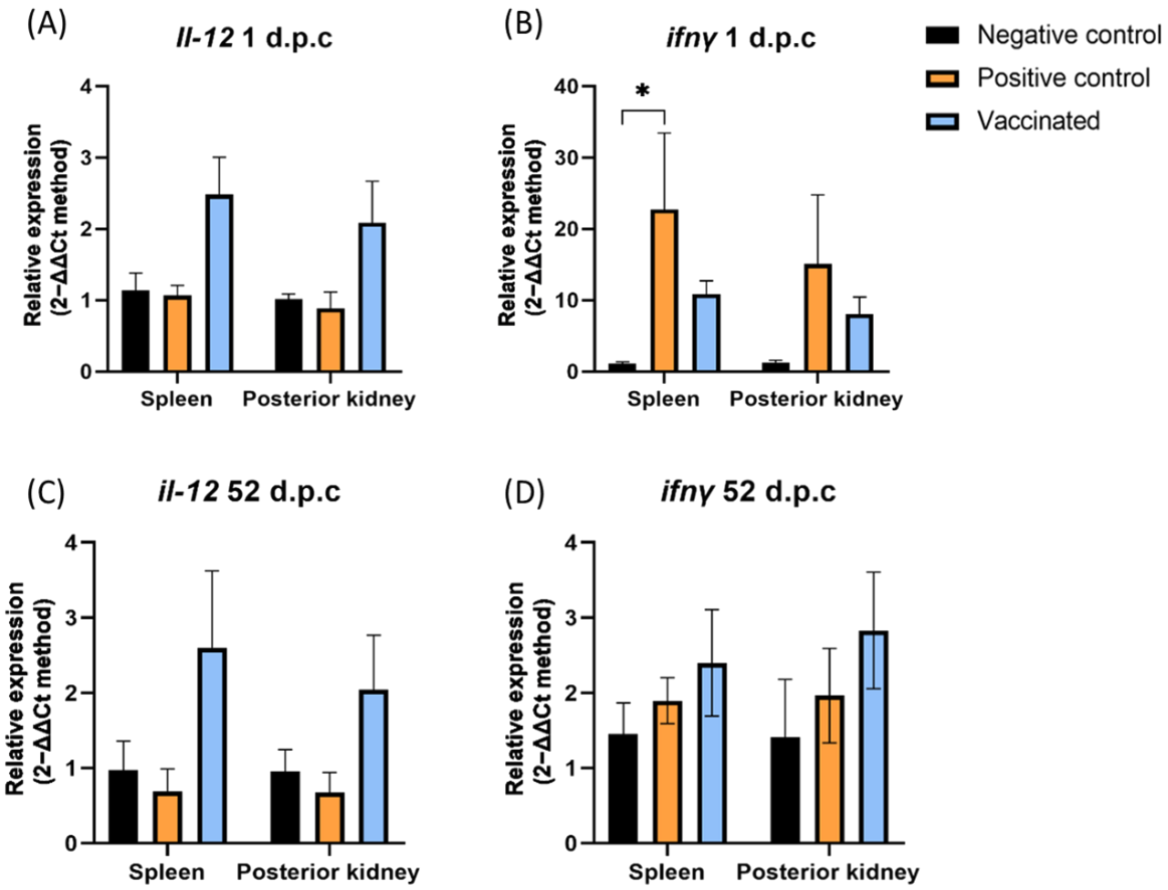

Figure 55. Trial 1*; RTqRT-PCR analysis of the expression of immune-related genes interleukin 12 (IL-12) and interferon gamma (IFN-γ) in posterior kidney and spleen at 1 (A-B) and 52 (C-D) days post challenge (d.p.c). The relative expression level of each immune-related gene was normalized to that of β-actin (ACTB) and elongation factor ($EF1A_A$) housekeeping genes. Error bars represent standard error. Two-way ANOVA and Tukey's multiple tests were performed for group comparison (*$p < 0.05$).*

6.4.2 Trial 2: vaccination and immune response

In Trial 2, goldfish were vaccinated both intracelomically or orally with $4x10^6$ CFU/fish of Δ*M. chelonae*. One day after vaccination, both the injected and orally vaccinated fish exhibited elevated levels of *IL-12* and *IFN-γ* transcripts, compared to the negative control. Notably, a

significantly higher abundance of *IL-12* transcripts was detected in the intestine and posterior kidney of the vaccinated group compared to the negative control, particularly in the injected vaccine group (*Fig. 56A*). Additionally, a significantly higher abundance of *IFN-γ* transcripts was observed in the intestine of the vaccinated group one day post-vaccination (*Fig. 56B*). During the 90 days after the challenge 2/20 (10%) fish deceased in the positive control group and only 1/40 (2.5%) in the oral vaccinated ones (*Fig. 57*).

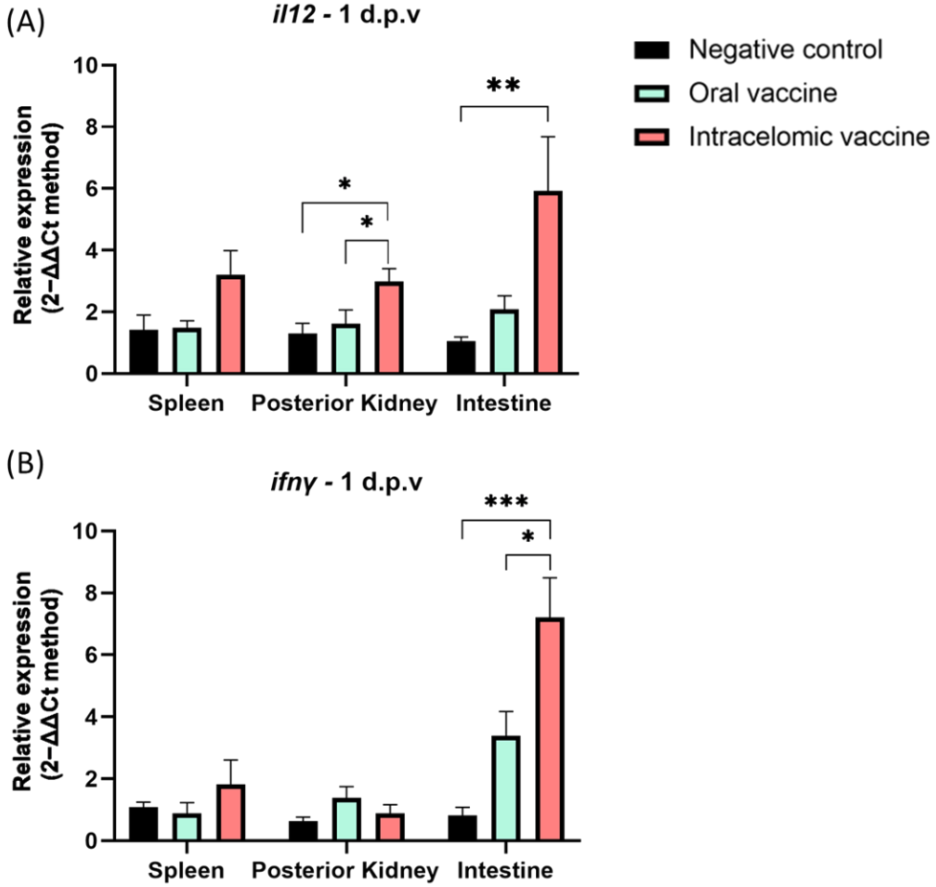

Figure 56. *Trial 2. (A) qRT-PCR analysis of the expression of immune-related genes interleukin 12 (IL-12) in posterior kidney, spleen and the distal part of the intestine at 1 day post vaccination (d.p.v). The relative expression level of each immune-related gene was normalized to that of β-actin (ACTB) and elongation factor ($EF1A_A$) housekeeping genes. (B) qRT-PCR analysis of the expression of immune-related genes interferon gamma (IFN-γ) in posterior kidney, spleen and the distal part of the intestine at 1 d.p.v. Bars represent the mean relative expression of two biological replicates and error bars represent standard error. Two-way ANOVA and Tukey's multiple tests were performed for group comparison (*p < 0.05, *** p < 0.001).*

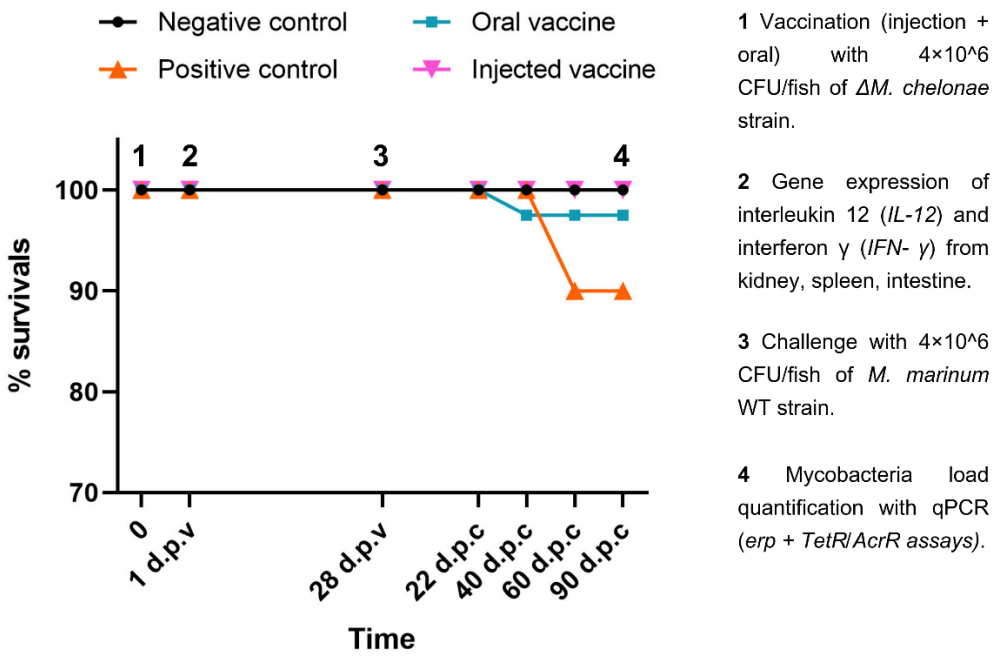

Figure 57. Survival curve of vaccinated and control groups during Trial 2.
Day 0*: Fish were vaccinated (oral/injected, ΔM. chelonae, 4 × 10⁶ CFU/fish) or received the same dose of PBS (negative control).* ***1 day post vaccination (d.p.v.)****: 8 fish/treatment were sacrificed and samples of posterior kidney, spleen, distal intestine were collected for gene expression analysis (IL-12 and IFN-γ gene).* ***28 d.p.v.****: Fish were challenged (WT M. marinum strain, 4 × 10⁶ CFU/fish). During the monitoring period, 2.5% mortality occurred in the oral vaccined group, while in the positive control group experienced a 10% mortality.* ***90 days post-challenge (d.p.c.)****: All survived fish were euthanized, and mycobacterial loads were quantified from the spleen and the posterior kidney via qPCR (erp, TetR/AcrR assays).*

The qPCR assays targeting *atpE*, *erp*, and *TetR/AcrR* genes demonstrated robust amplification and linearity across six orders of magnitude for their respective DNA templates.

The *atpE* qPCR assay reliably quantified *Mycobacterium* spp. DNA with a limit of quantifiable detection of 8.45 GE/reaction (*Fig. 58*). Below this threshold, amplification became inconsistent, with Cq values exceeding 36 and often no observed signal. This assay was tested using DNA from *M. marinum* WT, *M. chelonae* WT, and Δ*M. chelonae*, yielding consistent results across all templates.

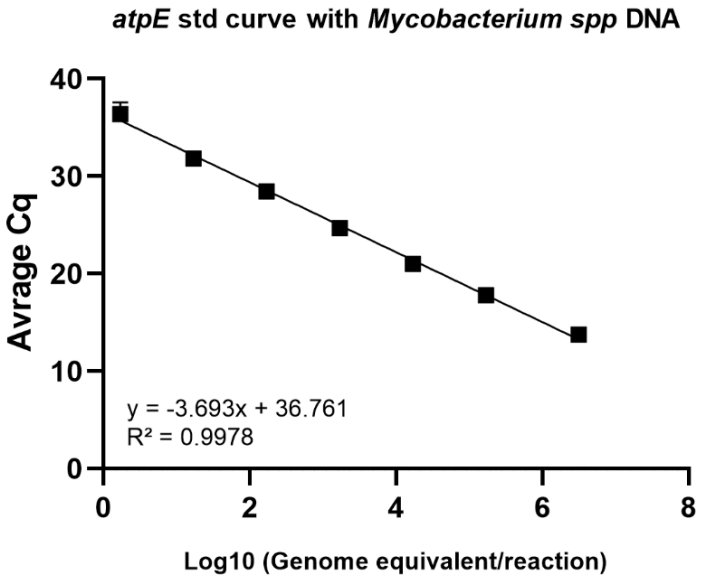

Figure 58. *Standard curve for the atpE qPCR assay using known quantities of M. chelonae and M. marinum DNA.*

The *erp* qPCR assay designed for *M. marinum* WT DNA, this assay achieved a limit of quantifiable detection of 7.06 GE/reaction (*Fig. 59*). Reactions below this threshold showed inconsistent amplification, with Cq values >36 or no signal. No cross-reactivity was observed with the Δ*M. chelonae* strain DNA.

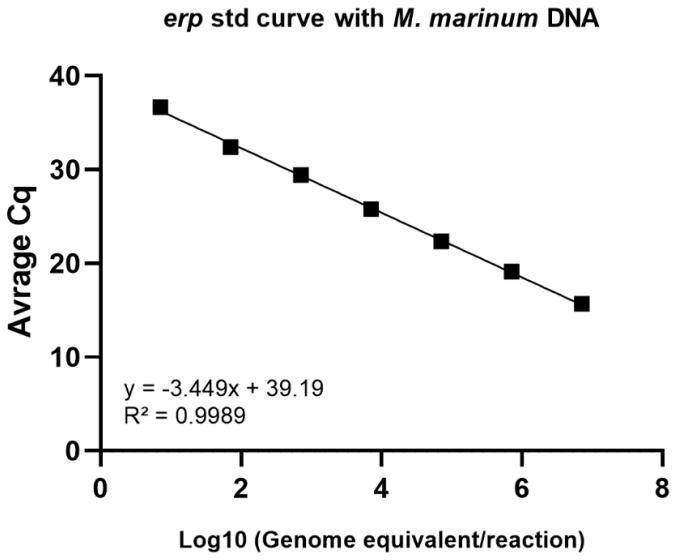

Figure 59. *Standard curve for the erp qPCR assay using known quantities of M. marinum WT DNA.*

The *TetR/AcrR* qPCR assay designed to be specific to Δ*M. chelonae* DNA, this assay had the limit of quantifiable detection at 0.9 GE/reaction (*Fig. 60A*). Weak cross-reactivity with *M. marinum* DNA was observed, with a detection limit of 7065 GE/µg. Amplification under these conditions was poor, with Cq values exceeding 36 and often no detectable signal (*Fig. 60B*)

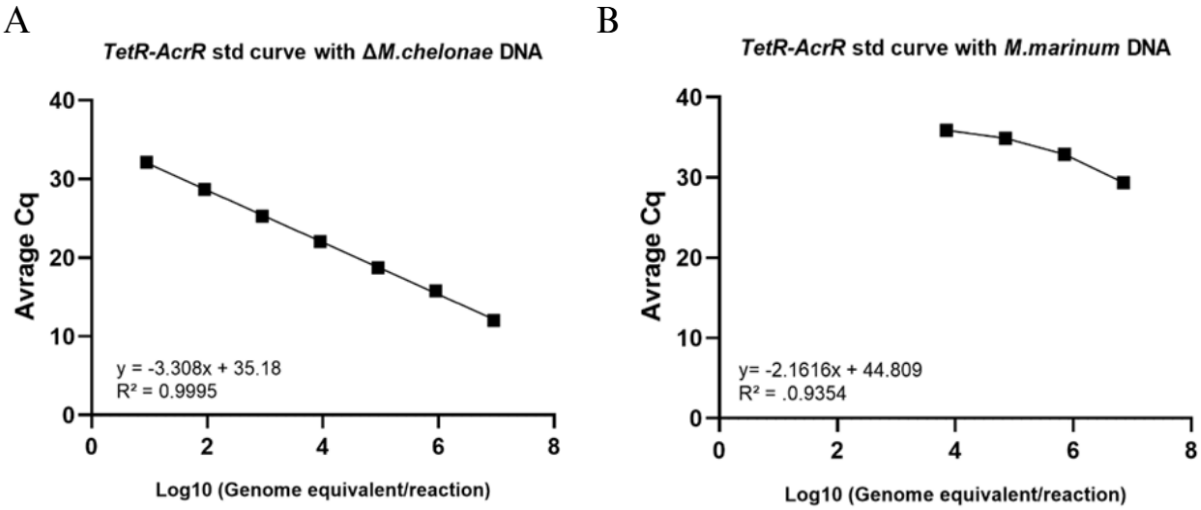

Figure 60. Standard curve for the TetR/AcrR qPCR assay. *(A) Standard curve for the TetR/AcrR qPCR assay using known quantities of ΔM. chelonae DNA. (B) Standard curve for the TetR/AcrR qPCR assay using known quantities of M. marinum WT strain DNA.*

6.4.4 Mycobacteria quantification.

Trial 1: total mycobacteria load

In Trial 1, the *atpE* qPCR revealed a significantly higher total mycobacterial load in the posterior kidney of vaccinated fish at 1 d.p.c. compared to both the positive and negative control groups. At 52 d.p.c., the total mycobacterial load in the vaccinated group was significantly higher than the negative control but not significantly different from the positive control (*Fig. 61*).

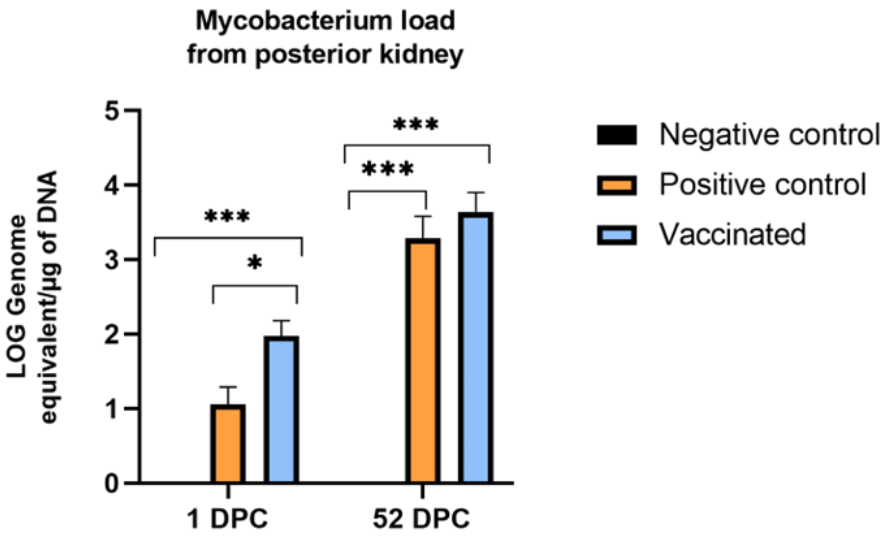

Figure 61. *Abundance of Mycobacterium spp. DNA in the posterior kidney at 1 and 52 days post-challenge (d.p.c.), determined by atpE qPCR assay. Bars represent standard error. Two-way ANOVA with Tukey's multiple comparisons test was used (*p < 0.05, ***p < 0.001).*

Trial 2**:** *M. marinum* and the cohabitation challenge

After 28 days, fish except negative control were challenged with *M. marinum* WT. Different mycobacteria loads were quantified using qPCR assays targeting the *erp* and *TetR/AcrR* genes from spleen and posterior kidney tissues. In both organs, the *erp* qPCR showed reduced *M. marinum* loads in both vaccine groups compared to the positive control, statistically significant in the posterior kidney (*Fig. 62*).

The *TetR/AcrR* qPCR assay revealed variations in Δ*M. chelonae* loads among vaccinated fish, with the injected vaccine group showing significantly higher levels compared to the oral vaccine group (*Fig. 63*).

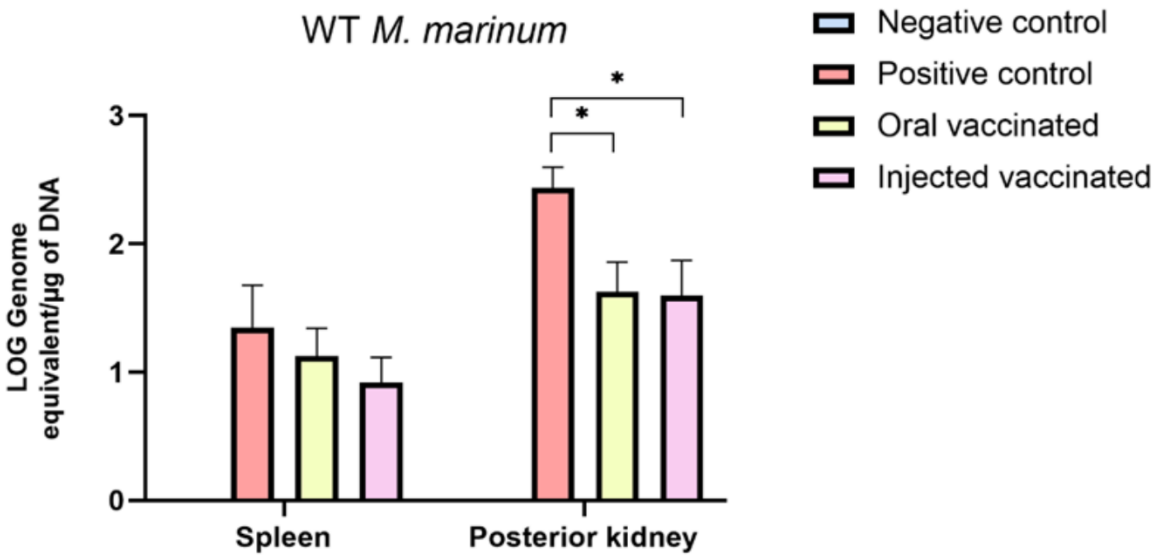

Figure 62. *Abundance of Mycobacterium marinum DNA in the spleen and posterior kidney at 90 days post-challenge (d.p.c.), determined by erp qPCR assay. Bars represent standard error. Two-way ANOVA with Tukey's multiple comparisons test was used (*p < 0.05, ***p < 0.001).*

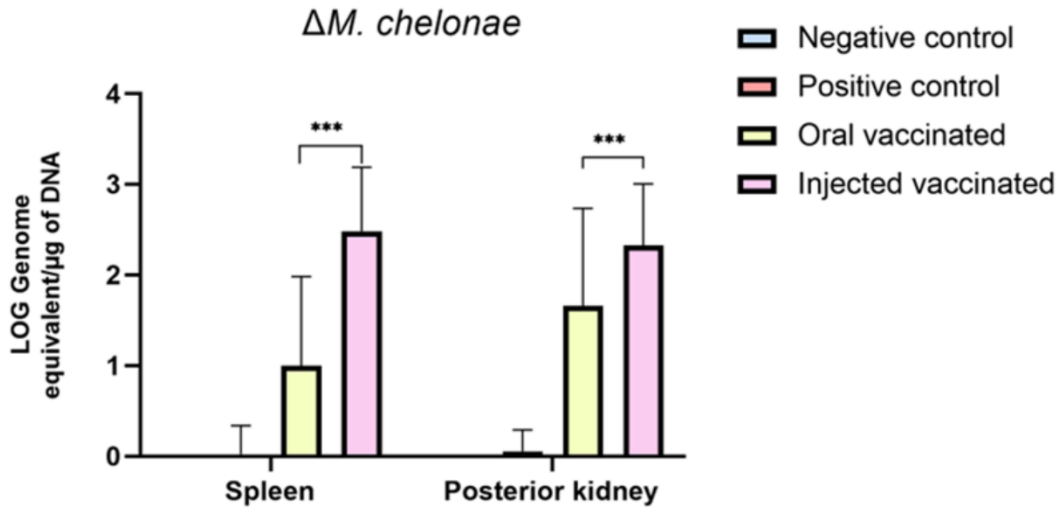

Figure 63. *Abundance of ΔM. chelonae DNA in the spleen and posterior kidney at 90 days post-challenge (d.p.c.), determined by TetR/AcrR qPCR assay. Bars represent standard error. Two-way ANOVA with Tukey's multiple comparisons test was used (***p < 0.001).*

To evaluate potential transmission dynamics and the extent of protection provided by the vaccine, pathogen loads were quantified with the *erp* qPCR in both shedders and cohabitants. Among vaccinated fish, *M. marinum* loads were consistently lower in the spleen and posterior kidney of

the shedders. However, *M. marinum* DNA was also detected in cohabitants, and no significant differences in pathogen load were observed between the positive control and the vaccinated groups.

6.4.5 ΔM. chelonae persistence

The safety of the ΔM. *chelonae* as a live-attenuated vaccine was evaluated through an in vivo study using 10 healthy goldfish. One month after vaccination, the ΔM. *chelonae* was reisolated on SBA in 3/5 of the vaccinated fish, while no bacterial growth was observed in the negative control group.

Total mycobacterial loads in vaccinated fish were quantified using the *atpE* qPCR assay, revealing bacterial loads of 1.72 log GE/µg in the spleen and 1.61 log GE/µg in the posterior kidney.

6.5 Discussion and conclusion

Vaccination remains a cornerstone strategy for mitigating disease outbreaks, reducing economic losses, minimizing reliance on antibiotics, and promoting sustainable aquaculture practices (Mondal & Thomas, 2022). Inactivated vaccines are widely employed due to their safety, cost-effectiveness, and efficacy. However, they predominantly stimulate humoral immunity, which have shown limited efficacy against intracellular pathogens like *Mycobacterium* spp. (Shoemaker et al., 2009; Flores-Valdez et al., 2022), that generally require robust cell-mediated immunity to be overcome (Munang'andu, 2018). In contrast, live-attenuated vaccines (LAVs) offer a significant advantage by mimicking natural infections, stimulating both humoral and cell immunity. Yet, a major LAVs challenge lies in ensuring the genetic stability of attenuated strains to prevent reversion to virulence (Shoemaker et al., 2009; Mohd-Aris et al., 2019; Irshath et al., 2023;).

In this study, we evaluated the efficacy, cross-protection, and safety of a Δ*M. chelonae* (mutant attenuated strain) as LAV in goldfish, focusing on its capacity to induce adaptive cell immunity.

Goldfish (*Carassius auratus*) were chosen for the *in vivo* experiments as they are an established model for studying mycobacteriosis (Talaat et al., 1998; Ruley et al., 2002, 2004). During both trials, mRNA expression levels of *IL-12* and *IFN-γ* were upregulated in the vaccinated group with Δ*M. chelonae* compared to the controls, suggesting a strong immunogenic potential of the LAV candidate. In particular, the prolonged expression of both cytokines at 52 d.p.c suggests that the vaccine can induce a durable and robust immunity. Interestingly, a previous study in not-vaccinated goldfish infected with virulent *Mycobacterium marinum*, reported a significant downregulation of pro-inflammatory cytokines, including *IL-12* and *IFN-γ*, by 56 days post-injection, suggesting a not durable immunity (Hodgkinson et al., 2012).

Furthermore, goldfish vaccinated with Δ*M. chelonae* and challenged with *M. chelonae* WT, showed no mortality or clinical signs in either the vaccinated or positive control groups throughout the 52 d.p.c period. The absence of mortality in the positive control group contrasts with findings by Nguyen Dinh-Hung et al. (2024), who reported acute mortality in betta fish when challenged with 1.0×10^7 CFU/fish of virulent *M. chelonae*. This discrepancy may be due to the differences between the species and differences between the *M. chelonae* isolates.

In Trial 2, where fish were vaccinated with Δ*M. chelonae* and challenged with *M. marinum* WT, mortality reached 10% in the positive control group and 2.5% in the orally vaccinated group. No mortality was observed in the intraperitoneally vaccinated group during the 90 days period of observation. These results suggest that the attenuated vaccine (Δ*M. chelonae*) provided full-protection in the intraperitoneally vaccinated group. However, the differences in mortality between vaccinated and non-vaccinated groups were not statistically significant, limiting the evaluation of vaccine efficacy.

However, bacterial load of *M. marinum* WT strain was lower in vaccinated fish compared to the positive control group, indicating that the LAV can provide robust cross-protection, particularly against *M. marinum* infection, especially in the intraperitoneally vaccinated group.

However, despite these promising results the persistence of the Δ*M. chelonae* in 60% of vaccinated fish, the small sample size and the limited observation period represent major limitations of this study.

Conclusion

This study provides evidence supporting the potential of the Δ*M. chelonae* as a live-attenuated vaccine for mycobacteriosis in fish. The vaccine elicited a strong cell-mediated immune response, reduced *M. marinum* burden, and showed no or low mortality in vaccinated fish. Further studies are needed to validate this approach for advancing the control of mycobacterial infections in aquaculture, improving both animal welfare and industry sustainability.

References

Ahmed, Imran, Simon Tiberi, Joveria Farooqi, Kauser Jabeen, Dorothy Yeboah-Manu, Giovanni Battista Migliori, and Rumina Hasan. 2020. "Non-Tuberculous Mycobacterial Infections—A Neglected and Emerging Problem." International Journal of Infectious Diseases 92 (March): S46–50. https://doi.org/10.1016/j.ijid.2020.02.022.

Anjur, N, S F Sabran, H M Daud, and N Z Othman. 2021. "An Update on the Ornamental Fish Industry in Malaysia: Aeromonas Hydrophila-Associated Disease and Its Treatment Control." Veterinary World 14 (5): 1143–52.

Assiri, Ahmad, Sylvie Euvrard, and Jean Kanitakis. 2019. "Cutaneous *Mycobacterium marinum* Infection (Fish Tank Granuloma) in a Renal Transplant Recipient: Case Report and Literature Review." Cureus, October. https://doi.org/10.7759/cureus.6013.

Aubry, Alexandra, Faiza Mougari, Florence Reibel, and Emmanuelle Cambau. 2017. "*Mycobacterium marinum*." Edited by David Schlossberg. Microbiology Spectrum 5 (2). https://doi.org/10.1128/microbiolspec.TNMI7-0038-2016.

Bedekar, Megha Kadam, and Sajal Kole. 2022. "Fundamentals of Fish Vaccination." In Vaccine Design. Methods in Molecular Biology, edited by S Thomas, 2411:147–73. Humana, New York, NY. https://doi.org/10.1007/978-1-0716-1888-2_9.

Bowker, J, J Trushenski, M Tuttle-Lau, D Straus, M Gaikowski, A Goodwin, and M Bowman. 2019. Guide to Using Drugs, Biologics, and Other Chemicals in Aquaculture. American Fisheries Society Fish Culture Section. https://drive.google.com/file/d/1zINB0VMIMplnCaOkeAxIH_OzvOBcHPZt/view.

Chapman, Frank A., Sharon A. Fitz-Coy, Eric M. Thunberg, and Charles M. Adams. 1997. "United States of America Trade in Ornamental Fish." Journal of the World Aquaculture Society 28 (1): 1–10. https://doi.org/10.1111/j.1749-7345.1997.tb00955.x.

Conyers, Liberty E, and Bernadette M Saunders. 2024. "Treatment for Non-Tuberculous Mycobacteria: Challenges and Prospects." Frontiers in Microbiology 15 (June). https://doi.org/10.3389/fmicb.2024.1394220.

Cui, Z, D Samuel-Shaker, V Watral, and M L Kent. 2010. "Attenuated *Mycobacterium marinum* Protects Zebrafish against Mycobacteriosis." Journal of Fish Diseases 33 (4): 371–75. https://doi.org/10.1111/j.1365-2761.2009.01115.x.

Das, Sweta, Arathi Dharmaratnam, Charan Ravi, Raj Kumar, and Thangaraj Raja Swaminathan. 2021. "Immune Gene Expression in Cyprinid Herpesvirus-2 (CyHV-2)–Sensitized Peripheral Blood Leukocytes (PBLs) Co-Cultured with CyHV-2-Infected Goldfish Fin Cell Line." Aquaculture International 29 (5): 1925–34. https://doi.org/10.1007/s10499-021-00721-6.

Delghandi, M. R., S. Menanteau-Ledouble, K. Waldner, and M. El-Matbouli. 2020. "Renibacterium Salmoninarum and Mycobacterium Spp.: Two Bacterial Pathogens Present at Low Levels in Wild Brown Trout (Salmo Trutta Fario) Populations in Austrian Rivers." BMC Veterinary Research 16 (1): 40. https://doi.org/10.1186/s12917-020-2260-7.

Delghandi, Mohammad Reza, Mansour El-Matbouli, and Simon Menanteau-Ledouble. 2020. "Mycobacteriosis and Infections with Non-Tuberculous Mycobacteria in Aquatic

Organisms: A Review." Microorganisms 8 (9): 1368. https://doi.org/10.3390/microorganisms8091368.

Dharmaratnam, Arathi, Arun Sudhagar, Sundar Raj Nithianantham, Sweta Das, and Thangaraj Raja Swaminathan. 2021. "Evaluation of Candidate Reference Genes for Quantitative RTqPCR Analysis in Goldfish (Carassius Auratus L.) in Healthy and CyHV-2 Infected Fish." Veterinary Immunology and Immunopathology 237 (6): 110270. https://doi.org/10.1016/j.vetimm.2021.110270.

Dinh-Hung, Nguyen, Ha Thanh Dong, Saengchan Senapin, Nguyen Vu Linh, Andrew P. Shinn, Nopadon Pirarat, Ikuo Hirono, Satid Chatchaiphan, and Channarong Rodkhum. 2024. "Infection and Histopathological Consequences in Siamese Fighting Fish (Betta Splendens) Due to Exposure to a Pathogenic Mycobacterium Chelonae via Different Routes." Aquaculture 579 (6): 740191. https://doi.org/10.1016/j.aquaculture.2023.740191.

Flores-Valdez, Mario Alberto, Andreas Kupz, and Selvakumar Subbian. 2022. "Recent Developments in Mycobacteria-Based Live Attenuated Vaccine Candidates for Tuberculosis." Biomedicines 10 (11): 2749. https://doi.org/10.3390/biomedicines10112749.

Francis-Floyd, R. 2011. "Mycobacterial Infections of Fish." United States Department of Agriculture, National Institute of Food and Agriculture. https://srac.msstate.edu/pdfs/Fact Sheets/4706 Myobacterial Infections of Fish.pdf.

Gauthier, David T., and Martha W. Rhodes. 2009. "Mycobacteriosis in Fishes: A Review." The Veterinary Journal 180 (1): 33–47. https://doi.org/10.1016/j.tvjl.2008.05.012.

Gcebe, Nomakorinte, Anita L. Michel, and Tiny Motlatso Hlokwe. 2018. "Non-Tuberculous Mycobacterium Species Causing Mycobacteriosis in Farmed Aquatic Animals of South Africa." BMC Microbiology 18 (1): 32. https://doi.org/10.1186/s12866-018-1177-9.

Guz, Leszek, and Krzysztof Puk. 2022a. "Antibiotic Susceptibility of Mycobacteria Isolated from Ornamental Fish." Journal of Veterinary Research 66 (1): 69–76. https://doi.org/10.2478/jvetres-2022-0011.

Hodgkinson, Jordan W., Jun-Qing Ge, Leon Grayfer, James Stafford, and Miodrag Belosevic. 2012. "Analysis of the Immune Response in Infections of the Goldfish (Carassius Auratus L.) with *Mycobacterium marinum*." Developmental & Comparative Immunology 38 (3): 456–65. https://doi.org/10.1016/j.dci.2012.07.006.

Irshath, Aadil Ahmed, Anand Prem Rajan, Sugumar Vimal, Vasantha-Srinivasan Prabhakaran, and Raja Ganesan. 2023. "Bacterial Pathogenesis in Various Fish Diseases: Recent Advances and Specific Challenges in Vaccine Development." Vaccines 11 (2): 470. https://doi.org/10.3390/vaccines11020470.

Kato, Goshi, Hidehiro Kondo, Takashi Aoki, and Ikuo Hirono. 2010. "BCG Vaccine Confers Adaptive Immunity against Mycobacterium Sp. Infection in Fish." Developmental & Comparative Immunology 34 (2): 133–40. https://doi.org/10.1016/j.dci.2009.08.013.

Kent, Michael L., Stephen W. Feist, Claudia Harper, Shelley Hoogstraten-Miller, J. mac Law, José M. Sánchez-Morgado, Robert L. Tanguay, George E. Sanders, Jan M. Spitsbergen, and Christopher M. Whipps. 2009. "Recommendations for Control of Pathogens and Infectious Diseases in Fish Research Facilities." Comparative Biochemistry and Physiology Part C: Toxicology & Pharmacology 149 (2): 240–48. https://doi.org/10.1016/j.cbpc.2008.08.001.

Klesius, Phillip H., and Craig A. Shoemaker. 1999. “Development and Use of Modified Live Edwardsiella Ictaluri Vaccine against Enteric Septicemia of Catfish.” In Advances in Veterinary Medicine, 523–37. Elsevier. https://doi.org/10.1016/S0065-3519(99)80039-1.

Ladisa, Claudia, Mirko Bruni, and Alessandro Lovatelli. 2017. “Overview of Ornamental Species Aquaculture.” FAO Aquaculture Newsletter; Rome, no. 56: 39–40.

Ma, Jie, Timothy J. Bruce, Evan M. Jones, and Kenneth D. Cain. 2019. “A Review of Fish Vaccine Development Strategies: Conventional Methods and Modern Biotechnological Approaches.” Microorganisms 7 (11): 569. https://doi.org/10.3390/microorganisms7110569.

McDermott, Colin, and Brian Palmeiro. 2020. “Updates on Selected Emerging Infectious Diseases of Ornamental Fish.” Veterinary Clinics of North America: Exotic Animal Practice 23 (2): 413–28. https://doi.org/10.1016/j.cvex.2020.01.004.

Mohd-Aris, Aslizah, Mohd Hafiz Ngoo Muhamad-Sofie, Mohd Zamri-Saad, Hassan Mohd Daud, and Md. Yasin Ina-Salwany. 2019. “Live Vaccines against Bacterial Fish Diseases: A Review.” Veterinary World 12 (11): 1806–15. https://doi.org/10.14202/vetworld.2019.1806-1815.

Mondal, Haimanti, and John Thomas. 2022. “A Review on the Recent Advances and Application of Vaccines against Fish Pathogens in Aquaculture.” Aquaculture International 30 (4): 1971–2000. https://doi.org/10.1007/s10499-022-00884-w.

Munang’andu, Hetron Mweemba. 2018. “Intracellular Bacterial Infections: A Challenge for Developing Cellular Mediated Immunity Vaccines for Farmed Fish.” Microorganisms 6 (2): 33. https://doi.org/10.3390/microorganisms6020033.

Nguyen, Diem Thu, David Marancik, Cynthia Ware, Matt J. Griffin, and Esteban Soto. 2021. “Mycobacterium Salmoniphilum and M. Chelonae in Captive Populations of Chinook Salmon.” Journal of Aquatic Animal Health 33 (2): 107–15. https://doi.org/10.1002/aah.10124.

Niskanen, Mirja, Henna Myllymäki, and Mika Rämet. 2020. “DNA Vaccination with the *Mycobacterium marinum* MMAR_4110 Antigen Inhibits Reactivation of a Latent Mycobacterial Infection in the Adult Zebrafish.” Vaccine 38 (35): 5685–94. https://doi.org/10.1016/j.vaccine.2020.06.053.

Pasnik, David J., and Stephen A. Smith. 2005. “Immunogenic and Protective Effects of a DNA Vaccine for *Mycobacterium marinum* in Fish.” Veterinary Immunology and Immunopathology 103 (3–4): 195–206. https://doi.org/10.1016/j.vetimm.2004.08.017.

Phillips Savage, Ayanna Carla N., Lemar Blake, Rod Suepaul, O’Shane McHugh, Ray Rodgers, Calvern Thomas, Christopher Oura, and Esteban Soto. 2022. “Piscine Mycobacteriosis in the Ornamental Fish Trade in Trinidad and Tobago.” Journal of Fish Diseases 45 (4): 547–60. https://doi.org/10.1111/jfd.13580.

Puk, Krzysztof, and Leszek Guz. 2020. “Occurrence of Mycobacterium Spp. in Ornamental Fish.” Annals of Agricultural and Environmental Medicine 27 (4): 535–39. https://doi.org/10.26444/aaem/114913.

Radomski, Nicolas, Adélaïde Roguet, Françoise S Lucas, Frédéric J Veyrier, Emmanuelle Cambau, Héberte Accrombessi, Régis Moilleron, Marcel A Behr, and Laurent Moulin. 2013. “AtpE Gene as a New Useful Specific Molecular Target to Quantify Mycobacterium in

Environmental Samples." BMC Microbiology 13 (1): 277. https://doi.org/10.1186/1471-2180-13-277.

Ramsay, J M, V Watral, C B Schreck, and M L Kent. 2009. "Husbandry Stress Exacerbates Mycobacterial Infections in Adult Zebrafish, *Danio rerio* (Hamilton)." Journal of Fish Diseases 32 (11): 931–41. https://doi.org/10.1111/j.1365-2761.2009.01074.x.

Ravid-Peretz, Shay, Angelo Colorni, Galit Sharon, and Michal Ucko. 2019. "Vaccination of European Sea Bass *Dicentrarchus labrax* with Avirulent *Mycobacterium marinum* (IipA::Kan Mutant)." Fish & Shellfish Immunology 90 (July): 317–27. https://doi.org/10.1016/j.fsi.2019.04.057.

Rovid, Spickler Anna, and Dvorak Glenda. 2020. "Mycobacteriosis." http://www.cfsph.iastate.edu/DiseaseInfo/factsheets.php.

Ruley, Kristin M, John H Ansede, Christopher L Pritchett, Adel M Talaat, Renate Reimschuessel, and Michele Trucksis. 2004. "Identification of *Mycobacterium marinum* Virulence Genes Using Signature-Tagged Mutagenesis and the Goldfish Model of Mycobacterial Pathogenesis." FEMS Microbiology Letters 232 (1): 75–81. https://doi.org/10.1016/S0378-1097(04)00017-5.

Ruley, Kristin M., Renate Reimschuessel, and Michele Trucksis. 2002. "Goldfish as an Animal Model System for Mycobacterial Infection." In Fish & Shellfish Immunology, 35:29–39. https://doi.org/10.1016/S0076-6879(02)58079-4.

Saxena, Saloni, Herman P Spaink, and Gabriel Forn-Cuní. 2021. "Drug Resistance in Nontuberculous Mycobacteria: Mechanisms and Models." Biology 10 (2): 96. https://doi.org/10.3390/biology10020096.

Shoemaker, Craig A., Phillip H. Klesius, John D. Drennan, and Joyce J. Evans. 2011. "Efficacy of a Modified Live Flavobacterium Columnare Vaccine in Fish." Fish & Shellfish Immunology 30 (1): 304–8. https://doi.org/10.1016/j.fsi.2010.11.001.

Shoemaker, Craig A., Phillip H. Klesius, Joyce J. Evans, and Covadonga R. Arias. 2009. "Use of Modified Live Vaccines in Aquaculture." Journal of the World Aquaculture Society 40 (5): 573–85. https://doi.org/10.1111/j.1749-7345.2009.00279.x.

Slany, M. 2014. "A New Cultivation-independent Tool for Fast and Reliable Detection of *Mycobacterium marinum*." Journal of Fish Diseases 37 (4): 363–69. https://doi.org/10.1111/jfd.12113.

Soto, Esteban, Benjamin R. LaFrentz, Susan Yun, Dorothea Megarani, Eileen Henderson, Chutchai Piewbang, Amber E. Johnston, et al. 2024. "Diagnosis, Isolation and Description of a Novel Amnoonvirus Recovered from Diseased Fancy Guppies, Poecilia Reticulata." Journal of Fish Diseases 47 (6): 1703–18. https://doi.org/10.1111/jfd.13937.

Talaat, Adel M., Renate Reimschuessel, Steven S. Wasserman, and Michele Trucksis. 1998. "Goldfish, Carassius Auratus , a Novel Animal Model for the Study of *Mycobacterium marinum* Pathogenesis." Infection and Immunity 66 (6): 2938–42. https://doi.org/10.1128/IAI.66.6.2938-2942.1998.

Tarashi, Samira, Seyed Davar Siadat, and Abolfazl Fateh. 2022. "Nontuberculous Mycobacterial Resistance to Antibiotics and Disinfectants: Challenges Still Ahead." Edited by Fu-Ming

Tsai. BioMed Research International 2022 (February): 1–12. https://doi.org/10.1155/2022/8168750.

Thomas, Jobin, Ana Balseiro, Christian Gortázar, and María A. Risalde. 2021. "Diagnosis of Tuberculosis in Wildlife: A Systematic Review." Veterinary Research 52 (1): 31. https://doi.org/10.1186/s13567-020-00881-y.

Wang, Tiehui, and Christopher J Secombes. 2013. "The Cytokine Networks of Adaptive Immunity in Fish." Fish & Shellfish Immunology 35 (6): 1703–18. https://doi.org/https://doi.org/10.1016/j.fsi.2013.08.030.

Wise, David J., Terrence E. Greenway, Todd S. Byars, Matt J. Griffin, and Lester H. Khoo. 2015. "Oral Vaccination of Channel Catfish against Enteric Septicemia of Catfish Using a Live Attenuated Edwardsiella Ictaluri Isolate." Journal of Aquatic Animal Health 27 (2): 135–43. https://doi.org/10.1080/08997659.2015.1032440.

Zanoni, R G, D Florio, M L Fioravanti, M Rossi, and M Prearo. 2008. "Occurrence of Mycobacterium Spp. in Ornamental Fish in Italy." Journal of Fish Diseases 31 (6): 433–41. https://doi.org/10.1111/j.1365-2761.2008.00924.x.

Ziklo, N., A. Colorni, L.-Y. Gao, S. J. Du, and M. Ucko. 2018. "Humoral and Cellular Immune Response of European Seabass *Dicentrarchus labrax* Vaccinated with Heat-Killed *Mycobacterium marinum* (IipA::Kan Mutant)." Journal of Aquatic Animal Health 30 (4): 312–24. https://doi.org/10.1002/aah.10042.

Conclusions

Within climate change, overexploitation of resources, and the escalating demand for high-quality protein, aquaculture has emerged as sustainable solution, addressing overfishing, promoting coastal economic development, and reducing the environmental footprint of food production. However, infectious diseases represent a growing threat, compromising animal welfare often resulting in substantial economic losses.

Bacterial infections, particularly those associated with granulomatous inflammation, are of particular concern due to their chronic nature, which impairs growth performance and increases vulnerability to secondary infections. Another significant concern is the risk associated with chronic fish diseases and human health.

The aim of this experimental work was primarily focused on detecting diseases with granulomatous histological patterns caused by bacteria, particularly atypical non-tuberculous mycobacteria (genus: *Mycobacterium*), in the most farmed fish species in Sardinia. The results obtained were unexpected, as all examined fish species revealed a low presence of bacteria belonging to the *Mycobacterium* genus associated with granulomas. Most of the granulomas observed in the organs of the fish were attributed to the presence of parasitic trematodes and myxozoa (in Mugilidae) and to possible nutritional causes in the meagre (*Argyrosomus regius*). These findings are encouraging for Sardinian aquaculture both in terms of fish health and for the economic impact that bacterial diseases typically have on aquaculture businesses. Comprehensively, the integrated diagnostic approach adopted in this study provided valuable insights into the health status of farmed fish in Sardinia.

However, the detection of mycobacteria belonging to the *Mycobacterium chelonae* species, albeit with low prevalence in mullets and meagre, suggested us to not underestimate the issue, especially concerning the potential zoonotic role of these pathogens in humans.

Thus, the second aim of this work was to make a significant contribution to the potential prevention and vaccination against mycobacteriosis in fish. Our first step involved testing the resistance of *Mycobacterium* spp. biofilms to common disinfectants. Surprisingly, *M. chelonae* resisted all treatments, highlighting the hard challenge of preventing mycobacterial infections in aquatic environments.

The absence of a commercially available vaccine for mycobacteriosis has driven us to assess the immunogenic potential and efficacy of an attenuated *M. chelonae* as a live attenuated vaccine against fish mycobacteriosis, demonstrating the vaccine's cross-protective potential against mycobacterial infections.

Research and innovative solutions can play a crucial role in driving the global and regional development of the sector, promoting One Health management strategies that minimize risks to human, animals, and environmental health.

Acknowledgements

A PhD thesis is seldom the product of the sole candidate; it's rather the result of a team effort.
For this reason, I must acknowledge with gratitude the Pathological Anatomy team at the Department of Veterinary Medicine of the University of Sassari, who supported and guided me throughout every step of this research. In particular, I wish to express my deepest gratitude to my tutor Elisabetta Antuofermo and to Giovanni Pietro Burrai, Tiziana Cubeddu, Marta Polinas, and Marina Antonella Sanna: their support, availability, and encouragement were essential in reaching this milestone.

I would also like to thank the entire research team of the fish disease laboratory of IZSPLV (Turin), especially Giuseppe Esposito, Paolo Pastorino and Marino Prearo, for giving me the opportunity to conduct microbiological analyses on the samples and expand my expertise in microbiology and fish diseases. A sincere thank you also goes to Prof. Maria Filippa Addis, and the entire team at the Infectious Diseases Laboratory (University of Milan) for their invaluable contribution and help to the antibody's validation study.

Another huge thank you goes to the Aquatic Animal Health (AHHL) team at UC Davis. I wish to express my deepest gratitude to Prof. Esteban Soto, an incredible mentor whose professionalism and enthusiasm have always motivated and supported me. A special thank you goes to Renata, who welcomed me in California and made me feel at home from day one. Her friendship, support, and help in difficult times have been of immeasurable value to me. Obrigado para tudo!
I am also deeply grateful to the entire AHHL research team: Zeinab, Susan, Darbi, Eva, Kim, Taylor, and Miku. You have been incredible colleagues, who created amazing memories and contributed to my personal and professional growth.

I am deeply grateful to the cooperatives and companies that provided the fish and made this study possible from the very beginning. I would like to thank Maricoltura RiservAzzurra, Marina Torre Grande (Cabras, OR), Compagnie Ittiche Riunite Società Agricola S.r.l. (Golfo Aranci, SS), Stagno di San Teodoro S.p.A. (San Teodoro, SS), and Arrubia (Stagno di S'Ena Arrubia) for their availability and collaboration.

Finally, a special thought goes to my family and my brother, my guiding light and constant source of inspiration. Thank you for supporting me through these years of effort and sacrifice, for always believing in me, and for giving me the strength to never give up. You have taught me the value of commitment and determination, showing me that with dedication and passion, results will always come. I also want to express my heartfelt gratitude to all my friends who have been by my side throughout this journey, sharing both its challenges and milestones.

I believe that research is also about finding and appreciating beauty in every effort and discovery. Because while it is true that everything is just a dance of electrons to complete their octet, it is up to us to recognize the wonder in it and celebrate it.

Thank you.

Claudio Murgia